Imperial College London

Development of antimicrobial vaccines and monoclonal antibodies against carbapenem-resistant *Acinetobacter baumannii*

Sophie Louise Higham

Imperial College London

Department of Infectious Disease

Thesis submitted for the degree of Doctor of Philosophy

“You have to believe. Otherwise, it will never happen.”

Neil Gaiman, Stardust

Abstract

Acinetobacter baumannii is a Gram negative bacterium associated with high levels of antibiotic resistance and difficult to treat hospital acquired infections such as ventilator associated pneumonia. The development of carbapenem resistance by *A. baumannii* has left colistin as a last resort antibiotic treatment option. However, colistin resistance is developing resulting in an urgent requirement for the development of new antimicrobials and preventatives. Using clinically relevant *A. baumannii* isolates from ventilator associated pneumonia patients in Vietnam, a robust and reproducible murine respiratory infection model was developed. Intranasal challenge of mice resulted in significant weight loss, inflammation and bacterial burden. Outer membrane vesicles naturally produced by *A. baumannii* clinical isolates were used to immunise mice intramuscularly, subcutaneously and intranasally. Immunisation with OMVs provided high levels of protection against challenge, reducing weight loss and bacterial burden with intranasal immunisation being the most protective and completely preventing bacterial dissemination. Using serum from immunised mice to measure reactivity, three highly conserved antigens were identified using phage expression cloning and western blotting. The three proteins FilF, OXA-23 and PAL showed high levels of similarity across different *A. baumannii* strains collected from the National Center for Biotechnoloy Information database and potential for use in future vaccine development. Fully human monoclonal antibodies generated using the Kymouse platform at Kymab were raised against OMVs from the same clinical strains. These mAbs were tested in the infection model, showing mixed results. An antibody directed to the carbohydrate capsule antigen was the most effective at reducing disease severity. This work developed clinically relevant *in vivo* infection models in BALB/c mice that allowed for effective testing of the use of OMVs as vaccines against respiratory *A. baumannii* infection. Intramuscular and subcutaneous vaccination with OMVs provided some protection against challenge but intranasal vaccination was the most effective. OMVs delivered intranasally in a prime boost approach prior to challenge led to a significant IgA response and more effective protection against challenge which was most likely due to a stronger mucosal immune response. The three potential vaccine antigens identified require further testing to determine if they have any protective efficacy *in vivo*. Additionally, individual antibodies

showed mixed results when tested *in vivo* with capsular targeting antibodies being more effective than protein or lipooligosaccharide targeting antibodies, which could be due to capsule preventing antibody binding to the target. The work performed within this thesis highlighted the importance of immunisation route and the likelihood of a multivalent approach being the most efficacious for future *A. baumannii* vaccine and monoclonal antibody development.

Acknowledgments

I would like to thank Dr John Tregoning for being an outstanding supervisor throughout my PhD. Being responsible for coming up with the original concept behind this work he provided invaluable ideas and guidance throughout the project. By being enthusiastic, supportive and understanding John really helped me to build my confidence and resilience in scientific research. I believe I got very lucky being able to do my PhD in John's lab and I will be forever grateful for all of his help and support throughout my time working with him.

I would also like to give a big thank you to Dr Stephen Reece for all of the ideas, support and guidance he provided as a co-supervisor throughout my PhD, especially when it came to making the phage expression library and writing my thesis. It was always a pleasure to go and work with the Infectious Diseases and Vaccine group at Kymab, who showed me how to produce OMVs and helped me to produce phylogenetic trees.

Thank you also to Professor Paul Kellam for helping throughout, providing ideas and guidance for the project as well as for my thesis.

Another thank you must go out to Professor Stephen Baker for giving valuable advice throughout the project and for providing the clinical strains of *A. baumannii* that were so vital to the success of this project.

A huge thank you must also go to the Tregoning lab group. To Katie Flight for performing MSD analysis on some of my samples for me as well as everyone who helped me out with sample processing and animal studies. I am particularly grateful to Zee, David, Lucy, Hadi, Katie and Rob for being amazing and helpful people to work with as well as great friends to laugh the days and stupid mistakes away with.

I'd like to thank my parents for always telling me I could do whatever I put my mind to and for supporting me through all the ups and downs of my education and life. Thank you also to the rest of my family and my friends for providing that extra bit of motivation and support whenever I needed it.

Finally, a big thank you to my partner, Elliot. Thank you for always being there at the end of a long day, for listening to all my worries and for always telling me everything will be ok.

Thank you also for celebrating the highs with me and making me feel proud of myself and everything that I achieved.

This PhD was funded by the Biotechnology and Biological Sciences Research Council

Declaration of originality

The work presented here in this thesis is all my own. Any ideas or quotations belonging to other people or work performed by other people has been fully acknowledged and referenced where appropriate.

This thesis contains methodology, figures and intellectual content that have been submitted for publication.

Copyright Declaration

This thesis has been presented for the examination of the PhD degree of Imperial College London. The copyright of this thesis rests with the author. Unless otherwise indicated, its contents are licensed under a Creative Commons Attribution-Non Commercial 4.0 International License (CC BY-NC). Under this license, you may copy and redistribute the material in any medium or format. You may also create and distribute modified versions of the work. This is on the condition that: you credit the author and do not use it, or any derivative works, for a commercial purpose.

When reusing or sharing this work, ensure you make the license terms clear to others by naming the licence and linking to the licence text. Where a work has been adapted, you should indicate that the work has been changed and describe those changes.

Please seek permission from the copyright holder for uses of this work that are not included in this license or permitted under UK Copyright Law.

Table of contents

List of Tables 13

List of Figures 13

1 – Introduction 17

1.1 – Bacterial Lower Respiratory Tract Infections 18

1.1.1 – Clinical Burden 19

1.1.2 – Pneumonia 21

1.1.3 – Pneumonia Risk Factors 23

1.1.4 – Microbiology of Hospital Acquired Pneumonia (HAP) 24

1.1.5 – Current Animal Models of VAP 25

1.2 – *Acinetobacter* 27

1.2.1 – *Acinetobacter baumannii* 28

1.2.2 – A. baumannii Pathogenesis and Infection 31

1.2.3 – Mechanisms of *A. baumannii* Antimicrobial Resistance 36

1.3 – Host Response to *A. baumannii* Infection 37

1.3.1 – Innate Immune Response 38

1.3.2 – Adaptive Immune Response 41

1.4 – Vaccines and monoclonal antibodies for Antimicrobial Resistant Bacterial Infections 42

1.4.1 – Vaccines 43

1.4.2 – Monoclonal antibodies 48

1.5 – Hypothesis and Aims 51

1.5.1 – Aims: 51

2. Materials and Methods 52

2.1 – Reagents 53

2.1.1 – Consumables 53

2.1.2 – Reagents 54

2.1.3 – Antibodies 56

2.2 – Microbiology 56

2.2.1 – Bacterial culture and growth assays 58
2.2.2 – OMV production 59
2.3 – *in vivo* methods 59
2.3.1 – Challenge 59
2.3.2 – Clinical Scoring 60
2.3.3 – Vaccination 61
2.3.4 – mAb pre-treatment 62
2.3.5 – Harvest 62
2.4 – Enzyme-Linked Immunosorbent Assays 64
2.4.1 – IL-6 ELISA 64
2.4.2 – IgG, IgG1, IgG2a & IgM ELISA 64
2.4.3 – IgA ELISA 64
2.5 – Multiplex assay 65
2.6 – Protein identification via Western blotting and mass spectrometry 65
2.6.1 – Western Blot 65
2.6.2 – Protein extraction 66
2.7 – Phage expression cloning 66
2.7.1 – Lambda phage library generation 67
2.7.2 – Adsorption of Antisera with *E. coli* proteins 70
2.7.3 – Serological expression screening 71
2.7.4 – Plasmid excision, sequencing and protein identification 72
2.8 – Phylogenetic tree generation 73
2.9 – Statistical analysis 73
3 – Murine model development of *Acinetobacter baumannii* respiratory tract infection 75
3.1 – Introduction 76
3.1.2 – Chapter aims and hypothesis 78
3.2 – Results 79
3.2.1 – Optical density read at 600nm is a good estimate for the density of *A. baumannii* in liquid culture 79
3.2.2 – Increasing the intranasal challenge dose of *A. baumannii* ATCC 17978 increases disease severity and bacterial burden 80

3.2.3 – A minimum challenge dose of around 5x10^6 CFU per mouse of *A. baumannii* ATCC 17978 is required to reliably cause disease 82

3.2.4 – BALB/c mice recover quickly from intranasal challenge with *A. baumannii* ATCC 17978 that causes limited colonisation and disease 84

3.2.5 – Increasing the dose of clinical strain *A. baumannii* BAL_276 increases disease severity and bacterial burden 86

3.2.6 – Increasing the dose of clinical strain *A. baumannii* BAL_084 increases disease severity and bacterial burden 88

3.2.7 – Increasing the dose of clinical strain *A. baumannii* BAL_191 increases disease severity and bacterial burden 91

3.2.8 – Increasing the dose of clinical strain *A. baumannii* BAL_215 increases disease severity and bacterial burden 93

3.2.9 – Intranasal challenge of BALB/c mice with *A. baumannii* BAL_084 causes more severe disease and bacterial burden than ATCC 17978 94

3.2.10 – Intranasal challenge of BALB/c mice with *A. baumannii* BAL_276 causes severe disease and systemic dissemination 97

..... 99

3.3 – Discussion 100

4 – Comparison of vaccination routes in BALB/c mice immunised with OMVs derived from three A. baumannii strains 105

4.1 – Introduction 106

4.1.2 – Chapter aims and hypothesis 109

Aims 109

4.2 – Results 110

4.2.1 – *A. baumannii* ATCC 17978 OMVs provide limited protection against homologous infection. 110

4.2.2 – *A. baumannii* BAL_276 derived OMVs provide protection against homologous intranasal challenge 112

4.2.3 – Intramuscular immunisation reduced bacterial load in lungs during challenge with *A. baumannii* BAL_276 114

4.2.4 – *A. baumannii* BAL_084 derived OMVs did not protect against homologous intranasal challenge 117

4.2.5 – Intramuscular immunisation reduced bacterial load in the spleen during 48-hour challenge with *A. baumannii* BAL_084 119

4.2.6 – *A. baumannii* BAL_276 OMVs given subcutaneously provide better protection against homologous intranasal challenge than intramuscular vaccination. 122

4.2.7 – Route of vaccination did not alter antibody avidity.....124
4.2.8 – Use of an Imject Alum adjuvant led to increased antibody responses in BALB/c mice. 126
4.2.9 – The addition of an Imject Alum adjuvant did not provide a significant improvement to *A. baumannii* BAL_276 OMV vaccination. 130
4.2.10 – Intranasal vaccination with OMVs provides the high levels of protection against homologous infection out of the tested routes. 133
.....135
4.3 – Discussion 136
5 – Antigen discovery for *A. baumannii* vaccines and *in vivo* monoclonal antibodies.....140
5.1 – Introduction.....142
5.1.2 – Chapter Aims and hypothesis 144
Aims: 144
5.2 – Results 145
5.2.1 – Three antigens were identified as potential vaccine candidates for *A. baumannii using a reverse vaccinology approach* 145
5.2.2 – Phylogenetic analysis shows FilF, OXA-23 and PAL are highly conserved between different strains of *A. baumannii* 147
5.2.3 – Cocktail of 29 *A. baumannii* mAbs did not protect against intranasal *A. baumannii* challenge in BALB/c mice 149
5.2.4 – Conformational binding mAb cocktail 2 reduces inflammation in the lungs of BALB/c mice after *A. baumannii* BAL_276 challenge 152
5.2.5 – Intravenous anti-LOS mAb1042 did not protect against 24 or 48 hour challenge with *A. baumannii* BAL_276 in BALB/c mice 155
5.2.6 – Intravenous anti-LOS mAb1042 did not protect against *A. baumannii* BAL_191 challenge in BALB/c mice.....158
5.2.7 – Anti-OXA-23 mAb1349 does not protect against challenge with *A. baumannii* BAL_276 in BALB/c mice.....160
5.2.8 – Intravenous anti-OXA-23 mAb1349 did not protect against intranasal challenge with *A. baumannii* BAL_191 163
5.2.9 – Anti-KL-49 capsule mAb1416 provided some protection against challenge with *A. baumannii* BAL_191 in BALB/c mice 165
5.2.10 – Anti-KL-49 capsule mAb1416 provides better protection against challenge with *A. baumannii* BAL_191 when given to BALB/c mice intranasally.....167
5.3 – Discussion 169

6 – Discussion 173
6.1 – Summary 174
6.2 – Limitations 174
6.3 – Future work 176
6.4 – Vaccines against *A. baumannii* 177
6.5 – Potential of mAbs in the treatment of *A. baumannii* 179
6.6 – Conclusions and future perspectives 180
7 – Bibliography 183

List of Tables

Table 2.1	Common consumables used	53
Table 2.2	Common reagents used	54-56
Table 2.3	Common antibodies used	56
Table 2.4	Clinical strains of *A. baumannii* used	57
Table 2.5	Clinical scoring of coat	60
Table 2.6	Clinical scoring of activity levels	61
Table 2.7	Clinical scoring of stance	61
Table 2.8	Clinical scoring of breathing	61
Table 3.1	Summary of *in vivo* disease severity of the 5 *A. baumannii* strains used	102
Table 4.1	Summary of *in vivo* OMV vaccination routes and their effect on protective efficacy against homologous challenge	136
Table 5.1	Summary of *in vivo* mAb pre-treatments and their effect on protective efficacy against intranasal challenge	169

List of Figures

Figure 1.1	Comparison of the lungs in health and disease	21
Figure 1.2	Map to show global prevalence of carbapenem resistant *Acinetobacter baumannii*	30
Figure 1.3	Summary of *A. baumannii* virulence factors	32
Figure 1.4	Summary of *A. baumannii* host immune response	38
Figure 1.5	Time taken for detection of resistance of bacteria to antibiotics and vaccines	44
Figure 1.6	Figure to show a summary of some *A. baumannii* vaccine studies	46
Figure 2.1	Serial dilution and plating out to determine bacterial concentration	58
Figure 2.2	Phage expression cloning technique to identify target antigens using polyclonal serum from immunised mice	67
Figure 3.1	OD is a good estimate of concentration for *in vitro* growth of *A. baumannii*	80

Figure 3.2	Increasing the challenge dose of *A. baumannii* ATCC 17978 increases disease severity and bacterial burden	82
Figure 3.3	The dose of *A. baumannii* ATCC 17978 needs to be over ~$8x10^5$ to reliable cause disease	84
Figure 3.4	Intranasal infection with *A. baumannii* ATCC 17978 causes limited colonisation and disease	86
Figure 3.5	Infection with a clinical isolate BAL_276 causes disease in a dose related fashion	88
Figure 3.6	Increasing the challenge dose of *A. baumannii* BAL_084 increases disease severity and bacterial burden	90
Figure 3.7	Increasing the challenge dose of *A. baumannii* BAL_191 increases disease severity and bacterial burden	92
Figure 3.8	Increasing the challenge dose of *A. baumannii* BAL_215 increases disease severity and bacterial burden	94
Figure 3.9	Intranasal infection with *A. baumannii* BAL_084 causes severe disease and systemic colonisation	96
Figure 3.10	Intranasal infection with *A. baumannii* BAL_276 causes severe disease and systemic colonisation	99
Figure 4.1	OMVs from *A. baumannii* ATCC 17978 provide some protection against homologous challenge	111
Figure 4.2	OMVs from *A. baumannii* BAL_276 provide protection against homologous challenge	113
Figure 4.3	OMVs from *A. baumannii* BAL_276 provide protection against homologous challenge	116
Figure 4.4	OMVs from *A. baumannii* BAL_084 provide no protection against homologous challenge	118
Figure 4.5	OMVs from *A. baumannii* BAL_084 provide minimal protection against homologous challenge	121
Figure 4.6	OMVs from *A. baumannii* (strain BAL_276) protect better when injected subcutaneously	124

Figure 4.7	IgG avidity is reduced in subcutaneously immunised mice compared to intramuscularly immunised	126
Figure 4.8	Imject Alum adjuvant has little impact on antibody response against intramuscular or subcutaneous vaccination with *A. baumannii* BAL_276 OMV	129
Figure 4.9	Imject Alum adjuvant provides no benefit to intramuscular or subcutaneous vaccination with *A. baumannii* BAL_276 OMV	132
Figure 4.10	Intranasal vaccination with *A. baumannii* BAL_276 OMV provides the best protection against homologous challenge	135
Figure 5.1	Target identification by mass spectrometry and phage expression assay using antisera from immunised mice	146
Figure 5.2	Phylogenetic trees show high levels of similarity of FilF, OXA-23 and PAL between different *A. baumannii* strains	148
Figure 5.3	Cocktail of 23 mAbs does not provide protection against challenge with *A. baumannii* BAL_276	151
Figure 5.4	mAb cocktails provide some protection against disease following challenge with *A. baumannii* BAL_276	154
Figure 5.5	Intravenous anti-LOS mAb1042 does not provide protection against challenge with *A. baumannii* BAL_276	157
Figure 5.6	Intravenous anti-LOS mAb1042 does not provide protection against challenge with *A. baumannii* BAL_191	159
Figure 5.7	Intravenous anti-OXA-23 mAb1349 does not provide protection against challenge with *A. baumannii* BAL_276	162
Figure 5.8	Intravenous anti-OXA-23 mAb1349 does not provide protection against challenge with *A. baumannii* BAL_191	164
Figure 5.9	Intravenous anti-KL-49 capsule mAb1416 provides some protection against challenge with *A. baumannii* BAL_191	166
Figure 5.10	Intranasal administration of anti-KL-49 capsule mAb1416 provides improved protection against challenge with *A. baumannii* BAL_191 than intramuscular	168

Abbreviations

CDC – Centers for Disease Control and Prevention

CFU – Colony forming units

COPD – Chronic obstructive pulmonary disease

CT – Computerised tomography

FDA – Food and Drug Administration, USA

HAP – Hospital acquired pneumonia

ICU – Intensive care unit

LOS - Lipooligosaccharide

LPS – Lipopolysaccharide

LRTI – Lower respiratory tract infection

mAb – Monoclonal antibody

MDR – Multidrug-resistant

OMV – Outer membrane vesicle

PAMP – Pathogen-associated molecular pattern

PDR – Pan-drug-resistant

PRR – Pattern recognition receptor

VAP – Ventilator associated pneumonia

WHO – World Health Organisation

XDR – Extensively drug-resistant

1 – Introduction

1.1 – Bacterial Lower Respiratory Tract Infections

The air we breathe contains up to 100,000 bacteria per litre[1]. As a result, the lungs are constantly exposed to bacteria from both the air and upper respiratory tract[2]. Our respiratory tract hosts a distinct population of microorganisms that make up the lung microbiome[1,2], which is of similar density to what is found in the small bowel[1]. The most commonly found phyla in the lung are Firmicutes and Bacteroidetes, more specifically *Streptococcus* spp., *Veillonella* spp. and *Prevotella* spp.[1,2]. However, the microbiome of healthy lungs also frequently includes Fusobacteria, Actinobacteria and Proteobacteria[1].

If pathogens get into a niche of the human body where they wouldn't ordinarily be found in the healthy host, or the microbiota and/or immune system can no longer control the opportunistic pathogen population and the pathogens are able to outcompete the normal flora, it will result in a bacterial infection[3]. Acute bacterial respiratory tract infections most commonly affect the very young, old or those with pre-existing health conditions. However, they do affect healthy adults as well[1]. Chronic bacterial respiratory tract infections are most commonly a result of underlying disease, such as chronic obstructive pulmonary disorder or Cystic Fibrosis[1]. Acute and chronic respiratory tract infections are the most frequently occurring infections for which antimicrobial drugs are prescribed, with the respiratory tract being one of the largest reservoirs for multi-drug resistant bacteria[4].

Numerous genera of bacteria can cause lower respiratory tract infections. Some of the most clinically important bacteria that are commonly responsible for causing severe disease include *Staphylococcus aureus*, *Streptococcus pneumoniae*, *Klebsiella pneumoniae*, *Pseudomonas aeruginosa* and *Acinetobacter baumannii*[5]. Four of these species belong to a group of six pathogens with high levels of antibiotic resistance and virulence, named the ESKAPE pathogens: *Enterococcus faecium*, *S. aureus*, *K. pneumoniae*, *A. baumannii*, *P. aeruginosa* and *Enterobacter*[6]. The ESKAPE pathogens were highlighted by the World Health Organisation as having the highest risk of mortality of infection and are associated with increased health care costs when compared to other pathogens[6]. ESKAPE pathogens are the leading causes of hospital acquired infections and are extremely efficient in "escaping" treatment with antimicrobial agents due to development of antimicrobial resistance[6].

An infection caused by an antibiotic resistant strain of bacteria typically results in adverse outcomes at two-fold higher rates compared to similar infections caused by antibiotic

sensitive strains[7]. The increase in adverse outcomes can be as a result of delayed administration of effective antibiotic treatment, the emergence of antibiotic resistance during antibiotic treatment, reduced antibiotic efficacy and the requirement to use more toxic antibiotic treatment options, such as colistin[7]. The adverse outcome severity increases with pathogen virulence, patient vulnerabilities and disease severity. Antibiotic resistant infections can result in increased morbidity and mortality, which can be a result of increased length of mechanical ventilation and hospital stay; the requirement for intensive care; additional surgeries and physiological decline[7,8]. Extended-spectrum β-lactamase producing *K. pneumoniae* infections have nearly double the chance of antibiotic treatment failure compared to non-extended-spectrum β-lactamase producing *K. pneumoniae*. The risk of death caused by carbapenem resistant *K. pneumoniae* is two to five-fold higher than carbapenem sensitive strains. Additionally, treatment fails more frequently when patients are infected by antibiotic resistant *Neisseria gonorrhoeae*, resulting in continuation of the disease and infertility[7]. Antibiotic resistance results in a delay in the administration of effective antimicrobial therapies, often relying upon bacterial identification and potentially antibiotic sensitivity testing. This then allows the duration and severity of the infection to increase and can result in further complications, leading to increased morbidity and mortality. Additionally, it can result in increased periods of time when patients are infectious and therefore increases transmission[7,8].

1.1.1 – Clinical Burden

Based on data from 2019 and 2017, lower respiratory tract infections (LRTIs) were the leading cause of communicable death worldwide and the fourth most common cause of death overall[9,10]. LRTIs and pneumonia are two of the leading causes of death. Accounting for more than 4 million deaths each year, killing more people than HIV and malaria combined[1,10,11]. LRTIs are the highest cause of disease burden to humanity, resulting in the loss of 103,000 disability-life adjusted years[1]. In children under 5 years of age, pneumonia accounts for around 1.3 million deaths per year and 18% of all childhood mortality; it is the leading cause of death worldwide in children[1,10,11]. Acute LRTI in children also predisposes them for chronic respiratory disease later in life[10].

Multi-drug resistant bacteria are responsible for 15.5% of hospital acquired infections world-wide[6]. Although hospital acquired infections are most often preventable, they cause a

significant increase in mortality and morbidity and can greatly increase the length of stay in hospital as well as financial cost. They can cause serious complications post-surgery and are a big burden on health care systems[12,13]. Hospital acquired pneumonia (HAP) accounts for around 15% of all nosocomial infections[14] and is the most frequently occurring infection in intensive care units (ICUs) with a mortality rate of approximately 20%[15]. The Centre for Disease Control in the US estimated that in 2011 648,000 patients suffered from hospital acquired infections, with pneumonia being one of the most common at approximately 21.8%[16]. Similarly, in the UK the National Health Service (NHS) estimated that on average 300,000 patients develop hospital acquired infections every year with LRTIs being the most common at 22.8%[17]. Hospital acquired infections are estimated to cost the NHS over £1 billion annually[18].

One of the reasons for such high fatality rates due to LRTI is antimicrobial resistance. In 2019 there were approximately 2.49 million deaths caused by lower respiratory tract infections[19,20] with over 1.5 million of those deaths being associated with antimicrobial resistance[21]. Where a single causative agent has been identified, studies have found around 18-29% of LRTIs to be bacterial and 62-65% viral[22–24]. Despite the much lower incidence of disease seen in bacterial LRTIs, they are responsible for a disproportionate number of deaths. Showing the urgent need for research into new antimicrobials or alternative treatments.

Hospital acquired pneumonia is the second most common nosocomial infection but is responsible for the highest financial cost and greatest morbidity and mortality[25]. HAP is a serious issue in intensive care units (ICUs) where patients are often immunocompromised, more susceptible to infection and require mechanical ventilation. Mechanical ventilation results in a 20-fold increased risk for developing pneumonia[26]. Ventilator associated pneumonia (VAP) is pneumonia that occurs over 48 hours after ventilation. VAP is the most frequently occurring infection in ICUs[15,26–28]. Mortality is greatly increased in patients who develop VAP with mortality rates up to 50%[26,29,30]. VAP is also estimated to extend the duration of hospitalisation by 7 days and increase costs by $40,000 USD[30,31].

1.1.2 – Pneumonia

Pneumonia is most frequently caused by acute viral, bacterial or fungal lower respiratory tract infections, but it can also be non-infectious and drug-induced such as interstitial or eosinophilic pneumonia[32,33]. During pneumonia, alveoli fill with pus and fluid (Fig. 1.1); causing pain when breathing and reducing gas exchange in the alveoli, therefore reducing oxygen levels in the blood[34]. In the case of bacterial pneumonia, bacteria infiltrate the lower respiratory tract and lung parenchyma as a result of compromised host defences, a particularly virulent organism or an overwhelming inoculum in the case of experimental animal infection. A number of factors protect the respiratory system against microbial infection. These include the competing presence of the pulmonary microbiome as well as physical barriers such as the glottis and larynx, the cough reflex, mucociliary lining, tracheobronchial secretions, cell-mediated and humoral immunity, as well as a dual phagocytic system of alveolar macrophages and neutrophils. When these defence mechanisms work together effectively microorganisms fail to colonise, reducing the risk of disease. However, when host defences are compromised or overwhelmed, pneumonia occurs[30].

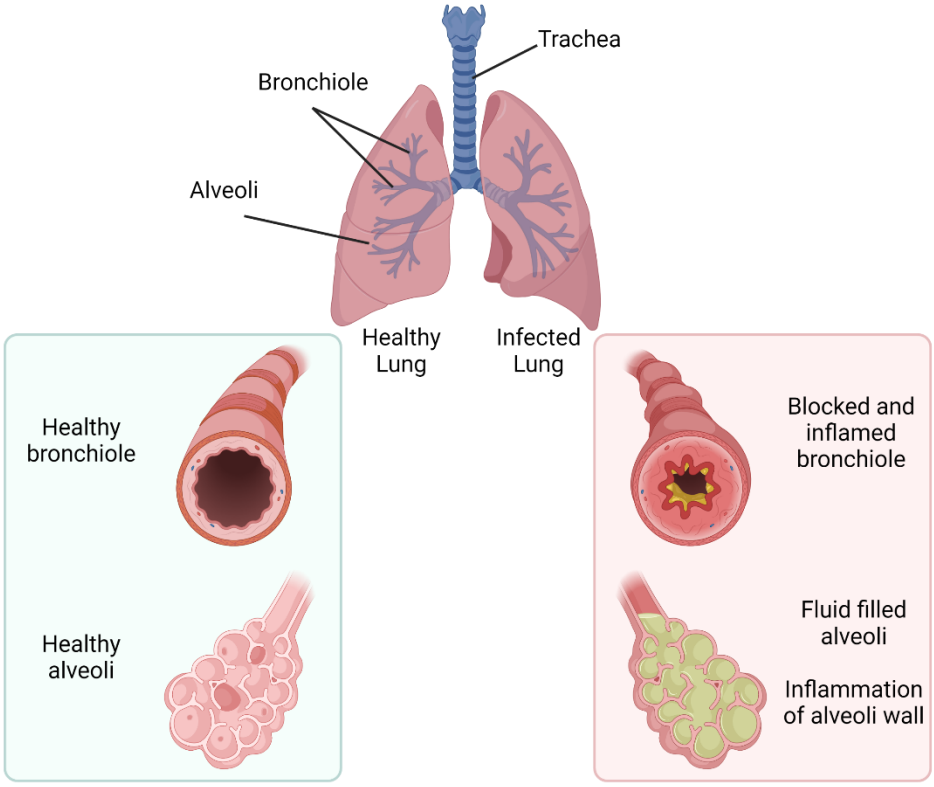


Figure 1.1 | Comparison of the lungs in health and disease. During infection, the bronchioles become inflamed and blocked up as alveoli walls also become inflamed and the alveoli fill with pus and fluid. Figure created using BioRender.com

In VAP, intubation of the patient breaks the barrier between the oropharynx and the trachea. Many VAP infections occur as a result of the aspiration of pathogens that have colonised the oropharyngeal mucosa[30] or from the formation of a biofilm on the surface of the endotracheal tube[35]. Mechanical ventilation facilitates the entry of pathogens into the lungs via contaminated secretions present on the endotracheal tube cuff[30]. As well as facilitating microbial entry into the lungs, mechanical ventilation increases chances of triggering pneumonia by disrupting normal respiratory defence mechanisms. Patients who have been intubated have abnormal swallowing function, an impaired cough reflex, compromised mucociliary clearance, sedative medication, supine positioning, gastroparesis, nasogastric feeding tubes and possibly additional compromising factors[36]. The length of stay of a patient prior to intubation influences the pathogens responsible for causing the VAP. Newly hospitalised patients often get VAP caused by bacteria that are a part of the normal mouth flora or pathogens generally associated with community acquired pneumonia. However, in patients who have been hospitalised for more than 5 days Gram negative bacteria and *S. aureus* typically colonise the airway and are therefore the primary pathogens causing VAP[30].

Diagnosing pneumonia can be challenging as it can cause symptoms that are non-specific and commonly seen in people with the flu or the common cold[37]. Medical professionals use chest X-rays to look for signs of inflammation in the lungs[37] and will look for signs of new or progressive infiltrate[38]. They also perform blood tests to look for leucocytosis and sputum tests to find the causative organism[37,38]. Additional tests can also include computerized tomography (CT) scans, pleural fluid culture, pulse oximetry, blood culture and bronchoscopy to further investigate causes, severity or for confirmation of the diagnosis[37]. A diagnosis of VAP will be made if a patient has new radiographic infiltrates as well as at least 2 of the following symptoms: fever or hypothermia, leucocytosis or leucopoenia, and purulent tracheobronchial secretions[39].

1.1.3 – Pneumonia Risk Factors

Risk factors for pneumonia include immunodeficiency, lack of proper immunisation within a population, malnutrition, extremes of age (young or old), cramped and crowded living conditions, exposure to particulates (through pollution or tobacco smoke), chronic health conditions and lack of breast feeding[10]. Lifestyle habits such as smoking and excessive alcohol consumption also put a person at higher risk of getting pneumonia. Pre-existing medical conditions increase the risk of pneumonia such as cystic fibrosis, asthma, COPD or bronchiectasis or having other serious diseases including diabetes, sickle cell anaemia and heart failure. Finally, being in an ICU especially when mechanically ventilated and immunocompromised, is a big risk factor in a patients potential to develop multidrug-resistant bacterial pneumonia[37]. The annual incidence of hospital acquired pneumonia globally is between 5 and 10 cases per 1,000 hospital admissions, in contrast VAP occurs in 10-25% of all mechanically ventilated patients[40].

Importantly, the prolonged use of antimicrobials to treat ICU patient's primary infections is thought to be a risk factor by creating a selective environment that more readily allows for colonisation with multi-drug resistant pathogens[30]. One study showed that patients who received antibiotic treatment within 15 days of developing a LRTI did not have an increased risk of developing VAP. However, 65% of 567 patients who were on broad spectrum antibiotics developed infections caused by *Pseudomonas* or *Acinetobacter* spp. compared to 19% of patients who received no antibiotics in the 15 days prior to developing a LRTI[30]. A study on baboons showed similar results, with the prevalence of multi-drug resistant bacterial infection being much higher in antibiotic treated mechanically ventilated baboons compared to the baboons that didn't receive antibiotic treatment[41]. There are strong arguments that prophylactic antibiotic use in the ICU may delay the onset of nosocomial infection but increases the risk of superinfection with multi-drug resistant pathogens[30]. During sequential sampling of patients with *P. aeruginosa* infection (7.6 ± 5.8 days apart) the primary antibiotic resistance rates were low to moderate for all antibiotics, ranging from 1.7% to 31.9%. However, during treatment, resistance developed and secondary resistance for at least one of the antibiotics reached 51%. The increase in resistance was found to be a consequence of mutant selection rather than clonal replacement of sensitive clones by resistant clones[42].

Mechanical ventilation is the most important factor associated with developing nosocomial pneumonia. 9-40% of patients who are mechanically ventilated for over 48 hours develop VAP however, HAP can occur less than 48 hours after intubation[14]. One study on 358 ICU patients, 223 of which were mechanically ventilated, showed that 12.1% of patients on mechanical ventilation developed pneumonia compared to 0.74% of patients who were not mechanically ventilated[43]. In addition, a multicentre study of 16 different ICUs results showed that on average 17.5% of patients developed VAP after being mechanically ventilated for over 48 hours[44]. The biggest risk of mechanical ventilation is found in the insertion of the endotracheal tube itself. This means that reducing the risk of mechanical ventilation is likely to be challenging[14].

1.1.4 – Microbiology of Hospital Acquired Pneumonia (HAP)

Many studies have investigated the etiological agents responsible for causing HAP. Gram-negative bacteria, including *P. aeruginosa*, *Enterobacter*, *Acinetobacter*, and enteric Gram-negative bacilli (such as *Salmonella* and coliform spp.)[14,45–47] are involved in between 55% and 85% of hospital acquired pneumonia (HAP) infections[14]. Gram-positive cocci are involved in 20%-30% of cases and 40%-60% of cases are polymicrobial[14]. Disease severity, duration of hospitalisation and prior antibiotic treatment are major determinants of the disease-causing pathogen. *P. aeruginosa*, *A. calcoaceticus* and *A. baumannii* account for 30%-50% of nosocomial pneumonia in mechanically ventilated ICU patients. These pathogens infrequently cause disease outside of an ICU setting[14]. In a study performed on the data of 24 investigations of VAP it was found that *P. aeruginosa* was the most common cause of VAP, followed by *Acinetobacter* spp[30].

Underlying diseases and risk factors alter the microbiology of disease, predisposing patients to infection with specific pathogens. COPD patients are at a higher risk of developing pneumonia caused by *Moraxella catarrhalis*, *S. pnuemoniae* or *H. influenzae*; cystic fibrosis patients are at a higher risk of developing pneumonia caused by *P. aeruginosa* and/or *S. aureus*. Many studies have been performed to try and identify the risk factors for specific pathogens[30]. One of these studies showed that neurosurgery, head trauma and large-volume aspiration were all risk factors for VAP caused by *A. baumannii*[30,48].

The time duration prior to infection also influences the microbiology of HAP. Early onset HAP occurs in the first 4 days of hospitalisation. The most common causative agents of early onset HAP are *H. influenzae*, *S. pneumoniae* or methicillin-susceptible *S. aureus*. Early onset HAP is often caused by antimicrobial susceptible organisms. On the other hand, late onset HAP is often caused by antimicrobial resistant organisms and occurs more than 4 days after hospitalisation. The most common causative agents of late onset HAP are *P. aeruginosa*, *Acinetobacter* spp., *Enterobacteriaceae* or methicillin-resistant *S. aureus*. Prior treatment with antibiotics in particular increases the risk factor for infection caused by these antibiotic resistant bacteria as well as others[14].

1.1.5 – Current Animal Models of VAP

Animal models are used in conjunction with human population studies to understand more about the disease. Such studies were critical in understanding the relationship between the microbiology of VAP and the resultant inflammatory response[39]. The process by which a mechanically ventilated patient develops VAP is often through prolonged microaspiration[39]. However, in animal models it is more commonly as a result of inoculation with a significant volume and dose of the chosen respiratory pathogen such that it causes a disease state[39,49–51]. Animal models allow for low cost, high impact research. They are widely available and make it possible to study in detail the mechanisms behind disease, often through invasive approaches that would not be possible in humans. Whether a study succeeds or fails, animal models provide a link between *in vitro* studies and clinical trials and are key in determining whether a study can continue into clinical trial[39,49].

There are many different animal models of pneumonia, the research question that is being asked is the biggest factor in determining what model is chosen. Non-mammalian studies using zebra fish, insects and roundworms are cheap and can be used to study innate immunity and host cell signalling. Non-mammalian models are also used for determining virulence of organisms. These organisms have fewer regulatory guidelines than if one were to use animals with higher-order sentience[49]. However, they lack a mammalian respiratory tract and adaptive immune system[49]. Non-human primates very closely model human physiology, pathophysiology and immune response and are also often susceptible to human pathogens but their use is expensive, raises major ethical concerns and is extremely highly regulated[49]. Rodent models can accurately model the human immune response, both innate

and adaptive, and are also susceptible to the majority of human pathogens that cause pneumonia. However, there are anatomical differences and drawbacks to rodent models. To induce pneumonia, animal models often rely on forced aspiration of large concentrations of bacteria rather than the more natural inhalation or aspiration from the upper airway, like in human pneumonia infections. Models also often use healthy, young adult rodents[49] although in human disease, pneumonia most commonly affects the very young, old or immunocompromised[1,10,18,43,44,49]. Despite these differences, there is still a large enough cross-over between the anatomy, immunology, physiology and cell biology of humans and rodents. This means animal models are still able to recapitulate many aspects of human respiratory infection[49].

1.1.5.1 Large animal models

Models in larger rodents or other mammals, such as pigs, allow for a more accurate representation of VAP as animals can be mechanically ventilated before they are infected[51–53]. One group developed a model of VAP in piglets where they were mechanically ventilated left to see if they developed endogenous pneumonia under different treatment conditions. They found that the majority of piglets subjected to prolonged mechanical ventilation developed pneumonia, which was usually polymicrobial but dominated by Gram-negative bacteria. They also found that animals that weren't mechanically ventilated and were inoculated with bacteria developed pneumonia that resolved spontaneously[52]. A different model of VAP was developed using immunocompetent rabbits where non-ventilator pneumonia was compared to VAP. In the VAP group rabbits were mechanically ventilated prior to bacterial challenge and non-ventilated rabbits were inoculated using an endobronchial catheter. This study developed an effective model of VAP in rabbits that resulted in histopathologic and bacteriologic features similar to those seen in human infection. They also found that the VAP group of rabbits had a more severe disease state than the non-ventilated group[53].

1.1.5.2 Rodent models

In murine models, it is a challenge to mechanically ventilate, so pneumonia is often induced through inoculation with large volumes/concentrations of bacteria[49,51]. One study used clinical isolates of *A. baumannii*, anaesthetising mice with isoflurane and preventing them from being able to swallow. This meant that when approximately $1x10^9$ colony forming units

(CFU) of bacteria in 50µl of PBS was pipetted into the oropharynx, the lungs were inoculated through reflexive aspiration. This method successfully induced pneumonia in mice[54]. Another study used a different clinical strain to develop a pneumonia model in mice. In this study mice were inoculated with $5x10^6$ – $1.5x10^7$ CFU/mouse by non-invasive intratracheal inoculation. Mice were then monitored for 7 days[55]. A lethal pneumonia model using particularly virulent clinical strains of *A. baumannii* were developed. Mice were inoculated by non-invasive intratracheal instillation of $1x10^8$ CFU/mouse and monitored over 7 days[50]. There are countless models available to use and develop, but the most important factor to consider is what the desired outcome of the study is and what model best fits the work being performed, while also considering the welfare and necessity of the animals and considering the 3Rs: replacement, reduction and refinement.

1.2 – *Acinetobacter*

The focus of this project is on *Acinetobacter* a Gram-negative coccobacillus[56]. *Acinetobacter* spp. are non-fastidious, strictly aerobic, non-motile, catalase-positive, indole-negative, oxidase-negative, non-lactose fermenting, citrate positive, non-glucose fermenting and encapsulated[57]. After significant taxonomic changes since its discovery in 1911, technological advances and better understanding of molecular methods and genetic makeup led to a wide acceptance of the current taxonomical classification; Domain: Bacteria, Phylum: Proteobacteria, Class: Gamma *Proteobacteria*, Order: Pseudomonadales, Family: Moraxellaceae, Genus: *Acinetobacter*. Only three species, *A. baumannii*, *A. haemolyticus* and *A. calcoaceticus*, are clinically relevant[57].

Acinetobacter are typically free-living saprophytes that can be found almost everywhere. Different species live in various habitats, which include soil, water, sewage, food, animals and humans. *Acinetobacter* spp. are considered to be a part of the skin, nasopharynx, mucous membrane and respiratory secretion normal flora. Typically, in hospitalised patients *Acinetobacter* spp. colonise the skin, oropharynx and digestive tract. *Acinetobacter* spp. are not only responsible for causing pneumonia, but also blood stream and wound/soft tissue infections[56,57].

Acinetobacter spp. are particularly good at surviving in arid environments for long periods of time, facilitating persistence and transmission. Translating this into a clinical setting is what

gives *A. baumannii* its uncanny ability to survive on and colonise reusable medical equipment. This includes ventilator tubing, arterial pressure monitoring devices, humidifiers, washbasins, plastic urinals and respirometers. It has also been possible to isolate *A. baumannii* from hospital personnel, mattresses and pillows as well as all ventilator equipment. Some *A. baumannii* strains are so well adapted to such conditions that they can persist on dry surfaces while remaining viable for over 4 months. This survivability allows *A. baumannii* to persist in hospitals, resulting in reservoirs of infection and prolonged hospital outbreaks[57].

1.2.1 – *Acinetobacter baumannii*

A. baumannii is recognised globally as a major health threat in hospitals. It is considered an opportunistic pathogen that primarily infects critically ill patients[58]. *A. baumannii* is able to cause problematic infections as a result of its ability to survive in conditions normally inhospitable to other more pathogenic bacteria that are in possession of typical virulence factors such as, toxins, pathogenicity islands, flagella and type 3 secretion systems[58–61]. The biggest problem with *A. baumannii* is its high genomic plasticity. This allows *A. baumannii* to easily and quickly acquire new antibiotic resistance and has resulted in the development of extensive and even pan-drug resistance at rates never seen before[58]. Infection rates of *A. baumannii* are lower than other Gram-negative bacteria, accounting for ~2% of all nosocomial infection in the United States and Europe and ~4% in Asia and the Middle East. However, approximately 45% of isolates are considered to be MDR globally[56,58]. In Latin America and the Middle East MDR rates can reach 70%[58] and over 90% in Asia[62]. The CDC recognised MDR *Acinetobacter* spp. as a serious threat and the World Health Organisation has placed carbapenem resistant *A. baumannii* in the critical group of bacteria that pose the biggest risk to human health[58,63]. It is *A. baumannii*'s high levels of drug resistance and mechanisms of resisting disinfection, oxidative stress and desiccation that allow for its survival within otherwise unfavourable conditions and ability to cause difficult to treat infections[58].

A. baumannii is the second most common causative agent of ventilator associated pneumonia with carbapenem resistant strains being associated with lengthy hospital stays and high mortality rates of up to 50%[64]. Treatments of such infections are a significant financial burden on the respective health service[64,65]. Without improvement, the future of

antimicrobial resistance looks bleak across the globe, with increased severity of antimicrobial resistant infection causing around 10 million deaths and significant cost increases from between $300 billion to over $1 trillion annually by 2050[65].

Carbapenem resistant *A. baumannii* is found across the globe (Fig. 1.2), with some of the highest rates of carbapenem resistance in the Mediterranean having been reported at over 90%[66]. Within the *Acinetobacter* genus, *A. baumannii* appears to be most clinically significant species[67]. It is primarily a healthcare associated pathogen and it is reported responsible for outbreaks of septicaemia, bacteraemia, VAP, wound sepsis, endocarditis, meningitis and urinary tract infections. Outbreaks most commonly occur in ICUs and burn units, often involving mechanical ventilation[57].

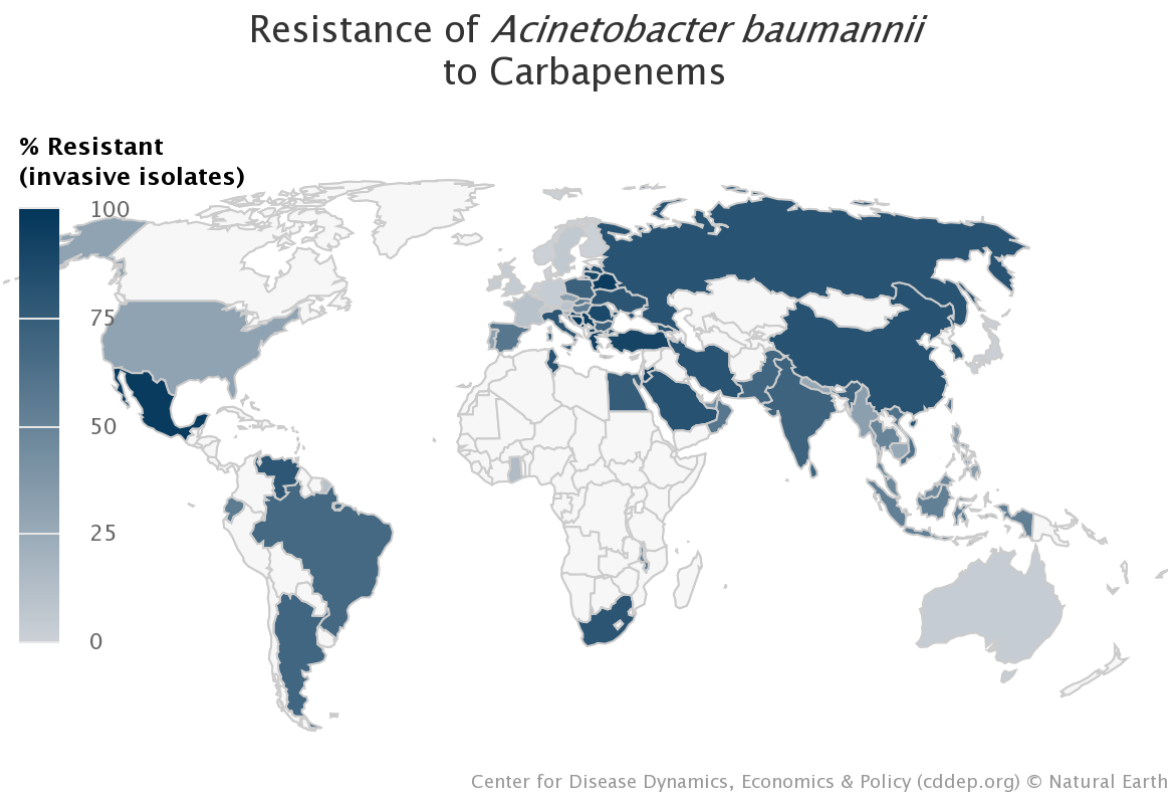


Figure 1.2 | Map to show global prevalence of carbapenem resistant *Acinetobacter baumannii*. Map to show the rates of *A. baumannii* carbapenem resistance across the globe, the darker the colour the higher the rate of carbapenem resistance. Map was produced by OneHealthTrust. ResistanceMap: Antibiotic resistance. 2022. https://resistancemap.onehealthtrust.org/AntibioticResistance.php . Date accessed: November 25, 2022.

1.2.2 – A. baumannii Pathogenesis and Infection

Phenotypic and genomic analysis has identified virulence factors possessed by *A. baumannii*[68]. Antibiotic resistance among *A. baumannii* isolates is rapidly spreading, posing a major threat to the health care systems across the globe[68,69]. The highly plastic genome of *A. baumannii* allows for horizontal gene transfer of genetic material that will aid survival under antibiotic and host selective pressure. Additionally, *A. baumannii* can produce biofilms and grow on both abiotic and biotic surfaces as well as adhering to, colonising and invading host cells[70]. All of these factors (Fig. 1.3) contribute towards *A. baumannii*'s high levels of persistence, survivability and transmission[69].

The outer membrane proteins (OMPs) of *A. baumannii* are incredibly important in allowing for its survival under antibiotic and host-induced stresses with each protein playing a distinct role[71]. The outer membrane of *A. baumannii* is host to a large range of OMPs that allow for the diffusion of small molecules across the outer membrane. These include OmpA, responsible for reducing β-lactam antibiotic diffusion across the outer membrane and mediating adherence to host cells[71]. CarO and OprD are two other outer membrane proteins that can be present in the outer membrane of *A. baumannii* that are related to antibiotic resistance, meditating the influx of β-lactam antibiotics[71]. There are many other OMPs found in the outer membrane of *A. baumannii* to help the bacteria respond to a number of environmental stressors reducing membrane permeability and to aid survival under osmotic, oxidative and antibiotic stressors as well as iron-limiting conditions[71].

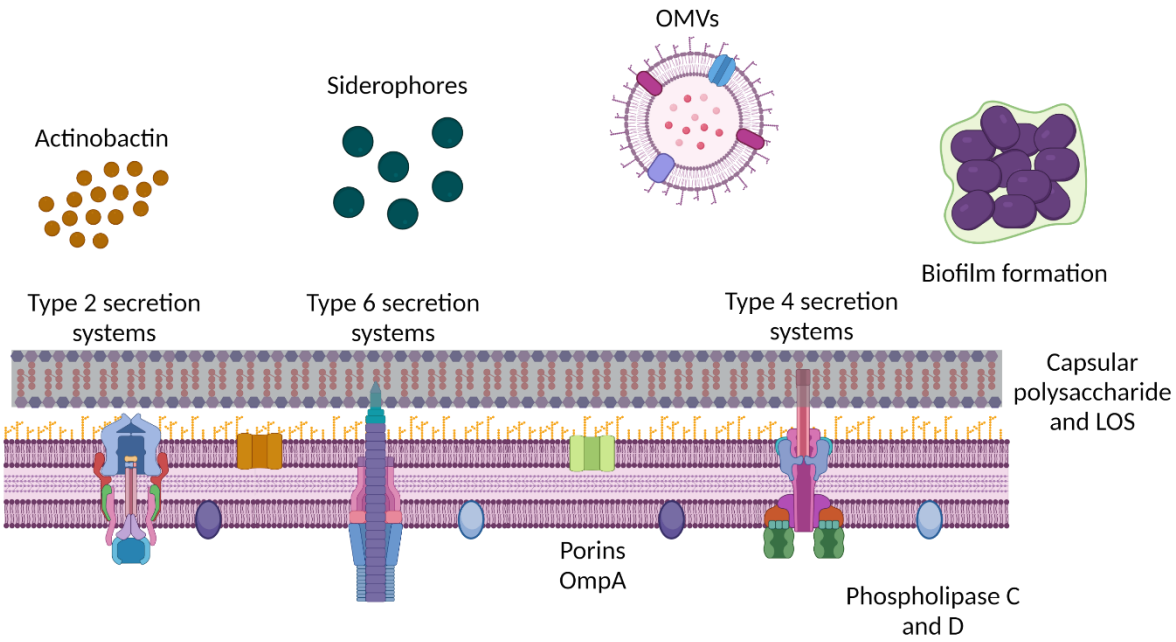


Figure 1.3 | Summary of *A. baumannii* virulence factors. Diagram of the bacterial membrane showing some of the virulence factors possessed by *A. baumannii* including OMVs, iron acquisition systems (actinobactin), capsule, lipooligosaccharide and porins. *A. baumannii* also make use of type 2, 4 and 6 secretion systems. The type 2 secretion systems are responsible for secreting effector proteins such as lipases and proteases; type 6 secretion systems for injecting effector proteins such as hemolysin co-regulated protein and valine glycine repeat protein into competing bacterial and host cells inducing cell death and could also be involved in horizontal gene transfer and type 4 secretion systems mediate the transfer of proteins and nucleoproteins between different bacterial cells through bacterial conjugation. Image made using BioRender.

1.2.2.1 – Porins

Porins are a type of outer membrane protein that are responsible for the regulation of cell permeability, OmpA is a highly abundant β-barrel porin. In *A. baumannii* OmpA is very well characterised and has a number of important roles in increasing the virulence of the organism. In *A. baumannii ompA* mutants, the ability to induce apoptosis of human epithelial cells is impaired[68]. It has been shown that OmpA helps to mediate bacterial binding and invasion of epithelial cells by interacting with fibronectin[68]. Secreted OmpA targets the host cell's mitochondria, inducing the release of proapoptotic molecules and subsequent apoptosis[68,71]. Another study showed that OmpA is able to translocate to the nucleus where it then induces cell death[68,70]. *A. baumannii* is also thought to avoid complement-mediated killing through OmpA's binding to factor H in human serum.

Functional OmpA has been shown to be important in the establishment of persistent colonisation of *A. baumannii* in murine lungs[68].

1.2.2.2 – Capsular Polysaccharides and Lipopolysaccharides (LPS)

Many clinically isolated *A. baumannii* strains express capsular polysaccharides and also possess a conserved gene cluster, the K locus, which includes genes involved in capsule export, the synthesis of activated sugar precursors, glycosyltransfer, glycan modification and oligosaccharide repeat-unit processing[68,72]. However, there are large amounts of variability within the *A. baumannii* capsule with over 100 distinct capsule types identified[73]. The capsular polysaccharides play important roles in virulence which is dependent upon the correct function of polymer assembly, export and subunit biosynthesis. *A. baumannii* that are mutated in any of these functions have been found to be deficient in their ability to grow in soft tissue infection sites, they're less lethal in murine septicaemia models, less able to defend themselves against serum killing and have impaired biofilm production capabilities[74].

LPS is a major part of the outer membrane of the majority of Gram-negative bacteria. LPS is immunogenic and induces the release of inflammatory cytokines like tumour necrosis factor and interleukin 8 from macrophages[68]. LPS consists of an endotoxic lipid A, an oligosaccharide core and a repetitive O-antigen. However, *A. baumannii* does not possess O-antigen so its LPS is instead termed lipooligosaccharide (LOS)[58]. LOS plays an important role in the survival of *A. baumannii* by helping to protect the bacteria from serum, opsonophagocytic killing and inflammatory responses. LpxC is an enzyme involved in the biosynthesis of lipid A. When LpxC is inhibited, clearance of *A. baumannii* is enhanced and protects the mice from what was previously a lethal dose[58,68].

1.2.2.3 – Phospholipase

Phospholipase is a lipolytic enzyme that is critical in the metabolism of phospholipids. Three classes of phospholipases have been defined. Phospholipase A (PLA) hydrolyses fatty acids from the glycerol backbone. Phospholipase C (PLC) cleaves the phosphorylated head from the phospholipid. Phospholipase D (PLD) cleaves off the head group. Phospholipid degradation reduces the stability of host cell membranes and interferes with cellular signalling and therefore alters the host immune response in various ways. *A. baumannii* has been shown to produce PLC and PLD. *A. baumannii* (ATCC 17978) possess two PLCs, which

improve the cytotoxic ability of *A. baumannii* (ATCC 17978). In *A. baumannii* (98-37-09) PLD enhances resistance to human serum and increases ability to invade epithelial cells in a murine pneumonia model. Another study showed that *A. baumannii* (ATCC 19606) possesses three PLD genes, all of which have important roles in epithelial cell invasion and virulence[68].

1.2.2.4 – Outer Membrane Vesicles (OMVs) as Virulence Factors

Many Gram-negative bacteria produce OMVs, which are spherical nanovesicles that are made of LPS, OMPs, periplasmic proteins, cytoplasmic proteins, lipids and DNA or RNA[68,75,76]. Two different proteomic analyses of *A. baumannii* OMVs have shown there to be well over 100 different proteins associated with the OMVs[77,78]. Additionally, capsular polysaccharide antibody responses were induced upon *Burkholderia pseudomallei* OMV vaccination[79], suggesting the presence of capsular polysaccharide antigens in OMVs of encapsulated bacteria. OMVs on average range between 20 and 250 nm and are typically used as delivery mechanisms between bacterial cells and from bacterial cells to host cells[68,75,76]. OMVs allow for the interaction of bacteria and host cells without the need for bacterial cells to be proximal to the host cells. Many OMVs are secreted from bacterial cells containing virulence factors such as OmpA, protease, phospholipase superoxide dismutase and catalase. *A. baumannii* OMVs deliver these virulence factors via lipid rafts, all ultimately resulting in cytotoxicity[68,76].

1.2.2.5 – Metal Acquisition System

Ferric iron does not solubilise easily under aerobic and pH neutral conditions making it relatively unavailable to bacteria. To overcome this many aerobic bacteria produce siderophores, which are high-affinity iron-chelating compounds. *A. baumannii* produces both siderophores and acinetobactin. Acinetobactin helps *A. baumannii* to persist within epithelial and alveolar cells and reduces the ability to cause cell damage. Acinetobactin production has been shown to occur more frequently in multidrug resistant *A. baumannii*[68]. *A. baumannii* are also able to overcome zinc and manganese limitation due to the possession of a zinc acquisition system and a manganese transporter, as well as a urea carboxylase[68].

1.2.2.6 – Protein Secretion Systems

Multiple protein secretion systems have been described in *A. baumannii*. *A. baumannii* has been shown to possess a type II secretion system (T2SS). T2SSs are multi-protein complexes that are similar in structure to type IV pili. T2SSs are responsible for the translocation of proteins from the periplasmic space to the outer membrane or extracellular milieu[68]. *A. baumannii* has also been shown to have a type VI secretion system (T6SS). T6SSs are often used by bacteria to inject effector proteins into host cells or competing bacteria in order to help colonisation by *A. baumannii*. T6SSs have also been shown to be involved in horizontal gene transfer in *Vibrio cholera* and is therefore likely involved in the transfer of antibiotic resistance plasmids[68]. The importance of T6SSs in *A. baumannii* and their function appears to be strain specific. It has been shown that multidrug resistant *A. baumannii* strains have large, self-transmissible plasmids that carry negative regulators for T6SSs. The expression of T6SS and ability to kill competing bacteria using T6SSs was also shown to make *A. baumannii* more susceptible to antibiotics. Such results suggest a molecular switch is at play, enabling the bacteria to choose between T6SS and antibiotic resistance[68,80]. The type V system autotransporter Ata has also been described in *A. baumannii.* This trimeric membrane protein is responsible for the mediation of biofilm formation, adherence and virulence[68]. Finally, *A. baumannii* have also been shown to possess the type IV secretion system (T4SS)[58], which are responsible for twitching motility, adhesion, biofilm formation, colonisation and transformation[81].

1.2.2.7 – Biofilm formation

A. baumannii is able to produce biofilms that protect themselves from the surrounding environment by increasing tolerances to extracellular stresses. Biofilms are populations of bacteria that are encased within an extracellular matrix of their own making. *A. baumannii* produces biofilms in wounds, on wound dressings and on abiotic surfaces. When it comes to producing and maintaining biofilms pili, adhesins and surface structures, such as capsular polysaccharides, are critical[58].

1.2.2.8 – Mechanism of Infection

Determining whether *A. baumannii* is colonising or infecting patients has proven to be challenging. Currently biomarkers, such as procalcitonin levels, are frequently used to determine the presence of an infection, but no study has been performed to confirm the

accuracy of this method[82]. One commonality between *A. baumannii* infections is the requirement for a break in a protective barrier enabling *A. baumannii* to reach the site of infection[58].

1.2.3 – Mechanisms of *A. baumannii* Antimicrobial Resistance

Multidrug resistant (MDR) strains of *A. baumannii* are defined as being resistant to at least 3 classes of antibiotics. An MDR strain that is also resistant to carbapenems is termed extensively drug resistant (XDR), while strains that are XDR and also resistant to polymyxins and tigecycline are termed pan-drug resistant (PDR)[57]. Some mechanisms by which these strains mediate resistance include through enzyme-mediated degradation of the antimicrobial drug, genetic alteration and efflux pumps[83]. Increasing drug resistance among *A. baumannii* has severely limited treatment options for infection, requiring urgent development for new antimicrobials and preventatives against *A. baumannii*.

The mechanisms by which beta-lactam antibiotic resistance is mediated is through the production of β-lactamase enzymes, alteration of outer membrane porins and expression of efflux pumps[83].

β-lactamases break down the β-lactam ring through hydrolysis, deactivating the molecules ability to kill bacteria[84]. The possession of beta-lactamase plasmids OXA23, OXA24 and OXA58 are the most frequently found carbapenemase encoding antibiotic resistance plasmids responsible for carbapenem resistance in *A. baumannii*[83]. Reduced outer membrane protein (OMP) and porin expression results in reduced entry of antimicrobial drugs into the cells. *A. baumannii* are also able to reduce antimicrobial entry by modifying penicillin binding proteins. Finally, efflux pumps are able to confer resistance to multiple classes of antibiotics by pumping antibiotics back out of the cell that have managed to get in. There are 6 families of efflux pumps. A member of the ATP-binding cassette (ABC) family, the AdeABC efflux pump, has been well characterised in *A. baumannii*. AdeABC mediates resistance to cefotaxime, chloramphenicol, erythromycin, aminoglycosides and fluoroquinolones. However, if overexpressed, AdeABC also confers resistance against carbapenems[83].

There are fewer mechanisms by which aminoglycoside resistance occurs than that of β-lactam antibiotic resistance. *A. baumannii* is able modify the amino and hydroxyl groups

of aminoglycosides with the use of aminoglycoside modifying enzymes. Adenylases, acetylases, phosphotransferases and methyltransferases are all aminoglycoside modifying enzymes and all have been identified in *Acinetobacter*. *A. baumannii* are also able to modify the aminoglycoside targeted ribosomal proteins and as already mentioned, *A. baumannii* are able to express efflux pumps that are effective against aminoglycosides[83].

The primary mechanism by which *A. baumannii* is resistant to quinolones is through mutations in the *gyrA* and *parC* genes. These mutations cause phenotypic changes to DNA gyrase and topoisomerase IV, which results in reduced drug affinity. Drug influx and efflux systems that are encoded for in chromosomal DNA mediate the regulation of expression of OMPs and efflux pumps. Reduced expression of OMPs and increased expression of efflux pumps results in active drug expulsion, which is also responsible for quinolone resistance in *A. baumannii*[83].

Colistin is a polymyxin, which works by disrupting the bacterial cell membrane. Positively charged cationic regions of the drug bind to negatively charged hydrophilic lipid tails of lipopolysaccharide. This reduces the integrity of the cell wall resulting in cell death[83]. There are two major mechanisms responsible for colistin resistance. Mutations in genes encoding lipid A result in the complete loss of lipid A, the target of colistin. The other mechanism of resistance involves mutations in the pmrAB system. The pmrAB system is responsible for monitoring the environmental conditions and regulating the expression of lipid A synthesis genes. Mutations in *pmrA* and *pmrB* upregulate their expression, which causes a remodelling of the outer membrane, reducing the ability for colistin to bind[83]. These mutations are the most commonly observed mechanism by which *A. baumannii* become resistant to colistin[58]. With colistin being a last resort option for treating multidrug resistant *A. baumannii* infection the potential for widespread colistin resistance is worrying.

1.3 – Host Response to *A. baumannii* Infection

Although understanding the mechanisms and types of antibiotic resistance found in *A. baumannii* is critical for the treatment and control of outbreaks; it is also important to understand the host response to *A. baumannii* infection (Fig. 1.4) and how the immune system works to rid the body of such infections. Characterisation of the molecular and

cellular responses to an infection provides valuable information that should guide the development of future therapies, treatments and preventions against *A. baumannii* infection[85].

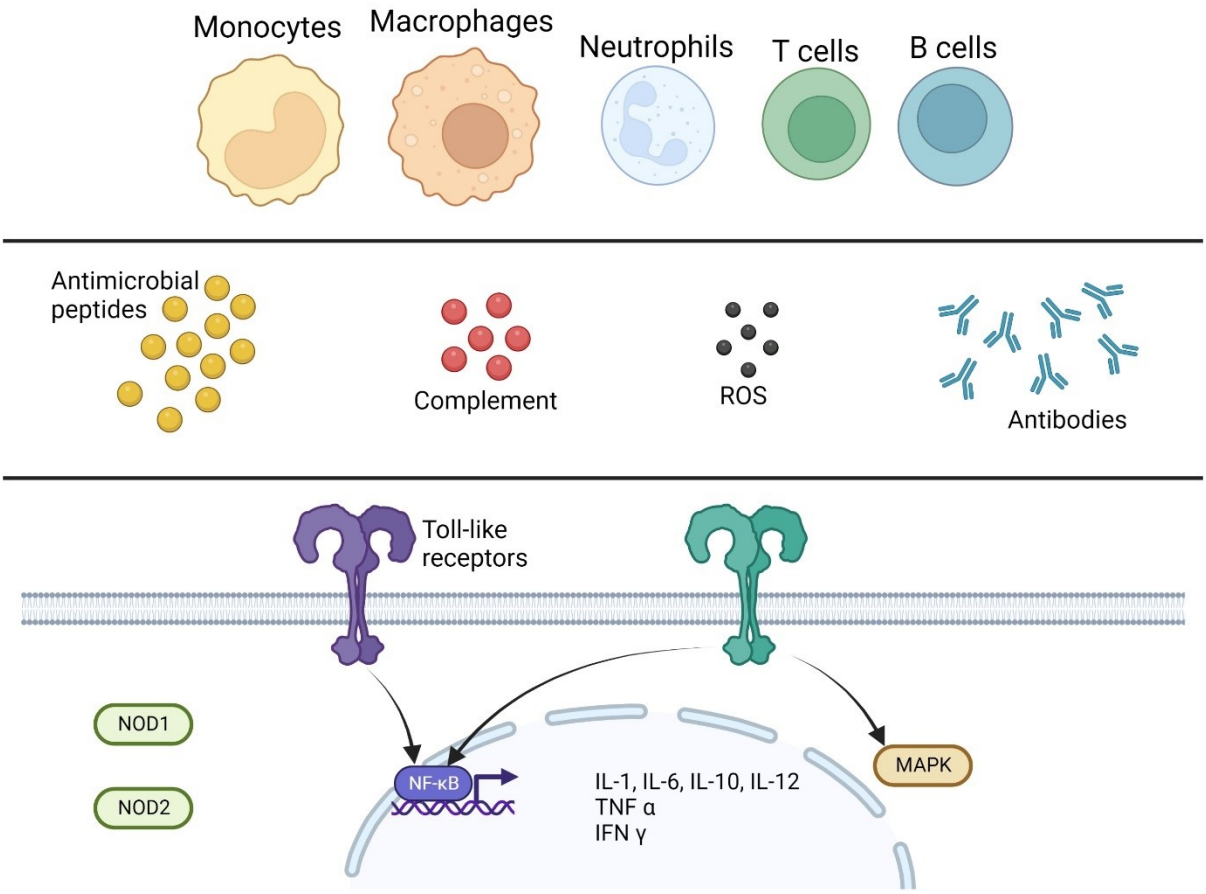


Figure 1.4 | Summary of *A. baumannii* host immune response. Diagram to show the host immune response to *A. baumannii* infection. Some of the immune cells involved in both innate and adaptive immunity include monocytes, macrophages, neutrophils, T cells and B cells. Components of the immune system that directly affect the bacterial cell include antimicrobial peptides, complement, ROS and antibodies. Finally, through bacterial ligand binding to toll-like receptors signalling cascades are activated resulting in the production of cytokines. Image made using BioRender.

1.3.1 – Innate Immune Response

Upon the detection of *A. baumannii*, the epithelial cell's first line of defence is to secrete antimicrobial peptides that inhibit the growth of the bacteria. At the same time, phagocytic cells are recruited to the site of infection through cytokine and chemokine signalling. Neutrophils are the first cells to arrive and are very important in controlling *A. baumannii* infection. Neutrophilic clearance of *A. baumannii* relies heavily on the production of reactive

oxygen species using the NADPH oxidase system. Macrophages and dendritic cells play minor roles in the clearance of *A. baumannii* but it is likely they have important sensing, signalling and regulatory roles[58]

1.3.1.1 – Pattern Recognition Receptors

A. baumannii interacts with mucosal epithelial cells of the respiratory tract and endothelial cells in the blood vessels. Adhesins such as *Acinetobacter* trimeric autotransporter, type IV pili and biofilm associated proteins are responsible for mediating such interactions by bringing the bacterial cells into close proximity of the host cells. Activation of immune cells is largely reliant upon the recognition of pathogen-associated molecular patterns by the host cell's pattern recognition receptors (PRRs)[85]. The host cell's PRRs are able to recognise pathogen-associated molecular patterns, initiating signalling cascades that ultimately result in the production and secretion of inflammatory mediators[86]. Research so far has found two types of PRRs to be responsible for the recognition of *A. baumannii*, toll-like receptors and NOD receptors[85]. *A. baumannii* pathogen-associated molecular patterns are known to activate the NF-κB and MAPK pathways. Activation of these pathways results in the release of many chemokines, which include macrophage inflammatory protein 2, monocyte chemoattractant protein and keratinocyte-derived chemokine, as well as a number of pro-inflammatory cytokines such as TNF-α, IL-1β and IL-6[86]. Some of the cell types that are involved in the recognition of *A. baumannii* PAMPs include dendritic cells, macrophages, monocytes, neutrophils and epithelial cells[85].

A. baumannii is generally considered to remain extracellular however, it does have the ability to invade host cells using a microtubule and microfilament dependent zipper-like mechanism. *A. baumannii* cells that have successfully invaded host cells are able to persist within membrane-bound vacuoles in the cytoplasm of host cells. This is where intracellular PRRs such as the endolysosomal toll-like receptor 9 (TLR9) become important. TLR9 detects bacterial DNA and subsequently initiates a signalling cascade. Nucleotide-binding oligomerisation domain containing protein 1 (NOD1) and NOD2 are cytosolic PRRs. NOD1 and NOD2 work with a downstream signalling partner in order to limit the proliferation of *A. baumannii* within epithelial cells. This suggests *A. baumannii* is able to escape the membrane-bound vacuoles[58].

1.3.1.2 – Neutrophils

Neutrophils are essential players in the host immune response against *A. baumannii*; making up the largest population of immune cells recruited to the site of infection with neutrophils critical for controlling infection[86]. There is therefore a high prevalence of *A. baumannii* infection in people who have neutropaenia[85]. During lung infection with *A. baumannii* the innate immune response is stimulated to produce chemokines, which in turn recruit immune cells to the site of infection[86]. Neutrophils are rapidly recruited to the lungs, sometimes as soon as 4 hours after infection. Neutrophil recruitment peaks around 24 hours after infection and increased disease severity and lethality is seen in neutrophil depleted mice. Neutropoenia causes delayed production of the majority of the early chemokines and proinflammatory cytokines mentioned above[87]. Similar results are also seen in other studies[88,89] and hold true in *A. baumannii* infection models representing bacteraemia[90], septicaemia[91] and soft tissue infection[92]. In response to infection, lymphocytes and granulocytes produce defensins, cathelicidins, reactive oxygen species and reactive nitrogen species, as well as other antimicrobial factors, to help kill bacteria[86].

A. baumannii have been shown to possess the ability to adhere to neutrophils. This process is independent of phagocytosis and is likely to involve Outer membrane protein A (OmpA) and pili. *A. baumannii* is thought to avoid neutrophil killing by adhering to the neutrophils and activating them. *A. baumannii* stimulates the production of IL-8, increasing levels compared to without *A. baumannii*. The increased levels of IL-8 then enhance the migration of both neutrophils and adherent *A. baumannii*[93].

1.3.1.3 – Monocytes and Macrophages

Monocytes and macrophages are also found among the first immune cells to be recruited to an infection site. In particular, tissue resident macrophages, such as alveolar macrophages, will be present at the site of infection prior to the arrival of neutrophils. This provides an advantage to the host during lung infection with macrophages phagocytosing *A. baumannii,* limiting their growth and the infection while the neutrophils are still being recruited. Macrophages have been seen to phagocytose *A. baumannii in vivo* 4 hours after infection, while the neutrophils are still being recruited. Macrophages produce high levels of IL-6, TNF-α and MIP-2 during *A. baumannii* infection and post-infection. Post-infection macrophages also produce high levels of IL-10 and IL-1β. Despite macrophages taking longer to kill

bacteria than neutrophils, the initial population of macrophages are able to kill 80% of all phagocytosed bacteria in 24 hours. However, macrophage depletion models have shown in both pneumonia and bacteraemia models that although there is an increased bacterial burden, the loss of macrophages does not increase lethality[85].

1.3.2 – Adaptive Immune Response

Upon intramuscular vaccination with a protein antigen, dendritic cells are activated through PRRs and trafficked to the draining lymph node. Within the lymph node, protein antigen peptides are presented by MHC II and MHC I molecules on the dendritic cells to $CD4^+$ and $CD8^+$ T cells. Along with signalling through B cell receptors, initiated by soluble vaccine antigen, the T cells mediate B cell proliferation and development. This results in T cell dependent maturation of the antibody response through affinity maturation and immunoglobulin class switching. Short-lived plasma cells are produced to rapidly secrete vaccine antigen specific antibodies into serum for approximately 2 weeks after vaccination. Additionally, memory B cells are also produced to provide long term immune memory against the vaccine antigen and reside within the bone marrow. $CD8^+$ memory T cells are also produced and proliferate rapidly upon activation with $CD8^+$ T cells being key for eliminating infected host cells[94].

1.3.2.1 *A. baumannii* Humoral Immunity

The adaptive immune response to *A. baumannii* has been studied extensively with regards to humoral immunity. Antibody-mediated protection against *A. baumannii* infection works via a number of different mechanisms including antibody-mediated complement activation, antibody opsonisation and neutralisation[95]. In an effort to design effective vaccines, many antigens have been proposed. It has been suggested in the case of an OmpA vaccine, that antibodies are protecting against infection via bacterial opsonisation and protection against infection is independent of complement activation[85,95]. Interestingly, immunisation with a recombinant OmpA vaccine did not enhance complement mediated killing of complement resistant strains as the vaccine failed to neutralise the ability of OmpA to inhibit complement. Suggesting these strains are resistant to direct bactericidal killing through the alternative complement pathway, even when mediated via antibody[95]. However, it has also been suggested that antibodies and C3 work synergistically to improve both opsonisation and phagocytosis of *A. baumannii* through the classical complement pathway[95]. The

importance of the humoral response against *A. baumannii* is further supported by a study performed in B cell knockout mice, with no protection seen in vaccinated mice in a murine pneumonia model[95]. It is highly likely that a strong antibody response that enhances opsonophagocytosis is an essential mechanism of protection against *A. baumannii* infection. However, *A. baumannii* specific antibody neutralisation capabilities have been understudied and could be a possible therapeutic strategy. Antisera to *Acinetobacter* trimeric autotransporter (Ata), a surface protein adhesin[96], inhibited Ata binding to collagen type IV[97]. Iron regulated outer membrane protein targeting antibodies have also been shown to bactericidal under low iron conditions, blocking siderophore mediated uptake of iron[98], suggesting the potential of antibodies targeting virulence factors and their bactericidal properties.

1.3.2.2 *A. baumannii* cellular immunity

Comparatively, the cellular response of the adaptive immune system to *A.* baumannii remains relatively unknown[85,95]. Many studies rely upon IgG isotype ratios to determine whether protection was driven by Th1 or Th2 responses. Whole-cell inactivated, live attenuated and OMV *A. baumannii* vaccinations all resulted in high levels of IgG1 and IgG2a, indicating both Th1 and Th2 responses are involved[95]. Immunisation with an *A. baumannii* live attenuated vaccine showed an increased Th1 response and significantly increased Th2 and Th17 responses in mice[99]. However, there are high levels of variance between strains and even vaccine doses eliciting different Th response profiles[85,95]. The optimal cell mediated immune response for *A. baumannii* is unknown and understudied[95], requiring further investigation to build a full picture of what an effective response involves.

1.4 – Vaccines and monoclonal antibodies for Antimicrobial Resistant Bacterial Infections

In 2019 it was estimated that 4.95 million people globally died from illness in which antimicrobial resistance (AMR) played a part, with 1.27 million of those deaths being directly attributable to AMR. By comparison, HIV/AIDS was the cause of 864,000 deaths and malaria was the cause of 643,000 deaths[100]. Without action, based on the increasing drug resistance of bacterial pathogens it has been predicted that by 2050 the number of deaths

will be almost 10x higher than it was in 2019 with an estimated 10,000,000 deaths each year as a result of AMR infections[100,101].

Antibodies and vaccines both have great potential for use in the treatment and/or prevention of AMR infections[102,103]. Vaccines are able to stop infection before it takes hold, preventing a person getting sick in the first place. However sometimes infections are a rare occurrence in a person's life, making whole population vaccines a less efficient way of managing infection[103]. Despite high costs of production and a potential poor shelf life, antibodies are highly specific towards bacterial strains and do not cause damage to the normal flora. Antibodies can either be used directly by targeting the bacterial cells themselves, or indirectly by targeting the toxins and virulence factors produced by the bacteria[102].

1.4.1 – Vaccines

Between 1915 and 1945 communicable diseases were the leading cause of death[104]. Now with vaccines, improved hygiene and other medical advancements the top 3 leading causes of death globally in 2019 were all noncommunicable[9]. In modern day vaccine development there are many approaches that can be taken with many different vaccine types such as whole virus/cell, protein based, viral vector, nucleic acid and nanoparticle based vaccines[105]. Additionally, with the advancement of sequencing technologies it is now possible to use reverse vaccinology based approaches using whole genomic or proteomic data to rationally design novel vaccines, such as the case of the meningococcus B vaccine[106,107].

Antibiotic resistance develops quickly and can be easily spread across the globe and between different bacterial pathogens[108]. While levels of antibiotic resistance are increasing, the development of new classes of antibiotics struggle to keep up due to the difficulty of producing a drug with a good balance of antibacterial activity, pharmacokinetic properties, drug metabolism and safety profile[103]. Researchers can try to improve existing antibiotic treatment efficacy through potentiation, such as efflux pump inhibition, or through active uptake approaches using membrane transporters[103]. Unfortunately, the emergence of new antibiotic resistances often occurs soon after implementation of a new antibiotic (Fig. 1.5)[107,108]. Vaccines provide a viable alternative to combat antimicrobial resistance. Vaccines work in several ways to help prevent antimicrobial resistance. Vaccines

can directly prevent infections caused by antimicrobial resistant bacteria but also indirectly by reducing antibiotic prescription and usage by reducing symptomatic disease[103,107,108]. Vaccination also prevents the start of a bacterial infection, therefore preventing replication to a point where numbers are high enough for new resistances to develop, whereas antibiotics are used on established infections when numbers are already high enough to develop new antibiotic resistances[103,107–109]. While development of new antibiotics could be short lived, the development of antimicrobial vaccines provides a more stable outlook in the control of antimicrobial resistant bacteria[107].

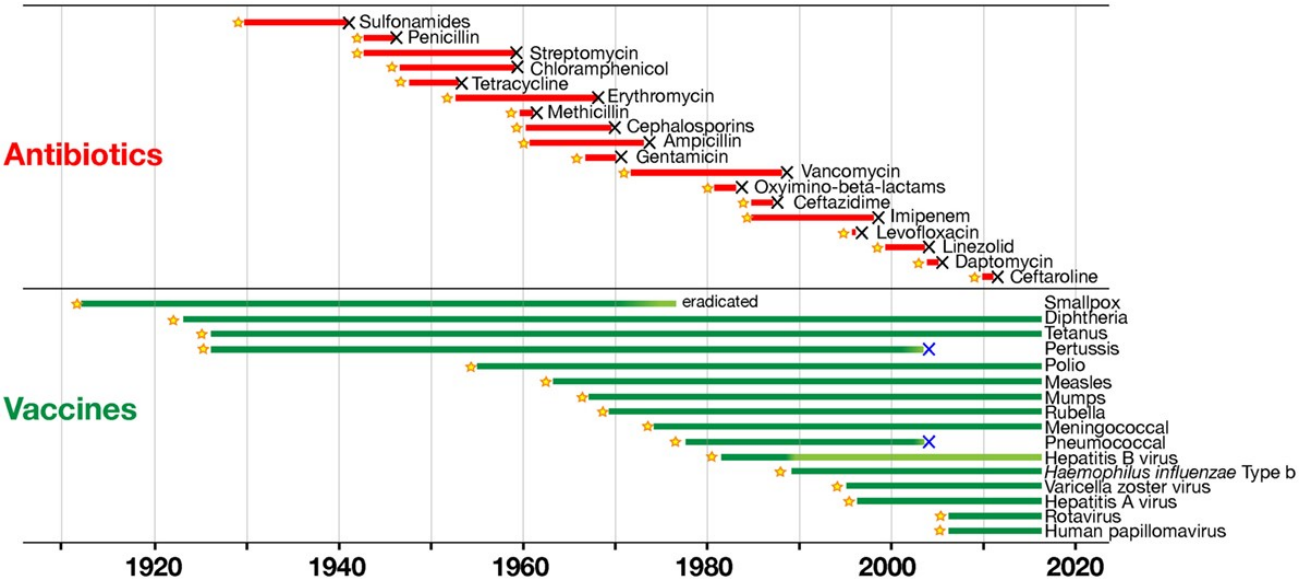


Figure 1.5 | Time taken for detection of resistance of bacteria to antibiotics and vaccines. A timeline to show the time taken for the detection of new resistances of bacteria to antibiotics (red) and vaccines (green). Black crosses represent detection of antibiotic resistance and blue crosses represent detection of resistance to vaccine. Yellow stars show product introduction; apart from Smallpox vaccination, which began much earlier. Figure copied from Tagliabue, A & Rappuoli, R. 2018. Changing Priorities in Vaccinology: Antibiotic Resistance Moving to the Top. *Front Immunol*. 9(1068). https://doi.org/10.3389/fimmu.2018.01068.

The *Haemophilus influenzae* type b Hib polysaccharide capsule conjugate vaccine showed high efficacy in preventing disease in immunised infants and also older children through herd immunity[108]. However, not only was it highly effective at preventing disease, it also significantly reduced antibiotic usage and the development of antibiotic resistance. Prior to introducing the vaccine, *H. influenzae* type b infections were affecting 3.5 to 601 per 100,000 children under 5 years of age in many countries throughout the world, with β-lactam resistance being detected from the early 1970s. However, between 1999 and 2000 it

was found that only 16.6% of *H. influenzae* type b strains possessed β-lactamase[108]. The introduction of the Hib vaccine significantly reduced disease rates among children across the globe, cases in Canada dropped from 2.6 cases per 100,000 to 0.08 cases per 100,000 and resulted in near elimination of the disease in children under 5 in the UK a few years after introduction of the vaccine from 21 to 44 cases per 100,000[108,110]. A reduction in circulating β-lactamase positive strains of *H. influenzae* type b was also observed[108].

Additionally, the *Streptococcus pneumoniae* vaccines have reduced both pneumonia cases and also the number of infections that are resistant to frontline antibiotic treatment. However, the fight against antimicrobial resistance with vaccines doesn't stop at bacterial vaccines. Effective use of influenza vaccines reduces the amount of antibiotics incorrectly prescribed to or taken by people experiencing flu symptoms[107].

1.4.1.1 – Outer membrane vesicles as vaccines

One example of a potential vaccine modality for development is outer membrane vesicles (OMVs). An OMV based vaccine has been used effectively to help control a meningococcus B outbreak in New Zealand between 2004 and 2008; protection was complement-mediated via vaccine induced antibodies. The New Zealand OMV was then used as a component of the 4CMenB vaccine, highlighting the potential of OMVs in vaccine development[103]. It is also relatively easy to engineer OMVs through bacterial genetic manipulation. By targeting genes responsible for membrane stabilisation, such as *tolR*, it is possible to increase OMV release. These OMVs will have the natural surface proteins of the bacteria on their surface, in their native conformation[103,111,112]. LC-MS was performed on the OMV proteins of Bexsero, showing around 100 proteins quantified from each preparation of OMV with approximately 90% of the proteins being consistent across lots, including OpcA, NspA and PorB[113,114]. This increases the protective potential of the OMVs[103,111,112]. There are high amounts of lipopolysaccharides (LPS) present as well and therefore the potential for high levels of LPS reactogenicity. However, this can also be modified by targeting genes responsible for LPS acylation[103]. It is also possible to display proteins and glycans on the surface of OMVs or even load them with therapeutic molecules, further increasing their potential usage[111].

Generalised modules for membrane antigens GMMA are engineered OMVs produced by introducing mutations into bacteria to destabilise the outer membrane and induce the release of GMMA particles, for example *gna33* in meningococcus and *tolR* in *Shigella sonnei*

and *Salmonella*[115–117]. Additional mutations can also be introduced to reduce toxicity and fine tune reactogenicity as well as to use GMMA as delivery systems for antigens of interest[117,118].

1.4.1.2 – Vaccines against *A. baumannii*

Increased prevalence of MDR, XDR and PDR *A. baumannii* infection has resulted in an increased research interest into developing new antimicrobials against *A. baumannii*. One such example is the development of preventative vaccines, which would be particularly useful in patients who are at a high risk of requiring mechanical ventilation, burn patients and military personnel who are at a high risk of war-related injuries and infections[119].

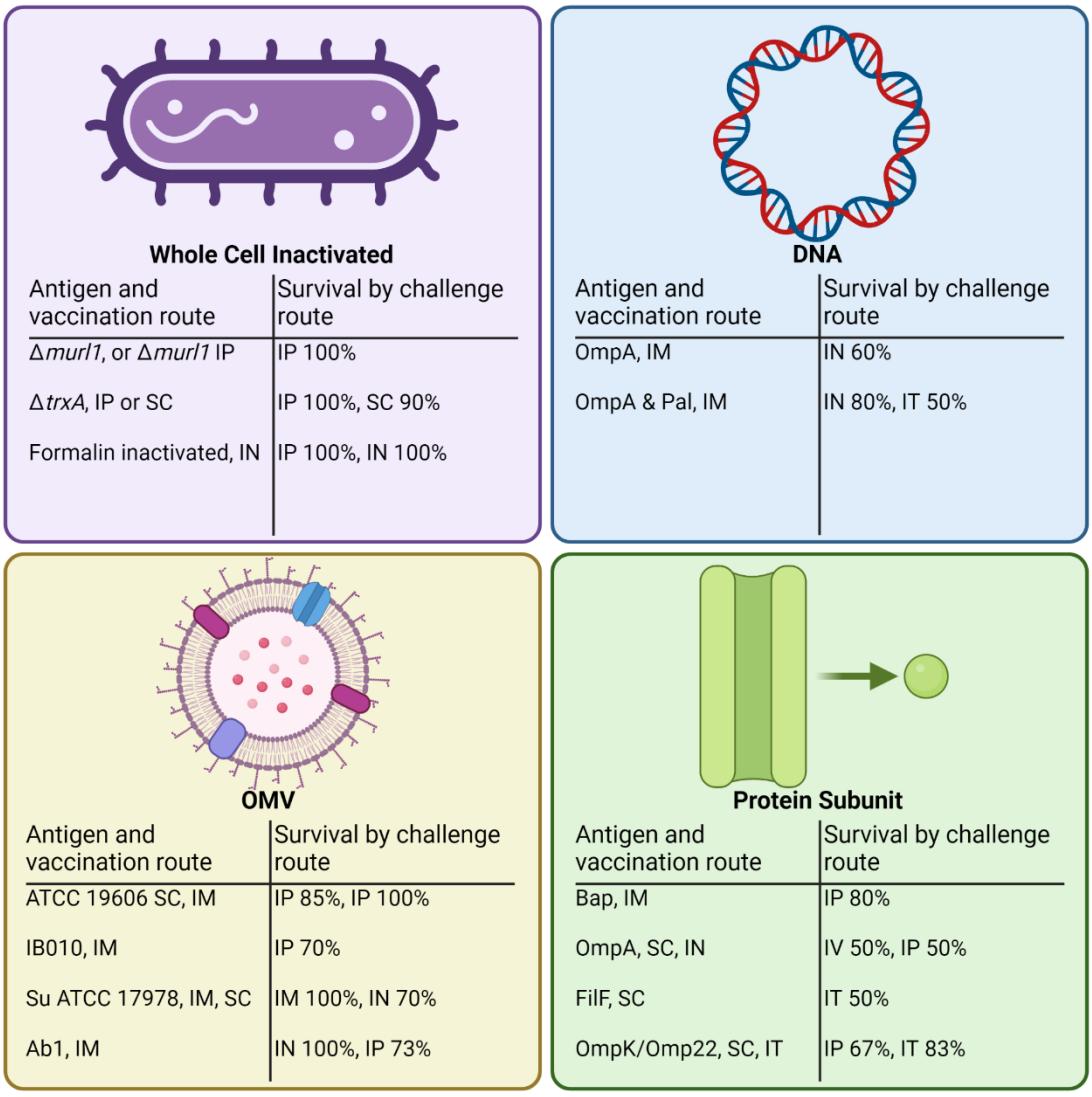


Figure 1.6 |Figure to show a summary of some *A. baumannii* vaccine studies. Schematic to show a summary of the different types of vaccines tested in murine models of *A. baumannii* infection whole cell inactivated, DNA, OMV and protein subunit. Tables within each show the antigen used for immunisation the routes of immunisation and routes of challenge respectively along with the vaccine efficacy determined by % survival of mice after challenge. Image generated in BioRender.

A whole cell inactivated vaccine proved to be highly immunogenic, resulting in the production of antibodies against multiple antigens and reduced the bacterial load in vaccinated mice compared to the unvaccinated controls in a murine sepsis model. The vaccine also proved to be cross protective against multiple strains of *A. baumannii* and serum from vaccinated mice was protective when used to passively immunise unvaccinated mice[119,120]. By introducing mutations into *murl1* and *murl2* a live attenuated strain of *A. baumannii* was generated that resulted in an infection in BALB/c mice with reduced virulence, but still induced an effective antibody response[121]. However, the use of a live attenuated vaccine for *A. baumannii* seems impractical. Target populations would likely involve the immunocompromised, so the potential for reversion and the difficulties immunocompromised individuals immune systems can have handling vaccines still capable of replication could hinder such vaccines[122].

OMVs and outer membrane complexes have been shown to be effective when used to vaccinate mice[123,124]. OMVs have demonstrated good antibody responses, significantly reducing bacterial burdens and increased survival rates compared to unvaccinated mice[121]. However, despite their success in murine models, the usage of such vaccines in humans is not without complication. There are high levels of LPS present in the vaccine preparations and it can be challenging to standardise the composition of the vaccine to ensure consistency across different production lots[119].

Protein sub-unit vaccines have been under development more recently with *A. baumannii* biofilm associated protein, Bap, and the bacterial porin outer membrane protein, OmpA, being the proteins of interest[119]. When mice were vaccinated with Bap they showed high levels of antigen-specific antibodies and reduced bacterial load after intraperitoneal challenge with a clinical isolate[119,125]. Vaccination of diabetic mice with OmpA showed high levels of antigen-specific antibodies and reduced bacterial loads when challenged intravenously with clinical strains[119,126]. Results also showed the sera of vaccinated mice provided passive immunisation by enhancing opsonophagocytic killing of *A. baumannii*[126]. Although these studies were successful, it is of note that they have only been tested in systemic *A. baumannii* infection models. It is therefore unknown if the vaccinations would also be protective against other clinically relevant *A. baumannii* diseases such as pneumonia.

DNA vaccines have also been explored against *A. baumannii*. Two vaccines were tested, one with OmpA alone in a eukaryotic expression vector pBudCD4.1 and a second consisting of OmpA and peptidoglycan associated lipoprotein (*pal*) inserted into the pVAX1 expression plasmid. Both vaccines were administered into mice intramuscularly in a prime boost approach and both vaccines resulting in 60% survival rates in mice compared to 0% survival in nonvaccinated mice after intranasal (for OmpA vaccinated) or intratracheal (for OmpA and *pal* vaccinated) challenge[121]. This suggests the potential for DNA based vaccines, and maybe RNA based vaccines, in the future of *A. baumannii* vaccine development.

1.4.2 – Monoclonal antibodies

Since the development of hybridoma technology, improvements to screening processes and modern antibody engineering capabilities the therapeutic potential of mAbs has significantly increased. Particularly in the case of antimicrobial resistance where few antibiotic treatment options remain, mAbs could provide another viable alternative[127]. This is particularly true in the case of infections that are a rare occurrence in a person's lifetime, such as hospital acquired infections. Due to their specificity mAbs would likely be reserved to second- or third- line therapy, after the causative agent has been identified. However, in the case of infections such as *A. baumannii*, where treatment options are severely limited, mAbs have high potential for success[103]. The specificity is also beneficial as treatment with mAbs is not going to disrupt the patient's microbiome as with antibiotics[128]. Antibacterial mAbs are able to work through a number of different mechanisms such as direct killing, anti-virulence, neutralisation, complement deposition and improving opsonophagocytosis[129].

It is of course important to consider that the efficacy of a mAb will depend largely on the availability, expression level and level of conservation of the target epitope. This is why toxin targeting mAbs are particularly successful, with two being approved for use already against anthrax and *Clostridium difficile* toxin B[127,130–132]. Anti-toxin mAbs may struggle to treat acute disease with large numbers of bacteria, limiting their usage to prophylaxis, however they can be administered alongside other mAbs with direct effects upon the bacteria as a cocktail of mAbs or even in combination with antibiotics to work synergistically together[127]. Suvratoxumab is a human IgG1 mAb targeting *Staphylococcus aureus* alpha toxin currently under development by Aridis Pharmaceuticals. The mAb works by neutralising the toxin, inhibiting alpha toxin binding to host cells, and is designed for use in

ventilator associated pneumonia patients. Suvratoxumab is currently undergoing phase III clinical trials in France to evaluate its safety and efficacy among high risk patients with VAP caused by *S. aureus* when given intravenously[133,134].

Many researchers are also trying to develop mAbs to surface targets and outer membrane proteins. Proteins involved in host cell adhesion, immune evasion, bacterial biosynthesis and porins are some examples of targets being explored. Multiple clinical trials have been run with mAbs targeting various *S. aureus* surface components such as clumping factor A (ClfA), GrfA, poly-N-acetylglucosamine (PNAG) and protein A[127,131]. Unfortunately, the ClfA and GrfA mAbs failed to show efficacy in phase III clinical trials[131]. Participants receiving XBiotech's *S. aureus* protein A mAb 514G3 experienced reduced hospitalisation times and no drug-related adverse events in a phase I/II trial. However, this study was unable to show any statistically significant outcomes as it was statistically underpowered[135]. The PNAG antibody F598 from Aloplexx has completed phase I and pilot phase II trials and was reported to be well tolerated with antibody levels in serum being maintained for 2-3 months[136].

Polysaccharide targets such as LPS and capsular polysaccharide (CPS) are also proving to be promising targets for mAbs. CPS is important in evasion of the host's immune system, making it favourable and effective in vaccine development. The binding of antibodies to CPS improves opsonophagocytosis. However, due to the high levels of selection pressure upon polysaccharide most are highly variable[127] resulting in, for example, over 100 different capsule types found amongst *A. baumannii* isolates[73] and more than 80 capsule types are found in *Klebsiella pneumoniae*[137]. This poses a difficulty in mAb development due to their high levels of specificity and limited cross-reactivity. This means a cocktail of mAbs would be required to cover multiple capsule types. Additionally, capsule targeting mAbs could increase selective pressure on certain capsule types, shifting bacterial populations away from the mAb target[127].

With the potential identification of new classes of antibiotics that will be long lasting looking bleak mAbs provide good alternative. Whether used individually, in multi-modal cocktails or in combination with antibiotics they could fill the gap between vaccine and antibiotic where antibiotic resistance has severely limited treatment options[129,131]. With options for use as

prophylactics and therapeutics as well as a lack of effective antibiotics, mAbs have a high potential for future success[132].

1.5 – Hypothesis and Aims

I hypothesise that *A. baumannii* derived OMVs will protect mice against challenge and that the route of immunisation will alter the immune response to the same OMV vaccine. Serum from such studies will allow for downstream analysis of antibody targets and mAbs raised against OMVs that provide protection against challenge will provide passive protection against challenge with *A. baumannii*.

1.5.1 – Aims:

1. To develop *in vivo* respiratory infection models in mice using clinically relevant *A. baumannii* isolates.
    - This will be achieved by intranasal challenge of BALB/c mice and disease severity will be assessed by measuring weight loss, inflammation and bacterial burden.

2. To determine whether inoculation with *A. baumannii* derived OMVs provides protection against challenge and whether the route of vaccination affects the level of protection given.
    - This will be achieved using the previously described infection model and immunising mice via different routes with OMV derived from *A. baumannii* followed by homologous challenge.
    - Protection will be determined by comparing weight loss, inflammation and bacterial burden between immunised and non-immunised mice.

3. To identify novel *A. baumannii* vaccine antigens and test protective efficacy of anti-*A. baumannii* mAbs.
    - Serum from immunised mice will be used to identify target antigens via Western blotting and phage expression cloning.
    - Mice will be pre-treated with mAbs raised against *A. baumannii* derived OMVs prior to intranasal challenge and protection will be determined by comparing weight loss, inflammation and bacterial burden between treated and un-treated mice.

2. Materials and Methods

2.1 – Reagents

2.1.1 – Consumables

Table 2.1 | Common consumables used

Consumable	Supplier	Product Code
Sterile 10 µl inoculating loops	VWR	612-9357P
50 ml Falcon tube	Corning	734-0453
1.8 ml Cryotube	ThermoFisher	NUNC379499
96-well U bottom tissue culture plate	Greiner bio-	392-0019
1.5 ml microcentrifuge tubes	VWR	211-0015
1 ml Syringe	BD Plastipak	613-4971
5 ml Bijou	Sigma-Aldrich	Z645338
70 µM cell strainer	Greiner bio-	542000
90 mm Petri dishes	ThermoFisher	101R20
150 mm Petri dishes	Corning	430599
Nitrocellulose membrane 132mm diameter	Whatman	WHA10402525
Nitrocellulose membrane 82mm diameter	Whatman	WHA10401116
26 G Needles	BD Medical	613-3835
96-well Nunc-Immuno microwell plate	Sigma-Aldrich	M5785
Cuvette 1.5 ml	VWR	634-0001

2.1.2 – Reagents

Table 2.2 | Common reagents used

Reagent	Supplier	Product Code
Dulbecco's Modified Eagle Medium/high glucose (DMEM)	Sigma-Aldrich	D5671
IPTG	Sigma-Aldrich	I6758
Tween-20	Sigma-Aldrich	P1379
Dulbecco's Phosphate Buffered Saline (PBS)	Gibco	14190-094
Lysogeny Broth (LB)	Sigma-Aldrich	L3022
Lysogeny Broth Agar (Lennox)	Sigma-Aldrich	L2897
Glycerol	Sigma-Aldrich	G5516
TMB Substrate Solution	Invitrogen	00-4201-56
Isoflurane-vet 100% w/w Inhalation Vapour, Liquid	Merial	SPC_1411147
Pentobarbital	Animalcare	Vm 10347/4014
Lambda ZAP II Undigested Vector Kit	Agilent	236201
Gigapack III Gold packaging extract	Agilent	200201
*Eco*RI adaptors	Stratagene	901110
TE buffer	Sigma-Aldrich	SRE0033
dNTP mix	Thermo Fisher	R0194
3M sodium acetate	Millipore	567422
Ethyl alcohol	Sigma-Aldrich	459836
T4 DNA polymerase	Invitrogen	18005017
10X ligase buffer	Thermo Fisher	B69
10mM rATP	Invitrogen	AM8110G
Phenol:Chloroform:Isoamyl Alcohol	Sigma-Aldrich	P2069
T4 DNA ligase	Thermo Fisher	EL0014
T4 polynucleotide kinase	Thermo Fisher	EK0031
10X STE buffer	Fisher Scientific	BP2479
Microspin S400 HR column	Cytiva	GE27-5140-01
Glycogen	Sigma-Aldrich	G0885

Reagent	Supplier	Product Code
XL1-Blue MRF cells	Agilent	236201-12
MgSO4	Sigma-Aldrich	M2773
Maltose	Millipore	1059120100
NaCl	Sigma-Aldrich	S3014
Yeast extract	Sigma-Aldrich	Y1625
NZ amine	Sigma-Aldrich	N4767
agar	Sigma-Aldrich	A1296
Tris-HCl	Roche	10812846001
Gelatin	Sigma-Aldrich	G2500
Tryptone	Millipore	T7293
DMSO	Sigma-Aldrich	D8418
PMSF	Roche	PMSF-RO
Leupeptin	Sigma-Aldrich	L2884
Gentamicin	Sigma-Aldrich	G1914
Kanamycin	Merck	BP861
Tetracycline	Sigma-Aldrich	87128
NBT/BCIP	Thermo Fisher	34042
SOLR cells	Agilent	236201-12
Ampicillin	Sigma-Aldrich	A9393
HiCrome Acinetobacter Agar Base	HIMEDIA	M1938
In-Gel Tryptic Digestion Kit	ThermoFisher	89871
FM 4-64	Invitrogen	T3166
Any KD MP TGX Gel	BioRad	4569033
10x Tris/Glycine/SDS Running Buffer	BioRad	161-0772
Pierce Lane Marker Reducing Sample Buffer	ThermoScientific	39000
Dual Color Standards	BioRad	1610374
Bovine Serum Albumin	Sigma-Aldrich	A2153
Trans-Blot Turbo Mini Nitrocellulose Transfer Packs	BioRad	170-4158
Mini-PROTEAN TGX Gels, 4-20%	BioRad	456-1093
Haematoxylin solution	Sigma-Aldrich	HHS16

Reagent	Supplier	Product Code
Eosin	Sigma-Aldrich	E4009

2.1.3 – Antibodies

Table 2.3 | Common antibodies used

Antibody	Supplier	Product Code
α mouse IgG-HRP	BioRad	STAR120P
α mouse IgG1-biot	BioRad	STAR132P
α mouse IgG2a-biot	BioRad	STAR133P
α mouse IgM-biot	Jackson Immuno	115-035-020
α mouse IgA-biot	SouthernBiotech	1040-08
α mouse IgG-AP	Jackson Immuno	115-055-003

2.2 – Microbiology

There were five different strains of *A. baumannii* used. Laboratory reference strain *A. baumannii* ATCC 17978 is an antibiotic sensitive strain that was originally isolated in the 1950's from a 4 month old baby with fatal meningitis[138–140]. ATCC 17978 was chosen for use due to its antibiotic sensitivity and the large amounts of information available in scientific literature. The other four strains (Table 2.4) are clinical isolates obtained from one hospital in Ho Chi Minh City, Vietnam, between 2009 and 2011[141]. The isolates were collected from VAP patients in the intensive care unit and were all high antibiotic resistant. Belonging to the Global clone 2 clonal complex the isolates spread across 3 GC subclades and 4 K loci, these 4 strains were representative of this collection of clinical strains.

Table 2.4 | Clinical strains of *A. baumannii* used. All strains were stored as glycerol stocks and originally collected by S. Baker (University of Cambridge) from Ho Chi Minh City, Vietnam.

ENA accession	Species	Strain	Specimen	Year	MIC IP	IP	AK	CAZ	CRO	CN	CIP	TZP	CO	Clonal complex	GC2 Subclade	K locus
ERR190418	*Acinetobacter baumannii*	BAL_084	VAP	2009	32	R	R	R	R	R	R	R	S	GC2	b	KL58
ERR190436	*Acinetobacter baumannii*	BAL_191	VAP	2010	64	R	R	R	R	R	R	R	S	GC2	e	KL49
ERR190448	*Acinetobacter baumannii*	BAL_215	VAP	2010	64	R	R	R	R	R	R	R	S	GC2	c	KL58
ERR190469	*Acinetobacter baumannii*	BAL_276	VAP	2011	64	R	R	R	R	R	R	R	S	GC2	d	KL2

*MIC IP: minimum inhibitory concentration imipenem, IP: imipenem, AK: amikacin, CAZ: ceftazidime, CRO: ceftriaxone, CN: gentamicin, CIP: ciprofloxacin, TZP: piperacillin-tazobcatam & CO: colistin. R resistant, S susceptible.

2.2.1 – Bacterial culture and growth assays

All bacteria grown planktonically were grown in LB broth at 37°C shaking at 200 rpm. For static growth, bacteria were grown on HiMedia Acinetobacter base with or without multi-drug resistance selective supplement at 37°C overnight. For glycerol stocks, a single colony was picked and cultured in 5 ml LB broth until OD 0.7 and then mixed 1:1 with 50% glycerol and stored at -80°C.

For growth assays, a glycerol stock was used to streak out an agar plate and grown overnight at 37°C. The following day, swipes from an area of dense growth were used to inoculate 50 ml falcons containing 5 ml LB broth and left to grow overnight at 37°C with shaking. The next morning, 200 µl was taken from each overnight and used to inoculate 20 ml of LB broth in an Erlenmeyer flask and incubated at 37°C with shaking. At 1, 2, 4, 8 and 24 hours after inoculation 1 ml of the culture was taken to measure the OD_{600} using a spectrophotometer. Another 20 µl was also taken to retrospectively calculate concentration in colony forming units/ml (CFU/ml). To do this, 180 µl sterile PBS was added to a sterile U bottom 96-well plate. Then 20 µl from each culture was added and serially diluted down the plate. Finally, 20 µl from 6 appropriate dilutions per sample were added and dripped down an agar plate, left to dry and incubated overnight at 37°C (figure 2.1).

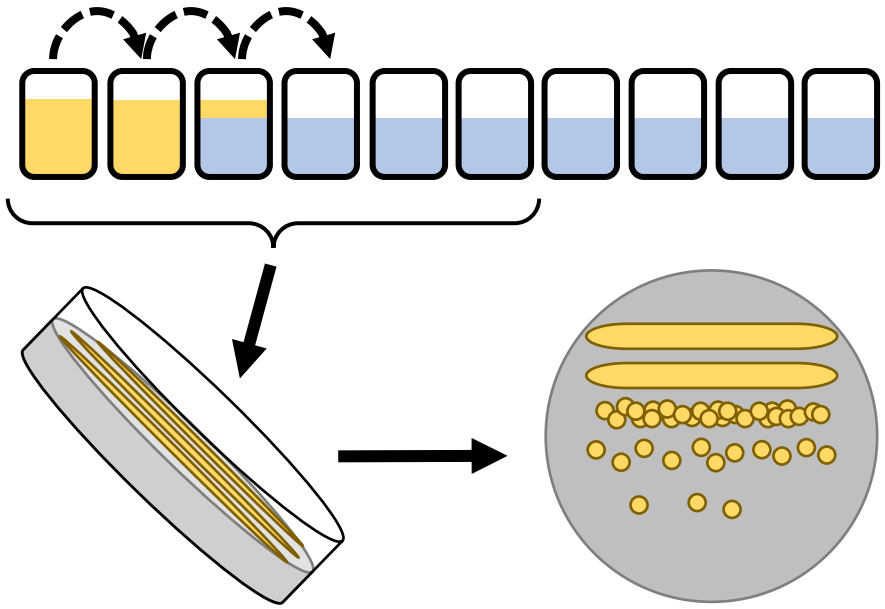


Figure 2.1 | Serial dilution and plating out to determine bacterial concentration. Bacteria was serially diluted 1:10 down a 96 well plate and mixed. A multichannel pipette was used to plate out 20 µl of 6 different dilutions onto one agar plate by tipping the plate and pipetting the culture onto the plate slowly until it has spread down the plate. The plates are left upright to dry and incubated overnight at 37°C.

2.2.2 – OMV production

A. baumannii naturally blebs out OMVs during normal growth. To generate OMVs an agar plate was streaked out from a glycerol stock and grown overnight at 37°C. The following day a swipe from an area of dense growth was taken and used to inoculate 200 ml LB broth which was incubated overnight with shaking. The liquid culture was centrifuged the next day at 7,200 x*g* for 15 minutes at 4°C. The supernatant containing the OMVs was taken off and vacuum filtered using a 0.45 µm Stericup. The OMVs were then pelleted via ultracentrifugation using a Beckman Optima L-100 XP at 100,000 x*g* for 2 hours at 4°C or via centrifugation at 7,200 x*g* overnight at 4°C. The OMV pellets were then re-suspended in PBS and a sample was taken to streak onto LB agar plates overnight to check for sterility.

To quantify OMVs, they were incubated at room temperature for 20 minutes with FM4-64 lipophilic dye in a black 96-well polypropylene microtiter plate and blanked against wells containing PBS and FM4-64. Fluorescence was then read using a FLUOstar Omega excitation 520 nm, emission 700 nm. The data was expressed as fluorescence units (FU) relative to volume of sample added to the well.

2.3 – *in vivo* methods

All *in vivo* studies were performed in accordance with the United Kingdom's Home Office regulations. All work was approved by Imperial College London's Animal Welfare and Ethical Review Board under Protocol number 1, project license number P4EE85DED. Animals were housed in autoclaved individually ventilated cages under positive pressure, in the Central Biomedical Services facilities at St Mary's Hospital Campus Imperial College London. Mice were specific-pathogen free and all studies were carried out in the same room under containment level 2 conditions. Mice were housed in groups wherever possible, unless they needed separating due to fighting, and groups were given the same experimental treatments. Rooms were kept to a 12-hour light/dark cycle, maintained at 20-24°C with 55 ± 10% humidity and mice received food and water *ad libitum*. Studies were performed using 6-8 week old female BALB/c mice from Charles River Laboratories UK.

2.3.1 – Challenge

To prepare bacteria for challenge infections a glycerol stock was streaked out onto an agar plate and incubated overnight. A swipe from an area of dense growth was used to inoculate

5 ml LB broth in a 50 ml falcon and incubate overnight with shaking. The next morning, 200 µl of overnight culture was used to inoculate 20 ml of LB and grown to OD_{600} 0.7. The culture was then centrifuged at 4,000 x*g* for 3 minutes and the pellet was resuspended in PBS. The PBS and *A. baumannii* solution was then centrifuged at 10,000 *xg* for 2 minutes and the pellet was resuspended in 400 µl PBS which should be at a concentration of approximately 10^{10} CFU/ml. This stock solution was diluted to the target challenge dose, from which a sample was taken to serially dilute and plate onto agar to retrospectively determine CFU/ml by counting the individual colonies and using the following formula: (number colonies x the dilution factor)/ volume of culture plated.

For challenge, mice were anaesthetised via inhalation of 2.5% isoflurane in oxygen at 2 L/minute and then 100 µl bacterial culture at the desired target concentration was pipetted onto their nose forming a bubble over both nostrils for mice to breathe in.

2.3.2 – Clinical Scoring

For clinical scoring mice were assessed by a blinded individual on the appearance of their coat, their level of activity, their stance and their breathing using the table below (Table 4). The scores were then totalled to give an overall clinical score.

Table 2.5 | Clinical scoring of coat. Mice were given clinical scores based on the appearance of their coat, with the description of what each score means below.

Coat

Score	Description
0	Clean and smooth
1	Slightly scruffy
2	Significant piloerection, thin coat
3	Severely unkempt, stained coat

Table 2.6 | Clinical scoring of activity levels. Mice were given clinical scores based on their level of activity, with the description of what each score means below.

Activity

Score	Description
0	Normal
1	Quiet, explores slowly
2	Lethargic with only some movement
3	No spontaneous movement, sits completely still

Table 2.7 | Clinical scoring of stance. Mice were given clinical scores based on their stance, with the description of what each score means below.

Stance

Score	Description
0	Normal
1	Slightly hunched
2	Very hunched, obvious even when moving
3	Lies on side

Table 2.8 | Clinical scoring of breathing. Mice were given clinical scores based on their breathing, with the description of what each score means below.

Breathing

Score	Description
0	Normal
1	Rapid, shallow
2	Rapid, abnormal
3	Laboured

2.3.3 – Vaccination

For vaccination the OMVs were diluted to either 100 FU in 50 µl sterile PBS for intramuscular or subcutaneous immunisation or 500 FU in 100 µl sterile PBS for intranasal immunisation. Mice were then immunised intramuscularly in their rear leg or

subcutaneously on their right flank. Intranasal immunisation was carried out in the same method as an intranasal challenge.

2.3.4 – mAb pre-treatment

For mAb pre-treatment mice were given mAbs diluted to the correct concentration in sterile PBS and given doses in 100 µl volumes. Mice were put into a heat box set to 37.5°C and warmed for 5-10 minutes prior to injection with mAbs intravenously in one of their lateral tail veins. For intranasal doses of mAb mice were treated in the same way as for intranasal challenge.

2.3.5 – Harvest

Upon meeting the scientific end point mice were culled via a terminal dose of 200 µl intraperitoneal pentobarbital followed by cutting of the femoral artery or exsanguination under terminal anaesthesia.

2.3.5.1 – BAL

Bronchoalveolar lavage (BAL) was performed by cutting a small hole in the trachea using a scalpel and inserting a flexible cannula attached to a 1 ml syringe containing 1 ml sterile PBS. Around 0.7 ml of PBS was pushed into the lungs and withdrawn back into the syringe. This was repeated two more times and then the BAL fluid was collected in a 1.5 ml microcentrifuge tube and stored on ice until it could be serially diluted and plated onto agar plates to determine bacterial load in the BAL fluid. The agar plates were incubated at 37°C overnight.

BAL fluid was then centrifuged at 11,000 x*g* to pellet cells and the supernatant was removed and stored at -80°C for later cytokine analysis. The remaining cell pellet was treated with ACK cell lysis buffer for 3 minutes at room temperature before quenching the reaction with DMEM, followed by another centrifugation at 11,000 x*g* for 1 minute. The supernatant was removed and the remaining cell pellet was resuspended in 500 µl DMEM and BAL fluid cells were counted using trypan blue. 50-200 µl of the cell suspension was loaded onto cytospin slides to spin at 30 x*g* for 5 minutes and the slides were left to dry. The following day, the slides were fixed in methanol for 5 minutes and then stained with haematoxylin for 5 minutes followed by a wash in water and 6 dips in eosin. The slides were washed once more and left to dry so coverslips could be mounted on each slide.

2.3.5.2 – Nasal lavage

Nasal lavage was performed by removing the bottom jaw of the mice and cutting the trachea above where the BAL had been performed. A flexible canula was attached to a 1 ml syringe containing 1 ml sterile PBS which was inserted into the trachea facing towards the nose of the mouse. The rear end of the mice was elevated so they were at an angle with their noses closest to the work surface. A 1.5 ml microcentrifuge tube was held underneath their nose to catch the PBS coming out of their nostrils after being pushed through their upper airways from the syringe. The nasal lavage fluid was then kept on ice until it could be serially diluted and plated onto agar to determine the bacterial load in the upper respiratory tract. The agar plates were incubated at 37°C overnight.

The remaining nasal lavage fluid was centrifuged at 11,000 x*g* for 1 minute and the supernatant was removed and stored at -80°C for future ELISA analysis.

2.3.5.3 – Lungs

Both lobes of the lungs were dissected out of the mice and placed into bijou tubes containing 5 ml sterile DMEM to be kept on ice until processing. The lungs were mashed through 0.7 µm cell strainers along with the 1 ml of DMEM they were stored in to generate the lung homogenate. Some of the lung homogenate was serially diluted and plated onto agar plates to determine bacterial loads in the lungs. The agar plates were incubated at 37°C overnight. The remaining lung homogenates were centrifuged at 400 x*g* for 5 minutes and the supernatant was removed and stored at -80°C for future cytokine analysis.

2.3.5.4 – Spleens

The spleens were dissected out from the mice into bijou tubes containing 1 ml of sterile DMEM and kept on ice until processing. The spleens were mashed through 0.7 µm cell strainers along with the 1 ml DMEM they were stored in to generate the spleen homogenates. The spleens were then serially diluted and plated onto agar to determine bacterial loads in the spleens. The agar plates were incubated overnight at 37°C.

2.3.5.5 – Blood

Blood was collected from the mice through exsanguination of the carotid artery, leading to around 100-300 µl of blood being collected from each mouse. Blood was left on ice to clot

for 3 hours before centrifugation at 11,000 x*g* for 10 minutes to pellet the clot. The serum was collected and stored at -80°C for future analysis.

2.4 – Enzyme-Linked Immunosorbent Assays

All enzyme-linked immunosorbent assays (ELISAs) were performed using Nunc-Immuno Micro-Well 96-well plates. All blocking was performed using 1% BSA in PBS and all plate washes were performed using 0.05% Tween-20 in PBS. All ELISAs were developed using TMB, the reactions were stopped using 2N H_2SO_4 and plates were read at 450 nm using a FLUOstar Omega microplate reader.

2.4.1 – IL-6 ELISA

IL-6 was measured in the BAL fluid and lung homogenate supernatant. IL-6 ELISAs were performed using the mouse IL-6 DuoSet ELISA kit (BioTechne, DY406). BAL samples were used neat and lung homogenate supernatants were run neat and 1 in 2.

2.4.2 – IgG, IgG1, IgG2a & IgM ELISA

IgG, Ig1, IgG2a and IgM levels were measured in the serum of mice using a semi-quantitative ELISA. Plates were coated with anti-kappa and anti-lambda murine light chain antibodies for standard wells and 500 Fluorescent units OMVs per well and incubated for 2 hours at room temperature. Plates were washed with PBST and blocked with BSA in PBS for at least 1 hour and washed again with PBST. Serum samples were diluted 1:250, 1:500 and 1:5,000, added to the plates and incubated at 4°C overnight. Plates were then washed again with PBST and horseradish peroxidase conjugated antibodies were added to the plates IgG (BioRad STAR120p), IgG1 (STAR132P), IgG2a (STAR133P), IgM (Jackson Immuno Research 115-035-020) and incubated for 2 hours at room temperature. Plates were then washed and TMB was added to plates and the reaction was stopped 1 minute and a half later with H_2SO_4 and plates were read at 450 nm.

2.4.3 – IgA ELISA

Levels of IgA were measured in the BAL fluid and nasal lavage fluid. Plates were treated in the same way as the serum ELISAs and the BAL and nasal lavage samples were used neat. Plates were coated with anti-kappa and anti-lambda wells for the standards and 500 FU OMVs per well for the samples. Plates were washed, blocked and washed again before

samples were added and plates were incubated at 4°C overnight. The following day the plates were washed and biotinylated anti mouse IgA (SouthernBiotech 1040-08) was added to plate and incubated for 2 hours at room temperature. The plates were washed with PBST and streptavidin-HRP was added to the plate for 20 minutes. The plates were washed with PBST again and then TMB was added to the plate and the reaction was stopped after 20 minutes with H_2SO_4 and the plates were read at 450 nm.

2.5 – Multiplex assay

The BAL supernatant was also used for Meso Scale Discovery Electrochemiluminescence (MSD) to measure the levels of 10 different cytokines 24 hours after challenge. A custom 10-spot U-PLEX kit was used to measure mouse cytokines: GM-CSF, IFN-γ, IL-5, IL-6, IL-10, KC, MCP-1, MIP-1α, MIP-1β and TNF. This work was performed by Katie E Flight, Imperial College London. The plates contain 10 spots within each well, 1 spot per analyte. Calibrator solution is 4-fold serially diluted to generate an 8 point standard curve and 20 µl added to the corresponding standard wells and 20 µl of BAL sample was added to the sample wells and the plate was incubated for 2 hours at room temperature with shaking. The plate was washed 3 x in PBS with 0.05% Tween-20 and then detection antibody was added. The plate was incubated for 2 hours at room temperature with shaking and washed 3 x again with PBST. Read buffer was added to each well and the plate was read using a SECTOR imager.

2.6 – Protein identification via Western blotting and mass spectrometry

OMVs were diluted in PBS and sample buffer and boiled at 95°C for 5 minutes before loading 1000 FU of OMV into mini-PROTEAN TGX gels and ran at 100 V for 45 minutes – 1 hour, until the dye front migrated to the bottom of the gel. Gels were either stained with Coomassie blue to visualise and image proteins or taken forwards for western blotting.

2.6.1 – Western Blot

For western blotting, proteins were separated by SDS-PAGE and then transferred using the Tans-blot Turbo and Trans-blot Turbo mini nitrocellulose transfer packs. The membrane was then removed and cut to size and blocked overnight with blocking buffer (1% BSA in PBS). Membranes were washed using wash buffer (0.1% Tween-20 in PBS). Serum was diluted

1:200 in blocking buffer and incubated on the membrane for 2 hours at room temperature with rotation. Membranes were washed with wash buffer before adding HRP conjugated anti-mouse IgG or anti-human IgG detection antibody and incubating for 1 hour at room temperature with rotation. The membranes were washed again and then left to develop in Immobilon Crescendo Western HRP Substrate (Millipore, WBLUR0500) for 5 minutes and imaged with a Biostep, Celvin S chemiluminescent imager.

2.6.2 – Protein extraction

The Thermo Scientific In-Gel Tryptic Digestion Kit was used to prepare excised bands from the SDS PAGE gel that corresponded to bands where serum from immunised mice was binding on the Western blot and for mass spectrometric analysis. Excised bands were de-stained and shrank using acetonitrile before allowing to air dry. Trypsin was then added to the dried pieces of gel and incubated at room temperature for 15 minutes before adding digestion buffer and incubating at 37°C for 4 hours. The digestion mix was removed and put into a clean tube and 1% formic acid was added to the gel pieces and incubated for 5 minutes. The extraction solution was then removed and added to the digestion mixture, inactivating the trypsin. The sample was then sent for mass spectrometric analysis by Dr Paul Hitchen, Department of Life Sciences Imperial College London.

2.7 – Phage expression cloning

The Lambda ZAP II Undigested Vector Kit from Agilent Technologies[142] was used for the phage expression cloning. The Expression Cloning method from Molecular Diagnosis of Infectious Diseases[143] was also used. In brief (Fig. 2.2), lambda phage library was generated containing random fragments of genomic *A. baumannii* DNA. The phage were then used to infect *E. coli* and protein expression was induced using isopropyl β-D-1-thiogalactopyranoside (IPTG) soaked into a nitrocellulose membrane. The membrane with the *A. baumannii* proteins bound on is washed and incubated with sera from immunised mice. The membrane was washed again and incubated with an alkaline phosphatase (AP) conjugated anti-mouse IgG antibody, followed by another wash and detection using NBT/BCIP substrate. Positive phage plaques corresponding to reactive spots on the membrane were then plugged and the lambda phage DNA was extracted and sent for sequencing to identify which proteins the antibodies bound.

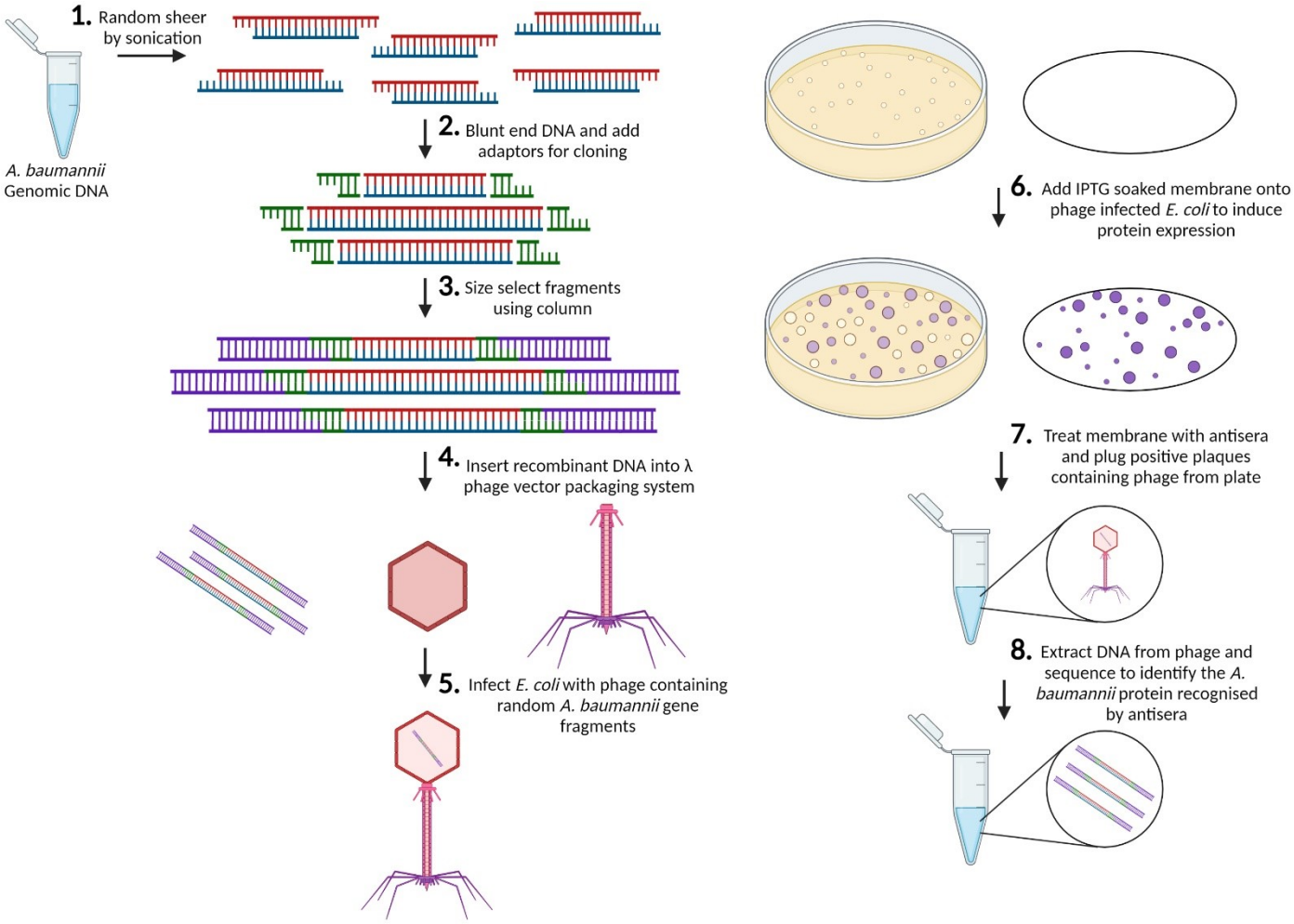


Figure 2.2 | Phage expression cloning technique to identify target antigens using polyclonal serum from immunised mice. Mice were immunised with *A. baumannii* BAL_276 OMVs intramuscularly and serum was collected and pooled to be used in phage expression cloning. A lambda phage library containing random fragments of *A. baumannii* genomic DNA was generated to screen with anti-sera and identify proteins the antibodies were binding to. Image made using BioRender.

2.7.1 – Lambda phage library generation

2.7.1.1 – Sonication, blunting and adding adaptors

Genomic DNA was extracted from 1.5 ml overnight culture of *A. baumannii* BAL_276 and BAL_084 using the GenElute Bacterial Genomic DNA Kit and quantified using a nanodrop. The gDNA was sonicated for 2 minutes, 10 seconds on, 10 seconds off and then precipitated overnight at -20°C in 3M sodium acetate and 100% ethanol. The precipitated DNA was centrifuged at 12,800 x*g* for 1 hour at 4°C, washed in 70% ethanol, centrifuged again and the supernatant was removed and the DNA left to dry before resuspending in ultrapure water.

To blunt the ends of the DNA fragments, 15 µg of DNA was mixed with 20µl T4 DNA polymerase buffer, 5µl 10 mM dNTPs, 3µl T4 DNA polymerase and ultrapure water to a final reaction volume of 100 µl and incubated for 30 minutes at 37°C. 100 µl TE buffer was then added to each tube along with 200 µl P/C/I and the tubes were mixed and centrifuged at 12,000 x*g* for 2 minutes. The aqueous top layers were removed and added to new tubes with 200 µl chloroform and centrifuged a second time. The aqueous layers were removed again and added to new tubes for DNA precipitation overnight at -20°C with sodium acetate and ethanol.

*Eco*RI adaptors needed to be added onto the blunted gDNA fragments to add *Eco*RI sticky ends for cloning. To add on the *Eco*RI adaptors, the DNA was cleaned and dried in the same way as before and the pellet resuspended in 12 µl *Eco*RI adaptors and incubated at 4°C for 30 minutes. 1.5 µl ligase buffer, 1 µl rATP and 1µl T4 DNA ligase was added and incubated overnight at 4°C. The reaction was heat inactivated at 70°C for 30 minutes and then the adaptors were phosphorylated by adding 1 µl ligase buffer, 2 µl rATP, 6 µl ultrapure water and 1 µl T4 DNA polynucleotide kinase and incubating for 30 minutes at 37°C. The reaction was heat inactivated again and the DNA extracted in the same way as before using P/C/I and chloroform. 10 µl 10x STE and 250 µl 100% ethanol were added and DNA was precipitated overnight at -20°C. The precipitated DNA was washed as before and left to dry. The pellet was resuspended in 1x STE buffer and stored at 4°C for size selection.

2.7.1.2 – Size selection, ligation to lambda ZAP express arms

Size selection columns were washed 3 times with 500 µl 1x STE by clamping the columns over a 15 ml falcon tube and waiting for the buffer to run through via gravity. The columns were put over clean tubes and the sample was added and left for 2 minutes to collect fraction 1. The column was then moved to a clean 15 ml falcon tube and 50 µl of 1x STE buffer was added to the column and left for 2 minutes to collect fraction tube. This was repeated until 9 fractions had been collected. The fractions were visualised on a 1% agarose gel and fractions 6-9 were pooled and precipitated by adding 2 µl glycogen and 2.5 volumes of 100% ethanol and incubated at -20°C for 1 hour. The mixture was centrifuged at 17,500 x*g* for 1 hour at 4°C and the pellet was then washed with 70% ethanol and centrifuged again. The supernatant was removed and the DNA pellet was left to dry and resuspended in 12 µl ultrapure water.

100 ng of fractionated DNA was added to 0.5 µl of ligase buffer, 0.5 µl rATP, 1 µl lambda phage arms, 0.5 µl T4 DNA ligase and ultrapure water up to 5 µl final volume and left at 4°C overnight. Another 0.5 µl of rATP and 0.5 µl ligase were added and the reaction was left overnight again at 4°C.

2.7.1.3 – Packaging, titration and amplification of library

To package the DNA, 2 µl of ligation reaction was added to the Gigapack III packaging extract and incubated at room temperature for 2 hours before adding 500 µl of SM buffer and 20 µl chloroform. The tube was centrifuged briefly to sediment the debris and the supernatant, containing the phage, was stored at 4°C.

To titrate the phage, a single *E. coli* XL1-Blue MRF colony was grown in 50 ml LB supplemented with 10 mM $MgSO_4$ and 0.2% maltose at 37°C with shaking for 4-6 hours until mid-log phase. The bacteria was pelleted by centrifugation at 500 x*g* for 10 minutes and resuspended in 25 ml 10mM $MgSO_4$. The solution was diluted to an OD_{600} 0.5 with 10mM $MgSO_4$ and the phage were serially diluted in SM buffer and 1 µl of the diluted phage was added to 200 µl of the diluted host cells. The phage and bacteria were then incubated at 37°C for 15 minutes to allow for the phage to attach to the cells. The phage and cell mixture was then mixed with 3 ml LB top agar and poured onto LB agar plates. The plates were then incubated overnight at 37°C. The next morning, the plaques were counted to determine the titre in plaque-forming units per ml (pfu/ml).

The quality of the library was checked by plugging plaques into sterile 1.5 ml microcentrifuge tubes and adding 500 µl SM buffer and 20 µl chloroform and the tubes were vortexed. Separate 50 ml cultures or XL1-Blue MRF and SOLR cells were grown in LB broth with supplements overnight at 30°C, centrifuged at 1000 x*g* for 10 minutes, resuspended in 25 ml $MgSO_4$ and then each adjusted to OD_{600} 1.0. In a 15 ml falcon tube, 200 µl XL1-Blue MRF cells, 250 µl phage and 1 µl ExAssist helper phage were mixed and incubated at 37°C for 15 minutes. Then 3 ml of LB broth with supplements was added to each tube and incubated for 2.5-3 hours at 37°C with shaking. The 15 ml falcon tubes were then incubated at 65-70°C for 20 minutes to lyse the cells and lambda phage particles. The tubes were centrifuged at 1000 x*g* for 15 minutes and the supernatant containing the excised pBluescript phagemid packaged as filamentous phage particles was removed. 200 µl of SOLR cells were mixed with 10-100 µl of the phage supernatant and incubated at 37°C for

15 minutes then plated onto LB-ampicillin agar plates and incubated overnight at 37°C. Single colonies from the plates were picked and a colony PCR using M13 forward and reverse primers and Q5 polymerase was run. A 1% agarose gel was run to check for different sized gDNA fragment inserts.

With a good quality library more XL1-Blue MRF cells were grown overnight, pelleted and adjusted to an OD_{600} of 0.5 in 10 mM $MgSO_4$. 600 µl of OD_{600} adjusted XL1-Blue MRF cells were mixed with the packaged library suspension containing approximately $5x10^4$ pfu and the tubes were incubated at 37°C for 15 minutes. The cell and phage mix was then added to 6.5 ml NZY top agar and poured onto 150 mm NZY agar plates and incubated for 6-8 hours at 37°C. After plaques start to touch, 8-10 ml SM buffer was added on top and the plates were incubated with gentle rocking at 4°C overnight so the phage diffuse into the SM buffer. The phage suspensions were then collected and pooled into sterile containers and the plates were rinsed with another 2 ml SM buffer and added to the pooled phage solution. Chloroform was added to a final concentration of 5% and the mixture was incubated for 15 minutes at room temperature. The tubes were centrifuged at 500 x*g* for 10 minutes to remove the debris and put the supernatant containing the phage into a clean, sterile falcon tube. Chloroform was added to the tube at a final concentration of 0.3% for storage at 4°C. To store aliquots of the library long term, DMSO was added to a final concentration of 7% for storage at -80°C. The aliquots were then re-titred to find the final concentration.

2.7.2 – Adsorption of Antisera with *E. coli* proteins

To ensure there is no binding to *E. coli* or *E. coli* proteins adsorption of antisera with *E. coli* proteins must be performed before serological expression screening. A single XL1-Blue MRF colony was used to inoculate 50 ml LB broth with supplements and incubated overnight at 30°C with shaking. The culture was then centrifuged and the bacterial pellet resuspended in 25 ml $MgSO_4$ and adjusted to OD_{600} 0.5 and 600 µl was added to 1.5 ml microcentrifuge tubes with ~2.5 – 3 $x10^4$ PFU of negative pick phage (phage containing empty vector, with no *A. baumannii* gDNA insert). The tubes were incubated for 15 minutes at 37°C and then mixed with 8 ml NZY top agar and poured onto pre-warmed 150 mm NZY agar plates, left to set and incubated at 42°C for 4-6 hours and plaques began to form. During the incubation, nitrocellulose membranes were soaked in 10 mM IPTG and left to dry. Once the plaques

were beginning to form, the IPTG soaked nitrocellulose filters were placed on top of the plate and the plates were incubated overnight at 37°C.

The filters were washed three times for 10 minutes with 0.1% Tween-20 in PBS and then blocked with 1% BSA, 1% Tween-20 PBS for 1 hour at room temperature with rocking. Filters were washed another three times with 0.1% PBST while 50 µl serum from immunised mice was mixed with 100 µl 0.5 M EDTA, 200 µl 0.1 M PMSF, 100 µl 10 mg/ml leupeptin, 100 µl 10 mg/ml gentamycin and PBS to a final volume of 10 ml. The serum mixture was then added to the membrane and incubated for 2 hours with rocking. The serum was poured off into a 50 ml falcon tube and a follow-up wash made up of the same components as the serum mixture, but without the serum, was added to the membrane and incubated for 40 minutes with rocking. The follow up wash was then poured into the falcon tube with the serum and sodium azide was added to a final concentration of 0.05% for storage at 4°C.

2.7.3 – Serological expression screening

2.7.3.1 – Primary screen

XL1-Blue MRF cells were grown the same way as before and diluted down to OD_{600} 0.5 in 10 mM $MgSO_4$ and 600 µl was added to each 1.5 ml microcentrifuge tube along with ~$2.5x10^4$ PFU positive phage. The phage and cells were incubated at 37°C for 15 minutes and then mixed with 8 ml NZY top agar and poured on top of 150mm NZY agar plates. The agar was allowed to set and then plates were incubated at 42°C for 4-6 hours until plaques began to form. Nitrocellulose membranes soaked in 10 mM IPTG and dried before they were added to the top of each plate and marked with sterile needles so they could be correctly orientated after screening was complete. The plates were then incubated at 37°C overnight and then cooled at 4°C for 15 minutes so the membrane could be removed without taking the top agar with it. The filters were washed 3 times in 0.1% PBST and then blocked with 1% BSA in 1% PBST and then washed 3 more times in 0.1% PBST. The pre-adsorped serum was then added to each membrane and incubated with rocking for 2 hours at room temperature. The membranes were then washed 3 times with 0.1% PBST and then the AP conjugated anti-mouse IgG was added and incubated for 1 hour with rocking at room temperature. Finally, the membranes were washed three more times in 0.1% PBST and then filters were added to NBT/BCIP for 5-15 minutes until purple spots developed. The membranes were then rinsed in ultrapure water and left to dry on filter paper. Positive

plaques corresponding to the purple spots on the membrane were removed and placed into 1 ml SM buffer containing 30 µl chloroform and stored at 4°C.

2.7.3.2 – Secondary screen

To confirm the phage were positive and to ensure clonality of the final phage a secondary screen was performed. XL1-Blue MRF cells were grown overnight again, centrifuged, resuspended and diluted down to OD_{600} 0.5 and 200 µl of cells were added to 1.5 ml microcentrifuge tubes along with 3.5 µl of the plugged phage after a 1:500 dilution in SM buffer. Tubes were incubated at 37°C for 15 minutes, mixed with 4 ml NZY top agar and poured onto 90 mm NZY agar plates. Plates were then incubated at 42°C for 4-6 hours until plaques began to form and the dried, IPTG soaked nitrocellulose membranes were added on top of the plates and incubated overnight at 37°C. The plates and membranes were treated in the same way as the primary screen, however the secondary phage picks were put into 500 µl SM buffer containing 20 µl chloroform. As the positive phage were confirmed and individual, clonal plaques were easy to pick a tertiary screen was not necessary.

2.7.4 – Plasmid excision, sequencing and protein identification

To excise the phagemids the plugged phage in SM buffer and 20 µl chloroform were vortexed and incubated for 1-2 hours at room temperature before storing at 4°C. XL1-Blue MRF and SOLR cells were grown overnight in 50 ml LB with supplements, centrifuged, resuspended and diluted to OD_{600} 1.0. In falcon tubes, 200 µl XL1-Blue MRF cells, 250 µl phage stock and 1 µl ExAssist helper phage were mixed and incubated for 15 minutes at 37°C. 3 ml LB broth with supplements was then added and the tubes were incubated for 2.5-3 hours at 37°C with shaking. The tubes were then incubated for 20 minutes at 65-70°C to lyse the lambda phage particles and the cells and the tubes were centrifuged at 1,000 x*g* for 15 minutes to pellet cell debris. The supernatant was removed and 10 – 100 µl was added to 1.5 ml microcentrifuge tubes along with 200 µl of the SOLR cells and the tubes were incubated for 15 minutes at 37°C. 200 µl of the cell mixture was plated onto LB ampicillin plates and incubated overnight at 37°C. Individual colonies were picked, glycerol stocks were made and plasmid DNA purifications were performed using Qiagen miniprep kits. Plasmids were checked for inserts via gel electrophoresis and then sent for sequencing using the T7 and M13 forward and reverse primers. Sequencing results were blasted against

the NCBI database and translated to see what proteins were able to be expressed as a whole protein or as a fusion protein with lacZ.

2.8 – Phylogenetic tree generation

To generate the phylogenetic trees the following search criteria were used on the NCBI protein database:

- “(carbapenem-hydrolyzing class D beta-lactamase OXA-23) AND "Acinetobacter baumannii"[porgn:__txid470]”
- (peptidoglycan-associated lipoprotein[Protein Name] OR (peptidoglycan-associated[All Fields] AND lipoprotein[All Fields])) AND "Acinetobacter baumannii"[porgn]
- (carbapenem-hydrolyzing class D beta-lactamase OXA-23[Protein Name] OR (carbapenem-hydrolyzing[All Fields] AND class[All Fields] AND D[All Fields] AND beta-lactamase[All Fields] AND OXA-23[All Fields])) AND "Acinetobacter baumannii"[porgn]

Amino acid sequences were collected for *pal*, *filF* and $bla_{\text{OXA-23}}$ and saved as a .txt files for each protein. The sequences were checked to make sure everything was written in FASTA format and then the .txt files were opened in BioEdit and saved as .FASTA files. Using the method published by B Hall[144] and the programme MEGA11 the FASTA sequence files were aligned using muscle alignment and the standard settings. For each protein’s alignment the model selector was then used to select the best model to use when generating a maximum likelihood tree. Each alignment was then used to generate a phylogenetic tree file in MEGA11 using the best model for each protein: FilF – JTT + G, Oxa-23 – JTT and PAL – JTT + G. The tree files were then save in the Newick format and opened FigTree to edit their appearances and collapse down long branches.

2.9 – Statistical analysis

All statistical tests were performed using GraphPad Prism V9 and described in the figure legends. *In vivo* and *in vitro* studies were performed in replicates with the graphs shown here being representative of all of the data collected. Where individual data points per experimental group are shown, the mean is also marked for each group on the graphs. Error bars are also included where points are representative of a group of data points, where

points are representative of means but error bars are not visible the data points are larger than the error bars. Statistical significance was shown on graphs using **p≤0.05, **p ≤0.01, ***p ≤0.001, ****p ≤0.0001*.

Pearson Correlation Coefficients were manually calculated to determine the level of correlation between OD_{600} and CFU based *A. baumannii* growth assays.

Significant differences in weight loss over 24 hours, IL-6 concentration, neutrophil infiltration and bacterial load between all experimental groups were determined using Kruskal-Wallis tests of multiple comparisons using Dunn's multiple comparison test where there were more than 2 experimental groups or time points.

Significant differences in time course challenge weight loss between all experimental groups were determined by multiple t tests.

Significant differences in antibody responses, weight loss, IL-6 concentration, neutrophil infiltration and bacterial load between all experimental groups were determined using two tailed Mann-Whitney tests where there were only 2 experimental groups.

Significant differences in antibody responses between all experimental groups where there were more than 2 experimental groups and more than one time point were determined using two-way ANOVAs with Tukey's multiple comparisons tests.

3 – Murine model development of *Acinetobacter baumannii* respiratory tract infection

3.1 – Introduction

There is clear need for the development of novel methods to control *A. baumannii* infections. To create new antimicrobials one needs to develop a method for testing their efficacy. Whether that is an *in vivo* or *in vitro* method will depend upon several factors such as costs, capabilities and what kind of results should be obtained to test a hypothesis. How one plans to use the final product, what kind of infection it is treating and what the infectious agent is will also have a bearing on what kind of method is used. In this case it was best to develop a murine infection model of *A. baumannii* to allow for future testing of vaccine efficacy and to get a more wholistic idea of the kind of infection caused in mice to therefore understand how the vaccine might work and establish correlates of protection.

It is also important to make sure you pick the correct bacterial strains to study. Laboratory reference strains tend to have the benefits of being well studied and understood, perhaps with more predictable behaviours *in vitro* and *in vivo* as well as fully sequenced and annotated genomes readily available[145]. This makes working with them easier and with more published data, can help to support, disprove and explain results. However, this also means that the strains have been around for a long time and were often subcultured decades ago. In the world of bacteria this can amount to numerous mutations and adaptations occurring in both the laboratory reference strain and the circulating strains resulting in very different bacteria[145]. Some laboratory reference strains will be less clinically relevant and therefore results will be less indicative of what is actually happening in humans infected with modern strains. *A. baumannii* ATCC 17978 could be a good example of this after being isolated in 1951 from a child with meningitis and has little to no antimicrobial resistances[146,147]. This shows how different laboratory reference strains can be from the circulating strains we see today.

Effective and reliable *in vivo* infection models provide a valuable way to investigate mechanisms of infection and aid in the development of novel treatment and prevention strategies[148]. There are many existing *A. baumannii* infection models available to study the conditions that best mimic human disease from respiratory tract and soft tissue infection to immunocompromised, immunocompetent or diabetic murine models[148,149]. There are high levels of similarity between experimental murine pneumonia models and pneumonia in humans[150].

Using laboratory reference strain *A. baumannii* ATCC 17978 and four different clinical strains we studied the *in vitro* growth of the strains before developing a murine respiratory tract infection model. The clinical strains were isolated from ventilator associated pneumonia patients from hospital outbreaks in Vietnam. The four chosen strains were representative across the different capsule types and subclades of the clinical strains collected. Of potential interest is the fact that clinical strain BAL_191 shares its capsule type with some *Klebsiella pneumoniae* strains[151], another ESKAPE pathogen that is also listed as critical on the WHO's list of pathogens for which urgent research into new antimicrobials is required[63].

3.1.2 – Chapter aims and hypothesis

I hypothesise that *A. baumannii* will cause respiratory tract infection in BALB/c mice with clinical strains causing more severe disease than laboratory reference strain ATCC 17978.

Aims:

1. Perform *A. baumannii* ATCC 17978 and clinical strain *in vitro* growth assays to compare their growth patterns and estimate colony forming units per ml at certain time points;

2. Intranasally challenge BALB/c mice with *A. baumannii* ATCC 17978 to find the best challenge dose and assess disease severity, bacterial burden and duration of infection;

3. Intranasally challenge BALB/c mice with different challenge doses of *A. baumannii* to find the best challenge strain and dose to assess disease severity, bacterial burden and duration of infection.

3.2 – Results

3.2.1 – Optical density read at 600nm is a good estimate for the density of *A. baumannii* in liquid culture

To determine whether the optical density at 600nm (OD_{600}) was a suitable estimate of concentration of *A. baumannii* in liquid culture, fresh cultures were set up from overnight cultures and their growth was measured across 24 hours. The OD_{600} was measured using a spectrophotometer and the concentration was determined by serially diluting the culture and plating onto LB agar. When *A. baumannii* ATCC 17978 was grown the OD_{600} (Fig. 3.1A) and the bacterial concentration (Fig. 3.1B) both increased quickly, entering log phase around 2 hours. Between 4 and 8 hours growth started to slow and then plateaued. The Pearson Correlation Coefficient was also calculated to determine the level of correlation between the OD_{600} and concentration of bacteria (represented by the r value in Fig. 3.1 B) showing good correlation between the OD_{600} and concentration of bacteria during *in vitro* growth of ATCC 17978. When the same study was performed using clinical strains of *A. baumannii*, all of the clinical strains had similar OD_{600} (Fig. 3.1C) and concentration (Fig. 3.1D) readings throughout. Between 2 and 4 hours the OD_{600} and concentration were both increasing rapidly as the bacteria entered the log phase which slowed between 4 and 8 hours, where OD_{600} and concentration plateaued. The Pearson Correlation Coefficients were calculated again for the four clinical strains, which all showed strong positive correlation between the OD_{600} and the concentration of bacteria in the culture. The OD_{600} and concentration of both *A. baumannii* ATCC 17978 and the clinical strains mimicked one another, particularly between 2 and 8 hours after inoculation and showed high levels of correlation. The OD_{600} therefore provides a good estimate of the concentration of bacteria within liquid culture.

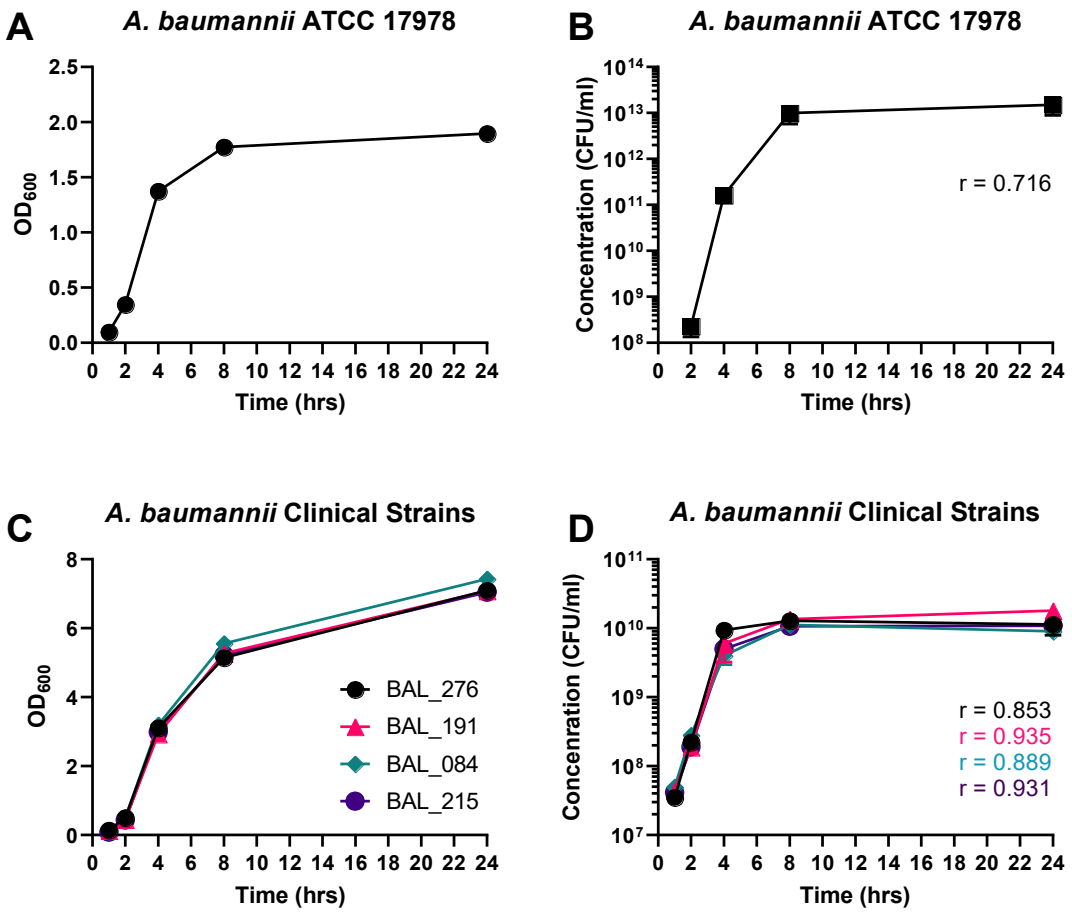


Figure 3.1 | OD is a good estimate of concentration for *in vitro* growth of *A. baumannii*. *A. baumannii* was grown *in vitro* to measure the OD_{600} and concentration of *A. baumannii* in culture with LB broth. *A. baumannii* ATCC 17978 growth was measured via a spectrophotometer **(A)** and plating out dilutions to establish colony forming units per ml **(B)**. Growth of clinical strains of *A. baumannii* was measured via a spectrophotometer **(C)** and plating out dilutions to establish colony forming units (CFU) per ml **(D)**. Pearson Correlation Coefficients were calculated and are represented by the r values on the graphs.

3.2.2 – Increasing the intranasal challenge dose of *A. baumannii* ATCC 17978 increases disease severity and bacterial burden

In order to see if it was possible for BALB/c mice to be infected with *A. baumannii* ATCC 17978, a fresh culture was grown until it reached an OD_{600} of 0.7, bacterial cells were washed and resuspended at a concentration of $1x10^{10}$ CFU/ml to dilute for the challenge doses. Doses were confirmed retrospectively by serially diluting each challenge dilution and plating onto agar to count individual colonies and determine the final CFU/ml and therefore CFU/mouse. Mice were intranasally challenged with $2.33x10^5$ CFU per mouse, $3.45x10^4$ CFU per mouse or sterile PBS (Naïve) and culled 24 hours later. Weight loss was measured after

infection (Fig. 3.2A) with only the $2.33x10^5$ CFU per mouse group losing weight at around 3% of their bodyweight, though this was not significant. IL-6 in the BAL fluid was measured by ELISA 24 hours after challenge (Fig. 3.2B) where a dose response was seen. The mice challenged with $3.45x10^4$ CFU per mouse had slightly raised IL-6 levels, but the mice challenged with $2.33x10^5$ had significantly increased levels of IL-6 in their BAL fluid compared to the naïve group ($p \leq 0.01$). Similar results were seen with the neutrophil infiltration into the lungs
(Fig. 3.2C), which was compared in BAL by H&E straining and manual counting. The mice challenged with $3.45x10^4$ CFU per mouse had slightly increased numbers of neutrophils in the lungs compared to the naïve group. However, the $2.33x10^5$ CFU per mouse group had significantly increased neutrophil infiltration into the lungs 24 hours after challenge compared to the naïve mice ($p \leq 0.01$).

The bacterial burden was measured in the BAL fluid and lungs by serially diluting BAL fluid and lung homogenate and plating onto LB agar. No bacteria were recovered from the BAL fluid of the naïve mice or the $3.45x10^4$ CFU per mouse group, but three mice challenged with $2.33x10^5$ CFU per mouse had some bacteria recovered from the BAL fluid (Fig. 3.2D). Increasing the dose of *A. baumannii* ATCC 17978 increased weight loss, inflammation and bacterial burden. However, doses were too low resulting in limited disease and low levels of bacterial recovery.

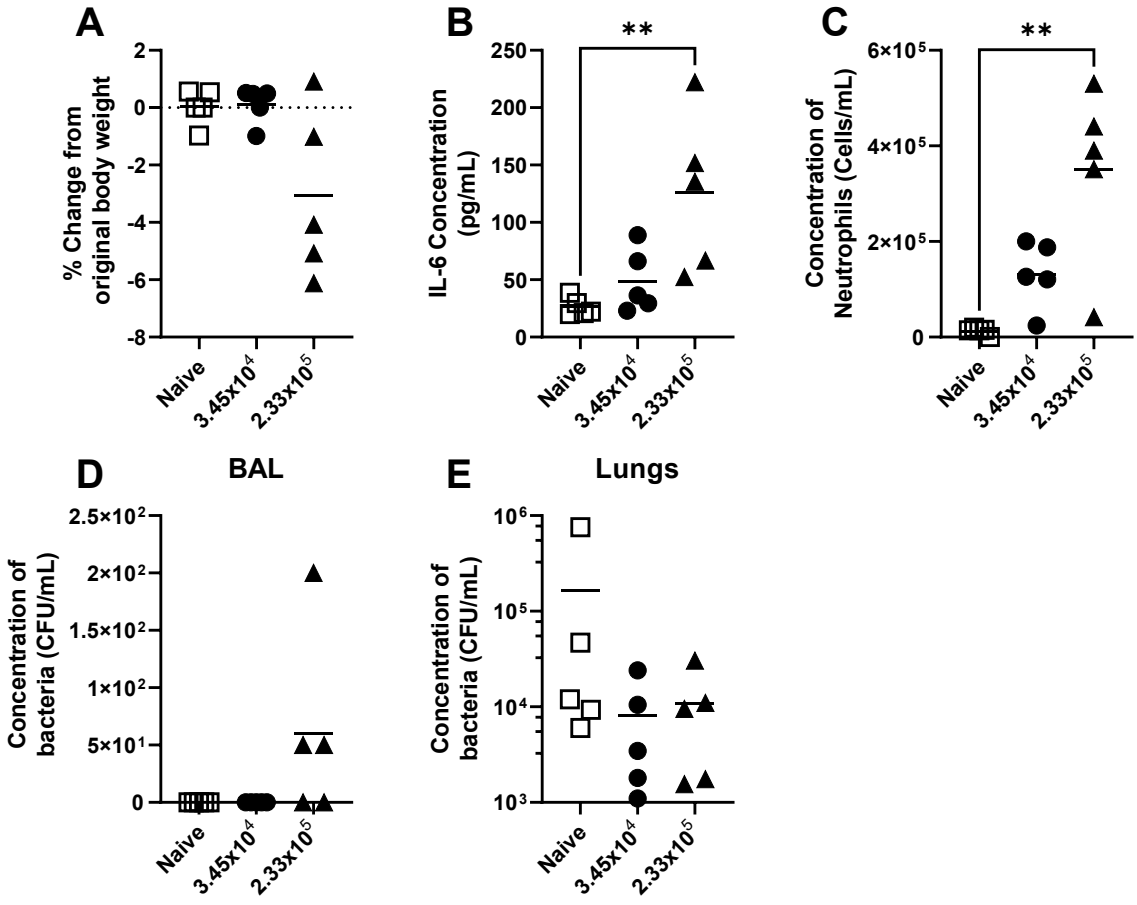


Figure 3.2 | Increasing the challenge dose of *A. baumannii* ATCC 17978 increases disease severity and bacterial burden. BALB/c mice were intranasally challenged with 2 different doses of *A. baumannii* ATCC 17978 in 100µl or 100µl sterile PBS (naïve) and culled 24 hours later. Change in weight was measured after 24 hour challenge **(A)**. IL-6 concentration in the BAL fluid was measured using ELISA **(B)**. Neutrophil infiltration into the lungs was measured by manually counting haematoxylin and eosin stained cytospin slides **(C)**. Bacterial load was estimated by serially diluting BAL fluid **(D)** and lung homogenate **(E)** and plating out onto LB agar. Kruskal-Wallis tests were used to test for significant differences. **p≤0.05, **p ≤0.01, ***p ≤0.001, ****p ≤0.0001.* Points represent individual animals.

3.2.3 – A minimum challenge dose of around 5x10^6 CFU per mouse of *A. baumannii* ATCC 17978 is required to reliably cause disease

As the previously tested challenge doses only resulted in very mild disease and did not result in a reliable bacterial burden, where all mice had bacteria recoverable from the BAL fluid, the study was repeated. Challenge doses were increased to 3.4x10^5, 8.3x10^5 and 4.9x10^6 CFU per mouse as well as a naïve group. Mice were culled 24 hours after challenge and the change in body weight was measured (Fig. 3.3A). The only group with measurable weight loss 24 hours after challenge was the group that were given 4.9x10^6 CFU per mouse, that

lost significantly more weight than $3.38x10^5$ CFU per mouse group ($p \leq 0.001$). The level of IL-6 in the BAL fluid was also measured 24 hours after challenge (Fig. 3.3B). There was a dose response seen in the amount of IL-6 present in the BAL fluid. The mice challenged with $8.25x10^5$ CFU per mouse and $4.9x10^6$ CFU per mouse both had significantly more IL-6 in their BAL fluid than the naïve mice ($p \leq 0.05$ and $p \leq 0.01$ respectively).

The bacterial burden in the BAL fluid and lungs was measured. In the challenge groups, only the highest dose group $4.9x10^6$ CFU per mouse had bacteria recoverable from BAL of all 5 mice (Fig. 3.3C). This group also had the highest bacterial load recovered from the BAL fluid, which was significantly higher than in the naïve group ($p \leq 0.01$). There was also a dose response in the lungs (Fig. 3.3D). The only group that had bacteria recoverable from all 5 mice was the highest dose group $4.9x10^6$ CFU per mouse. This group also had the most bacteria recovered from the lungs, which was significantly higher than the naïve group ($p \leq 0.01$) and the low dose group $3.38x10^5$ CFU per mouse ($p \leq 0.05$). A challenge dose of at least $5x10^6$ CFU per mouse of *A. baumannii* ATCC 17978 is required to cause significant weight loss, inflammation and bacterial burden in BALB/c mice where all 5 mice have recoverable bacteria from the lungs and BAL.

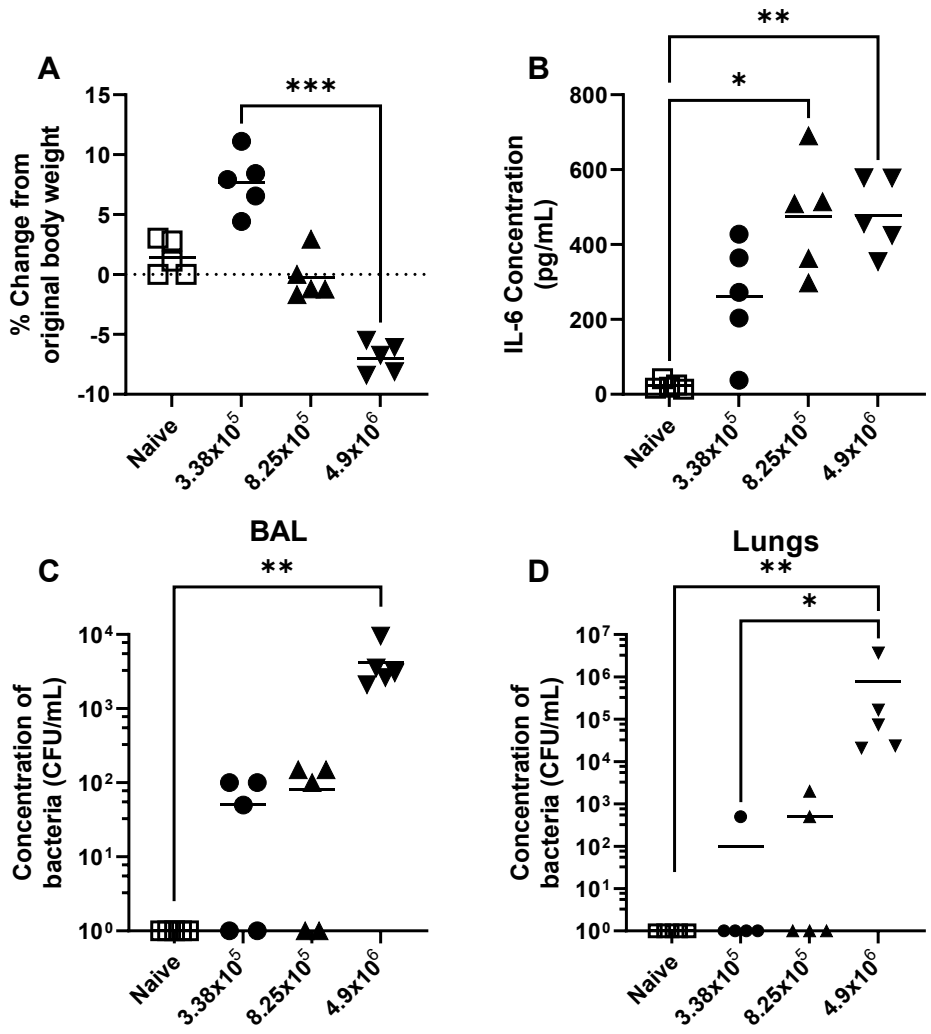


Figure 3.3 | The dose of *A. baumannii* ATCC 17978 needs to be over ~8x10^5 to reproducibly cause disease. BALB/c mice were intranasally challenged with 3 different doses of *A. baumannii* ATCC 17978 in 100µl or 100µl sterile PBS (naïve) and culled 24 hours later. Change in weight was measured after 24 hour challenge **(A)**. IL-6 concentration in the BAL fluid was measured using ELISA **(B)**. Bacterial load was estimated by serially diluting BAL fluid **(C)** and lung homogenate **(D)** and plating out onto LB agar. Kruskal-Wallis tests were used to test for significant differences. **p≤0.05, **p ≤0.01, ***p ≤0.001, ****p ≤0.0001.* Points represent individual animals.

3.2.4 – BALB/c mice recover quickly from intranasal challenge with *A. baumannii* ATCC 17978 that causes limited colonisation and disease

After establishing the optimum *A. baumannii* ATCC 17978 challenge dose we wanted to investigate whether there were still bacteria recoverable beyond 24 hours after infection. Mice were challenged with 5x10^6 CFU per mouse and culled 4, 24, 48 and 72 hours after

infection. Having already seen that naïve mice have IL-6 levels below the level of detection, very little neutrophil infiltration into the lungs and no recoverable bacteria, only one group of naïve mice was used. Naïve mice were given sterile PBS and culled 72 hours later. Mice were weighed throughout (Fig. 3.4A). Bacterial challenge mice had peak weight loss 24 hours after challenge, which was significantly more weight loss than the naïve mice ($p \leq 0.05$). Challenged mice then regained weight, returning to their original starting weights within 72 hours. The levels of IL-6 in the BAL fluid were measured (Fig. 3.4B). The levels of IL-6 in the BAL fluid were significantly increased in the challenge mice 4 ($p \leq 0.001$) and 24 ($p \leq 0.01$) hours after challenge compared to the naïve mice, with 4 hours being the peak and IL-6 levels returning to normal 48 hours after challenge. Neutrophil infiltration into the lungs of the challenge mice peaked around 24-48 hours after infection (Fig. 3.4C), where it was significantly increased compared to the naïve mice ($p \leq 0.01$) and returning to similar levels in naïve mice 72 hours after infection.

The bacterial loads were measured in the BAL fluid (Fig. 3.4D), lungs (Fig. 3.4E) and spleens (Fig. 3.4F). Peak bacterial load in the BAL fluid was seen 4 hours after challenge, which was significantly higher than the naïve mice ($p \leq 0.01$) after which all bacteria had been cleared from the BAL fluid by 48 hours after challenge. Peak bacterial load in the lungs was seen 4 hours after challenge, which was significantly higher than the naïve mice ($p \leq 0.001$). Bacterial load in the lungs was still significantly higher in the challenge mice 24 hours after challenge ($p \leq 0.001$) than the naïve mice and was still present in the lungs of some challenge mice 72 hours after challenge. The concentration of bacteria in the spleen remained relatively constant for the first 48 hours after challenge, with the bacterial loads at 4 and 24 hours after challenge being significantly higher than the naïve mice ($p \leq 0.05$ and $p \leq 0.01$ respectively). By 72 hours after challenge however, all mice had cleared bacteria from their spleens. Taken together, it was concluded that intranasal challenge with *A. baumannii* ATCC 17978 in BALB/c mice caused limited disease and colonisation which was cleared quickly from the sites tested.

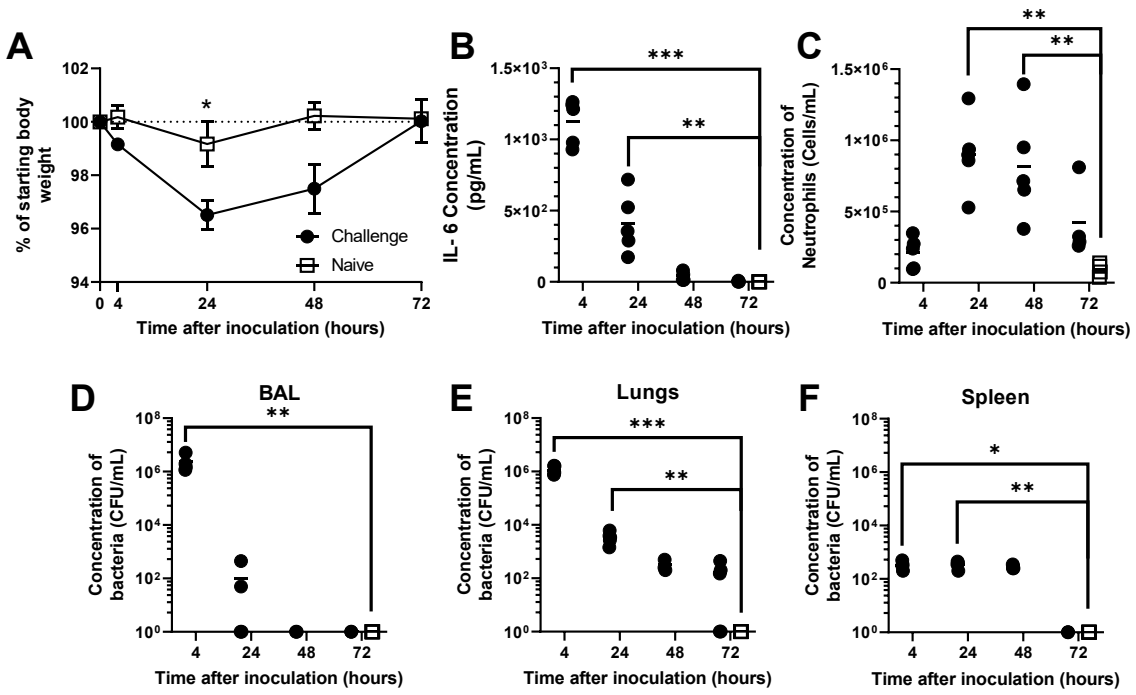


Figure 3.4 | Intranasal infection with *A. baumannii* ATCC 17978 causes limited colonisation and disease. BALB/c mice were intranasally challenged with 5x10^6 CFU per mouse *A. baumannii* ATCC 17978 in 100µl or 100µl sterile PBS (naïve) and culled 4, 24, 48 or 72 hours later. Mice were weighed after infection **(A)**. IL-6 concentration in the BAL fluid was measured using ELISA **(B)**. Neutrophil infiltration into the lungs was measured by manually counting haematoxylin and eosin stained cytospin slides **(C)**. Bacterial load was estimated by serially diluting BAL fluid **(D),** lung homogenates **(E)** and spleen homogenates **(F)** and plating out onto LB agar. Multiple t tests were used to test for significant differences in change in bodyweight. Kruskal-Wallis tests were used to test for significant differences in IL-6, neutrophil infiltration and bacterial loads. **p≤0.05, **p ≤0.01, ***p ≤0.001, ****p ≤0.0001.* Points represent means of mice (A). Points represent individual animals (B-F).

3.2.5 – Increasing the dose of clinical strain *A. baumannii* BAL_276 increases disease severity and bacterial burden

The clinical strains of *A. baumannii* collected from VAP patients in ICUs in Vietnam were used to develop more clinically relevant *in vivo* infection models. The strains were chosen as they were carbapenem resistant representatives of the isolates collected, covering four different GC2 subclades and three K loci. The isolates chosen were BAL_084 (GC2 subclade b, KL58), BAL_191 (GC2 subclade e, KL49), BAL_215 (GC2 subclade c, KL58) and BAL_276 (GC2 subclade d, KL2). By using the four representative strains any potential significant differences in disease severity as a result of GC2 subclade or capsule type should be accounted for.

A dose escalation study using a KL2 type clinical strain BAL_276 was performed to determine whether BAL_276 was able to cause disease in mice and determine disease severity caused by a KL2, GC2 subclade d isolate. Mice were intranasally challenged with a low ($1x10^5$ CFU per mouse), middle ($1.63x10^6$ CFU per mouse) and high ($1.45x10^7$ CFU per mouse) dose of *A. baumannii* BAL_276 or sterile PBS and culled 24 hours later. Bodyweight was measured after infection (Fig. 3.5A) and a dose response was seen but there were no significant differences between any of the groups. The bacterial load was measured in the BAL fluid (Fig. 3.5B), by plating onto selective HiCrome Acinetobacter agar base plates, where there a dose response was seen. The high dose group had the largest bacterial burden in the BAL fluid, which was significantly higher than the naïve group ($p \leq 0.05$). A dose response was also seen in the lungs (Fig. 3.5C), the highest dose challenge group had the largest bacterial load, which was significantly higher than the naïve group ($p \leq 0.05$) with around a 6-log increase. All challenge mice had bacteria recoverable from the lungs. Bacterial load in the upper respiratory tract was measured with nasal lavage (Fig. 3.5C). There was a dose response and the highest dose challenge group had significantly more bacteria recovered from the upper airways than the naïve group ($p \leq 0.05$). The lowest challenge dose did not lead to dissemination of the bacteria from the lungs to spleen in all mice (Fig. 3.5E). There was a dose response in the spleen with the highest challenge dose mice having the highest bacterial load on average, though this was not a statistically significant increase. The larger the challenge dose the more severe disease and greater the bacterial burden on the mice. Challenging the mice with around $1x10^7$ CFU per mouse *A. baumannii* BAL_276 caused the most weight loss and greatest bacterial burden that was significantly increased in the lungs and respiratory tract but also caused reproducible dissemination to the spleen in every mouse. Challenge with *A. baumannii* BAL_276 caused more severe disease at lower doses than challenge with ATCC 17978 (Fig 3.3 and Fig 3.5).

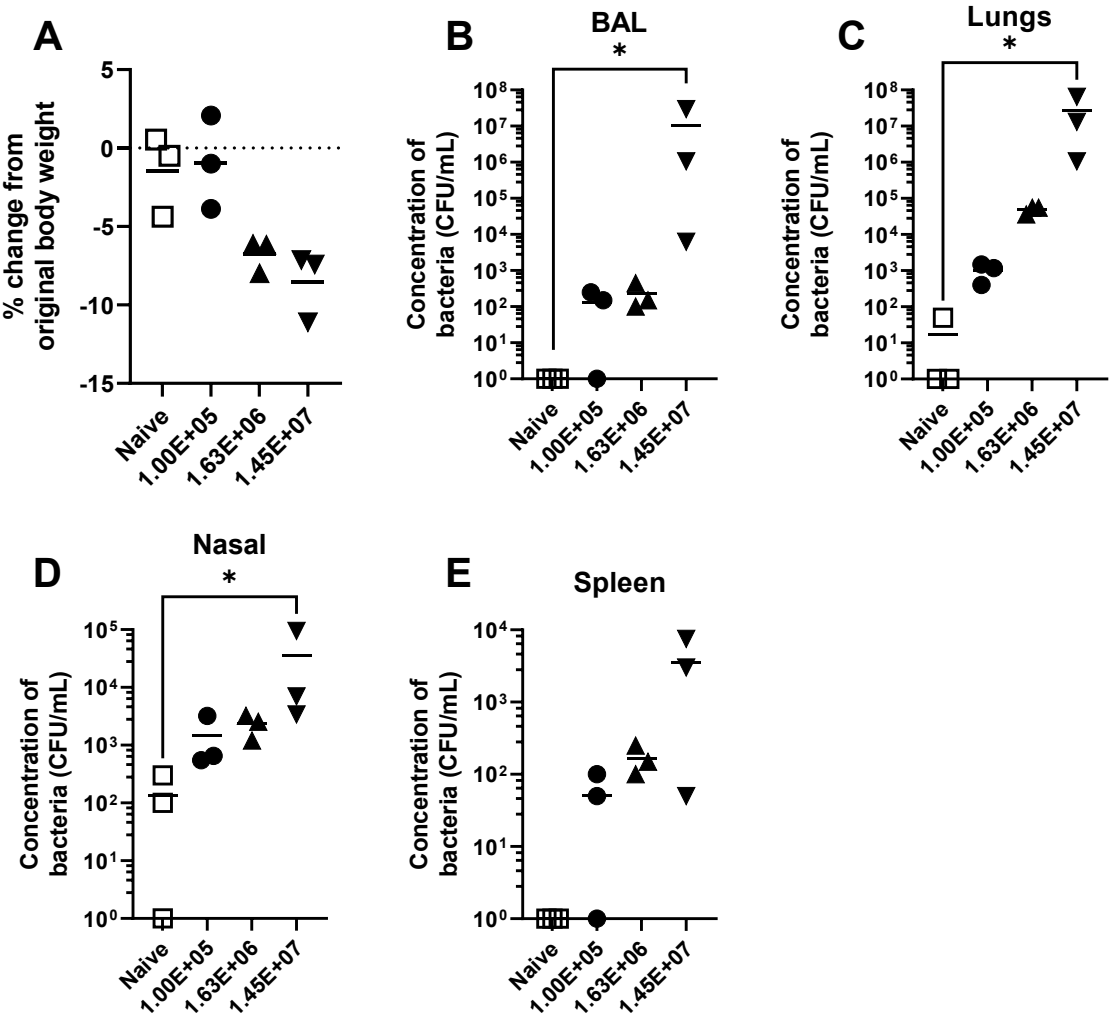


Figure 3.5 Infection with a clinical isolate BAL_276 causes disease in a dose related fashion. BALB/c mice were intranasally challenged with 3 different doses of clinical strain *A. baumannii* BAL_276 in 100µl or 100µl sterile PBS (naïve) and culled 24 hours later. Change in weight was measured after 24 hour challenge **(A)**. Bacterial load was estimated by serially diluting BAL fluid **(B),** lung homogenate **(C)**, nasal wash **(D)** and spleen homogenate **(E)** and plating out onto LB agar. Kruskal-Wallis tests were used to test for significant differences between naïve and challenge mice. **p≤0.05, **p ≤0.01, ***p ≤0.001, ****p ≤0.0001.* Points represent individual animals.

3.2.6 – Increasing the dose of clinical strain *A. baumannii* BAL_084 increases disease severity and bacterial burden

KL58 type, GC2 subclade b isolate *A. baumannii* BAL_084 was used to develop an infection model in BALB/c mice to see if infection differed significantly from KL2 type, GC2 subclade d isolate BAL_276. Three different doses and a naïve group were used, a low dose ($6x10^4$ CFU per mouse), middle dose ($6.5x10^5$ CFU per mouse) and high dose ($8.5x10^6$ CFU per mouse). Mice were challenged and culled 24 hours later. This time, mice were given clinical scores

based on their appearance 6 and 24 hours after challenge (Fig. 3.6A). There was a dose response in the clinical scoring of the mice, with the highest dose mice showing highest clinical scores. The high dose and middle dose groups had significantly higher clinical scores than the naïve mice at both 6 ($p \leq 0.001$, $p \leq 0.05$ respectively) and 24 ($p \leq 0.0001$ and $p \leq 0.001$ respectively) hours after challenge. A dose response was also seen in the change in weight 24 hours after challenge (Fig. 3.6B). Although all mice lost weight compared to the naïve mice, only the highest dose mice lost significantly more weight than the naïve mice ($p \leq 0.05$). The level of IL-6 was measured in the BAL fluid (Fig. 3.6C) and lung supernatant (Fig. 3.6D). A dose response was seen across both sites but only the highest dose group had significantly more IL-6 present in the BAL fluid and lungs compared to the naïve group ($p \leq 0.05$).

The bacterial burden was measured with dose responses seen in the BAL fluid (Fig. 3.6E), nasal wash (Fig. 3.6F) and lungs (Fig. 6G). In all cases, only the highest dose group had significantly increased bacterial loads compared to the naïve groups ($p \leq 0.05$). No dissemination of bacteria from the lungs to spleens was seen in the naïve, low and middle dose groups and in the high dose group only 2 mice had any bacteria disseminate to the spleen but this was not significant. Challenge with $8x10^6$ CFU per mouse of *A. baumannii* BAL_084 caused the most severe disease and greatest bacterial burden out of the tested challenge doses. However, there was little bacterial dissemination to the spleen when compared to BAL_276 or ATCC 17978.

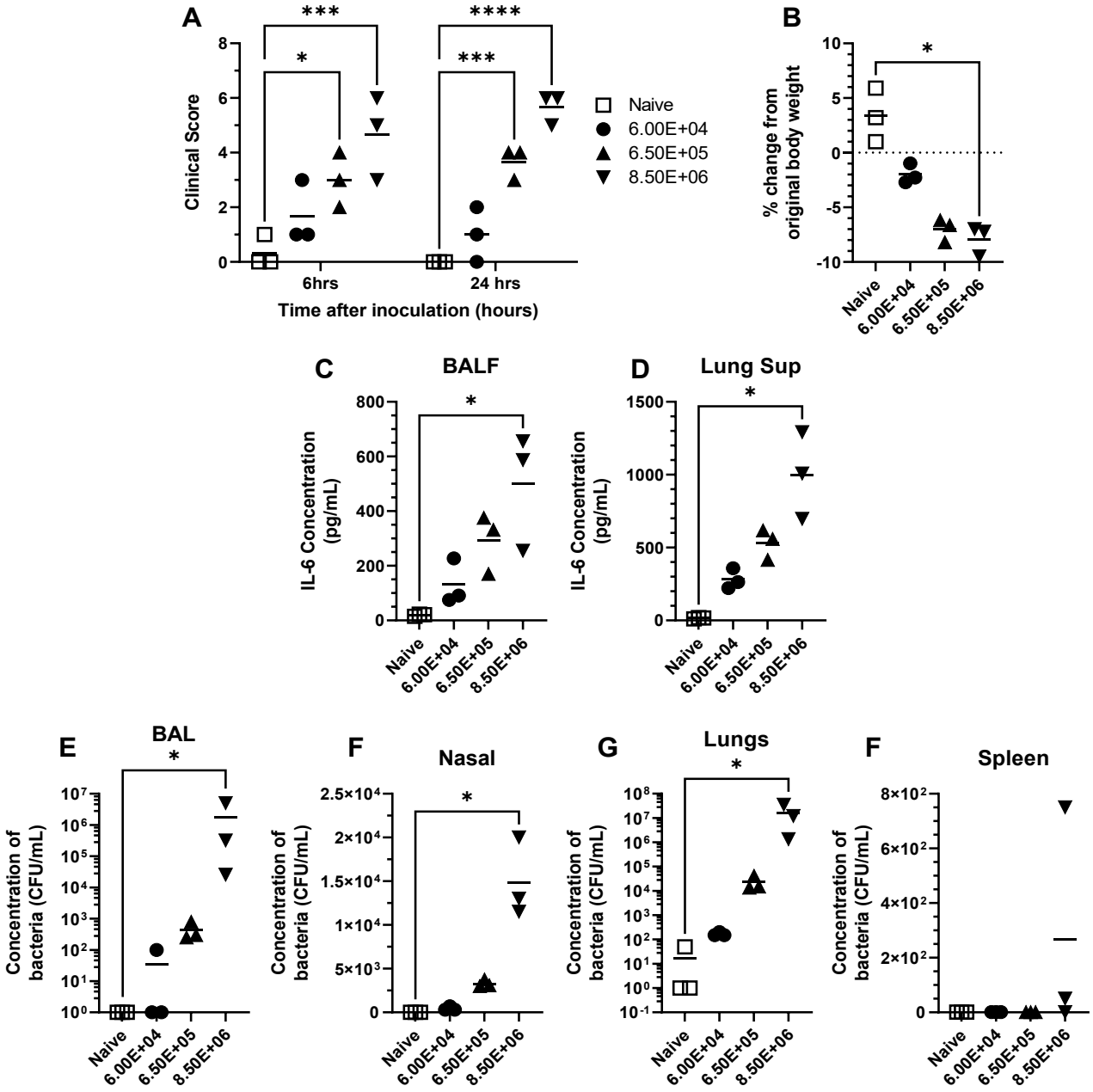


Figure 3.6 | Increasing the challenge dose of *A. baumannii* BAL_084 increases disease severity and bacterial burden. BALB/c mice were intranasally challenged with 3 different doses of clinical strain *A. baumannii* BAL_084 in 100µl or 100µl sterile PBS (naïve) and culled 24 hours later. Mice were given clinical scores as a marker of disease severity after challenge **(A)**. Change in weight was measured after 24 hour challenge **(B)**. IL-6 concentration in the BAL fluid **(C)** and lungs **(D)** was measured using ELISA. Bacterial load was estimated by serially diluting BAL fluid **(E)**, nasal wash **(F)**, lung homogenate **(G)** and spleen homogenate **(G)** and plating out onto LB agar. Kruskal-Wallis tests were used to test for significant differences. **p≤0.05, **p ≤0.01, ***p ≤0.001, ****p ≤0.0001.* Points represent individual animals.

3.2.7 – Increasing the dose of clinical strain *A. baumannii* BAL_191 increases disease severity and bacterial burden

A. baumannii BAL_191 represents a clinical strain with a third capsule type (KL49) and GC2 subclade (e) that mice were challenged with to assess infection severity. Mice were intranasally challenged with three different doses of *A. baumannii* BAL_191. A low dose ($8.5x10^4$ CFU per mouse), middle dose ($4.5x10^5$ CFU per mouse) and high dose ($6.5x10^6$ CFU per mouse) as well as a naïve group that received sterile PBS. The mice were then culled 24 hours after challenge. Clinical scores were given to mice (Fig. 3.7A). There was little to no difference between the clinical scores of the naïve mice and the low dose mice. The middle dose mice had increased clinical scores compared to the naïve mice which was significant 24 hours after challenge ($p \leq 0.001$). The high dose mice had significantly increased clinical scores compared to the naïve mice both 5 and 24 hours after challenge ($p \leq 0.0001$ and $p \leq 0.001$ respectively). Weight loss was measured during infection (Fig. 3.7B). The middle dose group lost the most weight which was significantly increased compared to the naïve mice ($p \leq 0.05$). However, the low and high dose groups did not lose much weight and the difference was not significant. The levels of IL-6 were measured in the BAL fluid (Fig. 3.7C) and lung supernatant (Fig. 3.7D). Similarly to the previous studies, there was a dose response and the high dose group was the only group with significantly increased IL-6 levels in the BAL fluid and lung supernatant compared to the naïve group ($p \leq 0.05$). Neutrophil infiltration into the lungs was measured (Fig. 3.7E) with all challenge mice having very similar levels of neutrophil infiltration into their lungs which was higher than the naïve mice but the difference was not significant.

Bacterial loads were measured in the BAL fluid, nasal wash and lungs. A dose response was seen in the bacterial load recovered from the BAL fluid (Fig. 3.7F) but only the high dose group had a significantly increased bacterial load compared to the naïve mice ($p \leq 0.05$). A dose response was also seen in the bacterial load recovered from the nasal wash (Fig. 3.7G). However, despite a large increase of around 4 logs in the high dose group compared to the naïve group the difference was not significant. There was also a dose response in the bacterial load recovered from the lungs (Fig. 3.7G). The high dose challenge group had a significantly increased bacterial load in the lungs compared to the naïve mice ($p \leq 0.05$). A challenge dose of $6.5x10^6$ CFU per mouse of *A. baumannii* BAL_191 caused the most severe

disease of the tested challenge doses with significantly increased clinical scores, inflammation and bacterial burden compared to naïve mice.

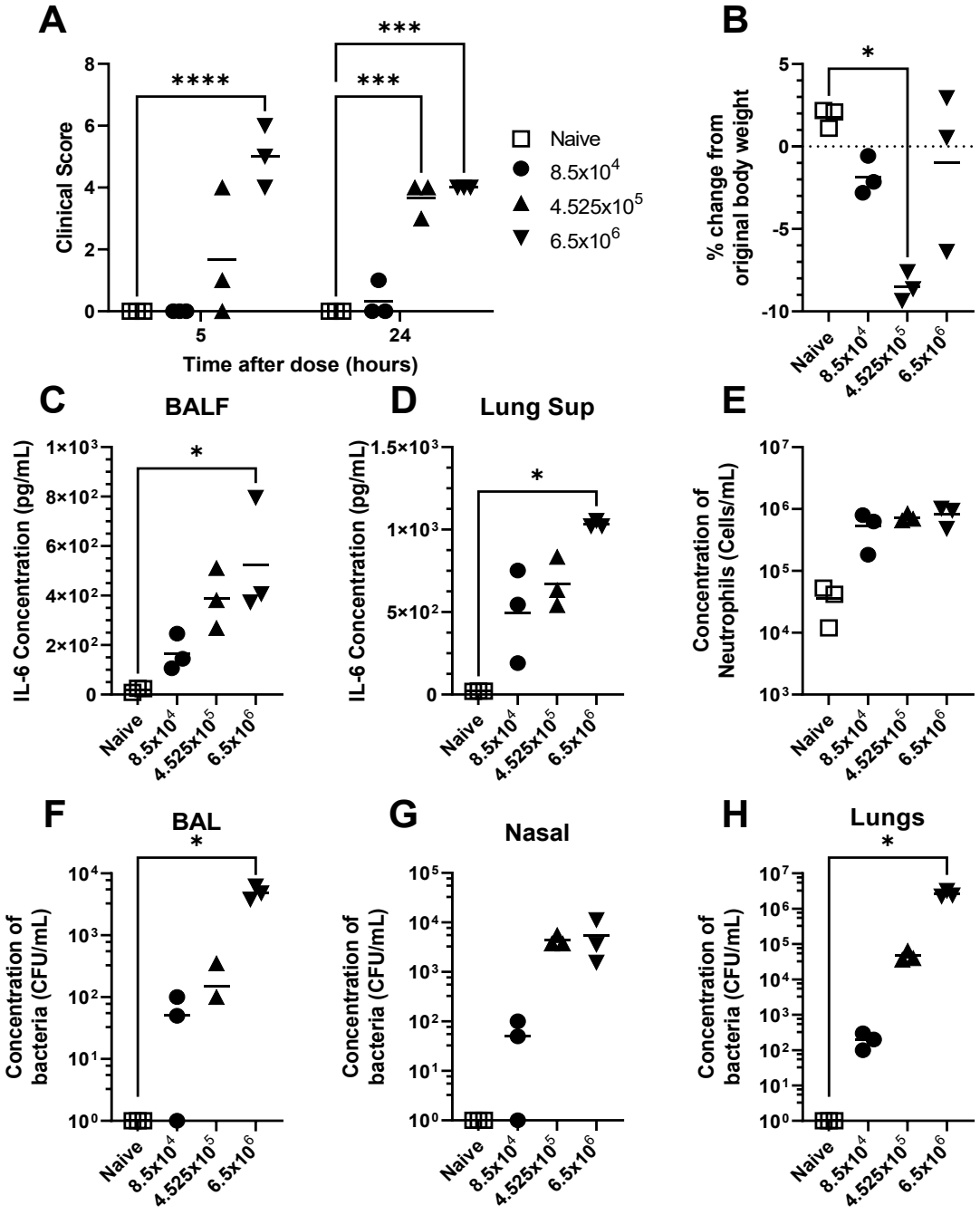


Figure 3.7 | Increasing the challenge dose of *A. baumannii* BAL_191 increases disease severity and bacterial burden. BALB/c mice were intranasally challenged with 3 different doses of clinical strain *A. baumannii* BAL_191 in 100µl or 100µl sterile PBS (naïve) and culled 24 hours later. Mice were given clinical scores as a marker of disease severity after challenge **(A)**. Change in weight was measured after 24 hour challenge **(B)**. IL-6 concentration in the BAL fluid **(C)** and lungs **(D)** was measured using ELISA. Neutrophil infiltration into the lungs was measured by manually counting haematoxylin and eosin stained cytospin slides **(E)**. Bacterial load was estimated by serially diluting BAL fluid **(F)**, nasal wash **(G)**, lung homogenate **(H)** and plating out onto LB agar. Kruskal-Wallis tests were used to test for significant differences. **p≤0.05, **p ≤0.01, ***p ≤0.001, ****p ≤0.0001.* Points represent individual animals.

3.2.8 – Increasing the dose of clinical strain *A. baumannii* BAL_215 increases disease severity and bacterial burden

The final clinical strain tested was *A. baumannii* BAL_215 and had the same capsule type as BAL_084 (KL58) but a different GC2 subclade (c). To determine how classification in this GC2 subclade affected infection, mice were challenged with three different doses of *A. baumannii* BAL_215 intranasally: a low dose ($2.05x10^5$ CFU per mouse), middle dose ($2.35x10^6$ CFU per mouse) and a high dose ($1.71x10^7$ CFU per mouse) as well as a naïve group that received sterile PBS. Mice were weighed throughout challenge (Fig. 3.8A). There was a dose response seen in the change in body weight and the high dose mice lost significantly more weight than the naïve mice ($p \leq 0.05$). The levels of IL-6 were measured in the BAL fluid (Fig. 3.8B) and lung supernatant (Fig. 3.8C). Similar dose responses were seen in the levels of IL-6 in both the BAL fluid and the lungs. In both the BAL fluid and the lungs, only the high dose group had significantly increased levels of IL-6 ($p \leq 0.05$).

The bacterial load was measured across the BAL fluid, lungs and nasal wash. The bacterial load in the BAL fluid (Fig. 3.8D) increased as the challenge dose increased. The bacterial load in the high dose group was significantly higher than the naïve group ($p \leq 0.5$). There was also a dose response in the lungs (Fig. 3.8E) with an increase of around 4 logs between the naïve mice and the high dose mice however this wasn't significant. There was a significant increase in bacterial load in the lungs of the high dose group compared to the low dose group ($p \leq 0.5$). In the nasal wash there was another dose response (Fig. 3.8F) with the high dose group having significantly increased bacterial load in the upper airways compared to the naïve mice ($p \leq 0.05$). When mice were challenged with *A. baumannii* BAL_215 a dose response was seen with higher challenge doses resulting in increased weight loss, inflammation (measured by IL-6) and bacterial burden. However, a challenge dose of at least $1.73x10^7$ CFU per mouse was required to cause significant differences.

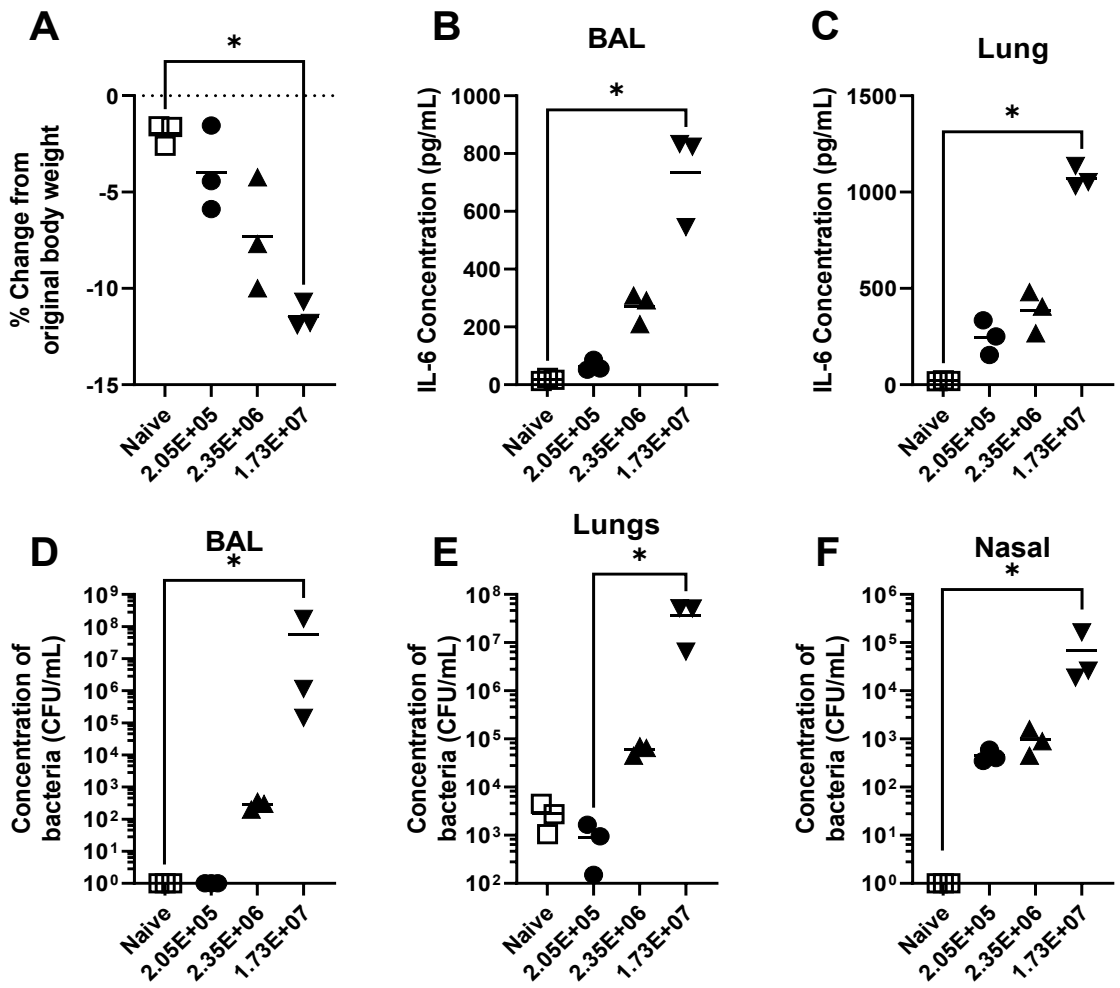


Figure 3.8 | Increasing the challenge dose of *A. baumannii* BAL_215 increases disease severity and bacterial burden. BALB/c mice were intranasally challenged with 3 different doses of clinical strain *A. baumannii* BAL_215 in 100µl or 100µl sterile PBS (naïve) and culled 24 hours later. Change in weight was measured after 24 hour challenge **(A)**. IL-6 concentration in the BAL fluid **(B)** and lungs **(C)** was measured using ELISA. Bacterial load was estimated by serially diluting BAL fluid **(D)**, lung homogenate **(E)** and nasal wash **(F)** and plating out onto LB agar. Kruskal-Wallis tests were used to test for significant differences. **p≤0.05, **p ≤0.01, ***p ≤0.001, ****p ≤0.0001.* Points represent individual animals.

3.2.9 – Intranasal challenge of BALB/c mice with *A. baumannii* BAL_084 causes more severe disease and bacterial burden than ATCC 17978

After establishing the best dose to challenge the mice with to reliably cause disease and increased bacterial loads while not exceeding severity limits, a time course of infection was run. In order to determine whether or not mice would recover from infection, mice were challenged and then culled 4, 24, 48 and 72 hours after challenge. Naïve mice were given sterile PBS intranasally and culled 72 hours later. Mice were weighed throughout the study

to assess the change in bodyweight (Fig. 3.9A). The challenged mice lost significantly more weight than the naïve mice 24, 48 and 72 hours after challenge ($p \leq 0.0001$, $p \leq 0.0001$ & $p \leq 0.01$ respectively). Peak weight loss was seen around 48 hours after challenge, but mice never recovered back to their original weight. The levels of IL-6 were measured in the BAL fluid (Fig. 3.9B) and the peak level of IL-6 was seen 4 hours after challenge which was significantly increased compared to naïve mice ($p \leq 0.0001$). IL-6 levels began to decrease thereafter but were still significantly increased 24 hours after challenge ($p \leq 0.01$). The level of neutrophil infiltration into the lungs was measured (Fig. 3.9C) and peaked between 24 and 48 hours after infection where it was significantly higher than the naïve mice 24 hours after challenge ($p \leq 0.05$), after which it began to decrease.

The bacterial load was measured in the BAL fluid, nasal wash, lungs and spleens of the mice. Peak bacterial recovery from the BAL fluid was 4 hours after challenge (Fig. 3.9D) which was significantly higher than the naïve mice ($p \leq 0.0001$). After this, the mice slowly cleared the bacteria from their lungs until only 2 mice had recoverable bacteria from BAL 72 hours after challenge. The numbers of bacteria recovered from the nasal wash of the challenge mice remained relatively steady, peaking around 4-24 hours after challenge (Fig. 3.9E). The bacterial load recovered from the upper airways was significantly higher in the challenge mice than the naïve mice at 4 and 24 hours after challenge ($p \leq 0.001$ & $p \leq 0.01$ respectively). There were only data for the 4 and 24 hour time points for bacteria recovered from the lungs (Fig. 3.9F) and spleens (Fig. 3.9G) due to plating issues. At 4 hours after challenge there were higher bacterial loads in both the lungs and the spleens than at 24 hours. Intranasal challenge with $1x10^7$ CFU per mouse of *A. baumannii* resulted in severe disease and bacterial burden, causing significantly increased weight loss, inflammation, neutrophil infiltration and bacterial burden compared to naïve mice. Challenged mice also did not fully recover within the time period tested.

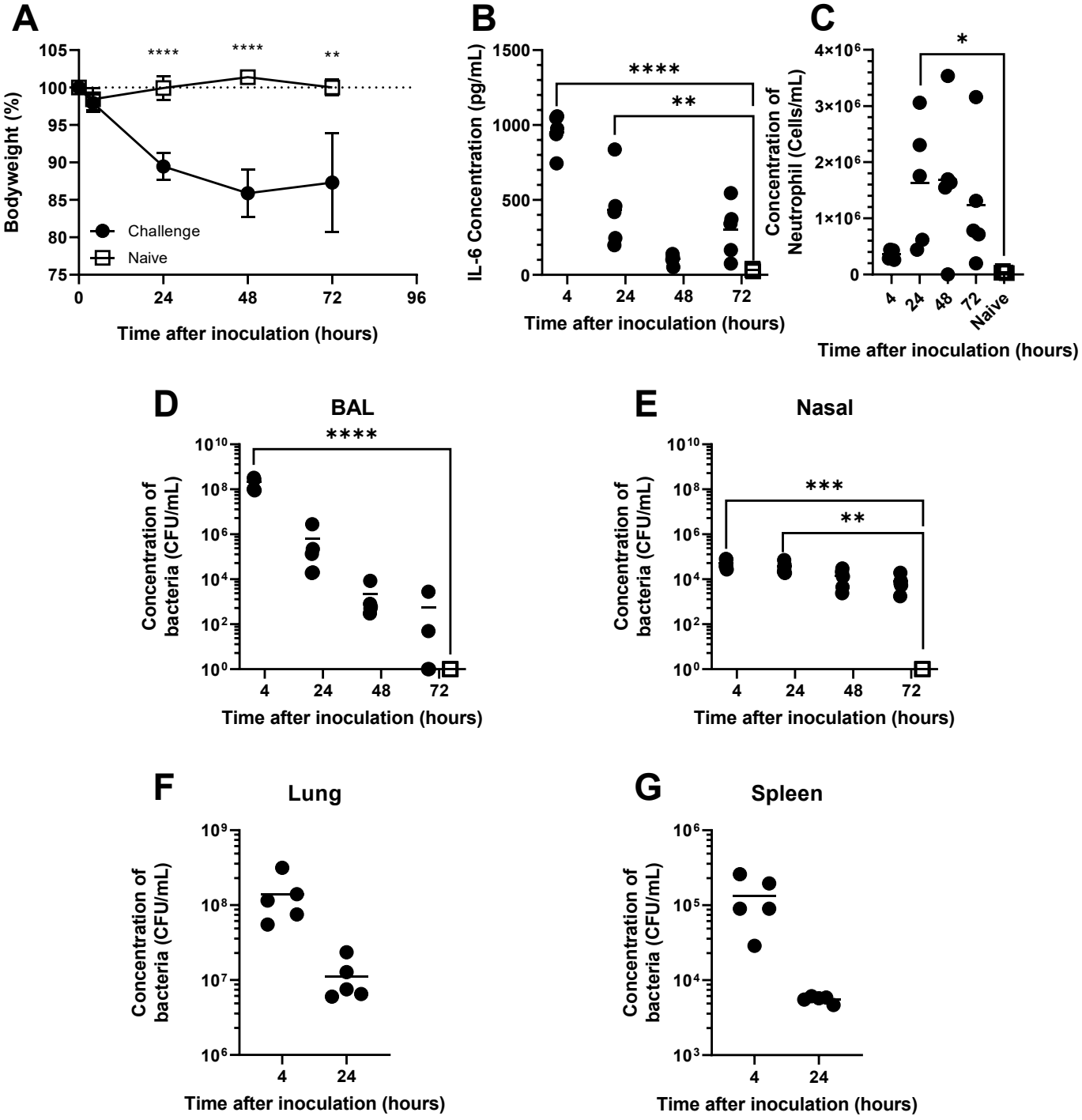


Figure 3.9 | Intranasal infection with *A. baumannii* BAL_084 causes severe disease and systemic colonisation. BALB/c mice were intranasally challenged with 1x10^7 CFU per mouse of clinical strain *A. baumannii* BAL_084 in 100µl or 100µl sterile PBS (naïve) and culled 4, 24, 48 or 72 hours later. Mice were weighed after infection **(A)**. IL-6 concentration in the BAL fluid was measured using ELISA **(B)**. Neutrophil infiltration into the lungs was measured by manually counting haematoxylin and eosin stained cytospin slides **(C)**. Bacterial load was estimated by serially diluting BAL fluid **(D),** nasal wash **(E)**, lung homogenate **(F)** and spleen homogenate **(G)** and plating out onto LB agar. Multiple t tests were used to test for significant differences in change in bodyweight. Kruskal-Wallis tests were used to test for significant differences in IL-6, neutrophil infiltration and bacterial loads. **p≤0.05, **p ≤0.01, ***p ≤0.001, ****p ≤0.0001.* Points represent means of mice (A). Points represent individual animals (B-G).

3.2.10 – Intranasal challenge of BALB/c mice with *A. baumannii* BAL_276 causes severe disease and systemic dissemination

A time course was also performed using *A. baumannii* BAL_276 to see how recovery from infection compared to BAL_084. Mice were challenged intranasally with $1x10^7$ CFU per mouse and culled between 4-72 hours or 7 days after challenge. Mice were weighed throughout challenge (Fig. 3.10A) and challenged mice lost significantly more weight than naïve mice 24, 48 and 72 hours after infection compared to naïve mice ($p \leq 0.0001$, $p \leq 0.0001$ & $p \leq 0.01$ respectively). Peak weight loss was seen 48 hours after challenge, after which mice began to regain weight. The level of IL-6 was measured in the BAL (Fig. 3.10B). The levels of IL-6 in the BAL fluid were significantly higher in the challenge mice compared to the naïve mice 4 and 24 hours after challenge ($p \leq 0.0001$ & $p \leq 0.01$ respectively). After peaking 4 hours after challenge IL-6 levels returned to normal 72 hours after challenge. Neutrophil infiltration into the lungs increased from 4 hours after infection until it peaked at 48 hours (Fig. 3.10C) and had almost returned to normal 72 hours after infection. At both 24 and 48 hours after challenge the infected mice had significantly increased levels of neutrophil infiltration into their lungs compared to naïve mice ($p \leq 0.01$ & $p \leq 0.0001$ respectively). The levels of different cytokines in the BAL fluid 24 hours after challenge were measured by Meso Scale Discovery Immunoassay (MSD) (Fig. 3.10D). All cytokines measured were significantly increased in the challenge mice compared to the naïve mice with p values ranging from 0.05-0.01.

The bacterial loads were measured across the BAL fluid, lungs, nasal wash and spleens of the mice. The bacteria recovered from the BAL fluid peaked 4 hours after infection and decreased after that, being completely cleared by 72 hours after challenge (Fig. 3.10E). Mice had significantly more bacteria recovered from the BAL fluid compared to the naïve mice 4 hours after challenge ($p \leq 0.0001$). The bacteria recovered from the lungs was highest 4 hours after challenge and reduced slightly but was never cleared within 72 hours after challenge (Fig. 3.10F). All time points tested had significantly increased bacterial loads in the challenge mice compared to the naïve mice ($p \leq 0.0001$). The bacteria recovered from the nasal wash also peaked 4 hours after infection and decreased slightly thereafter but was never completely cleared within 72 hours after challenge (Fig. 3.10G). Mice had significantly increased bacterial loads in their upper airways 4 hours after challenge ($p \leq 0.05$). The

bacterial load in the spleen (Fig. 3.10H) peaked 4 hours after challenge and then decreased until all bacteria were cleared from the spleen 72 hours after challenge. At 4, 24 and 48 hours after infection the challenge mice had significantly increased bacterial loads in their spleens compared to naïve mice ($p \leq 0.05$). Bacterial clearance between challenge and 72 hours after challenge across the different sides was compared (Fig. 3.10I). There was a steady decline of bacterial load seen in the BAL fluid and spleen. However, the bacteria in the lungs and nasal wash were being cleared more slowly than in the BAL fluid and the spleen.

In a second study, the time course was extended to 7 days to see if mice regained bodyweight and cleared all bacteria from their lungs and upper airways. Mice were challenged with $1x10^7$ CFU per mouse or given sterile PBS and were weighed before and throughout the challenge (Fig. 3.10J). Challenged mice lost significantly more weight than naïve mice from 1-7 days after challenge $p \leq 0.001$ between 1-4 days after challenge and $p \leq 0.01$ between 5 and 7 days after challenge. Peak weight loss was seen in the challenged mice 48 hours after challenge, after which the mice began to regain weight. However, by day 7 the mice still hadn't regained weight back to their starting bodyweight. At day 7 the bacterial loads were measured across all of the tested sites (Fig. 3.10K). There were no bacteria recovered from the BAL fluid, lungs or spleens of the challenge mice. However, there was still bacteria recoverable from the nasal wash of the challenge mice. Intranasal challenge with $1x10^7$ CFU per mouse of *A. baumannii* BAL_276 resulted in severe disease from which mice were still not fully recovered 7 days after challenge. Mice experienced significant weight loss, inflammation (as measured by MSD), neutrophil infiltration and systemic bacterial burden with prolonged colonisation of the upper respiratory tract.

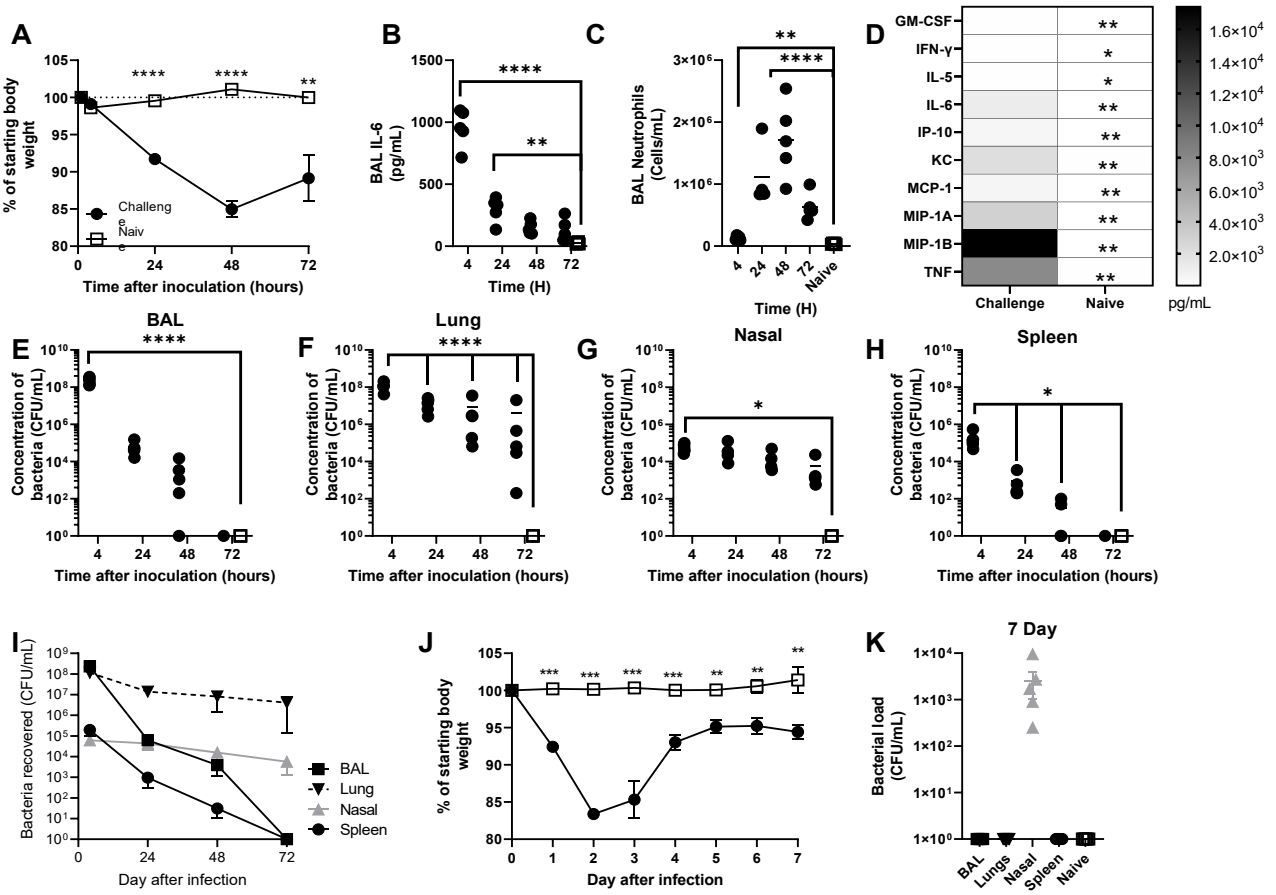


Figure 3.10 | Intranasal infection with *A. baumannii* BAL_276 causes severe disease and systemic colonisation. BALB/c mice were intranasally challenged with 1x10^7 CFU per mouse of clinical strain *A. baumannii* BAL_276 in 100µl or 100µl sterile PBS (naïve) and culled 4, 24, 48 or 72 hours later. Mice were weighed after infection **(A)**. IL-6 concentration in the BAL fluid was measured using ELISA **(B)**. Neutrophil infiltration into the lungs was measured by manually counting haematoxylin and eosin stained cytospin slides **(C)**. Cytokine levels in the BAL fluid were measured at 24 hours by MSD **(D)** Bacterial load was estimated by serially diluting BAL fluid **(D),** lung homogenate **(E)**, nasal wash **(F)** and spleen homogenate **(G)** and plating out onto LB agar. Comparison of bacterial clearance across the different compartments **(I)**. The study was repeated to take out to 7 days after challenge. Mice were weighed after challenge **(J)**. Bacterial load 7 days after challenge **(K)**. Multiple t tests were used to test for significant differences in change in bodyweight. Kruskal-Wallis tests were used to test for significant differences in IL-6, neutrophil infiltration, cytokines and bacterial loads. **p≤0.05, **p ≤0.01, ***p ≤0.001, ****p ≤0.0001.* Points represent means of mice (A, D, I & J). Points represent individual animals (B, C, E-H & K).

3.3 – Discussion

Results from this chapter have shown that optical density is a good estimate for bacterial concentration in liquid culture and that although *A. baumannii* ATCC 17978 is able to cause disease in BALB/c mice it is limited. It is difficult to achieve reliable and reproducible infection with *A. baumannii* ATCC 17978 in BALB/c mice. Mice recover quickly and bacteria are cleared within 48 hours of infection. Comparatively, clinical strains caused more severe disease in mice and greater levels of colonisation. At equivalent challenge doses, BAL_276 more reliably disseminated to the spleen from the lungs and resulted in increased clinical scores, with increased bacterial burden, inflammation and neutrophil infiltration into the lungs. It also took BALB/c mice more time to recover from infection with clinical strains, with mice still not returning to their original bodyweight and bacteria still remaining in the upper airways 7 days after challenge with BAL_276.

Optical density is widely used to estimate the concentration of bacteria within liquid culture[152]. The *in vitro* growth studies performed in this chapter have shown that the optical density of *A. baumannii* within liquid culture and concentration of clinical strains of bacteria closely reflect each other during growth. The OD_{600} and CFU/ml appear to be most similar during the log phase of growth, when the bacteria are growing exponentially with minimal cell death. This allows for a more accurate estimation of the concentration of bacteria in culture for subsequent dilution to different challenge doses as required to begin developing the infection models.

I have consistently seen that no matter what strain of *A. baumannii* used, disease severity and bacterial burden in BALB/c mice increases as the dose increases. Both disease severity and bacterial burden would be expected to increase until the dose reached a lethal level. Additionally, clinically relevant strains isolated from hospital outbreaks caused more severe disease and further increased bacterial burden in BALB/c mice compared to the laboratory reference strain *A. baumannii* ATCC 17978. The difference in disease severity and bacterial burden between *A. baumannii* ATCC 17978 and clinical strains when given at the same dose is most likely down to acquired virulence factors. *A. baumannii* is known for its capability to evolve rapidly, being able to take up extracellular DNA through its natural competence and incorporate the DNA into its genome as well as undergoing horizontal gene transfer with other organisms[153–156] . *A. baumannii* mobile genetic elements are known for encoding

antibiotic resistance genes but can also contain genes involved in iron acquisition, host cell invasion, haemolytic activity, biofilm formation and host cell adhesion[155]. Outbreak causing strains of *A. baumannii* have been shown to contain significantly more mobile genetic elements compared to non-outbreak strains. Additionally, virulence genes acquired by *A. baumannii* have been found to have derived from different bacterial organisms. This suggests these genes have been acquired through transposons and other mobile elements[154]. Due to selection pressures the pan genome of *A. baumannii* evolved towards increased antibiotic resistance. However, the high levels of genome plasticity seen in *A. baumannii* provides high potential for the acquisition of new virulence genes in the future[156].

It is very important to use modern clinically relevant strains in model development to provide a better understanding of the current mechanisms of infection when developing new vaccines. This results in the identification of more relevant antigen targets and more effective vaccines that work against currently circulating strains rather than a strain that was isolated decades ago like ATCC 17978. For example, *A. baumannii* ATCC 17978 is antibiotic sensitive and was isolated around 70 years ago and contains the pAB3 plasmid; a large conjugative plasmid containing one antibiotic resistance cassette. Since then, the pAB3 plasmid has gained 11 more resistance cassettes evolving into the pAB04 plasmid[157]. Another example is the secretion of glycoprotease CpaA by clinically relevant strains today[157,158] that is not found in ATCC 17978[157]. Although antibiotic resistance is not typically considered a virulence factor, in the case of *A. baumannii* infections increased antibiotic resistance is the biggest factor in poor clinical outcomes as a result of severely reduced treatment options[155].

Bacterial challenge with clinical *A. baumannii* strains and particularly BAL_276 resulted in a more severe and more reliable infection (Table. 3.1). This makes for a better challenge model as correlates of infection are more consistently raised when mice are challenged with clinical strains. This therefore allows for better measurement of vaccine efficacy as reductions in bacterial loads or inflammation will be greater and easier to see. As mice are specific pathogen free and culture methods are selective for *A. baumannii*, the bacteria recovered from tissues or BAL is as a result of the intranasal challenge. The high amounts of bacteria recoverable from the lungs and airways are reproduceable and remain consistently high when mice are challenged with the clinical strains. The clinical strains reliably result in dissemination of bacteria from the lungs to the spleen as well as having recoverable bacteria 24 hours after infection in all mice, indicative of more severe infection. It took mice more time to clear clinical strain bacteria from all of the tested physiological sites compared to the ATCC 17978 strain, giving a larger window of time for which protection can be assessed. There was also increased inflammation in the lungs of mice challenged with clinical strains with increased levels of inflammatory cytokines and neutrophil infiltration into the lungs, which ordinarily are found in the blood and pulmonary capillaries but begin to migrate to interstitial compartments and air spaces of the lungs within hours of infection[150], as seen here. The clinical strains also result in prolonged *A. baumannii* colonisation of the upper airways. Suggesting the clinical strains provide a more robust infection model with better and more correlates of infection to test and try to reduce that would be better suited for assessing vaccine efficacy than the ATCC 17978 strain.

Table 3.1 | Summary of *In vivo* disease severity of the 5 *A. baumannii* strains used. A summary of disease severity in BALB/c mice caused by each *A. baumannii* strain. Severity depicted as + (mild), ++ (moderate), +++ (severe) or – (no data available).

Bacterial strain	Weight loss	Inflammation (IL-6)	Bacterial dissemination
ATCC-17978	+	++	+
BAL_276	+++	+++	+++
BAL_084	+++	+++	++
BAL_191	++	++	-
BAL_215	+++	++	-

There were a number of limitations to the work performed within this chapter. The intranasal infection was a source of variation as the concentration of bacteria in the challenge dose must be calculated retrospectively, resulting variation in the challenge doses. There was also variation in the quality of the inoculum. Clinical strains appeared to be less effective after being stored in the freezer for multiple years. New stocks were grown and stored so that new *in vitro* growth assays could be performed and challenge doses re-titred until previous *in vivo* results were reproducible. This could have been due to low stability of the clinical isolates or loss of bacterial viability[159–161] both factors known affect bacterial storage and recovery. Inconsistent storage conditions, such as temperature fluctuations, can result in plasmid instability which could occur as a result of genetic damage over time[159]. Additionally loss of cell viability can result in selection from the small remaining population[162]. Further variation occurs as a result of intranasal challenge as it is impossible to know how much bacteria ends up in the lungs or how equally distributed it is between each lung. Additionally, intranasal inoculation has the potential for expulsion of inoculum from the nose adding more variability[150,163]. To reduce experimental variability and ensure bacteria enter the lungs a large inoculation volume was used.

Murine lungs differ from humans anatomically and physiologically, there are also differences between the pattern recognition receptors and mice also possess lower levels of circulating neutrophils compared to humans. These factors could influence the deposition and clearance of bacteria resulting in different infection pathologies and severities between humans and mice. Between different strains of mice different responses to infection are often also seen, so results should not be generalised to say similar results will be seen across all strains of mice [150]. The model developed here is an acute model that uses large doses of bacteria, causing disease to develop in mice soon after challenge and also rapid clearance of bacteria from the lungs and spleen. To develop a less acute model, bacteria can be passaged through mice to alter its virulence potential and increase capacity to persist within the host[164]. This would allow for smaller challenge doses and an infection that more closely mimics human disease. The number of similarities outweighs the differences in murine lower respiratory tract infection models[150], particularly for their use in pre-clinical research developing an effective vaccine. The mice challenged with clinical strains of *A. baumannii*

develop measurable signs of respiratory tract infection to determine whether a vaccine is effective.

The work performed within this chapter was an essential first step in developing an *A. baumannii* vaccine. Using *in vitro* growth curves, clinical *A. baumannii* strains and BALB/c mice we were able to develop an effective and robust *in vivo* infection model that could be used for testing vaccine efficacy in the next steps of the project.

4 – Comparison of vaccination routes in BALB/c mice immunised with OMVs derived from three A. baumannii strains

4.1 – Introduction

Current methods of treatment for *A. baumannii* infection are becoming increasingly less effective with clinical strains commonly being resistant to a broad range of antibiotics including β-lactams, fluoroquinolones and aminoglycosides[165]. Worryingly, strains are even growing resistance to the last resort antibiotic colistin[165] with rates of MDR reported to range between 47% at the lowest in North America and 93% at the highest in Europe and the Middle East[166]. With such high rates of antimicrobial resistance and high propensity to develop new resistances vaccines provide a promising alternative in the prevention of MDR *A. baumannii* infections. As it stands, there are no approved vaccines for use but lots of research is being done to find and develop a novel vaccine against *A. baumannii*[167–174]. A successful vaccine would help to prevent infection with *A. baumannii* and indirectly help to reduce the use of antibiotics by reducing symptoms and preventing proliferation of bacteria to help reduce the numbers of mutations resulting in antimicrobial resistance[103].

During normal growth *A. baumannii* produce OMVs, which are spherical proteoliposomes made up of outer membrane proteins, lipopolysaccharide, phospholipids and periplasmic content[175,176]. OMVs are highly immunogenic and can interact with many different types of host cells resulting in a range of inflammatory responses[177]. OMVs have many benefits in their potential use as vaccines as proteins are displayed in their native conformation, they have high levels of immunogenicity and they are non-infectious[175–177]. OMVs are also easy to isolate through centrifugation or precipitation[178]. Additionally, through genetic engineering techniques OMVs can be easily altered to display or anchor carbohydrate or protein antigens on their surface as well as by remodelling the LPS on their surface making them less reactogenic[178]. Bexsero is currently the only vaccine approved for human use containing OMVs. In human immunogenicity studies the recombinant protein group B meningitis vaccine (rMenB) induced a bactericidal antibody response in more than 80% of patients which was effective against three out of seven reference group strains. The addition of the Porin A expressing OMV into the vaccine formulation resulted in more than 90% of patients developing antibody titres over 4-fold greater than with rMenB alone for five out of the seven strains and 70% of patients developed a bactericidal antibody response against a sixth strain[179]. With the ease with which they can be isolated and engineered, OMVs have huge

potential in the development of new vaccines and in helping to combat antimicrobial resistance.

One of many additional and important factors to consider when developing a vaccine is the delivery route. When choosing a route of vaccination it's important to consider not only what gives the best immune response, but also the practicalities and safety[180]. Mixed results have been seen when comparing the efficacy of intramuscular vaccinations compared to subcutaneous, with some studies showing intramuscular vaccination having fewer reactions at the injection site and better antibody responses than subcutaneous vaccination and other studies showing there was no difference or even showing the opposite[180]. It is also assumed that antigens each have their own ideal route of immunisation[180], therefore it is down to the vaccine developer to weigh up the pros and cons of each and find the best route of vaccination. One murine study looking into different routes of vaccination of *Neisseria meningitidis* OMVs found there to be no discernible superiority between vaccination by intramuscular, subcutaneous or intraperitoneal injection[180].

Mucosal surfaces, such as the respiratory tract, have highly specialised innate and adaptive responses to protect against pathogens and control growth of commensal microorganisms[181]. Although locally produced IgG and IgM are important in humoral immunity at mucosal surfaces, secretory IgA has been shown to be key in developing a protective humoral response against mucosal infection[181]. Mucosal vaccinations elicit good local mucosal and systemic immune responses and would be easier to administer than injectable vaccines, resulting in a decreased risk of infection[181,182]. Additionally, removing the requirement for injection could also lead to increased vaccine uptake by the general population. Therefore, great effort is being put into producing safe and effective vaccines that can be delivered orally or intranasally[181]. Intranasal vaccination requires less antigen compared to oral vaccination[181] and in humans results in regional nasal and upper airway mucosal IgA response[182]. One study comparing oral and nasal vaccination with cholera toxin B subunit vaccination showed despite both oral and intranasal vaccines both eliciting good systemic IgG and IgA responses, only intranasal vaccination resulted in a significant increase of antigen specific IgA in nasal secretions[183]. The intranasal route elicited a later onset antibody response than the oral route however, the response was much longer lived after intranasal administration[183]. Studies have shown that subcutaneous vaccination results in

protective systemic and mucosal antigen-specific antibody responses in macaques and calves with calves also developing mucosal cell-mediated responses[181]. In the case of adenovirus-based coronavirus vaccines, studies have shown that intranasal vaccination was better than intramuscular vaccination. Although intranasal vaccination induced a systemic humoral immune response of comparable strength to intramuscular vaccination[184], intranasal vaccination also induced a local mucosal IgA response and created resident memory CD8 T cells in the airways and lungs[184,185]. This is of particular importance when you consider that increased levels of mucosal IgA, serum-neutralising antibodies and lung resident memory T cells are all associated with increased protection against infection as well as reduced viral loads and pulmonary damage[184,185].

In this chapter we wanted to determine whether *A. baumannii* derived OMVs could protect against homologous challenge using both the laboratory reference strain ATCC 17978 and two relevant clinical strains. Additionally, we wanted to investigate the antibody responses and levels of protection given by different routes of immunisation.

4.1.2 – Chapter aims and hypothesis

I hypothesise that immunising BALB/c mice with *A. baumannii* derived OMVs provides protection against intranasal infection and the route of immunisation will alter the quality of the immune response.

Aims

1. Immunise mice with *A. baumannii* ATCC 17978 derived OMVs and assess protective efficacy via homologous intranasal challenge;

2. Immunise mice with *A. baumannii* clinical strain derived OMVs and assess protective efficacy via homologous intranasal challenge;

3. Determine how the route of immunisation changes the immune response and how that affects protective efficacy via homologous intranasal challenge.

4.2 – Results

4.2.1 – *A. baumannii* ATCC 17978 OMVs provide limited protection against homologous infection.

To establish whether or not *A. baumannii* ATCC 17978 OMVs were protective against infection, BALB/c mice were immunised intramuscularly in a prime boost approach with a 30-day interval. The mice were then intranasally challenged with *A. baumannii* ATCC 17978 26 days after the second dose of OMVs. Blood was collected from the mice via tail bleeds before boosting and from terminal bleed when mice were culled 24 hours after challenge. The blood was allowed to clot and then centrifuged to collect the serum for ELISA. *A. baumannii* ATCC 17978 OMVs were used to coat the plate and measure the total OMV specific IgM and IgG titres. There was little difference in the amount of IgM present in the sera of OMV immunised mice and PBS mice (Fig. 4.1 B). The total levels of OMV specific IgG in the OMV immunised mice increased between the prime and boost (Fig. 4.1 C) and the level of OMV specific IgG in the serum at day 56 was significantly higher than that of the PBS group ($p \leq 0.05$). The bodyweight of the mice was measured over the 24 hour challenge and change in bodyweight was calculated (Fig. 4.1 D). There was little difference in the percent change in weight of the immunised mice compared to the PBS mice. IL-6 levels in the BAL fluid were measured by ELISA (Fig. 4.1 E), OMV immunised mice had significantly lower levels of IL-6 in the lungs compared to the PBS mice ($p \leq 0.05$). Cytospin slides were made from BAL fluid and neutrophils were counted (Fig. 4.1 F) but there was no difference in neutrophil infiltration into the lungs between the immunised and PBS mice. The bacterial load in the BAL fluid (Fig. 4.1 G) showed a significant reduction in the immunised mice compared to the PBS mice ($p \leq 0.05$). The bacterial load was also measured in the lungs (Fig. 4.1 H) however, despite around a half log reduction in bacterial load in the lungs of the OMV mice compared to the PBS group, this was not significant. Immunising mice with *A. baumannii* ATCC 17978 OMVs induced an immune response in BALB/c mice that was somewhat protective against challenge with significantly increased OMV specific IgG levels in serum, significantly reduced inflammation in the lungs and significantly fewer bacteria recovered from the BAL fluid.

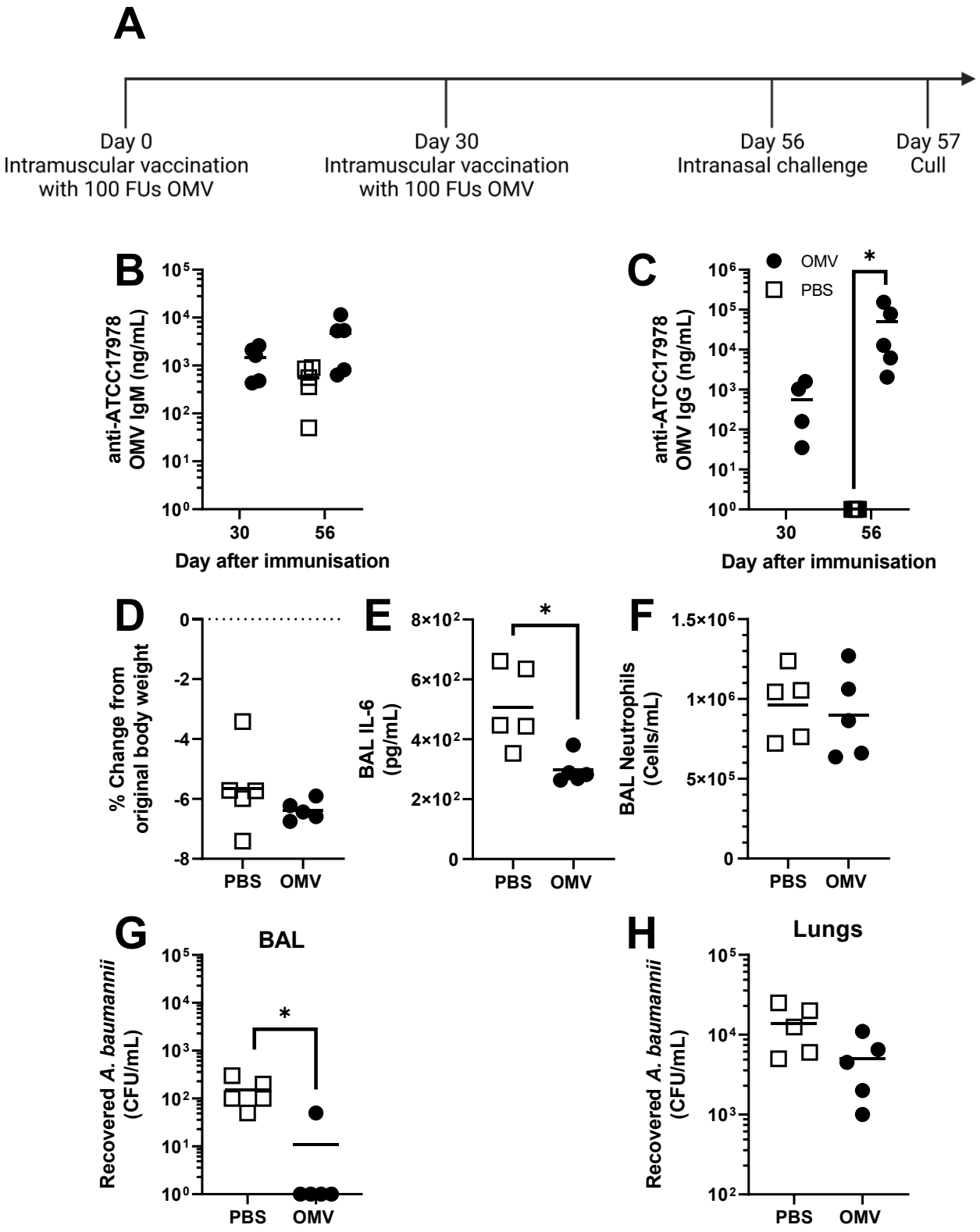


Figure 4.1 | OMVs from *A. baumannii* ATCC 17978 provide some protection against homologous challenge. Adult BALB/c mice were intramuscularly injected with 100 fluorescence units of ATCC 17978 OMV (OMV) or PBS (PBS) at day 0 and boosted at day 30 **(A)**. Anti-ATCC 17978 OMV IgM **(B)** or IgG **(C)** were measured in sera by ELISA. At day 56 mice were intranasally dosed with $5x10^6$ CFU *A. baumannii* ATCC 17978 and culled 24 hours later. Weight **(D)**, IL-6 **(E)** and neutrophil counts **(F)** were measured 24 hours after infection. Bacterial load at 24 hours in BAL **(G)** and lungs **(H)**. Mann-Whitney tests were used to test for significant differences. **p≤0.05, **p ≤0.01, ***p ≤0.001, ****p ≤0.0001.* Points represent individual animals.

4.2.2 – *A. baumannii* BAL_276 derived OMVs provide protection against homologous intranasal challenge.

A. baumannii ATCC 17978 OMVs provided some protection against challenge OMVs, but it wasn't yet known if OMVs derived from the clinical strain *A. baumannii* BAL_276 also protected BALB/c mice from infection. Mice were immunised intramuscularly in a prime boost approach with 21 day intervals and challenged intranasally with *A. baumannii* BAL_276 21 days after the second dose. Blood was collected from a terminal bleed and the serum was used for ELISAs. Plates were coated with either BAL_276 or BAL_084 OMVs and total specific IgM was measured (Fig. 4.2 B). The OMV immunised mice had significantly more IgM binding to BAL_276 OMVs ($p \leq 0.001$) and also BAL_084 OMVs ($p \leq 0.0001$) compared to the PBS mice. This was repeated for total specific IgG levels with similar results seen (Fig. 4.2 C). The BAL_276 OMV immunised mice had significantly increased levels of BAL_276 OMV specific IgG ($p \leq 0.01$) and BAL_084 OMV specific IgG ($p \leq 0.05$) compared to the PBS mice. Mice were also weighed either side of the 24 hour challenge, but there was no difference in weight loss between the immunised and PBS mice (Fig. 4.2 D). The level of IL-6 in the BAL fluid was measured by ELISA (Fig. 4.2 E), but there was no difference between the immunised mice or the PBS mice. Total white blood cell count in the BAL fluid was estimated (Fig. 4.2 F), with immunised mice having slightly increased levels but this was not significant. The bacterial burden was measured in the BAL fluid (Fig. 4.2 G), lungs (Fig. 4.2 H), spleen (Fig. 4.2 I) and nasal wash (Fig. 4.2 J). Immunised mice had significantly less bacteria recovered from all sites tested ($p \leq 0.05$-0.01). Intramuscular immunisation of BALB/c mice with *A. baumannii* BAL_276 OMVs elicited a significant antibody response, which was cross reactive and greater than that seen in *A. baumannii* ATCC 17978 immunisation. Additionally, the bacterial load was significantly reduced across all tested sites, a further improvement seen in BAL_276 immunisation compared to ATCC 17978.

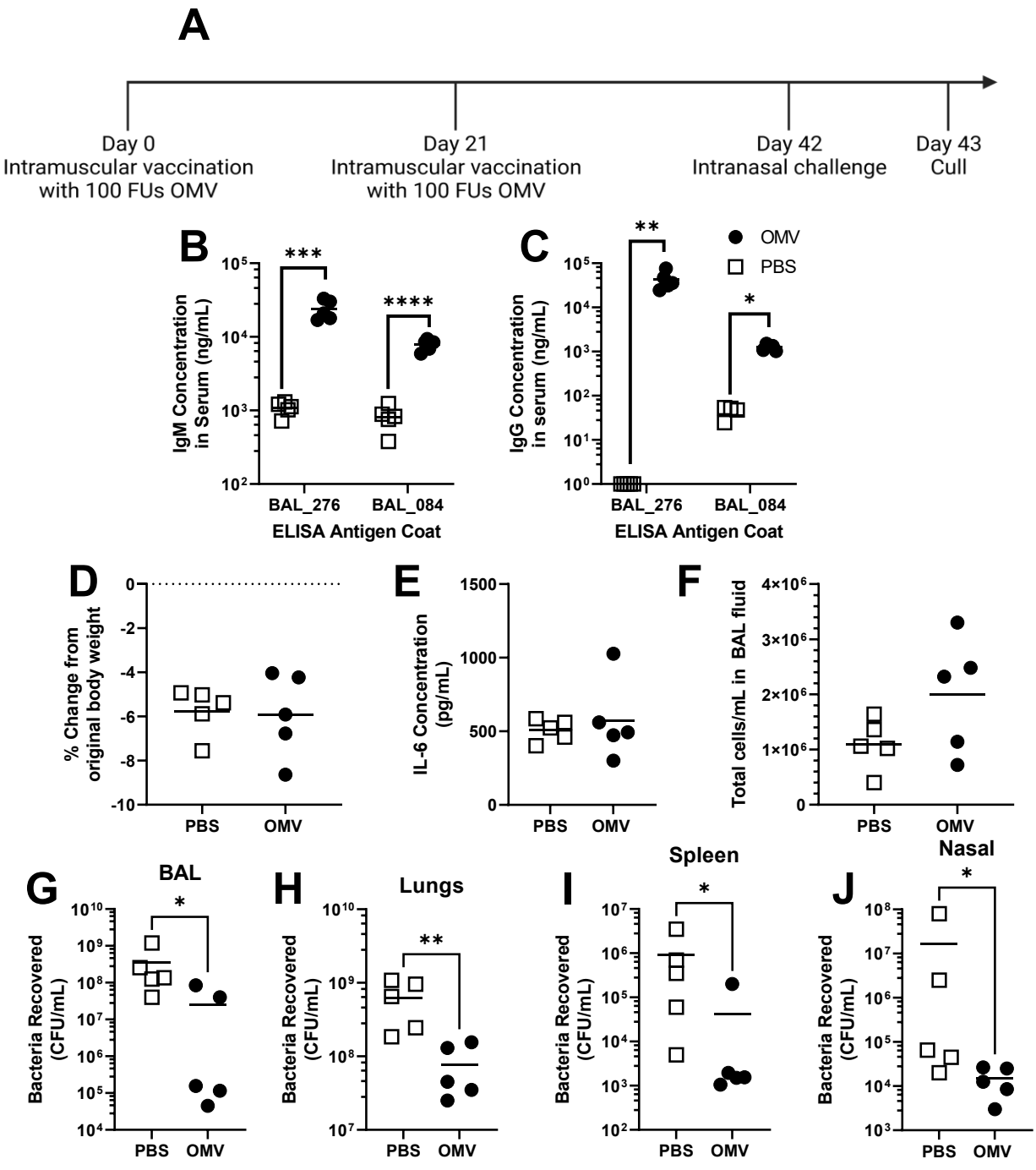


Figure 4.2 | OMVs from *A. baumannii* BAL_276 provide protection against homologous challenge. Adult BALB/c mice were intramuscularly injected with 100 fluorescence units of BAL_276 OMV (OMV) or PBS (PBS) at day 0 and boosted at day 21 **(A)**. Anti-BAL_276 and BAL_084 OMV IgM **(B)** or IgG **(C)** in sera at day 42 were measured by ELISA. At day 42 mice were intranasally dosed with $1x10^7$ CFU *A. baumannii* BAL_276 and culled 24 hours later. Weight **(D)**, IL-6 **(E)** and cell counts **(F)** were measured 24 hours after infection. Bacterial load at 24 hours in BAL **(G)** and lungs **(H)**, spleen **(I)** and nasal wash **(J)** . Mann-Whitney tests were used to test for significant differences. **p≤0.05, **p ≤0.01, ***p ≤0.001, ****p ≤0.0001.* Points represent individual animals.

4.2.3 – Intramuscular immunisation reduced bacterial load in lungs during challenge with *A. baumannii* BAL_276

Mice were immunised in a prime boost approach with *A. baumannii* BAL_276 OMVs with 21 day intervals. The mice were challenged intranasally with *A. baumannii* BAL_276 21 days after the second vaccine dose and were culled 24 or 48 hours after challenge. Mice were weighed throughout the challenge (Fig. 4.3 A) both groups of mice that were challenged with bacteria lost significantly more bodyweight than the naïve mice ($p \leq 0.0001$) however, there was no difference in weight loss between the PBS and OMV immunised mice. Bronchoalveolar lavage and nasal wash were performed 24 and 48 hours after challenge. Lungs and spleens were also dissected out and homogenised. Bacterial load in the BAL fluid was higher in both the PBS and OMV mice compared to the naive mice 24 and 48 hours after challenge (Fig. 4.3 B). Although the bacterial load in the BAL fluid of the OMV immunised mice was lower than the PBS group, the difference was not significant. Bacteria recovered from the BAL fluid of the PBS and OMV immunised mice decreased between 24 and 48 hours after challenge. The bacteria recovered from the nasal wash was increased in the PBS and OMV immunised mice compared to the naïve mice (Fig. 4.3 C). The amount of bacteria recovered from the nasal wash in the OMV immunised mice was lower than the PBS mice 24 hours after challenge, but the difference wasn't significant. There was little difference between the bacterial loads in the nasal wash of the PBS and OMV immunised mice 48 hours after infection. There was no difference in the amount of bacteria recovered from the nasal wash of the OMV immunised mice between 24 and 48 hours after challenge, but there was a slight reduction in the amount of bacteria recovered from the PBS mice 24 and 48 hours after challenge. Bacterial loads in the lung homogenate were much higher in the PBS and OMV groups compared to the naïve mice both 24 and 48 hours after challenge (Fig. 4.3 D). There was no difference in the bacterial load in the lungs of either the PBS or OMV mice 24 hours after challenge. However, 48 hours after challenge the bacterial load in the lungs of the OMV mice decreased while the bacterial load in the lungs of the PBS mice remained unchanged, but the difference was not significant. The bacterial load in the spleens was also measured (Fig. 4.3 E) but the OMV immunised mice had increased bacterial loads compared to the other two groups at both time points. The OMV immunised mice had reduced bacterial loads compared to the PBS mice and mice appeared to be clearing

bacteria from the lungs more quickly. However, the intramuscular OMV immunisation appears to do little to protect against colonisation of the upper airways and did not prevent dissemination to the spleen.

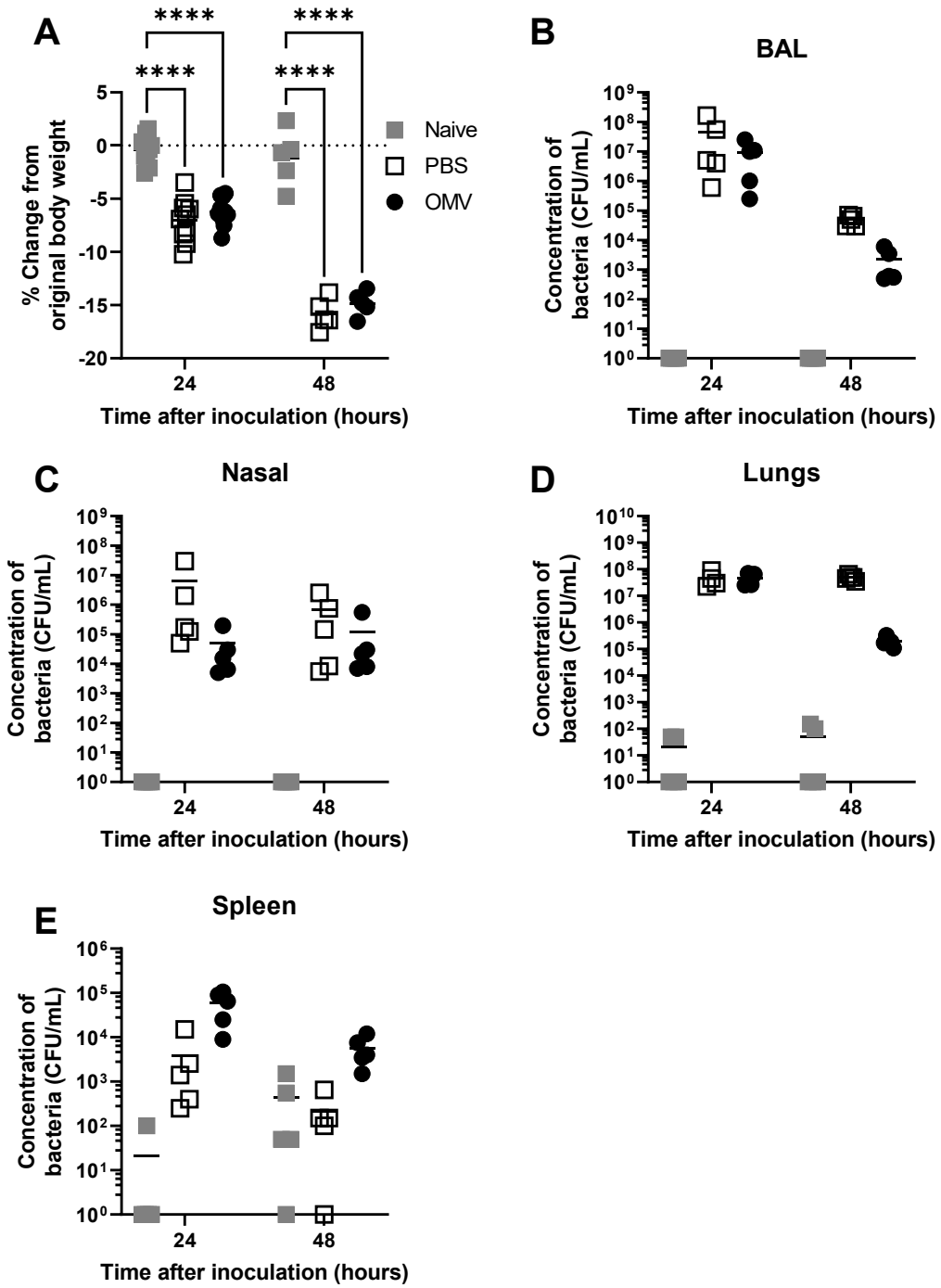


Figure 4.3 | OMVs from *A. baumannii* BAL_276 provide protection against homologous challenge. Adult BALB/c mice were intramuscularly injected with 100 fluorescence units of BAL_276 OMV (OMV) or PBS (PBS) at day 0 and boosted at day 21. At day 42 mice were intranasally dosed with 1x10^7 CFU *A. baumannii* BAL_276 and culled 24 or 48 hours later. Weight **(A)** was measured over the 24 and 48 hour challenge. Bacterial load at 24 and 48 hours in BAL **(B)**, nasal wash **(C)**, lungs **(D)** and spleen **(E)** . Two-way ANOVAs were used to test for significant differences in IgG and IgM concentrations in serum. **p≤0.05, **p ≤0.01, ***p ≤0.001, ****p ≤0.0001.* Points represent individual animals.

4.2.4 – *A. baumannii* BAL_084 derived OMVs did not protect against homologous intranasal challenge.

A second clinical strain, *A. baumannii* BAL_084, was then used to make OMVs and immunise BALB/c mice intramuscularly to investigate whether the OMVs could protect against infection. Mice were immunised in a prime boost approach with 21 day intervals and blood was collected from the terminal bleed. Plates were coated with *A. baumannii* BAL_084 OMVs and total IgG was measured using ELISA (Fig 4.4 A). Mice immunised intramuscularly with OMV had significantly increased levels of BAL_084 OMV specific IgG compared to PBS mice ($p \leq 0.01$). ELISAs were also performed to quantify the amount of BAL_084 specific IgM present in the serum (Fig. 4.4 B). OMV immunised mice had significantly increased levels of BAL_084 specific IgM compared to the PBS mice ($p \leq 0.01$). Mice were challenged intranasally with *A. baumannii* BAL_084, or sterile PBS (Naïve), 21 days after the second vaccination and culled 24 hours after challenge. Mice were weighed throughout the challenge (Fig. 4.4 C) with both the PBS and OMV groups losing significantly more weight than the naïve mice ($p \leq 0.05$). Bronchoalveolar lavage and a nasal wash were performed and the lungs and spleens were dissected out of mice. The BAL fluid and nasal wash as well as the lung and spleen homogenates were serially diluted and plated onto selective agar to determine bacterial loads 24 hours after challenge. Although the bacterial loads in the BAL fluid (Fig. 4.4 D), nasal wash (Fig. 4.4 E), lungs (Fig. 4.4 F) and spleen (Fig. 4.4 G) were all significantly higher in the PBS mice compared to the naive mice ($p \leq 0.05 – 0.01$) there wasn't much difference in the bacterial loads of the OMV immunised mice compared to the PBS mice in the lungs or upper airways. There was a slightly reduced bacterial load in the spleens of the immunised mice compared to the PBS mice, but this was not significant. The BAL_084 OMVs elicited a significant antibody response in BALB/c mice compared to the PBS treated mice however, this did not transfer to high levels of protection against infection with bacterial loads being very similar across the tested sites.

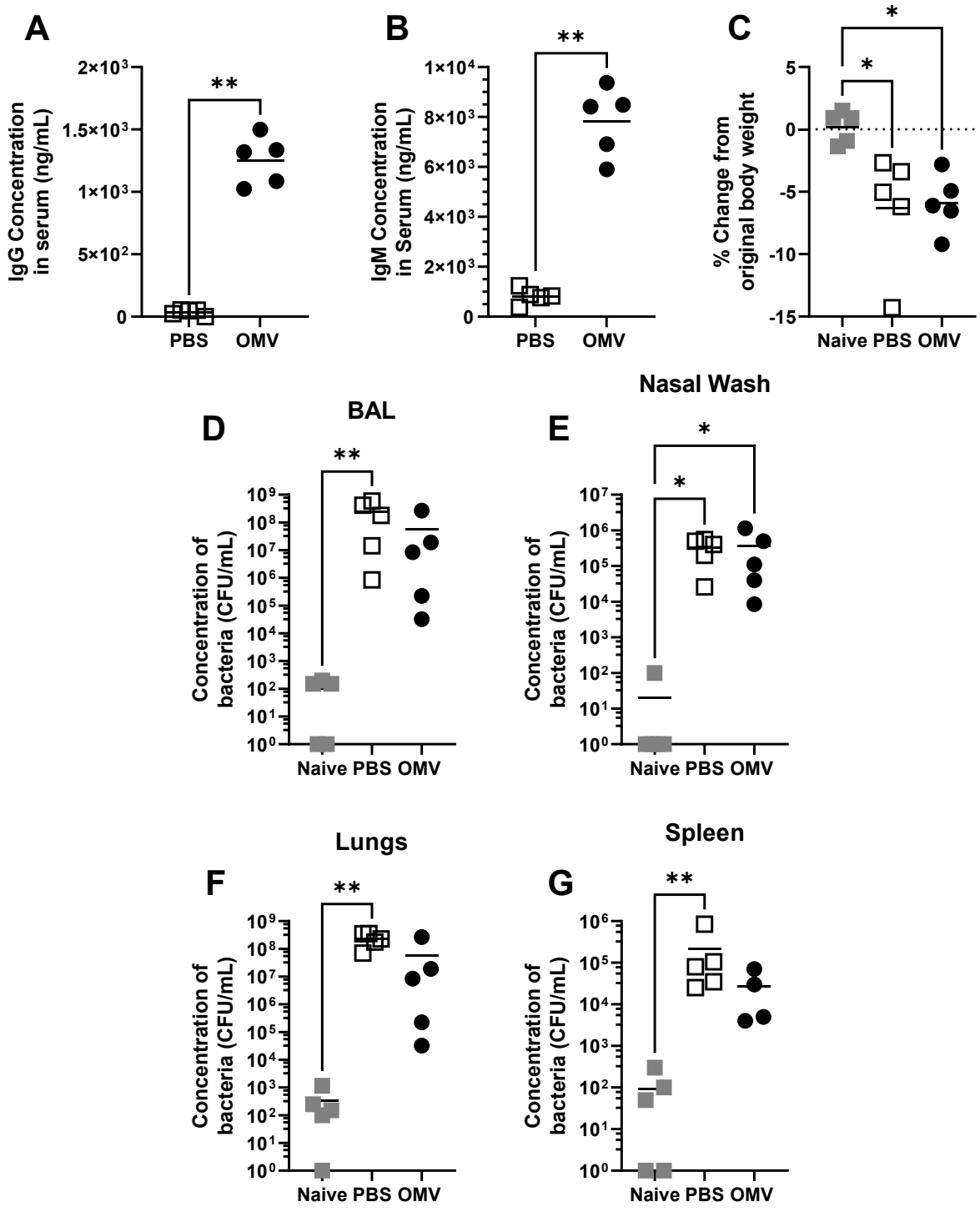


Figure 4.4 | OMVs from *A. baumannii* BAL_084 provide no protection against homologous challenge. Adult BALB/c mice were intramuscularly injected with 100 fluorescence units of BAL_084 OMV (OMV) or PBS (PBS) at day 0 and boosted at day 21. Anti-BAL_084 OMV IgG **(A)** or IgM **(B)** in sera at day 42 were measured by ELISA. At day 42 mice were intranasally dosed with $1x10^7$ CFU *A. baumannii* BAL_084 and culled 24 hours later. Weight **(C)** was measured over the 24 hour challenge. Bacterial load at 24 hours in BAL **(D)** nasal wash **(E)**, lungs **(F)** and spleen **(G)** . Kruskal Wallis was used to test for significant differences in bacterial load and change in weight. Mann-Whitney tests were used to test for significant differences in IgG and IgM concentrations in serum. **p≤0.05, **p ≤0.01, ***p ≤0.001, ****p ≤0.0001.* Points represent individual animals.

4.2.5 – Intramuscular immunisation reduced bacterial load in the spleen during 48-hour challenge with *A. baumannii* BAL_084

To better understand how *A. baumannii* BAL_084 vaccinated immunised mice cleared infection mice were intranasally challenged for 24-48 hours before culling. Mice were vaccinated in a prime boost approach with 21 day intervals and challenged intranasally with *A. baumannii* BAL_084 21 days after the second dose. Mice were culled 24 or 48 hours after challenge and their weight was measured over the course of the infection (Fig. 4.5 A). Both the OMV immunised mice and the PBS lost significantly more weight than the naïve mice 24 hours after challenge ($p \leq 0.0001$). The OMV immunised lost a similar amount of weight to the PBS mice 24 hours after challenge. However, 48 hours after challenge although both the OMV and PBS mice lost significantly more weight than the naïve mice ($p \leq 0.0001$) the OMV immunised mice lost significantly less weight than the PBS mice ($p \leq 0.01$). Bronchoalveolar lavage and nasal wash were performed 24 and 48 hours after challenge. Lungs and spleens were also dissected out and homogenised. The bacteria recovered from the BAL fluid was much higher in the OMV and PBS mice compared to the naïve mice both 24 and 48 hours after challenge (Fig. 4.5 B). However, both the OMV immunised and PBS groups of mice had very similar bacterial loads in their BAL fluid 24 hours after challenge which remained high 48 hours after challenge. Additionally, the amount of bacteria recovered from the nasal wash of the PBS and OMV immunised mice was much higher than that seen in the naïve mice at both 24 and 48 hours after challenge (Fig. 4.5 C). The OMV immunised mice had slightly increased bacterial loads in their upper airways compared to the PBS mice but both mice had increased numbers of bacteria in their upper airways 48 hours after infection than at 24 hours after infection. Similar results were seen in the lungs of the mice (Fig. 4.5 D). The PBS and OMV immunised mice had high levels of bacteria recovered from their lungs compared to the naïve mice at both 24 and 48 hours after infection. The levels of bacteria recovered from the lungs of the PBS and OMV immunised mice were very similar at both time points and there was an increase of bacteria recovered 48 hours after infection compared to 24 hours after infection. The bacterial loads in the lungs of the PBS and OMV immunised mice were significantly higher than the naïve mice 48 hours after infection ($p \leq 0.001$ and $p \leq 0.05$ respectively). Finally, the bacterial loads in the spleens of the PBS mice were much higher than the bacterial loads in the spleens of both the naïve and OMV

immunised mice 24 and 48 hours after infection (Fig. 4.5 E). At 48 hours after infection the PBS mice had significantly increased bacterial loads in their spleens compared to the naïve mice ($p \leq 0.0001$) and the OMV immunised mice ($p \leq 0.0001$). Intramuscular immunisation with *A. baumannii* BAL_084 derived OMVs followed by 24 and 48 hour homologous intranasal challenge resulted in little to no additional bacterial clearance in the airways or lungs. However, weight loss and bacterial load in the spleens 48 hours after infection were significantly reduced in OMV immunised mice.

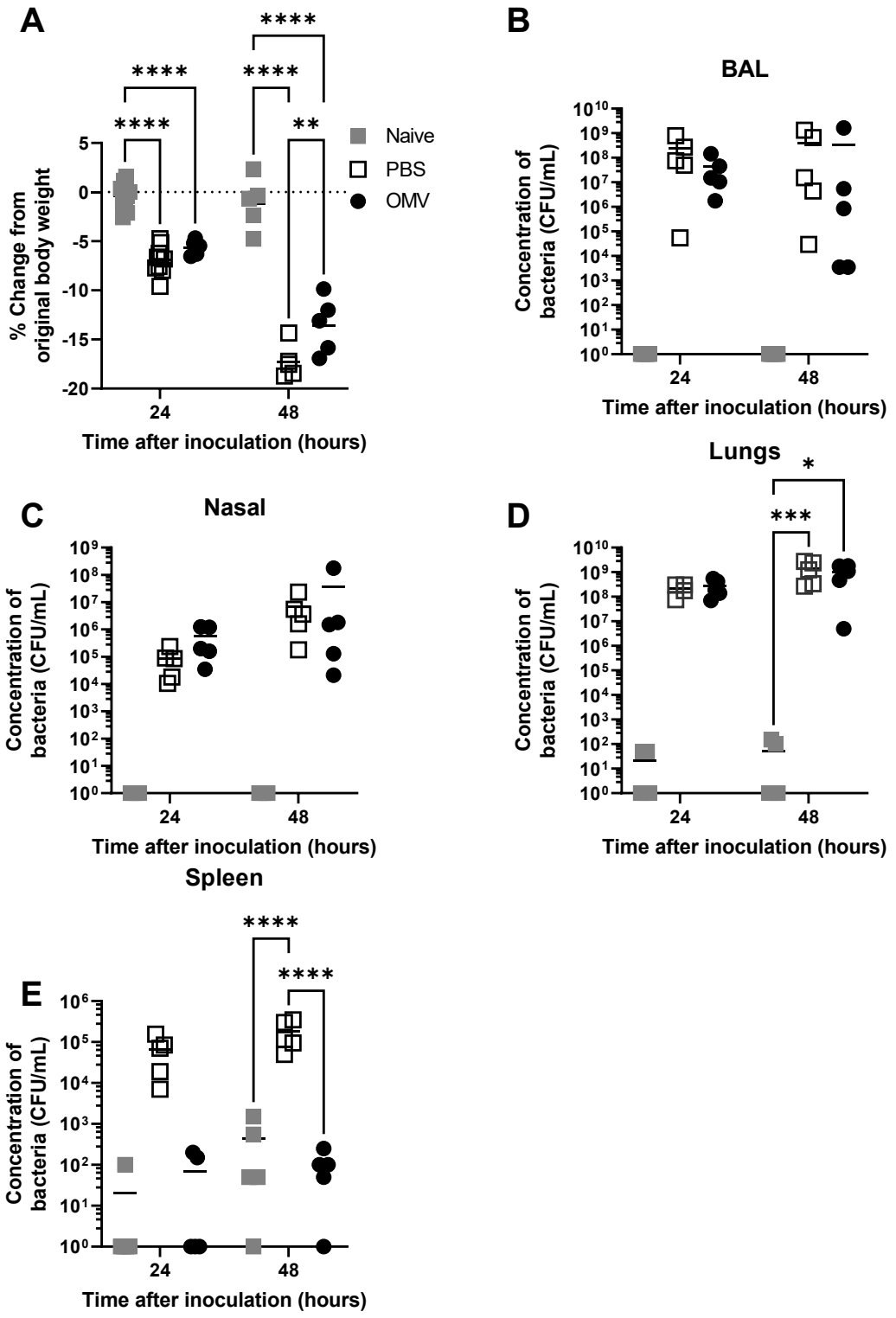


Figure 4.5 | OMVs from *A. baumannii* BAL_084 provide minimal protection against homologous challenge. Adult BALB/c mice were intramuscularly injected with 100 fluorescence units of BAL_084 OMV (OMV) or PBS (PBS) at day 0 and boosted at day 21. At day 42 mice were intranasally dosed with $1x10^7$ CFU *A. baumannii* BAL_084 and culled 24 or 48 hours later. Weight **(A)** was measured over the 24 and 48 hour challenge. Bacterial load at 24 and 48 hours in BAL **(B)**, nasal wash **(C)**, lungs **(D)** and spleen **(E)** . Two-way ANOVAs were used to test for significant differences. **p≤0.05, **p ≤0.01, ***p ≤0.001, ****p ≤0.0001.* Points represent individual animals.

4.2.6 – *A. baumannii* BAL_276 OMVs given subcutaneously provide better protection against homologous intranasal challenge than intramuscular vaccination.

To see if different routes of immunisation provided better protection, mice were immunised with *A. baumannii* BAL_276 derived OMVs intramuscularly and subcutaneously with 30 day intervals and then challenged intranasally with *A. baumannii* BAL_276 for 24 hours. Blood was assessed for antibody responses. After priming, both groups of immunised mice had significantly increased levels of BAL_276 OMV specific IgM in their serum (Fig. 4.6 B) compared to the PBS mice ($p \leq 0.001$). 30 days after the boost, the levels of IgM in the serum of the intramuscularly immunised mice had reduced to similar levels as seen in the PBS mice. The levels of BAL_276 OMV specific IgG in serum were raised after IM and SC OMV immunisation (Fig. 4.6 C). However, in this study only the SC immunised mice had significantly increased IgG compared to the PBS group at day 30 ($p \leq 0.0001$) and day 60 ($p \leq 0.01$). Although, both immunised groups of mice had very similar levels of BAL_276 OMV specific IgG present in their serum at the timepoints tested. Additionally, the levels of BAL_276 OMV specific IgG1 was tested in the OMV immunised mice (Fig. 4.6 D). The subcutaneously immunised mice had significantly more BAL_276 OMV specific IgG1 in their serum compared to the intramuscularly immunised mice. The levels of BAL_276 OMV specific IgG2 present in the serum were also tested (Fig. 4.6 E) however, there was no difference between the subcutaneously immunised and intramuscularly immunised mice. On day 60, 30 days after the second dose of *A. baumannii* BAL_276 OMV, the mice were challenged intranasally with *A. baumannii* BAL_276 and culled 24 hours later. The mice were weighed throughout the challenge (Fig. 4.6 F) but there was little difference in weight loss between the three groups of mice. An ELISA was performed on BAL fluid to measure the levels of IL-6 in the lungs (Fig. 4.6 G), which showed a reduction in IL-6 in the intramuscularly immunised mice compared to the PBS mice and further reduction in the subcutaneously immunised mice. The difference in IL-6 levels in the BAL fluid of the subcutaneously immunised mice was significantly lower than in the PBS mice ($p \leq 0.05$). Finally, the bacterial load in the BAL fluid, nasal wash, lungs and spleen was determined. In the BAL fluid the

amount of bacteria recovered from the intramuscularly immunised mice was on average only slightly reduced compared to the PBS mice (Fig. 4.6 H). However, the subcutaneous immunisation with BAL_276 OMVs significantly reduced the bacterial load in the BAL fluid compared to the PBS mice ($p \leq 0.05$). The bacterial load in the lungs was very similar to what was seen in the BAL fluid (Fig. 4.6 I). Intramuscularly immunised mice only had a slight reduction in bacterial load in the lungs compared to the PBS mice whereas, the subcutaneously immunised mice had a significantly reduced bacterial load in the lungs compared to the PBS mice ($p \leq 0.05$). The immunised mice all had reduced bacterial loads in their spleens compared to the PBS mice (Fig. 4.6 J). Additionally, not all mice in the immunised groups had bacteria recoverable from the spleen. However, in this case only the subcutaneously immunised mice had significantly reduced bacterial loads in the spleen compared to the PBS mice ($p \leq 0.01$). All three groups of mice had very similar levels of bacteria recovered from the nasal wash (Fig. 4.6 K), with no difference in bacterial load across the three groups. Subcutaneous immunisation resulted in a significantly increased antibody response compared to the non-immunised mice and also had a significantly increased level of IgG1 antibodies compared to the intramuscularly immunised mice. There was no difference in weight loss between the three groups, but the subcutaneously immunised mice had significantly reduced levels of IL-6 in the lungs. Finally, only the subcutaneous immunisation significantly reduced bacterial loads in the lungs and spleens but neither vaccination had any effect on the bacterial load in the upper respiratory tract.

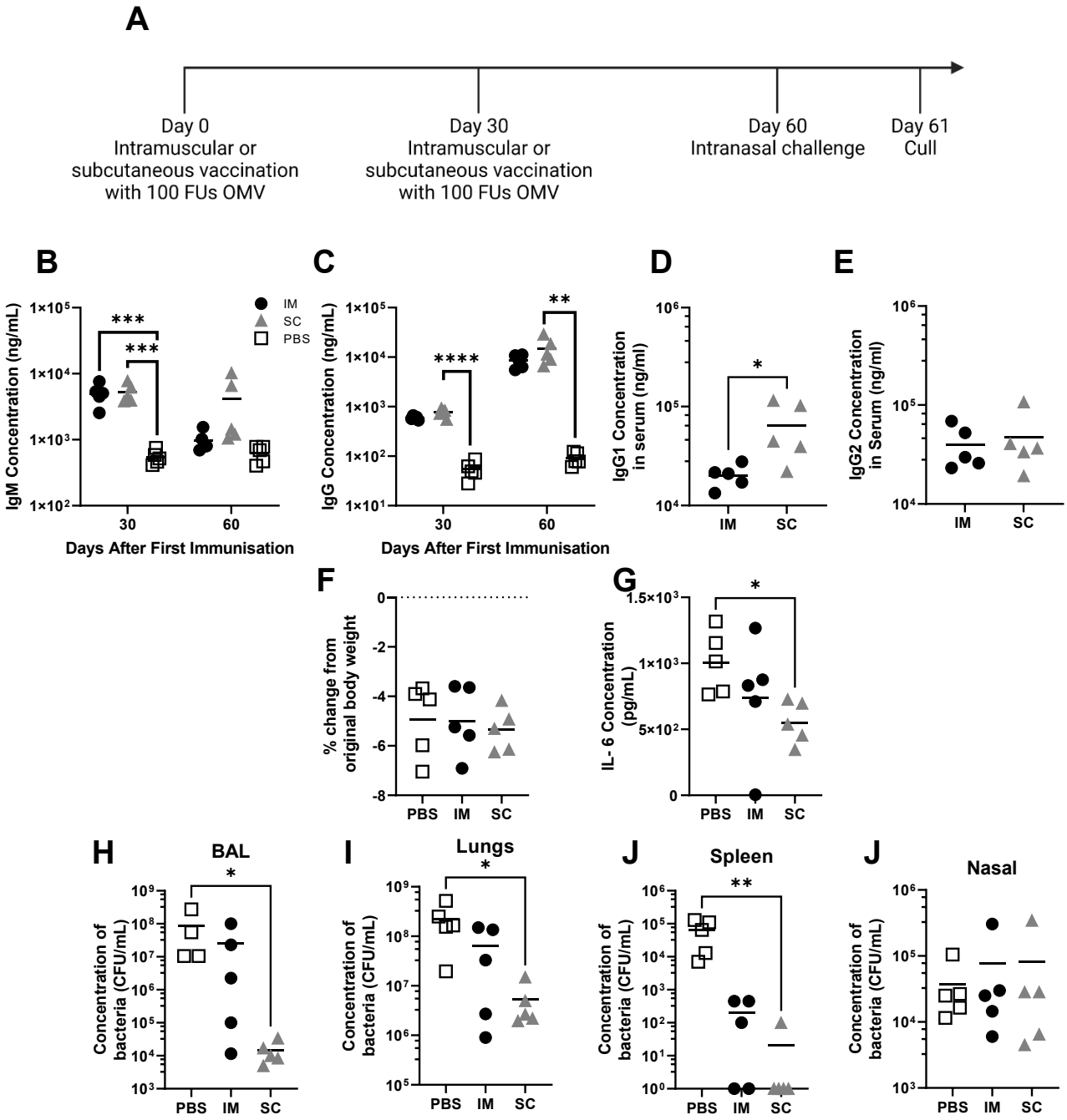


Figure 4.6 | OMVs from *A. baumannii* (strain BAL_276) protect better when injected subcutaneously. Adult BALB/c mice were injected with 100 fluorescence units of BAL_276 OMV intramuscularly (IM) or subcutaneously (SC) **(A)**. Control mice were intramuscularly injected with PBS (PBS) at day 0 and boosted at day 30. Anti-BAL_276 OMV IgM **(B)**, IgG **(C)**, IgG1 **(D)** or IgG2 **(E)** in sera. At day 60 mice were intranasally dosed with $1.4x10^7$ CFU *A. baumannii* BAL_276 and culled 24 hours later. Weight **(F)** and IL-6 **(G)** were measured 24 hours after infection. Bacterial load at 24 hours in BAL **(H)**, Lungs **(I)**, Spleen **(J)** and Nasal wash **(K)**. Kruskal Wallis was used to test for significant differences in bacterial load, change in weight and IL-6. Two-way ANOVAs were used to test for significant differences in IgG and IgM concentrations in serum. Mann-Whitney tests were used to test for significant differences in IgG1 and IgG2. **p≤0.05, **p ≤0.01, ***p ≤0.001, ****p ≤0.0001.* Points represent individual animals.

4.2.7 – Route of vaccination did not alter antibody avidity.

To determine whether there was a qualitative difference in the antibody response to IM or SC immunisation and determine whether SC immunisation resulted in improved antibody binding mice were immunised to collect serum. Mice were immunised with *A. baumannii* BAL_276 derived OMVs in a prime boost approach with 21 day intervals to determine whether there was a difference in antibody avidity. An ELISA was performed on serum collected from mice 21 days after the second dose of OMV. Plates were coated with *A. baumannii* BAL_276 OMV and total IgG was measured with and without a urea wash to calculate the avidity index. When total IgG was measured with no urea wash (Fig. 4.7 A) similarly to before, both immunised mice had increased levels of BAL_276 OMV specific IgG in their serum. However, only the subcutaneously immunised mice had significantly more OMV specific IgG in their serum compared to the PBS mice ($p \leq 0.01$). When a urea wash was performed and the total IgG still binding to BAL_276 derived OMVs was quantified (Fig. 4.7 B) both the intramuscularly and subcutaneously immunised mice still had very similar levels of IgG still bound to the OMVs, which was significantly increased compared to the PBS mice ($p \leq 0.05$). Finally, the avidity index was calculated (Fig. 4.7 C) but despite around a 10% difference in the avidities of the intramuscular and subcutaneous immunised mice IgG this was not significant. Subcutaneously immunised mice had significantly more total BAL_276 specific IgG compared to the PBS mice, but both groups of mice had significantly more BAL_276 specific IgG in their serum compared to the PBS mice after a urea wash was added into the ELISA protocol. However, despite a 10% decrease in avidity in the subcutaneously immunised mice compared to the intramuscularly immunised mice this was not a significant difference.

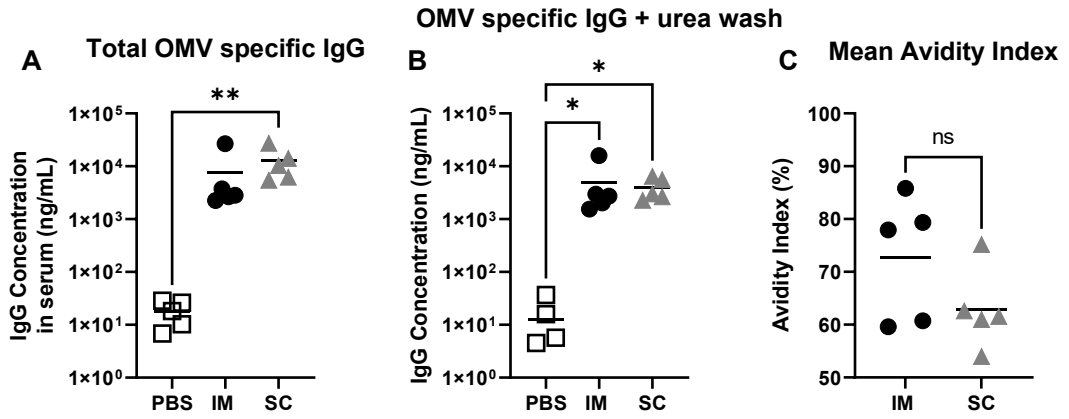


Figure 4.7 | IgG avidity is reduced in subcutaneously immunised mice compared to intramuscularly immunised. Adult BALB/c mice were injected with 100 fluorescence units of BAL_276 OMV intramuscularly (IM) or subcutaneously (SC). Control mice were intramuscularly injected with PBS (PBS) at day 0 and boosted at day 30. An ELISA was used to quantify anti-BAL_276 OMV IgG in sera without a urea wash **(A)** and with a urea wash included **(B)**. The mean avidity index was calculated for the two groups **(C)**. Kruskal Wallis was used to test for significant differences in total IgG. Mann-Whitney tests were used to test for significant differences in avidity index. **p≤0.05, **p ≤0.01, ***p ≤0.001, ****p ≤0.0001.* Points represent individual animals.

4.2.8 – Use of an Imject Alum adjuvant led to increased antibody responses in BALB/c mice.

Antibody responses to SC and IM immunisation of OMVs with and without Imject Alum were measured by ELISA to investigate what effect, if any, the route of immunisation and the addition of an alum-based adjuvant had on the immune response to *A. baumannii* OMVs. Mice were immunised subcutaneously and intramuscularly with *A. baumannii* BAL_276 OMVs with and without Imject Alum adjuvant mixed into the vaccine solution. Serum was collected 30 days after priming (day 30) and 30 days after boosting (day 60). It is important to note that shortly after receiving the boosting vaccination of OMV with Imject Alum, SC immunised mice developed injection site reactions. Lumps developed on the injection sites, one of which began to form an ulcer resulting in one mouse from the SC with Imject Alum group being euthanised after reaching its humane end point. Upon dissection of mice at the experimental end point, all mice that received Imject Alum in the vaccine formulation had formed depots at the injection sites.

To determine the total levels of BAL_276 OMV specific IgG, IgM, IgA, IgG1 and IgG2a present in the serum, plates were coated with BAL_276 OMV. All 4 groups of immunised mice had

increased levels of IgG in their serum before and after boosting compared to naïve mice (Fig. 4.8 A). After boosting, the subcutaneously immunised mice with alum also had significantly more BAL_276 specific IgG than the intramuscularly immunised mice with ($p \leq 0.001$) and without ($p \leq 0.01$) alum and the subcutaneously immunised mice without alum ($p \leq 0.01$). All immunised mice had increased levels of BAL_276 OMV specific IgM in their serum after priming compared to naïve mice, which decreased after boosting (Fig. 4.8 B). The subcutaneously immunised mice with alum had significantly increased levels of OMV specific IgM compared to the intramuscularly immunised mice with alum ($p \leq 0.01$) after priming. After boosting there were no significant differences in IgM levels of immunised mice. The levels of BAL_276 specific IgA were measured in the BAL fluid of all mice (Fig. 4.8 C). However, none of the mice had any OMV specific IgA present in their BAL fluid. The levels of BAL_276 OMV specific IgG1 were measured in the serum (Fig. 4.8 D) and all immunised mice had increased levels of IgG1 in their serum compared to non-immunised mice, but there was no difference between the immunised mice. As seen previously, the subcutaneously immunised mice had increased levels of IgG1 in their serum compared to intramuscularly immunised mice though this time the difference was not significant. The levels of BAL_276 OMV specific IgG2a were also increased in all immunised mice compared to non-immunised mice (Fig. 4.8 E). The addition of alum led to a slight increase in IgG2a titres in the serum of the mice compared to the mice immunised with OMV without alum. The subcutaneously immunised mice and intramuscularly immunised mice without alum had very similar levels of OMV specific IgG2a in their serum. The IgG1/IgG2 ratio was calculated (Fig. 4.8 F) and there was very little difference between the immunisation routes or with the addition of alum. An ELISA was also performed using whole bacterial cells of *A. baumannii* BAL_276 (Fig. 4.8 G). There was a slight increase in the levels of IgG binding to whole bacterial cells in the immunised mice. Subcutaneously immunised mice had slightly increased IgG responses compared to intramuscularly immunised mice and the addition of alum further increased the IgG response in subcutaneously immunised mice. LPS was isolated from *A. baumannii* BAL_276 and used to coat an ELISA plate and measure the amount of LPS specific IgG in the serum of mice
(Fig. 4.8 H). The amount of binding to LPS was very variable, but the subcutaneously immunised mice had the highest level of LPS specific IgG although it was not significantly different to any other groups. The only group of immunised mice not to respond to LPS

were the intramuscularly immunised mice. All routes of immunisation resulted in a broad antibody response against the OMVs with the subcutaneously immunised mice, with and without alum, often having the highest titres.

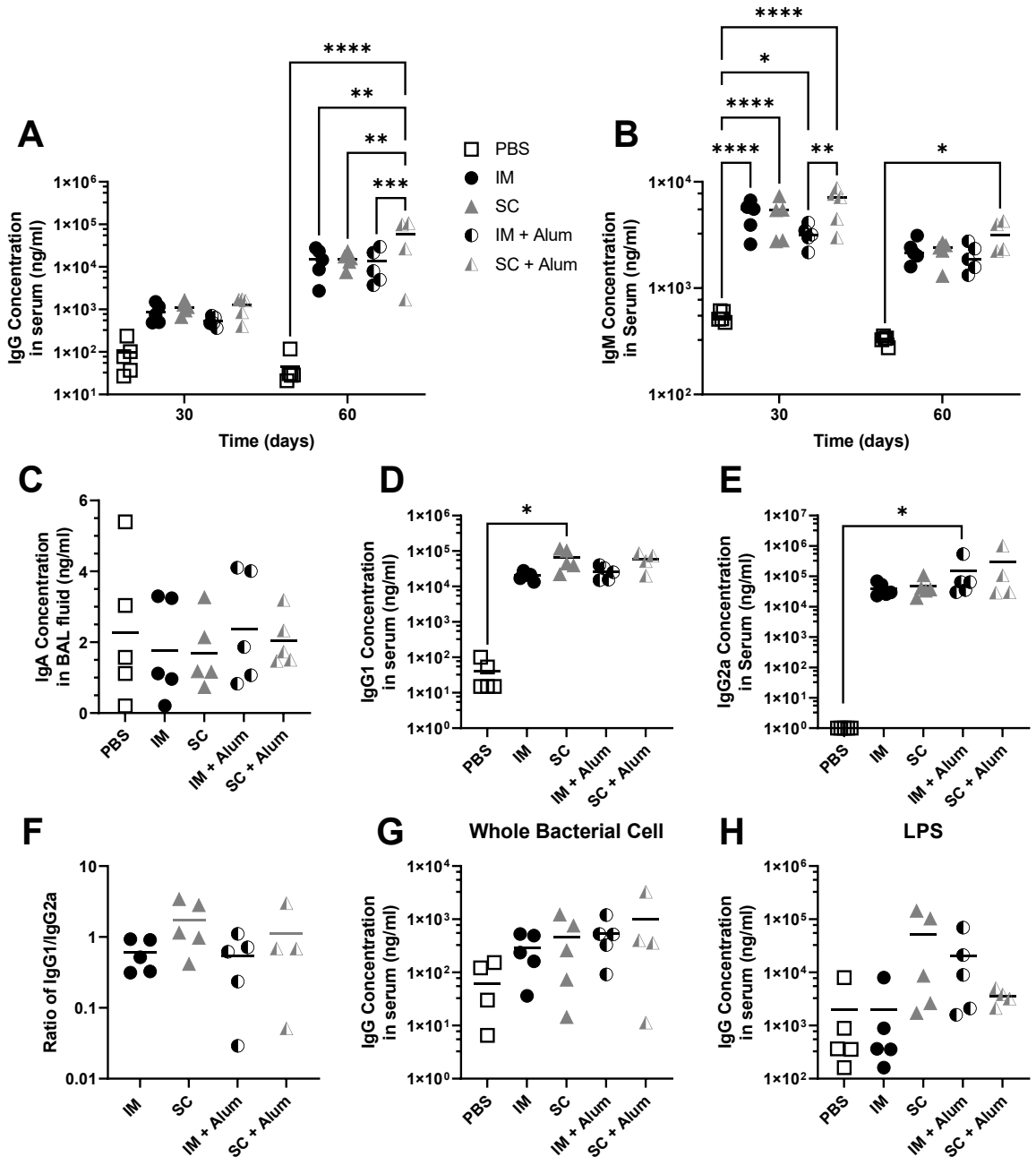


Figure 4.8 | Imject Alum adjuvant has little impact on antibody response against intramuscular or subcutaneous vaccination with *A. baumannii* BAL_276 OMV. Adult BALB/c mice were injected with 100 fluorescence units of BAL_276 OMV intramuscularly (IM) or subcutaneously (SC) with and without Imject Alum. Control mice were intramuscularly injected with PBS (PBS) at day 0 and boosted at day 30. Serum was collected at day 30 and day 60. Anti-BAL_276 OMV IgG **(A)**, IgM **(B)**, IgA **(C)**, IgG1 **(D)** and IgG2a **(E)** in sera. IgG1/IgG2a ratio was calculated **(F)** Total IgG in sera specific to whole bacterial cell **(G)** and LPS **(H)**. A two-way mixed effects ANOVA was used to test for significant differences in total BAL_276 OMV specific IgG and IgM. Kruskal Wallis tests were used to test for significant differences in IgA, IgG1, IgG2a, whole bacterial cell and LPS specific IgG. **p≤0.05, **p ≤0.01, ***p ≤0.001, ****p ≤0.0001.* Points represent individual animals.

4.2.9 – The addition of an Imject Alum adjuvant did not provide a significant improvement to *A. baumannii* BAL_276 OMV vaccination.

To try and induce a stronger Th2 response and determine whether that resulted in improved protection OMVs were mixed with Imject Alum, an alum based adjuvant, prior to immunisation[186]. Mice were immunised subcutaneously and intramuscularly with *A. baumannii* BAL_276 OMVs with and without Imject Alum adjuvant mixed into the vaccine solution. Mice were then challenged intranasally with *A. baumannii* BAL_276 and culled 24 hours later. Mice were weighed throughout the challenge to measure weight loss (Fig. 4.9 A). All 5 groups of challenge mice lost more weight than the naïve mice, on average between 7 and 10% of their starting bodyweight. Only the PBS and subcutaneously immunised mice lost significantly more weight than the naïve mice ($p \leq 0.05$ and $p \leq 0.01$ respectively). The bacterial load was measured in the BAL fluid, nasal wash, lungs and spleens of the mice 24 hours after challenge. All 5 challenged groups of mice had increased levels of bacteria recovered from their BAL fluid compared to the naïve (unchallenged) mice (Fig. 4.9 B). The intramuscularly immunised mice had the most bacteria recovered from their BAL fluid, which was significantly higher than the naïve mice ($p \leq 0.01$). The intramuscular OMV vaccination with alum mice had very similar levels of bacteria recovered from their BAL fluid as the mice immunised with PBS, followed by the subcutaneous vaccination with alum. The subcutaneously immunised mice had the lowest amount of bacteria recovered from their BAL fluid out of all of the challenge mice, which was approximately a 3-log decrease compared to the PBS mice but was not a significant difference. The bacteria recovered from the nasal wash was highest in the PBS mice (Fig. 4.9 C), which was significantly higher than the naïve mice ($p \leq 0.01$). The intramuscularly immunised mice also had significantly increased levels of bacteria recovered from their nasal wash than the naïve mice ($p \leq 0.01$). The subcutaneously immunised mice and subcutaneously immunised mice with alum had the lowest amounts of bacteria recovered from their nasal wash which was around a 2-log decrease compared to the PBS mice, but this was not significant. All groups of challenge mice had very similar levels of bacteria recovered from their lungs (Fig. 4.9 D), but the intramuscularly immunised mice with and without alum had significantly increased levels of bacteria recovered from their lungs compared to the naïve mice ($p \leq 0.05$ and $p \leq 0.01$ respectively). Finally, the bacterial loads

recovered from the spleens were again all increased in the challenge mice compared to the naïve mice (Fig. 4.9 E). Both the intramuscularly immunised groups of mice with and without alum had significantly increased bacterial loads in their spleens compared to the naïve mice ($p \leq 0.05$ and $p \leq 0.0001$). The subcutaneously immunised mice with alum had a slightly reduced bacterial load in their spleen compared to the PBS mice, but the subcutaneously immunised mice without alum had the lowest bacterial load in their spleen. The subcutaneously immunised mice without alum had significantly less bacteria recovered from their spleens compared to the intramuscularly immunised mice without alum ($p \leq 0.05$). Adding the alum adjuvant did little to further reduce bacterial loads or prevent weight loss compared to the equivalent vaccination without alum.

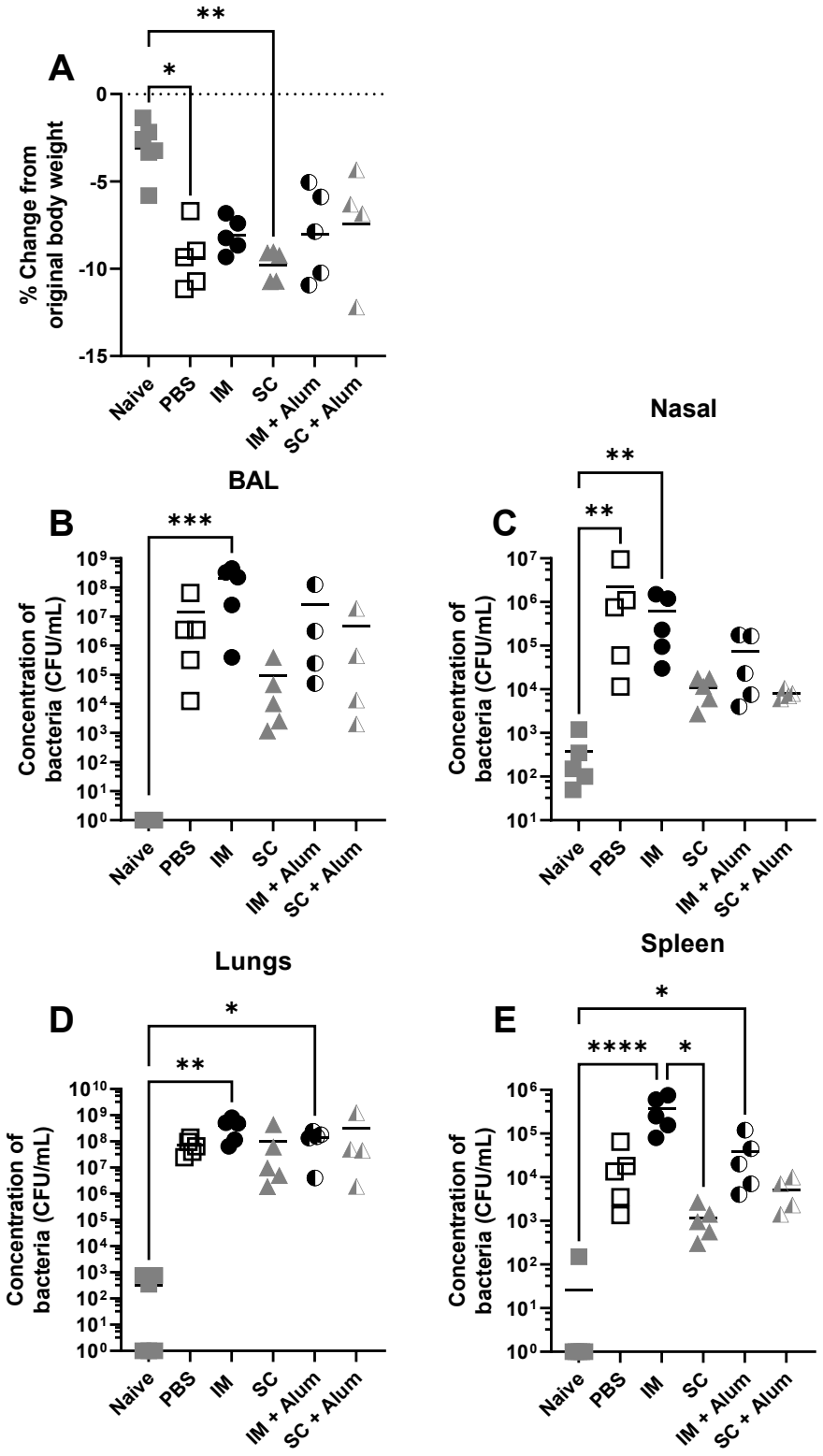


Figure 4.9 | Imject Alum adjuvant provides no benefit to intramuscular or subcutaneous vaccination with *A. baumannii* (strain BAL_276) OMV. Adult BALB/c mice were injected with 100 fluorescence units of BAL_276 OMV intramuscularly (IM) or subcutaneously (SC) with and without Imject Alum. Control mice were intramuscularly injected with PBS (PBS) at day 0 and boosted at day 30. At day 42 mice were intranasally dosed with $1x10^7$ CFU *A. baumannii* BAL_276 and culled 24 hours later. One group of mice (naïve) received no injection and were given 100µl PBS intranasally. Weight **(A)** was measured over the 24 hour infection. Bacterial load at 24 hours in BAL **(B)**, nasal wash **(C)**, lungs **(D)** and spleen **(E)**. Kruskal Wallis tests were used to test for significant differences in bacterial load and change in weight. **p≤0.05, **p ≤0.01, ***p ≤0.001, ****p ≤0.0001.* Points represent individual animals.

4.2.10 – Intranasal vaccination with OMVs provides high levels of protection against homologous infection out of the tested routes.

Due to the importance of mucosal immunity in respiratory tract infections, I chose to try intranasally immunising mice with OMVs. Mice were immunised intranasally with *A. baumannii* BAL_276 OMVs in a prime boost approach with 21 day intervals. On day 42 mice were challenged intranasally with *A. baumannii* BAL_276 and culled 24 and 48 hours later. Serum was collected after priming and upon culling mice to determine the OMV specific antibody titres. All immunised mice generated an IgG response against BAL_276 OMVs (Fig. 4.10 A). After boosting, on day 43 the levels of BAL_276 OMV specific IgG present in the serum had increased slightly since priming and was significantly increased in the immunised mice compared to the PBS mice ($p \leq 0.01$). The levels of BAL_276 OMV specific IgM were also measured (Fig. 4.10 B). After priming the immunised mice had slightly increased levels of BAL_276 OMV specific IgM in their serum compared to non-immunised mice, but this was not significant. The levels of IgM in their serum reduced after challenge but was still slightly higher than the PBS mice. The level of BAL_276 OMV specific IgA was measured in the nasal wash of the mice 24 and 48 hours after challenge (Fig. 4.10 C). Although the levels of IgA present in the nasal wash was increased at both 24 and 48 hours after infection, only 24 hours after challenge did the immunised mice have significantly increased levels of IgA in their upper respiratory tract compared to the PBS mice ($p \leq 0.05$). Mice were weighed throughout the infection to track their weight loss (Fig. 4.10 D) with the immunised mice experiencing significantly less weight loss 24 hours after infection compared to the PBS mice ($p \leq 0.01$). However, there was little difference in weight loss 48 hours after challenge. The levels of IL-6 in the BAL fluid were also measured after challenge (Fig. 4.10 E). At both 24 and 48 hours after challenge there wasn't much difference in the levels of IL-6 in the BAL fluid. The bacterial load was measured in the BAL fluid (Fig. 4.10 F), with immunised mice having significantly less bacteria recoverable from the BAL fluid 24 hours after challenge compared to the PBS mice ($p \leq 0.05$). Additionally, all 5 mice in the immunised group had completely cleared bacteria from inside their lungs 48 hours after challenge. The nasal wash was also used to determine the bacterial load in the upper respiratory tract (Fig. 4.10 G). The amount of bacteria recovered from the nasal wash of the immunised mice was significantly lower than the PBS mice 24 hours after challenge ($p \leq 0.01$). The amount of

bacteria present in the upper respiratory tract of PBS mice decreased 48 hours after challenge compared to 24 hours after challenge. Whereas the amount of bacteria recoverable from the immunised mice remained the same on average. However, one mouse had completely cleared all bacteria from its upper respiratory tract 48 hours after challenge. Similar results were seen in the lungs of the immunised mice when bacterial load in the lung homogenate was determined (Fig. 4.10 H). The immunised mice had significantly lower levels of bacteria recovered from their lungs compared to PBS mice 24 hours after challenge ($p \leq 0.01$). The amount of bacteria recovered from the lungs of PBS mice decreased between 24 and 48 hours after challenge however, the amount of bacteria recovered from the lungs of the immunised mice remained relatively similar between the two time points. Finally, the spleen homogenate was plated out to determine the bacterial load (Fig. 4.10 I). Immunised mice had significantly decreased bacterial loads in their spleens 24 hours after challenge compared to the PBS mice ($p \leq 0.01$). There were no bacteria recoverable from any spleens 48 hours after challenge. Intranasal vaccination with BAL_276 OMVs induced a significant antibody response and significantly reduced weight loss 24 hours after challenge. Intranasal immunisation significantly decreased bacterial burden across all of the tested sites 24 hours after challenge and intranasal vaccination completely prevented bacterial dissemination to the spleen.

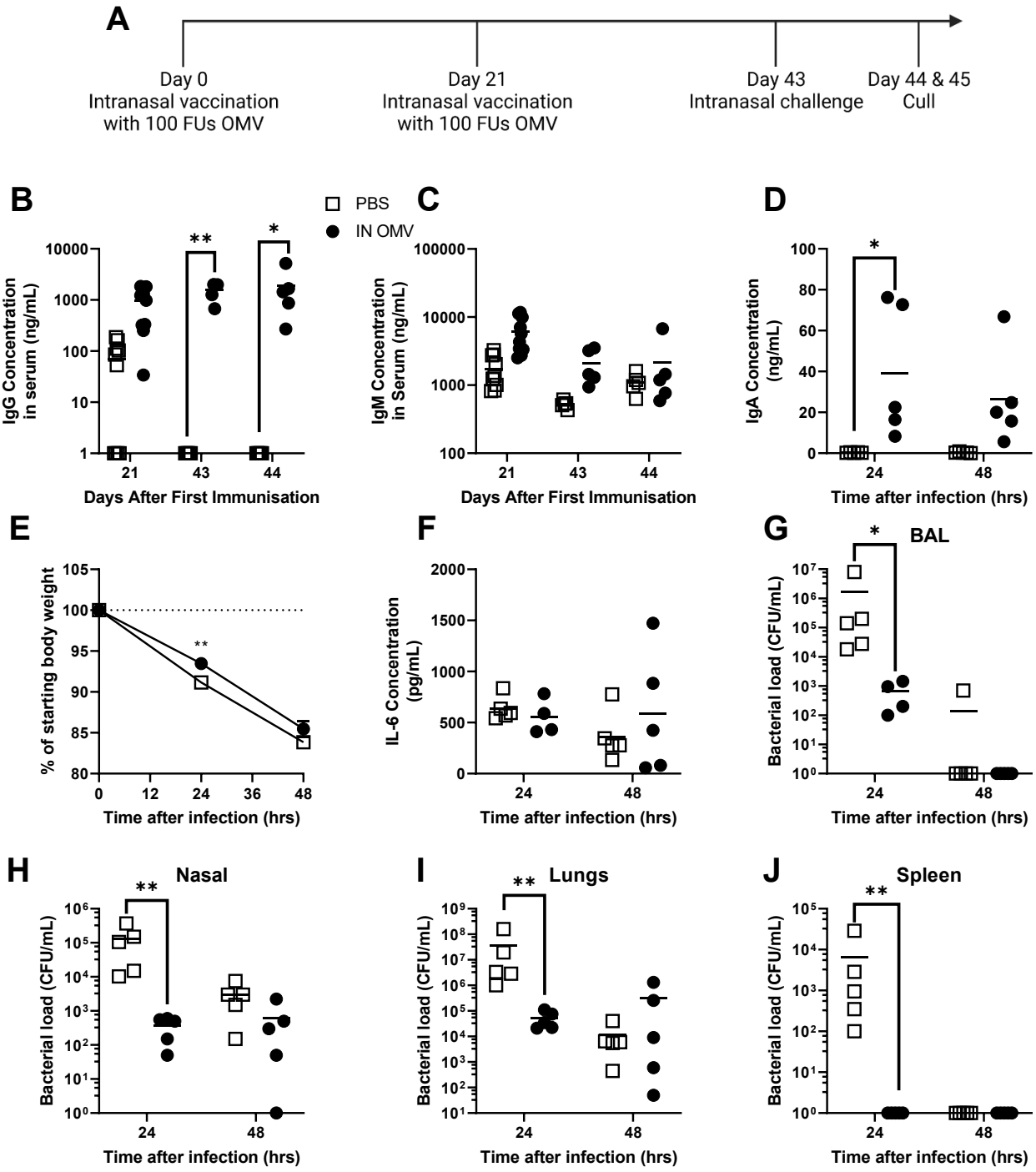


Figure 4.10 | Intranasal vaccination with *A. baumannii* BAL_276 OMV provides high levels of protection against homologous challenge. Adult BALB/c mice were intranasally dosed with 500 fluorescence units of BAL_276 OMV at day 0 and boosted at day 21 **(A)**. Control mice were intranasally dosed with PBS (PBS). At day 43 mice were intranasally dosed with $5x10^7$ CFU *A. baumannii* BAL_276 and culled 24 and 48 hours later. BAL_276 OMV specific IgG **(B)** or IgM **(C)** in serum or IgA **(D)** in nasal wash. Weight **(E)** and IL-6 **(F)** were measured. Bacterial load at 24 hours in BAL **(G)**, nasal wash **(H)**, lungs **(I)** and spleen **(J)**. Two-way ANOVAs were used to test for significant differences. **p≤0.05, **p ≤0.01, ***p ≤0.001, ****p ≤0.0001.* Points represent individual animals.

4.3 – Discussion

Results from this chapter show immunisation with OMVs derived from different strains of *A. baumannii* offer different levels of protection. This is likely to be down to differing immunogenicity levels and surface proteins as well as differing abundances of immunogenic antigens present on the surface of each OMV. Immunisation with *A. baumannii* ATCC 17978 derived OMVs, the least virulent of the three strains, resulted in the least protection and smallest reduction in bacterial load. Whereas immunisation with *A. baumannii* BAL_276 and BAL_084 derived OMVs resulted in larger reductions of bacterial load despite all three having similar serum antibody titres. Additionally, immunisation with *A. baumannii* BAL_276 derived OMVs elicited a cross reactive antibody response with serum IgG and IgM antibodies that also bound to *A. baumannii* BAL_084 derived OMVs. Subcutaneous vaccination was more effective than intramuscular, resulting in increased bacterial clearance and reduced inflammation which is most likely due to a qualitatively improved antibody response. However, intranasal vaccination was the most effective of all vaccination routes tested resulting in the greatest decreases in bacterial burden across all of the tested sites as well as a reduction in weight loss 24 hours after challenge (Table 4.1). This is most likely due to increased levels of mucosal IgA and the intranasal vaccination inducing a more potent mucosal immune response in the respiratory tract that can more effectively and more quickly work to eliminate respiratory infection by *A. baumannii*.

Table 4.1 | Summary of *in vivo* OMV vaccination routes and their effect on protective efficacy against homologous challenge. A summary of infection responses in BALB/c mice after OMV vaccination and homologous intranasal challenge. Responses depicted as + (mild increase), ++ (moderate increase), +++ (large increase), - (mild decrease), -- (moderate decrease), --- (large decrease) or ND (no difference).

Vaccination route	Antibody response	Weight loss	Inflammation (IL-6)	Bacterial load	Bacterial dissemination
Intramuscular	++	ND	-	-	-
Subcutaneous	++	ND	--	--	--
Intranasal	+++	ND	ND	---	---

Subcutaneously immunised mice experienced better protection against challenge with reduced inflammation in the lungs and reduced bacterial burdens compared to intramuscularly immunised mice. The only differences in antibody responses of the two routes of immunisation were that subcutaneously immunised mice had slightly increased levels of IgG1 compared to the intramuscularly immunised mice and perhaps increased binding to LPS and intramuscular route of vaccination had slightly increased levels of avidity. Suggesting, there could be a qualitative difference responsible for improved level of protection. Increased levels of IgG1 suggest subcutaneous immunisation could be skewing the immune response more towards a Th2 response[187] than intramuscular vaccination. Similar results have been seen upon vaccination with OmpA, where mice develop a Th2 response and varying the antigen dose altered the cytokine profile[188]. Additionally, as well as the IgG1 response a strong IgG2a response was also seen after subcutaneous and intramuscular immunisation, with similar results being reported in other *A. baumannii* OMV vaccination models[189]. Immune responses towards *A. baumannii* are often mixed, with dendritic cells presenting bacterial antigens to naive CD4 + T cells and polarizing the response toward a Th1 profile[190]. Due to its important role in neutrophil recruitment, it is suspected but not confirmed that IL-17 could be playing a role during *A. baumannii* infection which in turn would suggest a Th17 profile also[190].

Neutrophils play a key role in fighting *A. baumannii* infection[191,192]. Upon respiratory infection neutrophils are rapidly recruited to the lungs until the infection is cleared and levels return to baseline. When neutrophils are depleted prior to intranasal infection in mice, *A. baumannii* infections result in increased bacterial loads, dissemination and an increase in lethality. Conversely, when there was a chemokine induced recruitment of neutrophils into the lungs bacterial clearance was significantly improved[191]. Work performed within this thesis has shown intranasal *A. baumannii* infection in mice induces significant neutrophil infiltration into the lungs. This further suggests a strong Th17 response to a vaccine could help to improve protective efficacy. This could work similarly to a *Streptococcus pneumococci* challenge re-challenge model and *Helicobacter pylori* immunisation, where CD4 T cells produced IL-17 and lead to increased monocyte, macrophage and neutrophil recruitment and therefore increased bacterial clearance[193]. Additionally, in murine models using a live attenuated PA14 *Pseudomonas aeruginosa* strain

to immunise mice, CD4 T cells were responsible for producing IL-17, causing rapid neutrophil recruitment and increased clearance of bacteria. However, when IL-17 was depleted or the IL-17 receptor abrogated vaccine efficacy was reduced [193,194]. Multiple examples show how important IL-17 is in a vaccine induced immune response against extracellular bacterial infections[193–197]. Inducing an effective Th17 response with increased IL-17 levels and enhanced neutrophil recruitment could be highly beneficial when developing an *A. baumannii* vaccine.

The OMVs proved to be immunogenic on their own, without the need for an adjuvant. *A. baumannii* OMVs represent a multivalent vaccine approach, being made up of multiple surface proteins, LPS and phospholipids[111]. *A. baumannii* OMVs induced strong antibody responses that showed mixed Th1 and Th2 responses as well as the generation of an effective mucosal IgA response when mice were immunised intranasally. OMVs are also capable of eliciting protective Th17 responses[198], but this would require further investigation within the model used here. Immunisation with *A. baumannii* OMVs also reduced bacterial burden and dissemination. It is unknown if protection is heterologous and this requires further investigation, but antibodies raised against BAL_276 derived OMVs were able to bind to BAL_084 derived OMVs by ELISA. OMVs have a lot of potential for use in the future of *A. baumannii* vaccines as they elicit strong antibody responses and are capable of reducing bacterial burden with the potential for protective cross reactivity across different strains.

One limitation of the work performed in this chapter is that naturally produced *A. baumannii* derived OMVs were used for vaccination. These OMVs have had no modifications, which means LPS is abundant on the surface of the OMVs[111,198]. Due to the high levels of reactogenicity for use in real life situations the endotoxin present on the surface of OMVs must be removed or attenuated[199,200]. However, as the OMVs used here have not been modified in any way, further work would be required to remove or attenuate the LPS to make the OMVs more tolerable for future use. This naturally reduces the immunogenicity, so the immune response to the OMVs could lessen. This does not reduce the potential for use in a future *A. baumannii* vaccine as the 4C-MenB vaccine has shown with its effective OMV based component[199,201]. Other limitations include the protective efficacy of the OMVs in the model have so far only been tested against homologous

infection. It is possible that the immune response induced against the clinical isolate derived OMVs is not cross reactive. Additionally, the vaccination process proved to be challenging. It can be difficult to determine whether an intramuscular vaccine was correctly administered, where the vaccine may not have been accurately delivered into the muscle on both prime and boost immunisations immune responses may have been weaker causing more variation in the data. There may also have been variation between batches of OMVs produced resulting in differing responses. However, to try and reduce the effect this may have, each study was performed using the same batch of OMVs between the different groups and also for the subsequent ELISAs.

Intranasal immunisation was the best route of those tested. The presence of IgA on the mucosal surfaces of the upper respiratory tract could aid in the immediate clearance of bacteria leading to the significantly reduced bacterial loads in the upper airways[189]. Another possible mechanism of protection an intranasal vaccine could induce is tissue resident memory T cells. Studies have previously shown respiratory tract CD4+ Trm to contribute to bacterial clearance through IL-17 and IFNγ production and subsequent antigen-specific recruitment of neutrophils[202]. Given the important role of neutrophils in preventing *A. baumannii* infection this could be a particularly effective protective mechanism to induce via vaccination[190] however, further work would be required to confirm this. Preventing upper respiratory tract carriage of bacteria is likely to be an important factor of an effective vaccine as the upper airways, particularly the oropharynx, can act as a reservoir of infection in ventilator associated pneumonia[203–205]. An effective vaccine could prevent bacterial colonisation of the airways. With reduced or no bacterial carriage in the upper airways prior to mechanical ventilation the chances of a patient developing pneumonia through aspiration or upper airway flora being introduced to the lungs is likely to be reduced.

5 – Antigen discovery for *A. baumannii* vaccines and *in vivo* monoclonal antibodies

The work performed within this chapter was a part of a collaboration with Kymab. All mAbs used were developed and their targets identified by Kymab. Where work involves the mAbs, I performed the *in vivo* protection studies only.

5.1 – Introduction

The route of vaccination chosen is important in generating the desired and most effective immune response against infection. However, if the vaccine antigen is inaccessible or an immune response raised against it does not affect bacterial growth or infection no matter how "big" the immune response is, it will not protect against infection. Reverse vaccinology technologies use genomic and proteomic sequencing to identify novel vaccine candidates from whole genome sequencing or B cell repertoire analysis[106,206,207]. In the case of the original reverse vaccinology approach, *in silico* analysis was performed to screen multiple genomes of a pathogen/species and identify proteins that have the attributes of being a good vaccine target such as surface exposure and high levels of conservation between strains[206]. The 4CMenB vaccine was developed using reverse vaccinology. Using the complete whole genome sequence of *Neisseria meningitidis*, surface-exposed antigens were identified and used to immunise mice. The antisera was assessed for bactericidal properties and cross reactivity and the final vaccine contained 3 recombinant proteins as well as the epidemic New Zealand strain OMV component[201]. Subtractive genomics or proteomics can also be applied to remove proteins also produced by the host or closely related beneficial microorganisms. Proteomic analysis can provide additional information, for example, to identify proteins that are expressed during infection[207]. The *in silico* selected antigens can then be expressed and screened using animal models[206]. Comparatively, reverse vaccinology 2.0 relies upon B cell and antibody repertoire analysis using samples taken from vaccinated or infected individuals. Single B cell sorting is performed and antibodies are expressed for characterisation and functional assays before antigen identification. Using structural biological analysis, in-depth knowledge of the protective epitope can be obtained down to molecular levels of detail, the antigen can be engineered for presentation in the optimum immunogenic format with the best formulation or delivery system for *in vivo* testing[206].

Reverse vaccinology shows promise in antibacterial vaccine discovery[106,167,168,170,208]. Many essential proteins, virulence factors and resistance determinants have been identified as potential vaccine candidates or for use in small molecule drug development[167]. This has been done multiple times for *A. baumannii* resulting in the identification of a large number of potential vaccine antigens[167,168,170]. Targets belonged to a range of proteins involved in cell division, fimbriae, pili assembly, iron acquisition, biofilm formation, proteases and

hypothetical proteins[168,170]. One study resulted in the design of a vaccine construct that when used in computer generated models showed antigen interactions with host immunological complexes[167] suggesting the potential for use as a vaccine.

Due to the nature of the process, reverse vaccinology 2.0 also results in the production of pathogen specific monoclonal antibodies (mAbs)[106,206] which could be taken forward for use as bactericidal mAb treatment. Passive immunisation with mAbs has the potential to neutralise pathogens such as bacteria and also to induce a host immune response through constant fragment mediated antibody effector functions[209]. There are currently three antibacterial mAbs that have been approved for use in humans by the Federal Drug Administration, USA (FDA) and are used to treat *Bacillus anthracis* and *Clostridium difficile* infections[210]. Studies have shown mAbs against *A. baumannii* to be protective in sepsis, pneumonia and wound infection animal models, with multiple mAbs currently under development for XDR *A. baumannii*[210–212].

5.1.2 – Chapter Aims and hypothesis

I hypothesise that immunogenic antigens will be identifiable using sera from immunised mice and two different identification methods and that monoclonal antibodies will protect against infection with clinical *A. baumannii* strains in BALB/c mice.

Aims:

1. Use serum from immunised BALB/c mice to identify antigens via western blot and mass spectrometry as well as phage expression cloning;

2. Collect amino acid sequences for identified immunogenic antigens and generate phylogenetic trees to assess the level of homology between *A. baumannii* strains;

3. Pre-treat mice with anti-*A. baumannii* mAbs via different routes to find the most effective *in vivo* antimicrobial mAb in BALB/c mice.

5.2 – Results

5.2.1 – Three antigens were identified as potential vaccine candidates for *A. baumannii using a reverse vaccinology approach*

Serum from immunised mice was used in 1:100 dilutions to discover immunogenic antigens that could potentially be developed into vaccines, using western blotting followed by mass spectrometry or phage expression cloning.

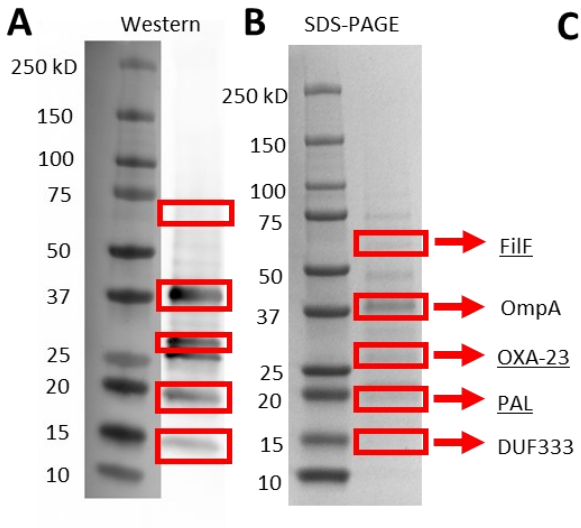
5.2.1.1 – Mass Spectrometry.

OMV bands from an SDS-PAGE gel (Fig. 5.1 B), that corresponded to bands detected via western blot (Fig. 5.1 A) using serum from immunised BALB/c mice, were excised for proteins to be extracted and analysed using mass spectrometry. There were 5 different proteins identified using this method: at 70kDa putative pilus assembly protein FilF[213,214], at 36-37kDa outer membrane protein A[71,215], at 31kDa class D carbapenem-hydrolysing-lactamase OXA-23[216,217], at 20kDa peptidoglycan-associated lipoprotein[218,219] and at 15kDa domain of unknown function 333[220].

5.2.1.3 – Phage expression cloning.

I generated a lambda phage library containing random fragments of genomic *A. baumannii* DNA. The phage were used to infect *E. coli* and induce protein expression onto nitrocellulose membranes. The membranes were soaked in sera from immunised mice and positive phage plaques were excised. The DNA from positive phage was extracted and sequenced to identify the proteins antibodies were binding to (Fig. 5.1 C). Many proteins were identified via this method however, 3 proteins were identified by both the western blot and mass spectrometry: FilF, OXA-23 and PAL.

Serum from a patient infected with *A. baumannii* was used in a western blot against different OMVs (Fig. 5.1 D) alongside an uninfected human control serum (Fig. 5.1 E). After infection there was strong binding to bands that are most likely to be OXA-23 and PAL however, there was no visible binding to FilF. Using two different methods of antigen identification 3 proteins have been identified through both, FilF, OXA-23 and PAL. Serum from an *A. baumannii* infected patient showed strong binding to both PAL and OXA-23 but not FilF.



C **Putative proteins from phage display**

Acetyl-Coa Carboxylase Carboxyltransferase Subunit Beta
Acyl-ACP--UDP-N-Acetylglucosamine O-Acyltransferase
Adenylosuccinate Lyase
ATP-Binding Protein
Bacterial Transferase Hexapeptide Family Protein
OXA-23
Cna B-Type Domain Protein
Cna Protein B-Type Domain Protein
Hypothetical Protein AB237_0812/NF038105 Family Protein
Hypothetical Protein ABNIH10_03641/Alpha/Beta Hydrolase
Hypothetical Protein DWA21_19730
Hypothetical Protein EXG27_19410
Hypothetical Protein F976_02086/GNAT Family N-Acetyltransferase
Hypothetical Protein J999_3850
Hypothetical Protein K041_3870
IS4-Like Element Isaba1 Family Transposase
Lac Repressor
Peptide Chain Release Factor 2
Peptidoglycan-Associated Lipoprotein (PAL)
FilF
Sigma-54 Dependent Transcriptional Regulator

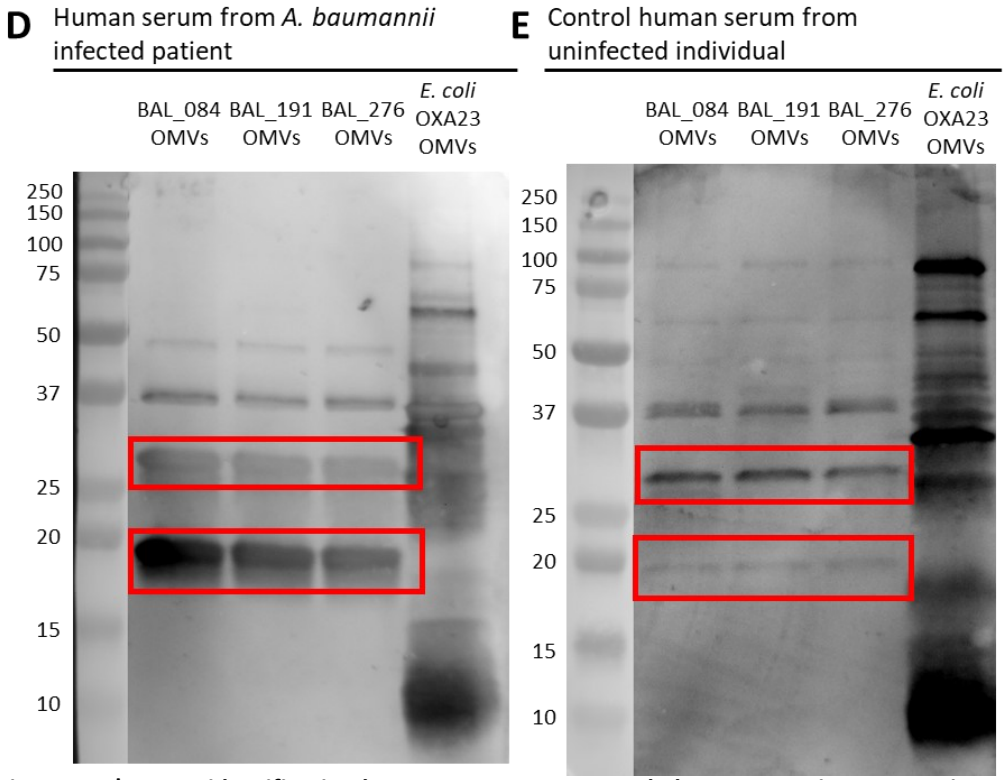
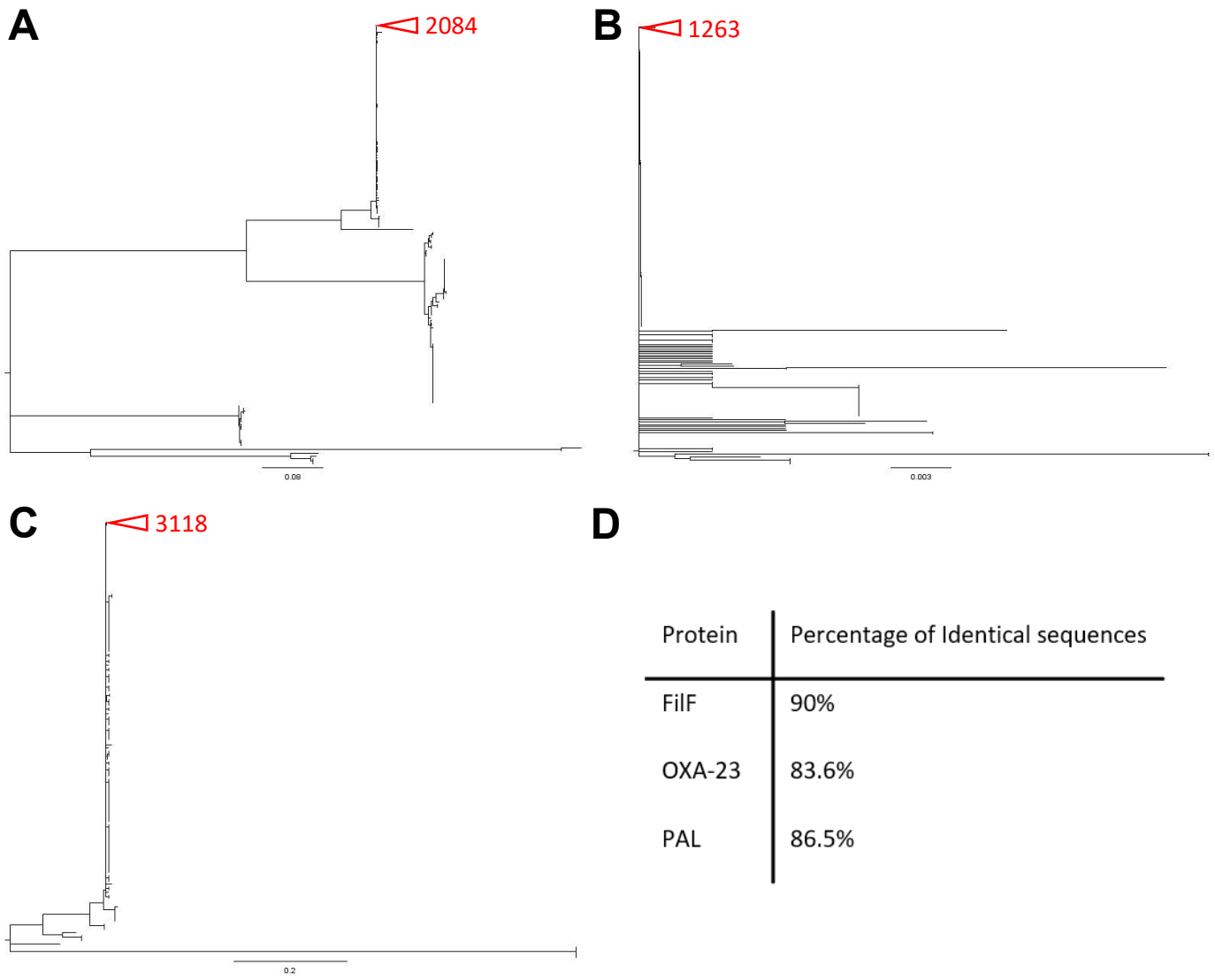


Figure 5.1 | Target identification by mass spectrometry and phage expression assay using antisera from immunised mice. *A. baumannii* (BAL_276) OMVs were run in parallel by SDS-PAGE. One gel was used for Western Blot **(A)** with antisera from mice immunised subcutaneously with *A. baumannii* (BAL_276) OMVs and the other gel was used for Coomassie staining and band excision for mass spectrometry analysis (red boxes) **(B)**. Putative proteins identified by phage expression assay **(C)**. Underlined gene names detected in both mass spectrometry and phage expression assays. *A. baumannii* OMVs were used for Western Blots using serum from an infected patient **(D)** and control uninfected patient **(E)**.

5.2.2 – Phylogenetic analysis shows FilF, OXA-23 and PAL are highly conserved between different strains of *A. baumannii*

Amino acid sequences were collated from the NCBI protein database for FilF, OXA-23 and PAL. The sequences were aligned, and a model selector was used to choose the best model for generating a maximum likelihood phylogenetic tree. Due to the size of the trees, the biggest branch showing identical sequences had to be collapsed, with the numbers of tips from each collapsed branch noted next to the collapsed branches. The phylogenetic tree representing FilF among different *A. baumannii* strains (Fig. 5.2.2 A) showed high levels of similarities of FilF between different strains: 90.4% of the 3448 collated sequences being identical. Additionally, the differences between those strains and the strains that were identical were minimal with the scale bar showing 0.08 substitutions. The phylogenetic tree showing the similarity of OXA-23 across different *A. baumannii* strains (Fig. 5.2.2 B) also showed high levels of similarity. The collapsed branch of identical sequences represented 83.6% of the 1510 sequences included in the tree. Additionally, any differences between those sequences and the variant sequences were very small with the scale bar showing 0.003 amino acid changes. Similarly, the tree representing PAL (Fig. 5.2.2 C) also showed high levels of similarity, with 86.5% of all of the collected sequences being identical and low levels of variation beyond that. Taken together, it can be concluded that all three proteins identified showed very high levels of similarity between different strains of *A. baumannii*.



Protein	Percentage of Identical sequences
FilF	90%
OXA-23	83.6%
PAL	86.5%

Figure 5.2 | Phylogenetic trees show high levels of similarity of FilF, OXA-23 and PAL between different *A. baumannii* strains. Amino acid sequences were collated and aligned for FilF, OXA-23 and PAL. The best model was selected for each maximum likelihood tree and the tree generated for FilF **(A)** with the scale bar representing 0.08 amino acid substitutions per site, OXA-23 **(B)** with the scale bar representing 0.003 amino acid substitutions per site, and PAL **(C)** with the scale bar representing 0.2 amino acid substitutions per site. The trees were rooted arbitrarily. Due to their size and the number of strains the tip labels were removed and the biggest branches with

5.2.3 – Cocktail of 29 *A. baumannii* mAbs did not protect against intranasal *A. baumannii* challenge in BALB/c mice

One alternative to vaccination is passive immunisation with antibodies. The protective efficacy of antibodies can be tested in the same way as a vaccine *in vivo*, enabling identification of protective antibodies. The antibodies were developed by Kymab, raised in human-immune repertoire mice against OMVs derived from the same four clinical isolates used here. B cells that produced antibody capable of binding to the surface of carbapenem resistant *A. baumannii* clinical isolates were singly sorted and sequenced to generate a library of OMV specific antibody sequences. Where sequence analysis indicated antibodies had undergone affinity maturation and a minimum level of binding to OMVs was identified VH/VL paired sequences to carry forwards for DNA synthesis and mAb expression in human embryonic kidney 293 cells. Kymab also performed target identification through phage expression cloning and western blotting.

A cocktail of 29 different mAbs was given to mice intravenously to determine whether the mAbs were protective against infection with *A. baumannii* BAL_276. Mice were intravenously given 5 mg/kg of IgG1 antibody cocktail in 50µl or 50µl PBS on day -1 and challenged intranasally with $5x10^7$ CFU in 100µl of *A. baumannii* BAL_276 or naïve mice were given 100µl PBS on day 0. Mice were weighed before challenge and 24 hours later (Fig. 5.2.3 A) with both challenge groups losing more weight than the naïve mice. The PBS group however, lost significantly more weight than the naïve mice ($p \leq 0.01$). An ELISA was performed on BAL fluid to quantify the amount of IL-6 (Fig. 5.2.3 B). The PBS mice had significantly more IL-6 in their BAL fluid compared to naïve mice ($p \leq 0.01$). The mice treated with mAbs had reduced IL-6 in their lungs compared to the PBS group, but the difference was not significant. The IL-6 was also measured in the lung homogenate supernatant (Fig. 5.2.3 C) with the PBS and mAb groups having very similar amounts of IL-6 in their lungs on average, both being significantly higher than the naïve mice ($p \leq 0.05$). Neutrophil infiltration into the lungs was measured by H&E staining and manual counting of the BAL cells (Fig. 5.2.3 D). The PBS mice had significantly more neutrophil infiltration into their lungs than the naïve mice ($p \leq 0.05$). The mAb treated mice had fewer neutrophils than the PBS mice and the increase between the naïve and mAb treated mice was not significant.

Lungs and spleens were dissected out of the mice and homogenised and BAL and nasal lavage were performed. BAL fluid, nasal lavage fluid, lung and spleen homogenates were all serially diluted and plated onto selective agar to estimate bacterial loads. Bacterial load in the BAL fluid was measured 24 hours after challenge (Fig. 5.2.3 E) with both the PBS and mAb treated groups having significantly more bacteria than the naïve mice ($p \leq 0.05$ and $p \leq 0.01$ respectively). The bacterial burden in the upper respiratory tract was measured by nasal lavage (Fig. 5.2.3 F) and the mAb treated mice had slightly reduced bacterial load compared to the PBS mice, but this was not significant. The PBS mice had significantly increased bacterial load in their upper respiratory tracts compared to the naïve mice ($p \leq 0.01$). Bacterial load in the lungs 24 hours after infection (Fig. 5.2.3 G) showed an increase in the mAb group compared to the PBS group. The amount of bacteria recovered from the lungs of the mAb treated mice was also significantly higher than the naïve mice ($p \leq 0.01$). The bacterial load was also measured in the spleen (Fig. 5.2.3 H) with the mAb treated mice having the highest bacterial load, which was significantly increased compared to the naïve mice ($p \leq 0.01$). Pre-treating mice intravenously with *A. baumannii* mAbs caused slightly reduced weight loss and reduced IL-6 in the BAL, but had no effect on bacterial loads across the tested sites. The cocktail of 29 mAbs therefore did not provide protection against challenge.

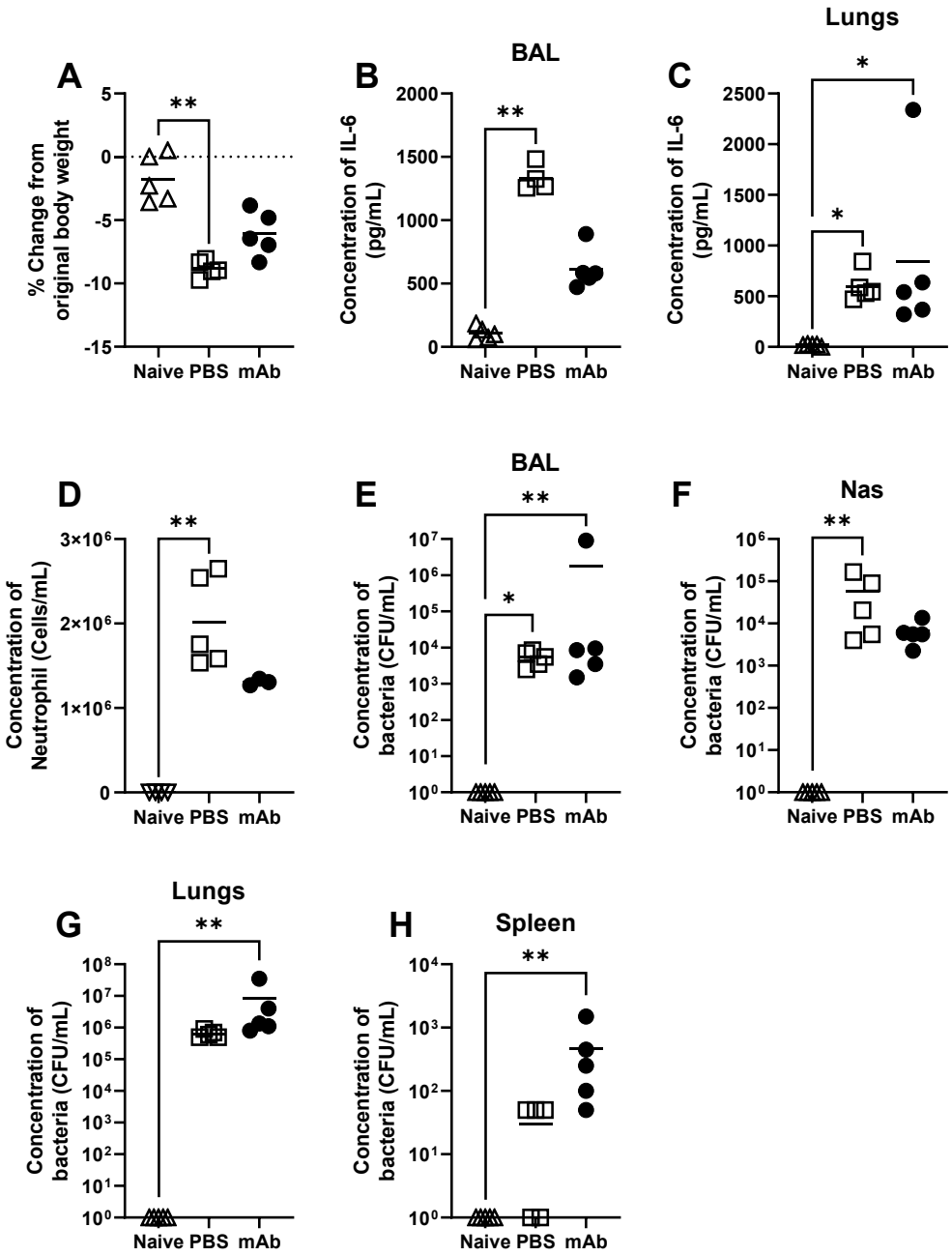


Figure 5.3 | Cocktail of 23 mAbs does not provide protection against challenge with *A. baumannii* BAL_276. Adult BALB/c mice were intravenously injected with 5 mg/kg cocktail of mAbs (mAb) or PBS on day -1, challenged on day 0 with $5x10^7$ CFU *A. baumannii* BAL_276 and culled 24 hours later. Weight **(A)**, IL-6 in the BAL **(B)** and lungs **(C)** and neutrophil counts **(D)** were measured 24 hours after infection. Bacterial load at 24 hours in BAL **(E)**, upper respiratory tract **(F)**, lungs **(G)** and spleen **(H)**. Kruskal-Wallis tests were used to test for significant differences. **p≤0.05, **p ≤0.01, ***p ≤0.001, ****p ≤0.0001.* Points represent individual animals.

5.2.4 – Conformational binding mAb cocktail 2 reduces inflammation in the lungs of BALB/c mice after *A. baumannii* BAL_276 challenge

The targets of the individual mAbs were identified by Kymab and 2 cocktails of 4 mAbs were suggested. Cocktail 1 contained antibodies against lipooligosaccharide (LOS) and OXA23 and cocktail 2 contained conformational binders, where the antigen could not be identified by western blot or screening of the phage expression library with binding therefore hypothesised as requiring recognition of a conformational epitope. Mice were pre-treated with 2 *A. baumannii* targeting mAb cocktails to determine whether increased amounts of each individual mAb, with known *A. baumannii* BAL_276 binding, could better protect mice against infection than the previous cocktail of 29 *A. baumannii* mAbs. The mice were given 5 mg/kg of each cocktail intravenously to see if having increased concentrations of each individual antibody targeting LOS and OXA23 or capsule would better protect against infection. The study would also give information on whether certain targets might have better potential for protective mAbs. Mice were given 5 mg/kg of either cocktail 1, cocktail 2, isotype control mAbs or 50µl PBS intravenously on day -1. On day 0 mice were challenged intranasally with $5x10^7$ CFU *A. baumannii* BAL_276 and culled 24 hours later. Mice were weighed before infection and 24 hours after (Fig. 5.2.4 A) with all groups of mice losing similar amounts of weight on average. IL-6 was measured in the BAL fluid (Fig. 5.2.4 B) both the cocktails of mAbs reduced the level of IL-6 compared to the isotype and PBS control groups. However, only cocktail 2 was significantly reduced BAL IL-6 compared to the PBS group ($p \leq 0.01$). Neutrophil infiltration into the lungs was measured in the BAL (Fig. 5.2.4 C) with all of the antibody treatments slightly raising the numbers of neutrophils compared to PBS mice. However, none of the differences were significant.

The bacterial loads were also measured in the BAL (Fig. 5.2.4 D), upper respiratory tract (Fig. 5.2.4 E), lungs (Fig. 5.2.4 F) and spleen (Fig. 5.2.4 G). Bacterial load in the BAL fluid was very similar across all 4 groups. In the upper respiratory tract although cocktail one had the biggest bacterial load, the bacterial loads were very similar across all of the groups. In the lungs the mice that were treated with cocktail 1 and cocktail 2 had slightly reduced bacterial loads compared to the PBS and isotype control mice. However, the difference was not significant. There was also no difference in the amount of bacteria recovered from the spleens of any of the mice. These results have shown cocktail 1 and 2 both reduced

inflammation in the lungs, however only cocktail 2 was significant. Additionally, both cocktail 1 and 2 slightly reduced the bacterial burden in the lungs. However, neither cocktail had any effect on weight loss, neutrophil infiltration or bacterial load in the BAL, upper respiratory tract or spleens.

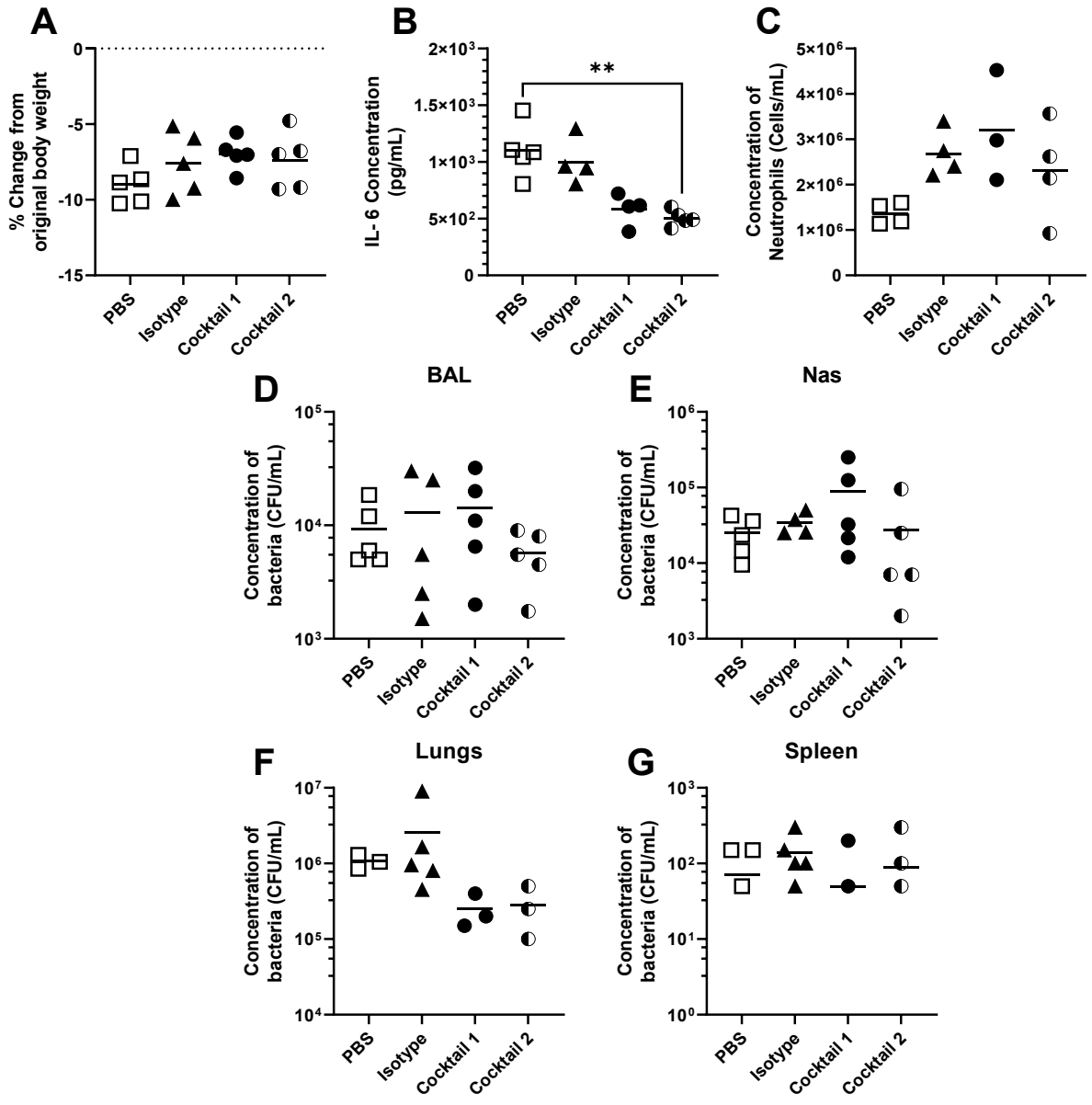


Figure 5.4 | mAb cocktails provide some protection against disease following challenge with *A. baumannii* BAL_276. Adult BALB/c mice were intravenously injected with 5 mg/kg cocktail 1 or cocktail 2 of mAb, 5 mg/kg isotype control or PBS on day -1, challenged on day 0 with $5x10^7$ CFU *A. baumannii* BAL_276 and culled 24 hours later. Weight **(A)**, IL-6 in the BAL **(B)** and neutrophil counts **(C)** were measured 24 hours after infection. Bacterial load at 24 hours in BAL **(D)**, upper respiratory tract **(E)**, lungs **(F)** and spleen **(G)**. Kruskal-Wallis tests were used to test for significant differences. **p≤0.05, **p ≤0.01, ***p ≤0.001, ****p ≤0.0001.* Points represent individual animals.

5.2.5 – Intravenous anti-LOS mAb1042 did not protect against 24 or 48 hour challenge with *A. baumannii* BAL_276 in BALB/c mice

To see if just an individual antibody targeting an antigen present on the challenge bacteria could protect against challenge mice were given a high or low dose of an anti-LOS mAb (mAb1042) and then challenged with *A. baumannii* BAL_276. Mice were intravenously injected with PBS, 10 mg/kg isotype control, mAb1042 or 1 mg/kg mAb1042 on day -1. On day 0 mice were then intranasally challenged with $5x10^7$ CFU *A. baumannii* BAL_276 and then culled 24 or 48 hours later. Weight was measured from the intravenous dose until 48 hours after challenge (Fig. 5.2.5 A). There was no difference in weight loss between any of the groups and all mice lost similar amounts of weight at similar rates. The amounts of IL-6 in the BAL (Fig. 5.2.5 B) and lungs (Fig. 5.2.5 C) were also measured. The levels of IL-6 in the BAL were similar across all groups 24 hours after challenge and 48 hours after challenge. Although there was little difference between the groups at each time point, the 10 mg/kg mAb1042 group did see a significant reduction in the amount of IL-6 in the BAL from 24 to 48 hours after challenge ($p \leq 0.05$). In the lungs however, there were very similar amounts of IL-6 across all groups at both 24 and 48 hours after challenge with similar rates of reduction.

The bacterial burden 24 and 48 hours after challenge was measured in the BAL, upper respiratory tract, lungs and spleens. The amount of bacteria recovered from the BAL (Fig. 5.2.5 D) was around 0.5 log higher in both of the mAb1042 treated mice compared to the PBS mice and around 1 log higher than the isotype control mice 24 hours after challenge. The bacterial load in the BAL 48 hours after challenge was similar across all groups however the mAb1042 treated mice had bigger decreases in bacterial load between 24 and 48 hours after challenge with the 1 mg/kg mAb1042 group having a significant reduction in bacterial load between 24 and 48 hours after challenge ($p \leq 0.05$). The bacterial load in the upper respiratory tract (Fig. 5.2.5 E) was similar across all groups at both 24 and 48 hours after infection. The amount of bacteria recovered from the lungs (Fig. 5.2.5 F) 24 hours after challenge was similar across all groups. However, 48 hours after challenge the 1 mg/kg mAb1042 treated mice had a significant reduction in bacterial load compared to 24 hours after challenge ($p \leq 0.05$). The bacterial load in the spleen (Fig. 5.2.5 G) was very similar across all groups 24 hours after challenge. However, 48 hours after challenge only the

isotype control and 10 mg/kg mAb1042 groups had bacteria recoverable from their spleens with the isotype control having significantly increased bacterial load compared to the PBS and 1 mg/kg mAb1042 groups ($p \leq 0.01$). The mAb1042 made no difference to weight loss, IL-6 levels or bacterial loads compared to the other groups.

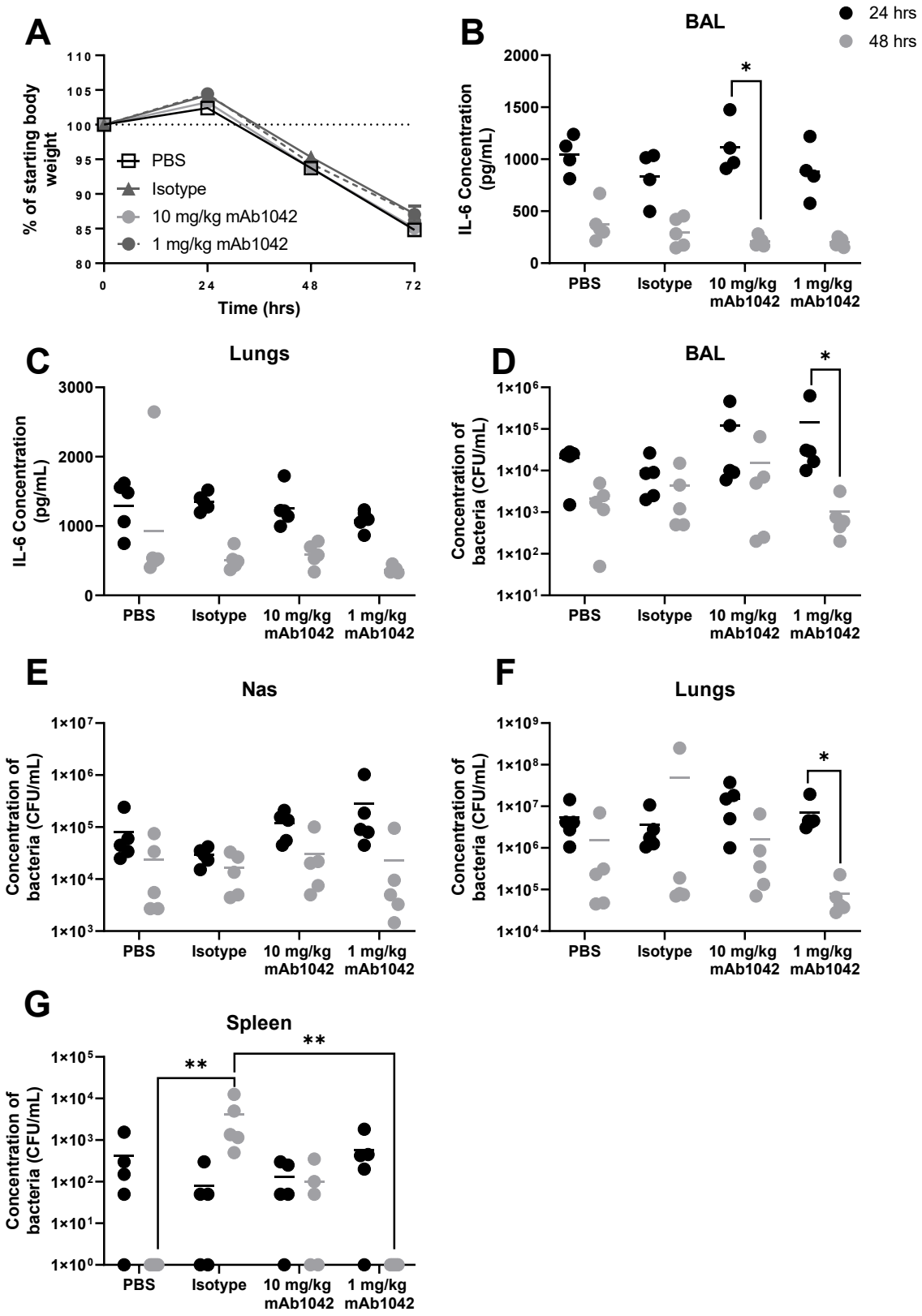


Figure 5.5 | Intravenous anti-LOS mAb1042 does not provide protection against challenge with *A. baumannii* BAL_276. Adult BALB/c mice were intravenously injected with 1 or 10 mg/kg of mAb1042, 10 mg/kg isotype control mAb or PBS on day -1, challenged on day 0 with $5x10^7$ CFU *A. baumannii* BAL_276 and culled 24 or 48 hours later. Weight **(A)** and IL-6 in the BAL **(B)** and lungs **(C)** were measured during infection. Bacterial load at 24 and 48 hours in BAL **(D)**, upper respiratory tract **(E)**, lungs **(F)** and spleen **(G)**. Kruskal-Wallis tests were used to test for significant differences. **p≤0.05, **p ≤0.01, ***p ≤0.001, ****p ≤0.0001.* Points for bodyweight represent means, all other points represent individual animals.

5.2.6 – Intravenous anti-LOS mAb1042 did not protect against *A. baumannii* BAL_191 challenge in BALB/c mice

Mice were intravenously dosed with 10 mg/kg anti-LOS mAb1042 to see if it would protect against challenge with a different bacterial strain *A. baumannii* BAL_191. Mice were given either mAb1042, isotype control mAb or nothing on day -1 and intranasally challenged with $5x10^7$ CFU *A. baumannii* BAL_191 on day 0 and culled 24 hours later. Weight was measured during infection (Fig. 5.2.6 A) with all three groups of mice losing very similar amounts of weight. Bacterial burden was also measured in the BAL (Fig. 5.2.6 B), upper respiratory tract (Fig. 5.2.6 C), lungs (Fig. 5.2.6 D) and spleen (Fig. 5.2.6 E) 24 hours after challenge. Bacterial loads in the BAL, upper respiratory tract and lungs were very similar in all three groups with no significant differences. In the spleen, the mice treated with mAb1042 and the control mice had very similar amounts of bacteria recovered. However, the isotype control mice had significantly more bacteria recovered from their spleens compared to the control mice. Anti-LOS mAb1042 did not protect against infection with *A. baumannii* BAL_191 in BALB/c mice with no difference in bacterial loads or weight loss.

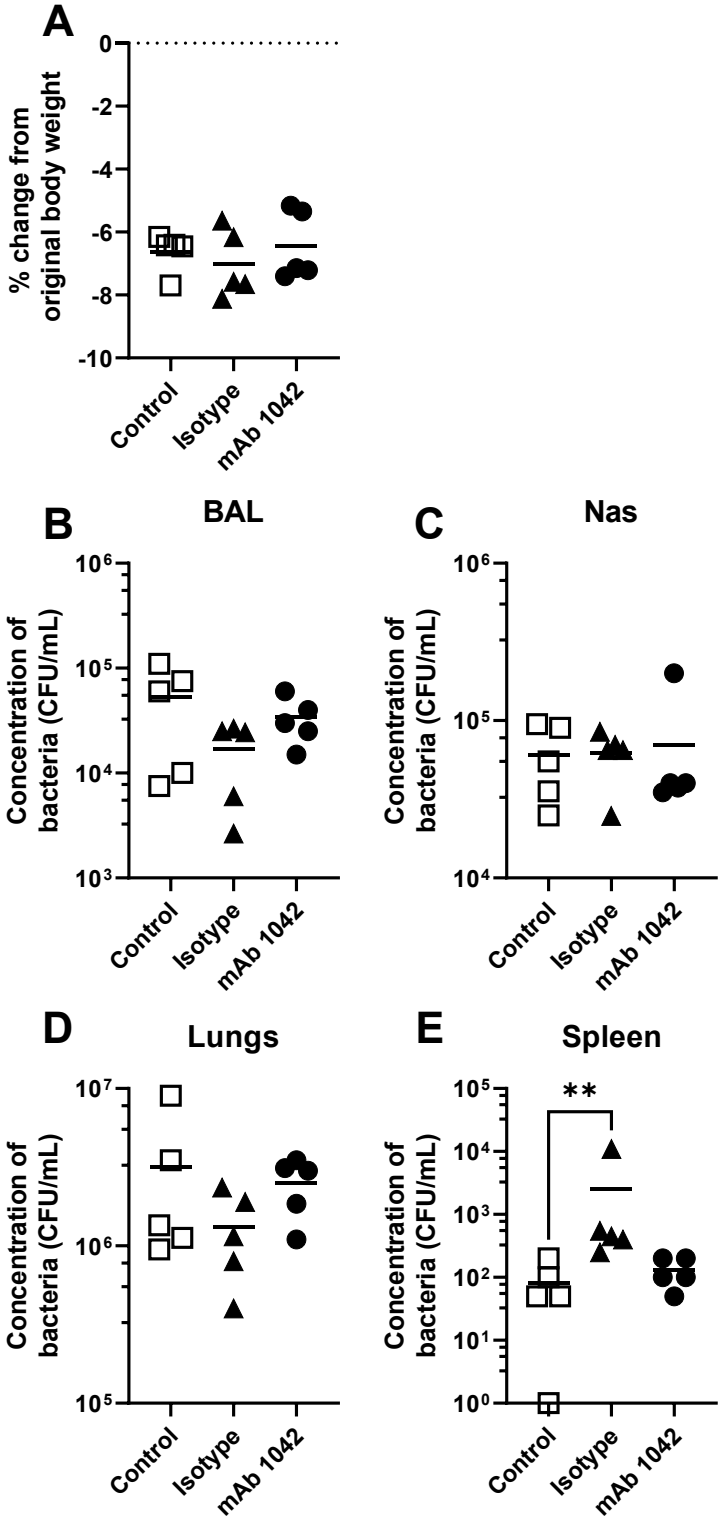


Figure 5.6 | Intravenous anti-LOS mAb1042 does not provide protection against challenge with *A. baumannii* BAL_191. Adult BALB/c mice were intravenously dosed with 10 mg/kg of mAb1042 or isotype control mAb on day -1 and day 0, challenged on day 0 with $5x10^7$ CFU *A. baumannii* BAL_191 and culled 24 hours later. Weight **(A)** and bacterial load at 24 hours in BAL **(B)**, upper respiratory tract **(C)**, lungs **(D)** and spleen **(E)**. Kruskal-Wallis tests were used to test for significant differences. **p≤0.05, **p ≤0.01, ***p ≤0.001, ****p ≤0.0001.* Points represent individual animals.

5.2.7 – Anti-OXA-23 mAb1349 does not protect against challenge with *A. baumannii* BAL_276 in BALB/c mice

To see if an anti-OXA-23 mAb alone was able to protect mice against challenge, mice were given mAb1349 24 and 4 hours prior to challenge. The mAb was also given via two different routes, intravenous and intranasal, to compare whether there are different levels of efficacy depending on the route. Mice were intravenously or intranasally dosed with 10 mg/kg mAb1349 or isotype control in 100 µl or nothing. Mice given mAb1349 intravenously were dosed on day -1 and 4 hours before challenge on day 0. Mice given mAb1349 intranasally were only given mAb 4 hours before challenge on day 0. On day 0, mice were intranasally challenged with $5x10^7$ CFU *A. baumannii* BAL_276 and culled 24 hours later. Mice were weighed during challenge (Fig. 5.2.7 A), all mice lost between 5 and 10% of their bodyweight prior to challenge. There was some variation in weight loss between the different treatment groups however, there were no significant differences. The amount of IL-6 was measured in the BAL (Fig. 5.2.7 B) and lungs (Fig. 5.2.7 C). Mice given mAb1349 intranasally had significantly less IL-6 in their BAL compared to intranasal isotype control ($p \leq 0.01$) or intravenous mAb1349 ($p \leq 0.05$). The mice given isotype control mAb also had low levels of IL-6 in their BAL compared to the other mice, but this was not significant. In the lungs however, the intranasal treated mAb1349 mice had the highest amount of IL-6 compared to the other groups, which was significantly increased compared to the PBS control mice ($p \leq 0.01$). There was no difference in the amount of IL-6 in the lungs of the other mAb groups. The total number of cells in the BAL was counted after lysing red blood cells with ACK buffer (Fig. 5.2.7 D). The mice given mAb1349 intranasally had significantly less white blood cells in their lungs compared to the mice given mAb1349 IV ($p \leq 0.01$).

Bacterial load was measured in the BAL fluid, upper respiratory tract, lungs and spleen 24 hours after challenge. There was not much difference in the amount of bacteria recovered from the BAL of any of the groups (Fig. 5.2.7 E). However, mice given intravenous isotype control mAb had significantly lower bacterial loads compared to the mice given mAb1349 intranasally ($p \leq 0.05$). The bacteria recovered from the upper respiratory tract was very similar across all groups (Fig. 5.2.7 F) with no significant differences between any of the groups. The bacterial load in the lungs (Fig. 5.2.7 G) showed little difference in the bacterial loads of any mouse treated with mAb. All mice given mAb however, had slightly raised

bacterial loads compared to the PBS mice but this was not significant. Bacterial load was also measured in the spleen (Fig. 5.2.7 H) where the amount of bacteria recovered was lowest in the intranasal isotype control group which was significantly reduced compared to the mice given mAb1349 IN ($p \leq 0.01$). The mice given mAb1349 intravenously had very similar amounts of bacteria recovered from their spleens as the PBS mice. The results from this study showed that anti-OXA-23 mAb1349 given either intravenously or intranasally did not result in significantly reduced weight loss, inflammation or bacterial burden and there was no difference between the two routes.

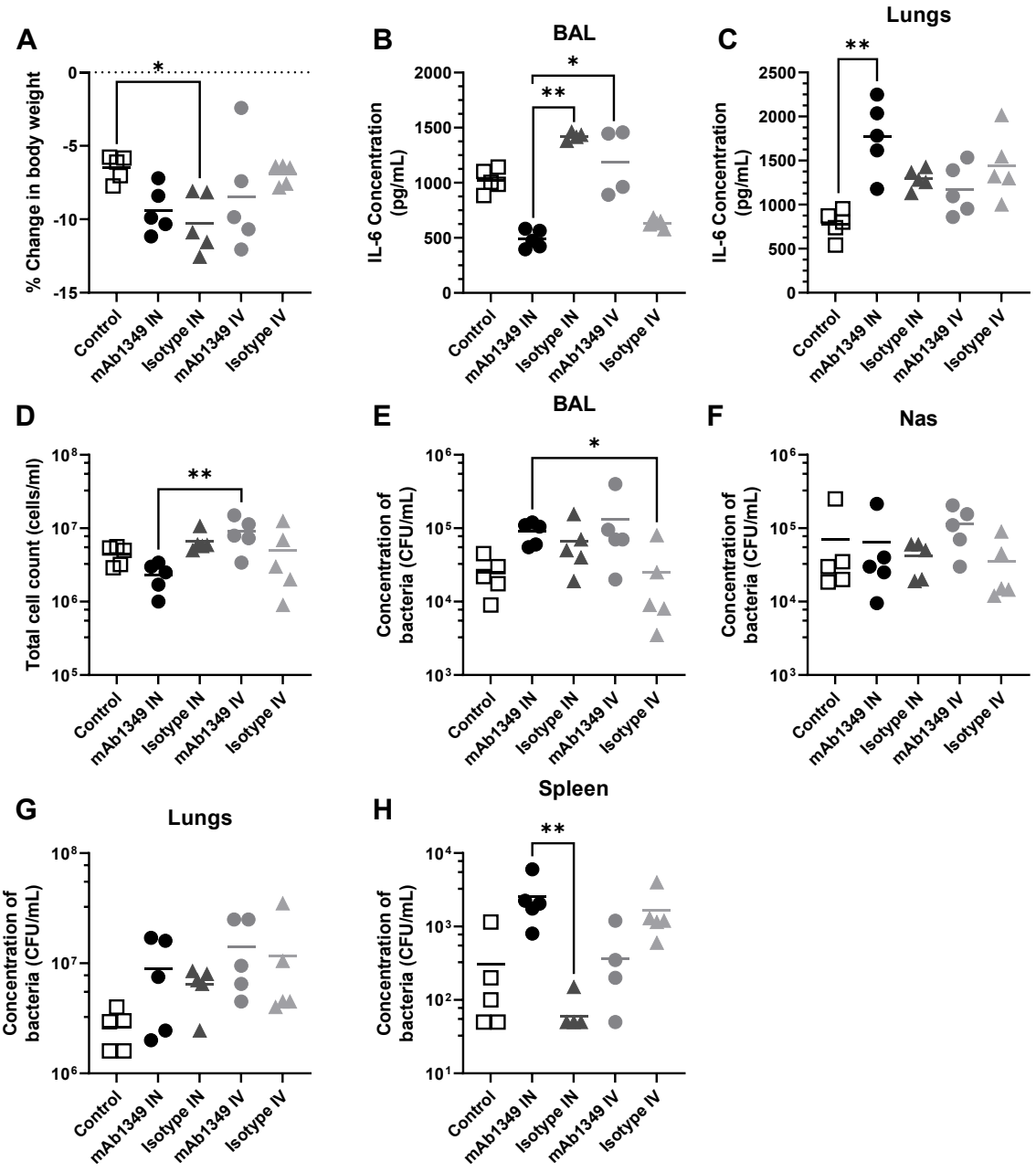


Figure 5.7 | Intravenous anti-OXA-23 mAb1349 does not provide protection against challenge with *A. baumannii* BAL_276. Adult BALB/c mice were intravenously or intranasally dosed with 10 mg/kg of mAb1349, 10 mg/kg isotype control mAb or nothing on day -1 and day 0, challenged on day 0 with $5x10^7$ CFU *A. baumannii* BAL_276 and culled 24 hours later. Weight **(A)** and IL-6 in the BAL **(B)** lungs **(C)** and total cells in the BAL **(D)** were measured 24 hours after challenge. Bacterial load at 24 in BAL **(E)**, upper respiratory tract **(F)**, lungs **(G)** and spleen **(H)**. Kruskal-Wallis tests were used to test for significant differences. **p≤0.05, **p ≤0.01, ***p ≤0.001, ****p ≤0.0001.* Points represent individual animals.

5.2.8 – Intravenous anti-OXA-23 mAb1349 did not protect against intranasal challenge with *A. baumannii* BAL_191

To see if anti-OXA-23 mAb1349 protected against a different strain with a different capsule type (KL49), mice were intravenously dosed with 10 mg/kg anti-OXA-23 mAb1349 24 and 4 hours prior to intranasal challenge with *A. baumannii* BAL_191. Two control groups were used, one group received nothing but the intranasal challenge (control) and the other was given 10 mg/kg isotype control mAb IV instead of mAb1349. All mice were culled 24 hours after challenge. Change in bodyweight was measured before and after 24 hour challenge (Fig. 5.2.8 A) and all mice lost very similar amounts of weight. Bacterial load was also measured 24 hours after challenge in the BAL, upper respiratory tract, lungs and spleen. The bacterial load in the BAL (Fig. 5.2.8 B) was lowest in the isotype control, but this wasn't significant and there was very little difference between any of the groups. The amount of bacteria recovered from the upper respiratory tract (Fig. 5.2.8 C) was lowest in the mice given mAb1349, however it wasn't significant and all of the groups were very similar. There was also very little difference in bacterial load in the lungs (Fig. 5.2.8 D). The bacterial load in the spleens (Fig. 5.2.8 E) of the mAb1349 mice was very similar to the control mice that received nothing, but significantly less than the isotype control. However, not all mice in either the control or mAb1349 group had bacteria recoverable from the spleens of all mice. In this study the anti-OXA-23 mAb1349 given at 10 mg/kg IV was not protective and did not decrease weight loss or bacterial loads in BALB/c mice challenged with *A. baumannii* BAL_191.

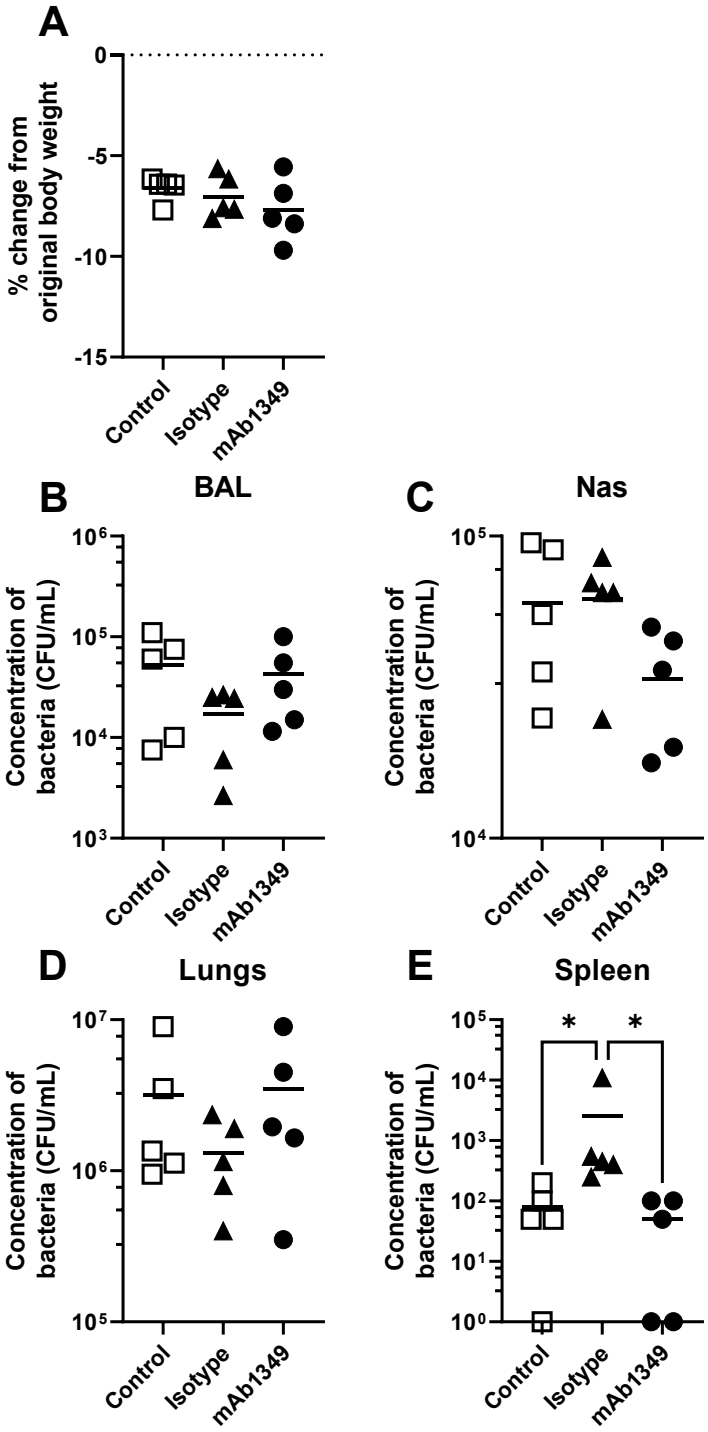


Figure 5.8 | Intravenous anti-OXA-23 mAb1349 does not provide protection against challenge with *A. baumannii* BAL_191. Adult BALB/c mice were intravenously dosed with 10 mg/kg of mAb1349 or isotype control mAb on day -1 and day 0, challenged on day 0 with $5x10^7$ CFU *A. baumannii* BAL_191 and culled 24 hours later. Weight **(A)** and bacterial load at 24 hours in BAL **(B)**, upper respiratory tract **(C)**, lungs **(D)** and spleen **(E)**. Kruskal-Wallis tests were used to test for significant differences. **p≤0.05, **p ≤0.01, ***p ≤0.001, ****p ≤0.0001.* Points represent individual animals.

5.2.9 – Anti-KL-49 capsule mAb1416 provided some protection against challenge with *A. baumannii* BAL_191 in BALB/c mice

To see whether capsule targeting mAbs rather than those targeting LOS or OXA-23 could be protective against infection mice were pre-treated with anti-KL-49 capsule mAb1416 before challenge with a KL-49 type clinical strain of *A. baumannii*. Mice were given 10 mg/kg mAb1416, isotype control mAb IV or nothing 24 and 4 hours before challenge. Mice were challenged intranasally with $5x10^7$ CFU *A. baumannii* BAL_191 intranasally and culled 24 hours later. Mice were weighed before and after challenge (Fig. 5.2.9 A) but there was little difference in weight loss between the 3 groups. Bacterial load was measured in the BAL, upper respiratory tract, lungs and spleen 24 hours after challenge. The amount of bacteria recovered from the BAL (Fig. 5.2.9 B) showed no difference between the mAb1416 and isotype control groups, which were also very similar to the control mice. The bacterial load in the upper respiratory tract (Fig. 5.2.9 C) showed a very similar average between the control and isotype control groups with a slight reduction in the amount of bacteria recovered from the mAb1416 group. However, this difference was not significant. The amount of bacteria recovered from the lungs (Fig. 5.2.9 D) of the mAb1416 treated mice was significantly decreased compared to the control mice. However, there was no difference between the mAb1416 mice and the isotype control mice. Only 2 out of the 10 mice in the mAb1416 treated mice had bacteria recoverable from the spleen (Fig. 5.2.9 E) which was significant reduction compared to the control ($p \leq 0.05$) and isotype control groups ($p \leq 0.001$). Despite there being no difference in weight loss, mice given IV mAb1416 had significantly reduced bacterial loads in their spleens compared to the control groups and a slight reduction of bacterial load in the upper respiratory tract suggesting low levels of protection against infection.

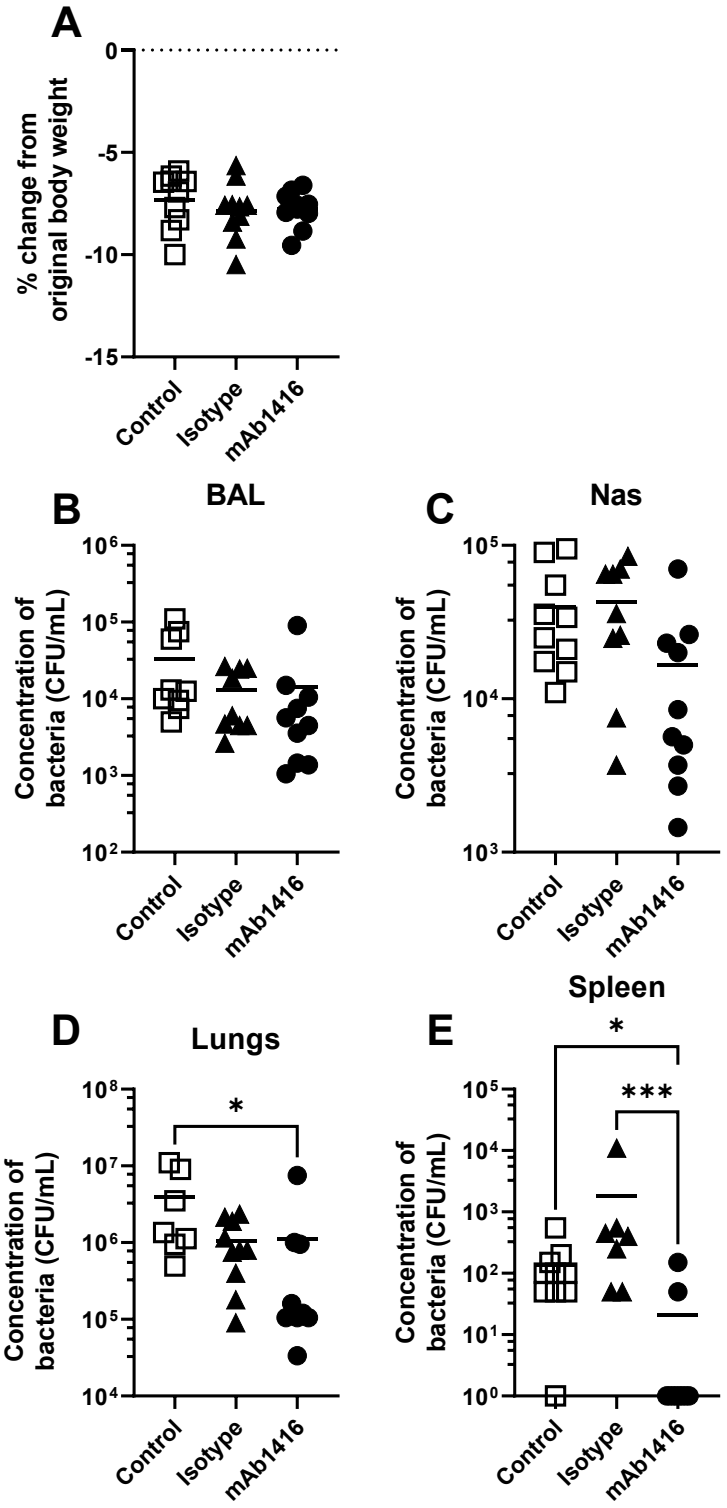


Figure 5.9 | Intravenous anti-KL-49 capsule mAb1416 provides some protection against challenge with *A. baumannii* BAL_191. Adult BALB/c mice were intravenously dosed with 10 mg/kg of mAb1416 or isotype control mAb on day -1 and day 0, challenged on day 0 with $5x10^7$ CFU *A. baumannii* BAL_191 and culled 24 hours later. Weight **(A)** and bacterial load at 24 hours in BAL **(B)**, upper respiratory tract **(C)**, lungs **(D)** and spleen **(E)**. Kruskal-Wallis tests were used to test for significant differences. **p≤0.05, **p ≤0.01, ***p ≤0.001, ****p ≤0.0001.* Points represent individual animals.

5.2.10 – Anti-KL-49 capsule mAb1416 provides better protection against challenge with *A. baumannii* BAL_191 when given to BALB/c mice intranasally

To see if the route of administration of mAbs would affect levels of protection, like vaccination, mice were given mAb1416 intranasally before challenge. Mice were given 10 mg/kg mAb1416 or isotype control intranasally 4 hours before intranasal challenge with $5x10^7$ CFU *A. baumannii* BAL_191and culled 24 hours later. Mice were weighed before and after challenge (Fig. 5.2.10 A) with very little difference in weight loss between the 3 groups. The amount of white blood cells in the BAL after being treated with ACK cell lysis buffer were counted with trypan blue (Fig. 5.2.10 B). Mice treated with mAb1416 prior to challenge had significantly lower concentrations of cells in their BAL compared to the control ($p \leq 0.05$) and isotype control groups ($p \leq 0.05$). Bacterial loads in the BAL, upper respiratory tract, lungs and spleen were measured 24 hours after challenge. The amount of bacteria recovered from the BAL (Fig. 5.2.10 C) was lowest in the mAb1416 mice compared to both the control and isotype control mice, but the difference was not significant. The bacterial load in the upper respiratory tract (Fig. 5.2.10 D) of mAb1416 treated mice was significantly lower than the control mice ($p \leq 0.05$) and was also lower than the isotype control mice, but this difference was not significant. The bacterial load in the lungs (Fig. 5.2.10 E) was the lowest in the mAb1416 treated mice, but the difference was not significant due to the numbers of mice with quantifiable samples. The mice pre-treated with mAb1416 also had no bacteria recovered from their spleens (Fig. 5.2.10 F), which was a significant decrease compared to the control mice ($p \leq 0.01$). The bacterial load recovered from the spleens of the mAb1416 mice was also much lower than the isotype control mice, but this was not significant. Pre-treating mice intranasally with mAb1416 provided better protection against challenge than when it was given intravenously, reducing the amount of white blood cell infiltration into the lungs and reducing the bacterial burden in the upper respiratory tract, lungs and spleen.

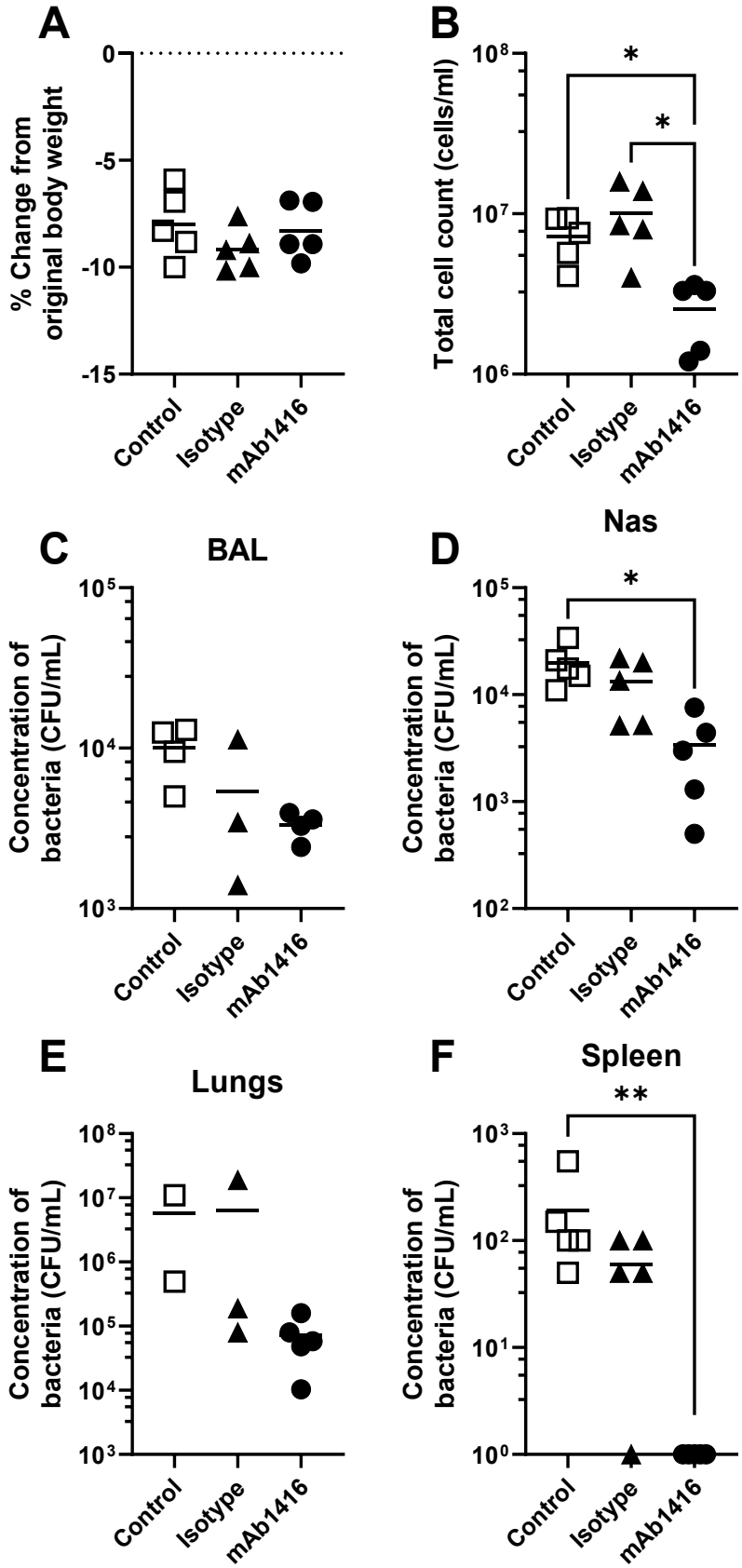


Figure 5.10 | Intranasal administration of anti-KL-49 capsule mAb1416 provides improved protection against challenge with *A. baumannii* BAL_191 than intravenous. Adult BALB/c mice were intranasally dosed with 10 mg/kg of mAb1416 or isotype control mAb on day -1 and day 0, challenged on day 0 with $5x10^7$ CFU *A. baumannii* BAL_191 and culled 24 hours later. Weight **(A)** and bacterial load at 24 hours in BAL **(B)**, upper respiratory tract **(C)**, lungs **(D)** and spleen **(E)**. Kruskal-Wallis tests were used to test for significant differences. **p≤0.05, **p ≤0.01, ***p ≤0.001, ****p ≤0.0001.* Points represent individual animals.

5.3 – Discussion

The work performed here showed that three potential vaccine targets, identified through two different methods, elicited antibody responses in both mice and humans. Phylogenetic trees of FilF, OXA-23 and PAL across different *A. baumannii* strains obtained from the NCBI protein database showed high levels of similarity of the proteins among strains where 84-90% of sequences were identical. Additionally, mAbs had been produced by Kymab that were raised against the same clinical strains used so far in this work. The mAbs bound to multiple targets, but OXA-23 binding was also identified independently by Kymab. The mAbs showed mixed results in the *in vivo* infection model (Table 5.1).

Table 5.1 | Summary of *In vivo* mAb pre-treatments and their effect on protective efficacy against intranasal challenge. A summary of infection responses in BALB/c mice after different mAb pre-treatments prior to intranasal challenge. Responses depicted as + (mild increase), ++ (moderate increase), +++ (large increase), - (mild decrease), -- (moderate decrease), --- (large decrease) or ND (no difference).

mAb and route of administration	Weight loss	Inflammation (IL-6)	Bacterial load	Bacterial dissemination
23 mAb cocktail - IV	ND	--	ND	+
Conformational mAb cocktail - IV	ND	--	ND	ND
LOS and OXA-23 mAb cocktail - IV	ND	-	ND	ND
LOS mAb1042 - IV	ND	NA	+	ND
OXA-23 mAb1349 - IV	+	+	+	-
OXA-23 mAb1349 - IN	+	--	+	++
Capsule mAb1416 - IV	ND	NA	--	--
Capsule mAb1416 - IN	ND	NA	--	---

FilF is a putative pilus assembly protein of *A. baumannii* found in the outer membrane[214,221] that has shown efficacy in animal models[222,223]. FilF has been identified a number of times via reverse vaccinology as a protein with good potential as a novel vaccine candidate[214,221,223]. Among the different serovars of *A. baumannii* FilF has been found to be one of the most conserved proteins[214] supporting its potential in the development of a broadly protective vaccine. Although FilF's role in virulence is unknown it resulted in

increased survival rate of 50% when used to vaccinate mice in an *in vivo A. baumannii* pneumonia survival model, resulting in good humoral responses and significant reduction in neutrophil infiltration into the lungs, inflammatory responses and bacterial load in the lungs[223].

PAL is a peptidoglycan associated lipoprotein found in the cell membrane and is a part of the Tol-Pal complex, which is involved in cell division[219,224]. The Tol-Pal system is physiologically important with mutations in the system resulting in increased drug and detergent sensitivity, periplasmic leakage, increased blebbing of OMVs and an upregulation of an extra cytoplasmic stress response[224]. Using a murine pneumonia model a DNA vaccine against OmpA and Pal mice elicited strong humoral responses resulting in a reduction of bacterial load and pathology in the lungs as well as reduced inflammation and cell inflammation in BAL[219].

The main mechanism of carbapenem resistance among *A. baumannii* strains is the acquisition of carbapenem-hydrolysing oxacillinase-encoding genes for which *oxa23* is the most widespread[225,226]. The *oxa23* gene can move between strains on plasmids, transposons and genomic resistance islands[225]. It has been shown previously that animals immunised with β-lactamases were able to produce strong neutralising antibody responses resulting in reduced bacterial burden and pathology[221].

The western blot using sera from infected human patients showed clear binding to both OXA-23 and PAL but no visible binding to FilF. This could be due to lower concentrations of anti-FilF antibodies present in the sera compared to the OXA-23 and PAL antibodies. Another explanation could be due to the sensitivity of the method of detection and perhaps needing longer incubation times to be able to see any band for FilF as during other performed in the lab, this was a particularly difficult protein to image alongside OXA-23 and PAL so this would need further testing to confirm. Particularly as it looks as though there could be some binding in the uninfected individual.

A similar antigen discovery process was used to identify mAb with protective capacity. *A. baumannii* targeting mAbs were then tested *in vivo* to see whether they were protective against infection with *A. baumannii* clinical strains. Mice treated with cocktails of mAbs experienced a reduction in inflammation in the lungs and in the case of cocktail 1 and 2,

slightly reduced bacterial loads in the lungs. Individual antibodies were then tested to see if larger doses of an effective antibody could provide better protection against challenge. Neither the LOS nor OXA-23 targeting mAbs were able to protect BALB/c mice against challenge with *A. baumannii* BAL_276. The OXA-23 targeting mAb, mAb1349, could even be having some off target effects causing an increase in bacterial load compared to isotype and PBS controls and maybe even resulting in antibody-dependent disease enhancement. KL-49 capsule targeting mAb1416 was able to protect against challenge with KL-49 type *A. baumannii* BAL_191. Pre-treatment with mAb1416 given IV before intranasal challenge resulted in reduced bacterial loads in the lungs and spleens of BALB/c mice while also reducing dissemination from the lungs. Giving mice mAb1416 intranasally further increased efficacy leading to reduced white blood cell infiltration into the lungs and reduced bacterial burden in the upper respiratory tract, lungs and complete prevention of bacterial dissemination to the spleen.

Although, many of the mAbs were ineffective the capsule targeting mAb was able to provide some protection against challenge. This could be due to the surface polysaccharides found on *A. baumannii* shielding the antibody targets resulting in decreased binding and reduced opsonisation and complement action[227]. This is supported not only by our own data, but also with other research. Most effective *A. baumannii* mAbs that have shown efficacy in *in vivo* infection models were raised against capsule or biofilm targets[211,212,227–230]. A combination of mAbs might be able to combat this problem by disrupting the capsule or outer membrane and allow for better access for other mAbs[211], which might be why there were low levels of efficacy when the cocktails of mAbs were used. Further work to find effective combinations of mAbs that work synergistically could result in increased levels of protection. Additionally, the use of mAb in combination with antibiotic could provide further improvements in treating infection with *A. baumannii*[212]. The intranasal administration of mAb1416 was more effective than the intravenous, with a reduction of bacterial load seen across more sites. This is similar to the results seen in the previous chapter with intranasal vaccination being the most effective, suggesting that the route of administration is important too. Intranasally administered mAbs might be able to target the bacteria more quickly due to already being in the lungs and upper respiratory tract in large quantities further increasing the protective efficacy of mAb treatment against *A. baumannii*.

Interestingly, the intravenous administration of mAb1416 had a small effect on the lungs but a greater effect in the spleen at reducing bacterial load. This could be due to lower levels of bacteria in the spleen so the mAbs are not overloaded and are better able to have an effect. Or potentially the human IgG1 mAbs could be better at translocating to the spleen than the lungs.

Due to not knowing the epitopes of the antigens it is difficult to determine how important the high levels of sequence homology is between different *A. baumannii* strains. For example, if the antigens are highly conserved between bacterial strains everywhere but where the antibodies are binding then you'd need antigen present for each different strain in order to provide broad protection against infection. Additionally, the mAbs used here were human IgG1 mAbs. Depending on how the antibody dependent protection in the mice works best against *A. baumannii* it could have been more efficacious to use murine antibodies with murine Fc regions or to try using different antibody isotypes or subclasses that might have increased effector functions and translocation from the blood to the lungs and therefore increase their protective efficacy.

The work performed within this chapter has identified 3 potential vaccine antigens that are highly conserved among *A. baumannii* but also with human sera binding to at least 2 and a high likelihood of a vaccine based upon those targets being protective and broadly effective across multiple strains. Different cocktails of mAbs as well as individual mAbs were also tested using the murine *A. baumannii* infection model previously developed, which showed that an intranasally administered cocktail of mAbs or capsule targeting mAbs are the most likely to be efficacious against *A. baumannii* respiratory tract infection.

6 – Discussion

6.1 – Summary

The work presented in this thesis shows that using clinical isolates of *A. baumannii* results in a more robust respiratory infection model in BALB/c mice than the laboratory reference strain ATCC 17978. This provides a better basis to test the efficacy of potential antimicrobial therapeutics and preventatives. Clinical isolates result in more severe disease with greater bacterial loads and inflammation, giving a broader and more reliable range in which to assess the efficacy of vaccination or mAb pre-treatment. Naturally produced, clinical isolate derived OMVs prove most protective when vaccinated intranasally. This is likely due to an improved mucosal immune response in the respiratory tract. Immune sera from OMV immunised mice were used to identify 3 proteins FilF, OXA-23 and PAL through both western blotting and phage expression cloning. All 3 of which show high levels of conservation between different strains and good potential for use in future *A. baumannii* vaccine development. Additionally, mAbs raised against OMVs from the same clinical isolates were tested in the *in vivo* infection model showing mixed results. With only the capsular mAb showing any level of protective efficacy. This could be partly due to capsule making the targets of the other mAbs inaccessible. It is still uncertain as to whether the mAbs could be more effective when used in combination, either as cocktails or with antibiotics. Additionally, further work is required to establish whether the identified proteins can provide protective immunity or not when used to immunise mice against *A. baumannii* respiratory tract infection.

6.2 – Limitations

There are a number of limitations in the work performed within this thesis. There's a wide range of variation in the bacterial growth and *in vivo* challenge. Due to the dose being calculated retrospectively it is never known at the time of challenge what challenge dose is given to the mice. Additionally, different mice challenged with the same dose of bacteria can develop disease of varying severity. This could be due to bacterial fitness or virulence upon challenge or potentially variability between the mice themselves. The clinical strains of *A. baumannii* we possess have also proven to be unstable compared to laboratory reference strain ATCC 17978, requiring the preparation of new glycerol stocks due to original glycerol stocks losing potency during *in vivo* challenge and an increase in intranasal challenge dose to result in the same disease severity. To reduce the effect of these variabilities, the

numbers of mice used were increased and data shown was representative of multiple repeats that show similar patterns in the data.

Further limitations are seen in the vaccination process where it can be difficult to know for certain if the vaccine administered via the correct route. For example, with intramuscular vaccination incorrect injection technique could result in the administration of the vaccine into subcutaneous fat, or a blood vessel accidentally. This increases the variability in the data and could even lead to complete vaccine failure[231]. Using naturally produced OMVs as a vaccine also introduces variation due to batch to batch variation between OMVs. For example, one batch could possess a particularly effective antigen that the next batch is missing. However, to help reduce the effects of this batch to batch variation either multiple batches can be produced and mixed together to provide the OMV vaccines or for each study the same batch of OMVs should be used throughout. Finally, without defined correlates of protection it is difficult to determine what protection means. In this case, the overall picture is taken into consideration of how the mice respond to vaccination and infection. Reducing bacterial load and preventing dissemination to the spleen is particularly important as these are the areas where the greatest difference is seen between vaccinated and non-vaccinated mice. Additionally, if the bacterial load at one site isn't often affected by vaccination but one particular route, or vaccine formulation reduces the bacterial load in that site as well as others it shows increased potential for use as a vaccine/route and therefore is providing increased protection.

Although upon phylogenetic analysis of the identified antigens shows high levels of conservation between different strains this information means nothing unless the sequences are conserved in the correct regions. For example, if the antigens that are highly variable in the areas of protein are accessible to the immune system then a vaccine antigen based upon that would not be cross protective across different strains. However, if the region of protein accessible to the immune system was highly conserved between strains the vaccine antigen would have good potential for use in the development of a cross protective vaccine. As important of a choice of vaccine antigen is the choice of antibody given to prevent infection. In this case human IgG1 mAbs were used to determine protective efficacy in mice against *A. baumannii*. However, I do not know how much the mAbs translocated within the mice. When given intravenously mAbs provided less protection

against challenge than when given intranasally. This could be due to lower concentration of antibody present in the lungs of the intravenously administered mice and poor translocation of mAbs from the blood to the lungs where they could be required to provide better protection.

6.3 – Future work

Further work to be performed could include liquid chromatography-mass spectrometry to identify the proteins present in the OMVs and determine the batch to batch variability between OMVs derived from the same strain of *A. baumannii*. As well as this, it would be interesting to compare this data between OMVs derived from different clinical strains of *A. baumannii* as well as identifying the proteins in the outer membrane of those strains to identify the percentage coverage of the OMV proteome to the proteins present on the outer membrane of the bacteria.

By performing antigen-specific single B cell sorting, mAb cloning and sequencing it would also be possible to identify the sequences of the variable heavy and light regions of the antibody. This would then allow for modelling and epitope mapping and characterisation. By finding out more information about the epitope it will be easier to understand how well conserved that region of each protein antigen is and therefore suggest whether it could have good potential for use as a vaccine. Additionally more rationally designed vaccines can be produced that are more likely to be effective and provide increased levels of protection.

The generation of new nucleic acid vaccines such as mRNA or saRNA vaccines against *A. baumannii* and testing routes of vaccination to determine whether or not they are effective at protecting against infection could provide a viable and more reproducible alternative to OMVs. The use of nucleic acid vaccines that only express a single antigen *in vivo* would also shed some light on how effective single antigens could be in the development of an *A. baumannii* vaccine. The nucleic acid vaccines could also be tested in combination to determine synergistic antigen combinations that increase levels of protection against infection. Additionally, producing GMMA containing *A. baumannii* antigens on their surface would provide a more standardised vaccine than naturally produced OMVs with reduced batch to batch variation. By using prime pull approaches it would be interesting to determine how the levels of protection against *A. baumannii* varies when mice are primed and boosted via different routes with different vaccines.

Finally, by further developing the mAbs it would be possible to determine whether certain isotypes or subclasses have increased protective efficacy against *A. baumannii* infection. As well as this, it would be important to identify synergistic combinations of individual mAbs and see if their use in combination with antibiotics can improve the therapeutic efficacy of the antibiotic. Potentially even re-sensitising resistant strains to an antibiotic.

6.4 – Vaccines against *A. baumannii*

Being responsible for around 50% of total ICU antibiotic use, nearly 15% of all hospital acquired infections and having the highest morbidity and mortality rates in ICUs, multidrug resistant *A. baumannii* is an ever-growing problem[232]. Resistance to carbapenems is alarmingly high with reported resistance rates of 70%, 92% and 100% in Chile, Korea and Portugal as well as 85% and 62%-100% in India and Pakistan[232]. Even more of a concern is the emergence of last resort treatment options colistin and tigecycline resistance with India, Iran and Spain reporting the highest levels of colistin resistance at 53%, 48% and 40.7% respectively along with 66% of isolates being resistant to tigecycline in Israel and 81% in Turkey[232]. Those most at risk include immunocompromised or elderly individuals, neonates with low birth weights and those with underlying conditions such as COPD, diabetes, smoking or alcoholism. In addition to these factors, prolonged stays in hospital, ICU stays, previous treatment with broad spectrum antibiotics, immunosuppression, tube feeding, catheterisation and mechanical ventilation all add additional risk to developing *A. baumannii* infections[232].

Bearing this information in mind, it is unlikely to be cost effective to immunise a whole population against such infections. Potential vaccination strategies would likely involve targeting most at risk populations. A vaccine has the potential to help people who are immunocompromised, patients in hospitals and military personnel[233]. Any person admitted to hospital who is likely to have a central line, catheter or ventilation tube inserted as well as patients being given broad spectrum antibiotics are all at risk[233]. This is particularly true for patients in areas of the world with high rates of *A. baumannii* infection and high rates of resistance where infection carries the greatest morbidity and mortality rates. Additionally, if a future vaccine was able to prevent carriage of *A. baumannii* it could be worth vaccinating health workers to help reduce potential transmission[121]. An additional avenue would be to vaccinate military personnel and patients who are admitted to hospital for longer durations

such that they have enough time to develop a protective response. However, in cases where hospitalisation cannot be predicted, passive immunisation could be a viable alternative.

It is also likely that a multivalent vaccine would be more effective than a vaccine based upon one antigen or multiple antigens with related functions. An effective multivalent vaccine would provide better levels of protection against challenge by inducing an immune response across multiple strains of *A. baumannii* and multiple virulence mechanisms. Using such a vaccine could make it possible to target biofilm and host cell adhesion neutralisation antigens as well as bactericidal metabolomic and growth related antigens[234]. Multivalent vaccines have shown to provide effective protection in both *A. baumannii*[234] and *Staphylococcus aureus*[235] *in vivo* infection models. Additionally, a monovalent vaccine carries the risk of vaccine escape variants developing due to mutation, down-regulation or elimination of the antigen[236]. This is particularly important to consider when developing a vaccine against an organism such as *A. baumannii* that is able to rapidly mutate and evolve to better survive in unfavourable conditions[237–239]. Pan-genomic analysis of *A. baumannii* military isolates showed numerous and rapid environmental adaptations, resulting in the acquisition or deletion of host cell adhesion, iron acquisition and efflux related virulence factors[239]. Using a multivalent approach has the potential to increase both longevity and protective efficacy of a future *A. baumannii* vaccine.

One other approach that could prove useful in a case such as *A. baumannii* could be to develop a combinational vaccine. If the demand for an *A. baumannii* vaccine on its own is not enough then it could be combined with other bacterial vaccines. Combined vaccines are not uncommon, with the diphtheria, tetanus and pertussis (DTP); measles, mumps and rubella (MMR) and the diphtheria, tetanus, pertussis, polio, Hib and hepatitis B 6-in-1 vaccines, among others currently used in the UK[240–242]. Combination vaccines provide a number of advantages such as reduced administration costs, fewer injections, higher rates of compliance and they allow for the new vaccines to be included in existing vaccination schedules[240]. A combinational vaccine approach could provide a more cost-effective way to protect against *A. baumannii* infections. Currently, *A. baumannii* infection leads to increased treatment costs, duration of hospital stay and increased mortality rates[243], but there is potential for *A. baumannii* to become completely resistant being untreatable with all

current antibiotics[121]. The need for alternative approaches to treat infections with *A. baumannii* is likely to increase in which case vaccines could be even more important.

6.5 – Potential of mAbs in the treatment of *A. baumannii*

Where a potential infection can't be predicted in time for a vaccination to be worth using mAbs could fill the gap. By treating patients prophylactically with *A. baumannii* mAbs, infection could be prevented. Alternatively, if a mAb was effective enough it may have therapeutic potential to treat a patient once they have an established infection. However, this would incur costs and time delays of ineffective antibiotic treatment and would require identification of the causative agent. This means mAbs would most likely be a second- or third-line defence. Although they could be an effective treatment if used in this manner, it also increases the chances of *A. baumannii* developing new antibiotic resistances compared to prophylactic use or vaccines.

A successful mAb treatment strategy for *A. baumannii* will likely consist of a cocktail of mAbs that work via multiple mechanisms and target different virulence, growth or phenotypic factors[244]. As with a vaccine, this would likely increase the breadth of reactivity and improve efficacy and longevity of the treatment due to the high variation seen between *A. baumannii* strains[244]. Along with their long biological half-lives, which can be increased through Fc modifications, mAbs have the potential to provide safe, effective and high levels of protection[245,246]. With antibody engineering capabilities Fc modifications can also increase complement activation and improve PK/PD propterties[131] to further improve their efficacy.

Synergistic relationships have been seen between mAbs and antibiotics. By giving mAbs in combination with antibiotics, antibiotic treatment time is reduced[247]. This in turn reduces some of the risks associated with taking antibiotics. Not only are treatment times reduced, but protection and bactericidal activity can be significantly improved compared to monovalent therapies, which has been seen using *in vivo* models of *A. baumannii* infection[211,248]. The use of low levels of antibiotics can also alter the expression profile of bacteria. This could lead to increased availability of certain antigens and result in increased efficacy or synergy between antibiotic and mAb combined treatment[131]. Alternatively, mAbs could be used as delivery vehicles for antibiotics or other cytotoxic compounds through

antibody drug conjugates. This could not only reduce the doses required, but also increase drug specificity and reduce side effects[131].

One potential outcome could be cocktails of mAbs being used prophylactically to prevent drug resistant *A. baumannii* infections taking hold in the first place in patients with wounds or requiring mechanical ventilation, catheterisation or a central line. However, if infection still manages to break through and *A. baumannii* identified as the causative agent it is possible a mAb and antibiotic combination therapy could be effective in the future. Significant steps still need to be made in developing an effective *A. baumannii* mAb based therapy. However, identifying effective antigens and improving the efficacy of mAbs provides a promising outlook for the treatment of drug resistant *A. baumannii*. They provide a safe and already well tested alternative to antibiotics after being used for years as treatments in other fields, such as cancer. Further development of antibacterial mAbs provides a realistic solution to help combat antibiotic resistance in the future.

6.6 – Conclusions and future perspectives

Combatting antibiotic resistance is going to be a difficult feat and there's unlikely to be one single solution, but a combination of solutions. In the case of *A. baumannii* using multivalent vaccines to target those most at risk and mAbs, or a combination of mAbs and antibiotics, in cases where hospitalisation could not have been predicted provides one potential solution. However, with *A. baumannii* infections likely occurring as a rare event in a person's life, if safety and efficacy prevailed it would be more cost effective to include an *A. baumannii* vaccine in an already existing vaccination programme as a combinational vaccine. Further research into effective antigens is required for both mAb and vaccine development. Another important factor to consider is epitope shielding by capsule, which could prove problematic. Potentially a combinational approach could combat this using a mixture of capsular and protein antigens, where disrupting the capsule provides better access to protein antigens.

With regards to future vaccine development, the work in this thesis has shown the impact the route of vaccination has on the level of protection against *A. baumannii* respiratory tract infection. Not only may some routes offer increased protective efficacy, but if that route does not require injection it could lead to increased vaccine uptake, easier introduction and reduced distribution costs. Intranasal vaccination would not require a sterile environment or

trained healthcare professional for administration and avoids any risks associated with improper needle usage, reducing the chances of blood borne disease transmission[249]. In the case of *A. baumannii* the intranasal immunisation provided the most effective and robust protection against infection suggesting developing effective mucosal immunity is most likely a key factor in active protection against infection. This is likely to be true of other respiratory pathogens too and is currently under investigation for the next phase of COVID-19 vaccines[249]. Intranasal immunisation is outperforming intramuscular immunisation and inducing effective mucosal and systemic immunity, preventing infection and transmission of SARS-CoV-2 in animal models[249]. This clearly highlights the importance of targeting the correct compartment to generate the desired and most effective immune response during vaccine development.

Based upon the work presented in this thesis, future studies to be considered could include investigating the protective efficacy of the three identified antigens. Using *E. coli* expressing FilF, OXA-23 or PAL on their surface recombinant OMVs can be generated and used to immunise mice and assess their protective efficacy against *A. baumannii* respiratory infection in the *in vivo* infection model. This would show whether the proteins are capable of inducing protection on their own or in combination against *A. baumannii*. Additional work could also be performed to study the mechanisms of protection underlying the intranasal OMV vaccination. This could determine whether tissue-resident memory cells are playing a role and if so, how important that role is in protective efficacy. Additionally, there could be an increased Th17 response to intranasal immunisation with *A. baumannii* OMVs compared to subcutaneous or intramuscular immunisation as seen with an intranasal pertussis vaccine[250] which requires further investigation.

Developing a vaccine or mAbs against carbapenem resistant *A. baumannii* presents a number of challenges such as the variability between strains, capsule as well as the ease with which *A. baumannii* can mutate and evolve. However, the data presented in this thesis and by others in the field suggests the generation of a protective immune response against *A. baumannii* is possible. Additionally, protective mAbs could also be viable with combinations of mAb cocktails and also mAb antibiotic combination therapies. Provided an appropriate strategy is chosen an *A. baumannii* vaccine could prove very effective at preventing disease in those who are at highest risk, while mAb cocktails or mAbs and

antibiotics can fill the gaps where necessary. Further research is required to determine the best antigens to target with vaccination and mAb therapies. However, for a bacterium such as *A. baumannii* where treatment options are severely limited and antibiotic resistances are increasing, vaccines and mAbs provide realistic and viable alternatives for the future.

7 – Bibliography

1. Cookson, W. O. C. M., Cox, M. J. & Moffatt, M. F. New opportunities for managing acute and chronic lung infections. *Nat. Rev. Microbiol.* **16**, 111–120 (2018).
2. Dickson, R. P., Erb-Downward, J. R., Martinez, F. J. & Huffnagle, G. B. The Microbiome and the Respiratory Tract. *Annu. Rev. Physiol.* **78**, 481–504 (2016).
3. Drexler, M. & Medicine (US), I. of. *How Infection Works*. *What You Need to Know About Infectious Disease* (National Academies Press (US), 2010).
4. Prat, C. & Lacoma, A. Bacteria in the respiratory tract—how to treat? Or do not treat? *Int. J. Infect. Dis.* **51**, 113–122 (2016).
5. Gadsby, N. J. *et al.* Development of two real-time multiplex PCR assays for the detection and quantification of eight key bacterial pathogens in lower respiratory tract infections. *Clin. Microbiol. Infect.* **21**, 788.e1-788.e13 (2015).
6. Mulani, M. S., Kamble, E. E., Kumkar, S. N., Tawre, M. S. & Pardesi, K. R. Emerging Strategies to Combat ESKAPE Pathogens in the Era of Antimicrobial Resistance: A Review. *Front. Microbiol.* **10**, (2019).
7. Friedman, N. D., Temkin, E. & Carmeli, Y. The negative impact of antibiotic resistance. *Clin. Microbiol. Infect.* **22**, 416–422 (2016).
8. Niederman, M. S. Impact of antibiotic resistance on clinical outcomes and the cost of care. *Crit. Care Med.* **29**, N114 (2001).
9. The top 10 causes of death. https://www.who.int/news-room/fact-sheets/detail/the-top-10-causes-of-death.
10. Forum of International Respiratory Societies & European Respiratory Society. *The global impact of respiratory disease*. (2017).
11. Bosch, A. A. T. M., Biesbroek, G., Trzcinski, K., Sanders, E. A. M. & Bogaert, D. Viral and Bacterial Interactions in the Upper Respiratory Tract. *PLOS Pathog.* **9**, e1003057 (2013).

12. Ishigami, J. *et al.* Estimated GFR and Hospital-Acquired Infections Following Major Surgery. *Am. J. Kidney Dis.* **73**, 11–20 (2019).

13. Peleg, A. Y. & Hooper, D. C. Hospital-Acquired Infections Due to Gram-Negative Bacteria. *N. Engl. J. Med.* **362**, 1804–1813 (2010).

14. Lynch, J. P. Hospital-Acquired Pneumonia: Risk Factors, Microbiology, and Treatment. *Chest* **119**, 373S-384S (2001).

15. Leone, M. *et al.* Hospital-acquired pneumonia in ICU. *Anaesth. Crit. Care Pain Med.* **37**, 83–98 (2018).

16. Monegro, A. F. & Regunath, H. Hospital Acquired Infections. in *StatPearls* (StatPearls Publishing, 2020).

17. Mackley, A., Baker, C. & Bate, A. Raising standards of infection prevention and control in the NHS. Preprint at researchbriefings.files.parliament.uk/documents/CDP-2018.../CDP-2018-0116.pdf (2018).

18. Bate, A., Mackley, A. & Baker, C. Raising standards of infection prevention and control in the NHS. (2018).

19. Kang, L., Jing, W., Liu, Q., Liu, J. & Liu, M. The trends of mortality, aetiologies and risk factors of lower respiratory infections in China from 1990 to 2019: Findings from the Global Burden of Disease Study 2019. *J. Infect. Public Health* **15**, 870–876 (2022).

20. Lower respiratory infections — Level 3 cause. *Institute for Health Metrics and Evaluation* https://www.healthdata.org/results/gbd_summaries/2019/lower-respiratory-infections-level-3-cause (2020).

21. Murray, C. J. Global burden of bacterial antimicrobial resistance in 2019: a systematic analysis. **399**, 27 (2022).

22. Ieven, M. *et al.* Aetiology of lower respiratory tract infection in adults in primary care: a prospective study in 11 European countries. *Clin. Microbiol. Infect.* **24**, 1158–1163 (2018).

23. Noviello, S. & Huang, D. B. The Basics and the Advancements in Diagnosis of Bacterial Lower Respiratory Tract Infections. *Diagnostics* **9**, 37 (2019).

24. Creer, D. D. *et al.* Aetiological role of viral and bacterial infections in acute adult lower respiratory tract infection (LRTI) in primary care. 5.

25. Torres, A., Ferrer, M. & Badia, J. R. Treatment Guidelines and Outcomes of Hospital-Acquired and Ventilator-Associated Pneumonia. *Clin. Infect. Dis.* **51**, S48–S53 (2010).

26. Bielen, K. *et al.* Animal models of hospital-acquired pneumonia: current practices and future perspectives. *Ann. Transl. Med.* **5**, (2017).

27. Arnold, H. M., Sawyer, A. M. & Kollef, M. H. Use of Adjunctive Aerosolized Antimicrobial Therapy in the Treatment of Pseudomonas aeruginosa and Acinetobacter baumannii Ventilator-Associated Pneumonia. *Respir. Care* **57**, 1226–1233 (2012).

28. Nhu, N. T. K. *et al.* Emergence of carbapenem-resistant Acinetobacter baumannii as the major cause of ventilator-associated pneumonia in intensive care unit patients at an infectious disease hospital in southern Vietnam. *J. Med. Microbiol.* **63**, 1386–1394 (2014).

29. Chaari, A. *et al.* Acinetobacter baumannii ventilator-associated pneumonia: epidemiology, clinical characteristics, and prognosis factors. *Int. J. Infect. Dis.* **17**, e1225–e1228 (2013).

30. Chastre, J. & Fagon, J.-Y. Ventilator-associated Pneumonia. *Am. J. Respir. Crit. Care Med.* **165**, 867–903 (2002).

31. Timsit, J.-F., Esaied, W., Neuville, M., Bouadma, L. & Mourvillier, B. Update on ventilator-associated pneumonia. *F1000Research* **6**, (2017).

32. Brinker, A., Cheng, C. & Chan, V. Association of Noninfectious Pneumonia With Ustekinumab Use. *JAMA Dermatol.* **155**, 221–224 (2019).

33. Alves dos Santos, J. W. *et al.* Non-infectious and unusual infectious mimics of community-acquired pneumonia. *Respir. Med.* **98**, 488–494 (2004).

34. Pneumonia. https://www.who.int/news-room/fact-sheets/detail/pneumonia.

35. Gil-Perotin, S. *et al.* Implications of endotracheal tube biofilm in ventilator-associated pneumonia response: a state of concept. *Crit. Care* **16**, R93 (2012).

36. Miko, B. A., Pereira, M. R. & Safdar, A. Respiratory Tract Infections: Sinusitis, Bronchitis, and Pneumonia. in *Principles and Practice of Transplant Infectious Diseases* (ed. Safdar, A.) 339–349 (Springer, 2019). doi:10.1007/978-1-4939-9034-4_20.

37. Pneumonia | National Heart, Lung, and Blood Institute (NHLBI). https://www.nhlbi.nih.gov/health-topics/pneumonia.

38. Koenig, S. M. & Truwit, J. D. Ventilator-Associated Pneumonia: Diagnosis, Treatment, and Prevention. *Clin. Microbiol. Rev.* **19**, 637–657 (2006).

39. Pulido, L., Burgos, D., García Morato, J. & Luna, C. M. Does animal model on ventilator-associated pneumonia reflect physiopathology of sepsis mechanisms in humans? *Ann. Transl. Med.* **5**, (2017).

40. Torres, A. *et al.* Pneumonia. *Nat. Rev. Dis. Primer* **7**, 1–28 (2021).

41. Johanson, W. G., Seidenfeld, J. J., de los Santos, R., Coalson, J. J. & Gomez, P. Prevention of nosocomial pneumonia using topical and parenteral antimicrobial agents. *Am. Rev. Respir. Dis.* **137**, 265–272 (1988).

42. Juan, C. *et al.* Contribution of clonal dissemination and selection of mutants during therapy to Pseudomonas aeruginosa antimicrobial resistance in an intensive care unit setting. *Clin. Microbiol. Infect.* **11**, 887–892 (2005).

43. George, D. L. *et al.* Epidemiology of Ventilator-acquired Pneumonia Based on Protected Bronchoscopic Sampling. *Am. J. Respir. Crit. Care Med.* **158**, 1839–1847 (1998).

44. Cook, D. J. Incidence of and Risk Factors for Ventilator-Associated Pneumonia in Critically Ill Patients. *Ann. Intern. Med.* **129**, 433 (1998).

45. Jonas, M. & Cunha, B. A. Bacteremic Escherichia coli Pneumonia. *Arch. Intern. Med.* **142**, 2157–2159 (1982).

46. O'dempsey, T. J. D. *et al.* Importance of enteric bacteria as a cause of pneumonia, meningitis and septicemia among children in a rural community in The Gambia, West Africa. *Pediatr. Infect. Dis. J.* **13**, 122 (1994).

47. Saeed, N. Salmonella pneumonia complicated with encysted empyema in an immunocompromised youth: Case report and literature Review. *J. Infect. Dev. Ctries.* **10**, (2016).

48. Baraibar, J. *et al.* Risk factors for infection by Acinetobacter baumannii in intubated patients with nosocomial pneumonia. *Chest* **112**, 1050–1054 (1997).

49. Orihuela, C. J., Maus, U. A. & Brown, J. S. Can animal models really teach us anything about pneumonia? Pro. *Eur. Respir. J.* **55**, (2020).

50. Zeng, X. *et al.* A lethal pneumonia model of Acinetobacter baumannii: an investigation in immunocompetent mice. *Clin. Microbiol. Infect.* **25**, 516.e1-516.e4 (2019).

51. Waack, U., Weinstein, E. A. & Farley, J. J. Assessing Animal Models of Bacterial Pneumonia Used in Investigational New Drug Applications for the Treatment of Bacterial Pneumonia. *Antimicrob. Agents Chemother.* **64**, (2020).

52. Marquette, C.-H., Wermert, D., Wallet, F., Copin, M.-C. & Tonnel, A.-B. Characterization of an Animal Model of Ventilator-Acquired Pneumonia. *Chest* **115**, 200–209 (1999).

53. Charles, P.-E. *et al.* New model of ventilator-associated pneumonia in immunocompetent rabbits*. *Read Online Crit. Care Med. Soc. Crit. Care Med.* **30**, 2278–2283 (2002).

54. Wang-Lin, S. X. *et al.* Antibody Dependent Enhancement of Acinetobacter baumannii Infection in a Mouse Pneumonia Model. *J. Pharmacol. Exp. Ther.* **368**, 475–489 (2019).

55. Gu, H. *et al.* Aging exacerbates mortality of Acinetobacter baumannii pneumonia and reduces the efficacies of antibiotics and vaccine. *Aging* **10**, 1597–1608 (2018).

56. Munoz-Price, L. S. & Weinstein, R. A. Acinetobacter Infection. *N. Engl. J. Med.* **358**, 1271–1281 (2008).

57. Almasaudi, S. B. Acinetobacter spp. as nosocomial pathogens: Epidemiology and resistance features. *Saudi J. Biol. Sci.* **25**, 586–596 (2018).

58. Harding, C. M., Hennon, S. W. & Feldman, M. F. Uncovering the mechanisms of Acinetobacter baumannii virulence. *Nat. Rev. Microbiol.* **16**, 91–102 (2018).

59. Kao, C.-Y., Sheu, B.-S. & Wu, J.-J. Helicobacter pylori infection: An overview of bacterial virulence factors and pathogenesis. *Biomed. J.* **39**, 14–23 (2016).

60. Mainil, J. Escherichia coli virulence factors. *Vet. Immunol. Immunopathol.* **152**, 2–12 (2013).

61. Mitchell, A. M. & Mitchell, T. J. Streptococcus pneumoniae: virulence factors and variation. *Clin. Microbiol. Infect.* **16**, 411–418 (2010).

62. Yadav, S. K. *et al.* Burden of Multidrug-Resistant Acinetobacter baumannii Infection in Hospitalized Patients in a Tertiary Care Hospital of Nepal. *Infect. Drug Resist.* **13**, 725–732 (2020).

63. Asokan, G. V., Ramadhan, T., Ahmed, E. & Sanad, H. WHO Global Priority Pathogens List: A Bibliometric Analysis of Medline-PubMed for Knowledge Mobilization to Infection Prevention and Control Practices in Bahrain. *Oman Med. J.* **34**, 184–193 (2019).

64. Alsulaiman, D. *et al.* Evaluation of acinetobacter baumannii pneumonia among critically ill patients in a tertiary care hospital in Saudi Arabia. *Heliyon* **6**, e03976 (2020).

65. Dadgostar, P. Antimicrobial Resistance: Implications and Costs. *Infect. Drug Resist.* **12**, 3903–3910 (2019).

66. Ma, C. & McClean, S. Mapping Global Prevalence of Acinetobacter baumannii and Recent Vaccine Development to Tackle It. *Vaccines* **9**, 570 (2021).

67. Joly-Guillou, M.-L. Clinical impact and pathogenicity of Acinetobacter. *Clin. Microbiol. Infect.* **11**, 868–873 (2005).

68. Lee, C.-R. *et al.* Biology of Acinetobacter baumannii: Pathogenesis, Antibiotic Resistance Mechanisms, and Prospective Treatment Options. *Front. Cell. Infect. Microbiol.* **7**, (2017).

69. Gedefie, A. *et al.* Acinetobacter baumannii Biofilm Formation and Its Role in Disease Pathogenesis: A Review. *Infect. Drug Resist.* **14**, 3711–3719 (2021).

70. Cerqueira, G. M. & Peleg, A. Y. Insights into Acinetobacter baumannii pathogenicity. *IUBMB Life* **63**, 1055–1060 (2011).

71. Uppalapati, S. R., Sett, A. & Pathania, R. The Outer Membrane Proteins OmpA, CarO, and OprD of Acinetobacter baumannii Confer a Two-Pronged Defense in Facilitating Its Success as a Potent Human Pathogen. *Front. Microbiol.* **11**, (2020).

72. Kenyon, J. J. & Hall, R. M. Variation in the Complex Carbohydrate Biosynthesis Loci of Acinetobacter baumannii Genomes. *PLoS ONE* **8**, (2013).

73. Singh, J. K., Adams, F. G. & Brown, M. H. Diversity and Function of Capsular Polysaccharide in Acinetobacter baumannii. *Front. Microbiol.* **9**, (2019).

74. Geisinger, E. & Isberg, R. R. Antibiotic Modulation of Capsular Exopolysaccharide and Virulence in Acinetobacter baumannii. *PLoS Pathog.* **11**, (2015).

75. Zhang, K. *et al.* Proteome Analysis of Outer Membrane Vesicles From a Highly Virulent Strain of Haemophilus parasuis. *Front. Vet. Sci.* **8**, (2021).

76. Jun, S. H. *et al.* Acinetobacter baumannii Outer Membrane Vesicles Elicit a Potent Innate Immune Response via Membrane Proteins. *PLoS ONE* **8**, (2013).

77. Kwon, S.-O., Gho, Y. S., Lee, J. C. & Kim, S. I. Proteome analysis of outer membrane vesicles from a clinical Acinetobacter baumannii isolate. *FEMS Microbiol. Lett.* **297**, 150–156 (2009).

78. Mendez, J. A. *et al.* Extracellular Proteome of a Highly Invasive Multidrug-resistant Clinical Strain of Acinetobacter baumannii. *J. Proteome Res.* **11**, 5678–5694 (2012).

79. Nieves, W. *et al.* A Burkholderia pseudomallei Outer Membrane Vesicle Vaccine Provides Protection against Lethal Sepsis. *Clin. Vaccine Immunol. CVI* **21**, 747–754 (2014).

80. Elhosseiny, N. M. & Attia, A. S. Acinetobacter: an emerging pathogen with a versatile secretome. *Emerg. Microbes Infect.* **7**, 1–15 (2018).

81. Johnson, T. L., Waack, U., Smith, S., Mobley, H. & Sandkvist, M. Acinetobacter baumannii Is Dependent on the Type II Secretion System and Its Substrate LipA for Lipid Utilization and In Vivo Fitness. *J. Bacteriol.* **198**, 711–719 (2016).

82. Garnacho-Montero, J. & Timsit, J.-F. Managing Acinetobacter baumannii infections. *Curr. Opin. Infect. Dis.* **32**, 69–76 (2019).

83. Asif, M., Alvi, I. A. & Rehman, S. U. Insight into Acinetobacter baumannii: pathogenesis, global resistance, mechanisms of resistance, treatment options, and alternative modalities. *Infect. Drug Resist.* **11**, 1249–1260 (2018).

84. Murray, B. E. Beta-lactamase-producing enterococci. *Antimicrob. Agents Chemother.* **36**, 2355–2359 (1992).

85. García-Patiño, M. G., García-Contreras, R. & Licona-Limón, P. The Immune Response against Acinetobacter baumannii, an Emerging Pathogen in Nosocomial Infections. *Front. Immunol.* **8**, (2017).

86. Mortensen, B. L. & Skaar, E. P. Host–microbe interactions that shape the pathogenesis of Acinetobacter baumannii infection. *Cell. Microbiol.* **14**, 1336–1344 (2012).

87. Faassen, H. van *et al.* Neutrophils Play an Important Role in Host Resistance to Respiratory Infection with Acinetobacter baumannii in Mice. *Infect. Immun.* **75**, 5597–5608 (2007).

88. Qiu, H., KuoLee, R., Harris, G. & Chen, W. High susceptibility to respiratory Acinetobacter baumannii infection in A/J mice is associated with a delay in early pulmonary recruitment of neutrophils. *Microbes Infect.* **11**, 946–955 (2009).

89. Tsuchiya, T. *et al.* NK1.1+ cells regulate neutrophil migration in mice with Acinetobacter baumannii pneumonia. *Microbiol. Immunol.* **56**, 107–116 (2012).

90. Bruhn, K. W. *et al.* Host Fate is Rapidly Determined by Innate Effector-Microbial Interactions During Acinetobacter baumannii Bacteremia. *J. Infect. Dis.* **211**, 1296–1305 (2015).

91. Innate Immune Responses to Systemic Acinetobacter baumannii Infection in Mice: Neutrophils, but Not Interleukin-17, Mediate Host Resistance | Infection and Immunity. https://iai.asm.org/content/79/8/3317.short.

92. Grguric-Smith, L. M. *et al.* Neutropenia exacerbates infection by Acinetobacter baumannii clinical isolates in a murine wound model. *Front. Microbiol.* **6**, (2015).

93. Kamoshida, G. *et al.* A novel bacterial transport mechanism of Acinetobacter baumannii via activated human neutrophils through interleukin-8. *J. Leukoc. Biol.* **100**, 1405–1412 (2016).

94. Pollard, A. J. & Bijker, E. M. A guide to vaccinology: from basic principles to new developments. *Nat. Rev. Immunol.* **21**, 83–100 (2021).

95. Jeffreys, S. *et al.* Insights into Acinetobacter baumannii protective immunity. *Front. Immunol.* **13**, (2022).

96. Bentancor, L. V., Camacho-Peiro, A., Bozkurt-Guzel, C., Pier, G. B. & Maira-Litrán, T. Identification of Ata, a Multifunctional Trimeric Autotransporter of Acinetobacter baumannii. *J. Bacteriol.* **194**, 3950–3960 (2012).

97. Bentancor, L. V. *et al.* Evaluation of the Trimeric Autotransporter Ata as a Vaccine Candidate against Acinetobacter baumannii Infections. *Infect. Immun.* **80**, 3381–3388 (2012).

98. Goel, V. K. & Kapil, A. Monoclonal antibodies against the iron regulated outer membrane Proteins of Acinetobacter baumannii are bactericidal. *BMC Microbiol.* **1**, 16 (2001).

99. Cabral, M. P. *et al.* Design of live attenuated bacterial vaccines based on D-glutamate auxotrophy. *Nat. Commun.* **8**, 15480 (2017).

100. Thompson, T. The staggering death toll of drug-resistant bacteria. *Nature* (2022) doi:10.1038/d41586-022-00228-x.

101. Adams, E. *et al.* Tackling Drug-Resistant Infections Globally: Final Report and Recommendations. Preprint at https://amr-review.org/sites/default/files/160518_Final%20paper_with%20cover.pdf (2016).

102. Ghosh, C., Sarkar, P., Issa, R. & Haldar, J. Alternatives to Conventional Antibiotics in the Era of Antimicrobial Resistance. *Trends Microbiol.* **27**, 323–338 (2019).

103. Baker, S. J., Payne, D. J., Rappuoli, R. & De Gregorio, E. Technologies to address antimicrobial resistance. *Proc. Natl. Acad. Sci.* **115**, 12887–12895 (2018).

104. Causes of death over 100 years - Office for National Statistics. https://www.ons.gov.uk/peoplepopulationandcommunity/birthsdeathsandmarriages/deaths/articles/causesofdeathover100years/2017-09-18.

105. Acosta-Coley, I. *et al.* Vaccines platforms and COVID-19: what you need to know. *Trop. Dis. Travel Med. Vaccines* **8**, 20 (2022).

106. Bidmos, F. A., Siris, S., Gladstone, C. A. & Langford, P. R. Bacterial Vaccine Antigen Discovery in the Reverse Vaccinology 2.0 Era: Progress and Challenges. *Front. Immunol.* **9**, (2018).

107. Tagliabue, A. & Rappuoli, R. Changing Priorities in Vaccinology: Antibiotic Resistance Moving to the Top. *Front. Immunol.* **9**, (2018).

108. Jansen, K. U., Knirsch, C. & Anderson, A. S. The role of vaccines in preventing bacterial antimicrobial resistance. *Nat. Med.* **24**, 10–19 (2018).

109. Micoli, F., Bagnoli, F., Rappuoli, R. & Serruto, D. The role of vaccines in combatting antimicrobial resistance. *Nat. Rev. Microbiol.* **19**, 287–302 (2021).

110. Heath, P. T. The UK Hib vaccine experience. *Arch. Dis. Child.* **86**, 396–399 (2002).

111. Balhuizen, M. D., Veldhuizen, E. J. A. & Haagsman, H. P. Outer Membrane Vesicle Induction and Isolation for Vaccine Development. *Front. Microbiol.* **12**, (2021).

112. Schager, A. E. *et al.* IgG Responses to Porins and Lipopolysaccharide within an Outer Membrane-Based Vaccine against Nontyphoidal Salmonella Develop at Discordant Rates. *mBio* **9**, e02379-17 (2018).

113. Tani, C. *et al.* Quantification by LC–MSE of outer membrane vesicle proteins of the Bexsero® vaccine. *Vaccine* **32**, 1273–1279 (2014).

114. Viviani, V. *et al.* OpcA and PorB are novel bactericidal antigens of the 4CMenB vaccine in mice and humans. *Npj Vaccines* **8**, 1–15 (2023).

115. Koeberling, O. *et al.* A broadly-protective vaccine against meningococcal disease in sub-Saharan Africa based on generalized modules for membrane antigens (GMMA). *Vaccine* **32**, 2688–2695 (2014).

116. Sokaribo, A. S. *et al.* A GMMA-CPS-Based Vaccine for Non-Typhoidal Salmonella. *Vaccines* **9**, 165 (2021).

117. Micoli, F., Nakakana, U. N. & Berlanda Scorza, F. Towards a Four-Component GMMA-Based Vaccine against Shigella. *Vaccines* **10**, 328 (2022).

118. Launay, O. *et al.* Booster Vaccination With GVGH Shigella sonnei 1790GAHB GMMA Vaccine Compared to Single Vaccination in Unvaccinated Healthy European Adults: Results From a Phase 1 Clinical Trial. *Front. Immunol.* **10**, (2019).

119. García-Quintanilla, M., Pulido, M. R., López-Rojas, R., Pachón, J. & McConnell, M. J. Emerging therapies for multidrug resistant Acinetobacter baumannii. *Trends Microbiol.* **21**, 157–163 (2013).

120. McConnell, M. J. & Pachón, J. Active and passive immunization against Acinetobacter baumannii using an inactivated whole cell vaccine. *Vaccine* **29**, 1–5 (2010).

121. Gellings, P. S., Wilkins, A. A. & Morici, L. A. Recent Advances in the Pursuit of an Effective Acinetobacter baumannii Vaccine. *Pathogens* **9**, 1066 (2020).

122. Detmer, A. & Glenting, J. Live bacterial vaccines – a review and identification of potential hazards. *Microb. Cell Factories* **5**, 23 (2006).

123. McConnell, M. J. *et al.* Vaccination with outer membrane complexes elicits rapid protective immunity to multidrug-resistant Acinetobacter baumannii. *Infect. Immun.* **79**, 518–526 (2011).

124. McConnell, M. J., Rumbo, C., Bou, G. & Pachón, J. Outer membrane vesicles as an acellular vaccine against Acinetobacter baumannii. *Vaccine* **29**, 5705–5710 (2011).

125. Fattahian, Y. *et al.* Protection against Acinetobacter baumannii infection via its functional deprivation of biofilm associated protein (Bap). *Microb. Pathog.* **51**, 402–406 (2011).

126. Luo, G. *et al.* Active and Passive Immunization Protects against Lethal, Extreme Drug Resistant-Acinetobacter baumannii Infection. *PLoS ONE* **7**, (2012).

127. Motley, M. P., Banerjee, K. & Fries, B. C. Monoclonal Antibody-Based Therapies for Bacterial Infections. *Curr. Opin. Infect. Dis.* **32**, 210–216 (2019).

128. Nagy, E., Nagy, G., Power, C. A., Badarau, A. & Szijártó, V. Anti-bacterial Monoclonal Antibodies. in *Recombinant Antibodies for Infectious Diseases* (ed. Lim, T. S.) 119–153 (Springer International Publishing, 2017). doi:10.1007/978-3-319-72077-7_7.

129. Zurawski, D. V. & McLendon, M. K. Monoclonal Antibodies as an Antibacterial Approach Against Bacterial Pathogens. *Antibiotics* **9**, 155 (2020).

130. Rosini, R., Nicchi, S., Pizza, M. & Rappuoli, R. Vaccines Against Antimicrobial Resistance. *Front. Immunol.* **11**, (2020).

131. Oleksiewicz, M. B., Nagy, G. & Nagy, E. Anti-bacterial monoclonal antibodies: Back to the future? *Arch. Biochem. Biophys.* **526**, 124–131 (2012).

132. Wang, H., Chen, D. & Lu, H. Anti-bacterial monoclonal antibodies: next generation therapy against superbugs. *Appl. Microbiol. Biotechnol.* **106**, 3957–3972 (2022).

133. Suvratoxumab - Aridis Pharmaceuticals/Biosynexus/GlaxoSmithKline/Regeneron Pharmaceuticals - AdisInsight. https://adisinsight.springer.com/drugs/800017995.

134. Aridis Pharmaceuticals, Inc. *A Phase 3, Randomized, Double-blind, Placebo-controlled, Single-dose Study to Evaluate the Efficacy and Safety of Suvratoxumab in Mechanically Ventilated Adults and Adolescents for the Prevention of Nosocomial Pneumonia*. https://clinicaltrials.gov/ct2/show/NCT05331885 (2022).

135. XBiotech Announces Top-Line Results for 514G3 Antibody Therapy in Serious Staphylococcus aureus Infections | XBiotech. https://investors.xbiotech.com/news-releases/news-release-details/xbiotech-announces-top-line-results-514g3-antibody-therapy/.

136. Monoclonal Antibody F598. *Alopexx* https://www.alopexx.com/pipeline/monoclonal-antibody-f598.

137. Huang, X. *et al.* Capsule type defines the capability of Klebsiella pneumoniae in evading Kupffer cell capture in the liver. *PLoS Pathog.* **18**, e1010693 (2022).

138. Acinetobacter baumannii Bouvet and Grimont - 17978 | ATCC. https://www.atcc.org/products/17978.

139. Iacono, M. *et al.* Whole-Genome Pyrosequencing of an Epidemic Multidrug-Resistant Acinetobacter baumannii Strain Belonging to the European Clone II Group. *Antimicrob. Agents Chemother.* **52**, 2616–2625 (2008).

140. Fernando, D. M., Xu, W., Loewen, P. C., Zhanel, G. G. & Kumar, A. Triclosan Can Select for an AdeIJK-Overexpressing Mutant of Acinetobacter baumannii ATCC 17978 That Displays Reduced Susceptibility to Multiple Antibiotics. *Antimicrob. Agents Chemother.* **58**, 6424–6431 (2014).

141. Schultz, M. B. *et al.* Repeated local emergence of carbapenem-resistant Acinetobacter baumannii in a single hospital ward. *Microb. Genomics* **2**, e000050 (2016).

142. Agilent Technologies. Lambda ZAP II Undigested Vector Kit Instruction Manual. (2015).

143. Lodes, M. J., Dillon, D. C., Houghton, R. L. & Skeiky, Y. A. W. Expression Cloning. in *Molecular Diagnosis of Infectious Diseases* (eds. Decler, J. & Reischl, U.) 91–106 (Humana Press, 2004). doi:10.1385/1-59259-679-7:91.

144. Hall, B. G. Building Phylogenetic Trees from Molecular Data with MEGA. *Mol. Biol. Evol.* **30**, 1229–1235 (2013).

145. Fux, C. A., Shirtliff, M., Stoodley, P. & Costerton, J. W. Can laboratory reference strains mirror 'real-world' pathogenesis? *Trends Microbiol.* **13**, 58–63 (2005).

146. Moore, L. R., Kothari, A., Mackie, A., Paulsen, I. T. & Karp, P. D. Summary of Acinetobacter baumannii, Strain ATCC 17978, version 26.1 Tier 2 Curated Database. (2019).

147. ATCC Genome Portal. *ATCC Genome Portal* https://genomes.atcc.org.

148. Luo, G. *et al.* Diabetic murine models for Acinetobacter baumannii infection. *J. Antimicrob. Chemother.* **67**, 1439–1445 (2012).

149. Thompson, M. G. *et al.* Validation of a Novel Murine Wound Model of Acinetobacter baumannii Infection. *Antimicrob. Agents Chemother.* **58**, 1332–1342 (2014).

150. Mizgerd, J. P. & Skerrett, S. J. Animal models of human pneumonia. *Am. J. Physiol.-Lung Cell. Mol. Physiol.* **294**, L387–L398 (2008).

151. Zhao, J. *et al.* Genomic characteristics of clinically important ST11 Klebsiella pneumoniae strains worldwide. *J. Glob. Antimicrob. Resist.* **22**, 519–526 (2020).

152. Beal, J. *et al.* Robust estimation of bacterial cell count from optical density. *Commun. Biol.* **3**, 1–29 (2020).

153. Vesel, N. & Blokesch, M. Pilus Production in Acinetobacter baumannii Is Growth Phase Dependent and Essential for Natural Transformation. *J. Bacteriol.* **203**, e00034-21 (2021).

154. Chakravarty, B. Genetic mechanisms of antibiotic resistance and virulence in Acinetobacter baumannii: background, challenges and future prospects. *Mol. Biol. Rep.* **47**, 4037–4046 (2020).

155. Gheorghe, I. *et al.* Subtypes, resistance and virulence platforms in extended-drug resistant Acinetobacter baumannii Romanian isolates. *Sci. Rep.* **11**, 13288 (2021).

156. Imperi, F. *et al.* The genomics of Acinetobacter baumannii: Insights into genome plasticity, antimicrobial resistance and pathogenicity. *IUBMB Life* **63**, 1068–1074 (2011).

157. Harding, C. M., Hennon, S. W. & Feldman, M. F. Uncovering the mechanisms of Acinetobacter baumannii virulence. *Nat. Rev. Microbiol.* **16**, 91–102 (2018).

158. Haurat, M. F. *et al.* The Glycoprotease CpaA Secreted by Medically Relevant Acinetobacter Species Targets Multiple O-Linked Host Glycoproteins. *mBio* **11**, e02033-20 (2020).

159. Marston, C. K. *et al.* Effects of Long-Term Storage on Plasmid Stability in Bacillus anthracis. *Appl. Environ. Microbiol.* **71**, 7778–7780 (2005).

160. Oskouei, D. D., Bekmen, N., Ellidokuz, H. & Yılmaz, Ö. Evaluation of different cryoprotective agents in maintenance of viability of Helicobacter pylori in stock culture media. *Braz. J. Microbiol.* **41**, 1038–1046 (2010).

161. Michel, C. & Garcia, C. Virulence stability in *Flavobacterium psychrophilum* after storage and preservation according to different procedures. *Vet. Res.* **34**, 127–132 (2003).

162. Simione, F. P. Key issues relating to the genetic stability and preservation of cells and cell banks. *J. Parenter. Sci. Technol. Publ. Parenter. Drug Assoc.* **46**, 226–232 (1992).

163. Bergamini, G. *et al.* Mouse pneumonia model by Acinetobacter baumannii multidrug resistant strains: Comparison between intranasal inoculation, intratracheal instillation and oropharyngeal aspiration techniques. *PLOS ONE* **16**, e0260627 (2021).

164. Silva, W. M. *et al.* A shift in the virulence potential of Corynebacterium pseudotuberculosis biovar ovis after passage in a murine host demonstrated through comparative proteomics. *BMC Microbiol.* **17**, 55 (2017).

165. Gallagher, P. & Baker, S. Developing new therapeutic approaches for treating infections caused by multi-drug resistant Acinetobacter baumannii: Acinetobacter baumannii therapeutics. *J. Infect.* **81**, 857–861 (2020).

166. Lob, S. H., Hoban, D. J., Sahm, D. F. & Badal, R. E. Regional differences and trends in antimicrobial susceptibility of Acinetobacter baumannii. *Int. J. Antimicrob. Agents* **47**, 317–323 (2016).

167. Solanki, V. & Tiwari, V. Subtractive proteomics to identify novel drug targets and reverse vaccinology for the development of chimeric vaccine against Acinetobacter baumannii. *Sci. Rep.* **8**, 9044 (2018).

168. Moriel, D. G. *et al.* Identification of Novel Vaccine Candidates against Multidrug-Resistant Acinetobacter baumannii. *PLOS ONE* **8**, e77631 (2013).

169. McConnell, M. J. & Pachón, J. Active and passive immunization against Acinetobacter baumannii using an inactivated whole cell vaccine. *Vaccine* **29**, 1–5 (2010).

170. Fereshteh, S. *et al.* New putative vaccine candidates against Acinetobacter baumannii using the reverse vaccinology method. *Microb. Pathog.* **143**, 104114 (2020).

171. Mat Rahim, N., Lee, H., Strych, U. & AbuBakar, S. Facing the challenges of multidrug-resistant Acinetobacter baumannii: progress and prospects in the vaccine development. *Hum. Vaccines Immunother.* **17**, 3784–3794 (2021).

172. Pulido, M. R., García-Quintanilla, M., Pachón, J. & McConnell, M. J. A lipopolysaccharide-free outer membrane vesicle vaccine protects against Acinetobacter baumannii infection. *Vaccine* **38**, 719–724 (2020).

173. Li, S. *et al.* Development of Different Methods for Preparing Acinetobacter baumannii Outer Membrane Vesicles Vaccine: Impact of Preparation Method on Protective Efficacy. *Front. Immunol.* **11**, (2020).

174. Lei, L. *et al.* DNA vaccine encoding OmpA and Pal from Acinetobacter baumannii efficiently protects mice against pulmonary infection. *Mol. Biol. Rep.* **46**, 5397–5408 (2019).

175. Avila-Calderón, E. D. *et al.* Outer Membrane Vesicles of Gram-Negative Bacteria: An Outlook on Biogenesis. *Front. Microbiol.* **12**, (2021).

176. Schwechheimer, C. & Kuehn, M. J. Outer-membrane vesicles from Gram-negative bacteria: biogenesis and functions. *Nat. Rev. Microbiol.* **13**, 605–619 (2015).

177. Kaparakis-Liaskos, M. & Ferrero, R. L. Immune modulation by bacterial outer membrane vesicles. *Nat. Rev. Immunol.* **15**, 375–387 (2015).

178. Qing, G. *et al.* Natural and engineered bacterial outer membrane vesicles. *Biophys. Rep.* **5**, 184–198 (2019).

179. Petousis-Harris, H. Impact of meningococcal group B OMV vaccines, beyond their brief. *Hum. Vaccines Immunother.* **14**, 1058–1063 (2018).

180. Brito, L. T. *et al.* Study of different routes of immunization using outer membrane vesicles of Neisseria meningitidis B and comparison of two adjuvants. *Vaccine* **38**, 7674–7682 (2020).

181. Su, F., Patel, G. B., Hu, S. & Chen, W. Induction of mucosal immunity through systemic immunization: Phantom or reality? *Hum. Vaccines Immunother.* **12**, 1070–1079 (2016).

182. Czerkinsky, C. & Holmgren, J. Mucosal Delivery Routes for Optimal Immunization: Targeting Immunity to the Right Tissues. in *Mucosal Vaccines: Modern Concepts, Strategies, and Challenges* (ed. Kozlowski, P. A.) 1–18 (Springer, 2012). doi:10.1007/82_2010_112.

183. Rudin, A., Johansson, E.-L., Bergquist, C. & Holmgren, J. Differential Kinetics and Distribution of Antibodies in Serum and Nasal and Vaginal Secretions after Nasal and Oral Vaccination of Humans. *Infect. Immun.* **66**, 3390–3396 (1998).

184. Du, L. *et al.* Intranasal Vaccination of Recombinant Adeno-Associated Virus Encoding Receptor-Binding Domain of Severe Acute Respiratory Syndrome Coronavirus (SARS-CoV) Spike Protein Induces Strong Mucosal Immune Responses and Provides Long-Term Protection against SARS-CoV Infection. *J. Immunol. Baltim. Md 1950* **180**, 948–956 (2008).

185. Kim, M. H., Kim, H. J. & Chang, J. Superior immune responses induced by intranasal immunization with recombinant adenovirus-based vaccine expressing full-length Spike protein of Middle East respiratory syndrome coronavirus. *PLoS ONE* **14**, e0220196 (2019).

186. Cunningham, A. F. *et al.* Responses to the soluble flagellar protein FliC are Th2, while those to FliC on Salmonella are Th1. *Eur. J. Immunol.* **34**, 2986–2995 (2004).

187. Firacative, C. *et al.* Identification of T helper (Th)1- and Th2-associated antigens of Cryptococcus neoformans in a murine model of pulmonary infection. *Sci. Rep.* **8**, 2681 (2018).

188. Lin, L. *et al.* Acinetobacter baumannii rOmpA vaccine dose alters immune polarization and immunodominant epitopes. *Vaccine* **31**, 313–318 (2013).

189. Huang, W. *et al.* Immunization against Multidrug-Resistant Acinetobacter baumannii Effectively Protects Mice in both Pneumonia and Sepsis Models. *PLOS ONE* **9**, e100727 (2014).

190. García-Patiño, M. G., García-Contreras, R. & Licona-Limón, P. The Immune Response against Acinetobacter baumannii, an Emerging Pathogen in Nosocomial Infections. *Front. Immunol.* **8**, (2017).

191. van Faassen, H. *et al.* Neutrophils Play an Important Role in Host Resistance to Respiratory Infection with Acinetobacter baumannii in Mice. *Infect. Immun.* **75**, 5597–5608 (2007).

192. Qiu, H., KuoLee, R., Harris, G. & Chen, W. High susceptibility to respiratory Acinetobacter baumannii infection in A/J mice is associated with a delay in early pulmonary recruitment of neutrophils. *Microbes Infect.* **11**, 946–955 (2009).

193. Lin, Y., Slight, S. R. & Khader, S. A. Th17 cytokines and vaccine-induced immunity. *Semin. Immunopathol.* **32**, 79–90 (2010).

194. Priebe, G. P. *et al.* IL-17 is a critical component of vaccine-induced protection against lung infection by lipopolysaccharide-heterologous strains of Pseudomonas aeruginosa. *J. Immunol. Baltim. Md 1950* **181**, 4965–4975 (2008).

195. Lin, J.-S., Kummer, L. W., Szaba, F. M. & Smiley, S. T. IL-17 Contributes to Cell-Mediated Defense against Pulmonary Yersinia pestis Infection. *J. Immunol.* **186**, 1675–1684 (2011).

196. Brummelman, J., Wilk, M. M., Han, W. G. H., van Els, C. A. C. M. & Mills, K. H. G. Roads to the development of improved pertussis vaccines paved by immunology. *Pathog. Dis.* **73**, ftv067 (2015).

197. Lin, L. *et al.* Th1-Th17 Cells Mediate Protective Adaptive Immunity against Staphylococcus aureus and Candida albicans Infection in Mice. *PLOS Pathog.* **5**, e1000703 (2009).

198. Wang, S., Gao, J. & Wang, Z. Outer Membrane Vesicles (OMVs) for Vaccination and Targeted Drug Delivery. *Wiley Interdiscip. Rev. Nanomed. Nanobiotechnol.* **11**, e1523 (2019).

199. Beernink, P. T. *et al.* A Meningococcal Native Outer Membrane Vesicle Vaccine With Attenuated Endotoxin and Overexpressed Factor H Binding Protein Elicits Gonococcal Bactericidal Antibodies. *J. Infect. Dis.* **219**, 1130–1137 (2019).

200. Waterbeemd, B. van de *et al.* Improved Production Process for Native Outer Membrane Vesicle Vaccine against Neisseria meningitidis. *PLOS ONE* **8**, e65157 (2013).

201. Masignani, V., Pizza, M. & Moxon, E. R. The Development of a Vaccine Against Meningococcus B Using Reverse Vaccinology. *Front. Immunol.* **10**, (2019).

202. Zheng, M. Z. M. & Wakim, L. M. Tissue resident memory T cells in the respiratory tract. *Mucosal Immunol.* **15**, 379–388 (2022).

203. Bredin, S. *et al.* Impact of colonization with multidrug-resistant bacteria on the risk of ventilator-associated pneumonia in septic shock. *J. Crit. Care* **71**, 154068 (2022).

204. Alp, E. & Voss, A. Ventilator associated pneumonia and infection control. *Ann. Clin. Microbiol. Antimicrob.* **5**, 7 (2006).

205. Messika, J., La Combe, B. & Ricard, J.-D. Oropharyngeal colonization: epidemiology, treatment and ventilator-associated pneumonia prevention. *Ann. Transl. Med.* **6**, 426 (2018).

206. Rappuoli, R., Bottomley, M. J., D'Oro, U., Finco, O. & De Gregorio, E. Reverse vaccinology 2.0: Human immunology instructs vaccine antigen design. *J. Exp. Med.* **213**, 469–481 (2016).

207. Seib, K. L., Zhao, X. & Rappuoli, R. Developing vaccines in the era of genomics: a decade of reverse vaccinology. *Clin. Microbiol. Infect.* **18**, 109–116 (2012).

208. Tahir ul Qamar, M. *et al.* Designing multi-epitope vaccine against Staphylococcus aureus by employing subtractive proteomics, reverse vaccinology and immuno-informatics approaches. *Comput. Biol. Med.* **132**, 104389 (2021).

209. DiGiandomenico, A. & Sellman, B. R. Antibacterial monoclonal antibodies: the next generation? *Curr. Opin. Microbiol.* **27**, 78–85 (2015).

210. Isler, B., Doi, Y., Bonomo, R. A. & Paterson, D. L. New Treatment Options against Carbapenem-Resistant Acinetobacter baumannii Infections. *Antimicrob. Agents Chemother.* **63**, e01110-18.

211. Nielsen, T. B. *et al.* Monoclonal Antibody Therapy against Acinetobacter baumannii. *Infect. Immun.* **89**, e00162-21 (2021).

212. Xiong, Y. Q. *et al.* A Human Biofilm-Disrupting Monoclonal Antibody Potentiates Antibiotic Efficacy in Rodent Models of both Staphylococcus aureus and Acinetobacter baumannii Infections. *Antimicrob. Agents Chemother.* **61**, e00904-17 (2017).

213. filF - Pilus assembly protein FilF - Acinetobacter baumannii | UniProtKB | UniProt. https://www.uniprot.org/uniprotkb/A0A059ZH06/entry.

214. Mahapatra, S. R. *et al.* Immunoinformatics-guided designing of epitope-based subunit vaccine from Pilus assembly protein of Acinetobacter baumannii bacteria. *J. Immunol. Methods* **508**, 113325 (2022).

215. ompA - Outer membrane protein A - Acinetobacter baumannii | UniProtKB | UniProt. https://www.uniprot.org/uniprotkb/A4GVE5/entry.

216. bla(Oxa-23) - Carbapenemase - Acinetobacter baumannii | UniProtKB | UniProt. https://www.uniprot.org/uniprotkb/I0B613/entry.

217. Zhao, Y. *et al.* Outbreak of carbapenem-resistant Acinetobacter baumannii carrying the carbapenemase OXA-23 in ICU of the eastern Heilongjiang Province, China. *BMC Infect. Dis.* **19**, 452 (2019).

218. pal - Peptidoglycan-associated protein - Acinetobacter baumannii | UniProtKB | UniProt. https://www.uniprot.org/uniprotkb/V5VAD5/entry.

219. Lei, L. *et al.* DNA vaccine encoding OmpA and Pal from Acinetobacter baumannii efficiently protects mice against pulmonary infection. *Mol. Biol. Rep.* **46**, 5397–5408 (2019).

220. DUF333 domain-containing protein - Acinetobacter shaoyimingii | UniProtKB | UniProt. https://www.uniprot.org/uniprotkb/A0A6G8RZU7/entry.

221. Ni, Z., Chen, Y., Ong, E. & He, Y. Antibiotic Resistance Determinant-Focused Acinetobacter baumannii Vaccine Designed Using Reverse Vaccinology. *Int. J. Mol. Sci.* **18**, 458 (2017).

222. Ren, S. *et al.* Design and evaluation of a multi-epitope assembly peptide vaccine against Acinetobacter baumannii infection in mice. *Swiss Med. Wkly.* (2019) doi:10.4414/smw.2019.20052.

223. Singh, R., Garg, N., Shukla, G., Capalash, N. & Sharma, P. Immunoprotective Efficacy of Acinetobacter baumannii Outer Membrane Protein, FilF, Predicted In silico as a Potential Vaccine Candidate. *Front. Microbiol.* **7**, (2016).

224. Gerding, M. A., Ogata, Y., Pecora, N. D., Niki, H. & de Boer, P. A. J. The trans-envelope Tol–Pal complex is part of the cell division machinery and required for proper outer-membrane invagination during cell constriction in E. coli. *Mol. Microbiol.* **63**, 1008–1025 (2007).

225. Hamidian, M. & Nigro, S. J. Emergence, molecular mechanisms and global spread of carbapenem-resistant Acinetobacter baumannii. *Microb. Genomics* **5**, e000306 (2019).

226. Tiwari, V., Kapil, A. & Moganty, R. R. Carbapenem-hydrolyzing oxacillinase in high resistant strains of Acinetobacter baumannii isolated from India. *Microb. Pathog.* **53**, 81–86 (2012).

227. Wang-Lin, S. X. *et al.* The Capsular Polysaccharide of Acinetobacter baumannii Is an Obstacle for Therapeutic Passive Immunization Strategies. *Infect. Immun.* **85**, e00591-17 (2017).

228. Nielsen, T. B. *et al.* Monoclonal Antibody Requires Immunomodulation for Efficacy Against Acinetobacter baumannii Infection. *J. Infect. Dis.* **224**, 2133–2147 (2021).

229. Nielsen, T. B. *et al.* Monoclonal Antibody Protects Against Acinetobacter baumannii Infection by Enhancing Bacterial Clearance and Evading Sepsis. *J. Infect. Dis.* **216**, 489–501 (2017).

230. Russo, T. A. *et al.* The K1 Capsular Polysaccharide of Acinetobacter baumannii Strain 307-0294 Is a Major Virulence Factor. *Infect. Immun.* **78**, 3993–4000 (2010).

231. Zuckerman, J. N. The importance of injecting vaccines into muscle. *BMJ* **321**, 1237–1238 (2000).

232. Asif, M., Alvi, I. A. & Rehman, S. U. Insight into Acinetobacter baumannii: pathogenesis, global resistance, mechanisms of resistance, treatment options, and alternative modalities. *Infect. Drug Resist.* **11**, 1249–1260 (2018).

233. Howard, A., O'Donoghue, M., Feeney, A. & Sleator, R. D. Acinetobacter baumannii. *Virulence* **3**, 243–250 (2012).

234. Ramezanalizadeh, F., Rasooli, I., Owlia, P., Darvish Alipour Astaneh, S. & Abdolhamidi, R. Vaccination with a combination of planktonic and biofilm virulence factors confers protection against carbapenem-resistant Acinetobacter baumannii strains. *Sci. Rep.* **12**, 19909 (2022).

235. Harro, J. M. *et al.* Clearance of Staphylococcus aureus from In Vivo Models of Chronic Infection by Immunization Requires Both Planktonic and Biofilm Antigens. *Infect. Immun.* **88**, e00586-19 (2019).

236. McConnell, M. J. & Martín-Galiano, A. J. Designing Multi-Antigen Vaccines Against Acinetobacter baumannii Using Systemic Approaches. *Front. Immunol.* **12**, (2021).

237. Wright, M. S., Iovleva, A., Jacobs, M. R., Bonomo, R. A. & Adams, M. D. Genome dynamics of multidrug-resistant Acinetobacter baumannii during infection and treatment. *Genome Med.* **8**, 26 (2016).

238. Hammerstrom, T. G., Beabout, K., Clements, T. P., Saxer, G. & Shamoo, Y. Acinetobacter baumannii Repeatedly Evolves a Hypermutator Phenotype in Response to Tigecycline That Effectively Surveys Evolutionary Trajectories to Resistance. *PLoS ONE* **10**, e0140489 (2015).

239. Chan, A. P. *et al.* A novel method of consensus pan-chromosome assembly and large-scale comparative analysis reveal the highly flexible pan-genome of Acinetobacter baumannii. *Genome Biol.* **16**, 143 (2015).

240. Skibinski, D. A., Baudner, B. C., Singh, M. & O'Hagan, D. T. Combination Vaccines. *J. Glob. Infect. Dis.* **3**, 63–72 (2011).

241. 6-in-1 Vaccine | Vaccine Knowledge. https://vk.ovg.ox.ac.uk/vk/6-in-1-vaccine.

242. 6-in-1-vaccine-overview. *nhs.uk* https://www.nhs.uk/conditions/vaccinations/6-in-1-infant-vaccine/ (2019).

243. Mirzaei, B. *et al.* Prevalence of multi-drug resistant (MDR) and extensively drug-resistant (XDR) phenotypes of Pseudomonas aeruginosa and Acinetobacter baumannii isolated in clinical samples from Northeast of Iran. *BMC Res. Notes* **13**, 380 (2020).

244. Tamehri, M. *et al.* Combination of BauA and OmpA elicit immunoprotection against Acinetobacter baumannii in a murine sepsis model. *Microb. Pathog.* **173**, 105874 (2022).

245. Dickey, S. W., Cheung, G. Y. C. & Otto, M. Different drugs for bad bugs: antivirulence strategies in the age of antibiotic resistance. *Nat. Rev. Drug Discov.* **16**, 457–471 (2017).

246. Ma, Y.-X. *et al.* Considerations and Caveats in Combating ESKAPE Pathogens against Nosocomial Infections. *Adv. Sci.* **7**, 1901872 (2020).

247. Watkins, R. R. A formidable foe: carbapenem-resistant Acinetobacter baumannii and emerging nonantibiotic therapies. *Expert Rev. Anti Infect. Ther.* **16**, 591–593 (2018).

248. Huang, W. *et al.* Anti-outer Membrane Vesicle Antibodies Increase Antibiotic Sensitivity of Pan-Drug-Resistant Acinetobacter baumannii. *Front. Microbiol.* **10**, (2019).

249. Alu, A. *et al.* Intranasal COVID-19 vaccines: From bench to bed. *eBioMedicine* **76**, 103841 (2022).

250. Raeven, R. H. M. *et al.* Intranasal immunization with outer membrane vesicle pertussis vaccine confers broad protection through mucosal IgA and Th17 responses. *Sci. Rep.* **10**, 7396 (2020).